

University of Lille

Faculty of Sciences and Technologies

Doctoral School 104 - Science of the Matter, of the Radiation, and of the Environment

Doctoral Thesis

by

Olena MOSKAIEVA

to obtain the degree of

Doctor of Lille University

Discipline: Organic, mineral, industrial chemistry

Molecular structure and ionic equilibria of fluorogenic dyes in polar aprotic solvents

Date of defence: 02 March 2023

Sophie	Fourmentin-Lamotte <i>Professor, University of the Littoral Opal Coast (ULCO)</i>	Referee
Oksana	Tananaiko <i>Associate Professor, National Taras Shevchenko University of Kyiv (Ukraine)</i>	Referee
Mykola	Mchedlov-Petrosyan <i>Professor, V.N.Karazin Kharkiv National University (Ukraine)</i>	Supervisor
Francois-Alexandre	Miannay <i>Assistant Professor, HDR, University of Lille</i>	Co-supervisor
Chazallon	Bertrand <i>Professor, University of Lille</i>	President
Minh-Huong	Ha-Thi <i>Assisitant Professor, Paris-Saclay University</i>	Examiner
Alexander	Ishchenko <i>Professor, Institute for Organic Chemistry, NAS of Ukraine (Ukraine)</i>	Examiner
Abdenacer	Idrissi <i>Professor, University of Lille</i>	Examiner

Université de Lille

Faculté des Sciences et Technologies

Ecole Doctorale 104 - Sciences de la Matière, du Rayonnement, et de l'Environnement

Thèse de Doctorat

par

Olena MOSKAIEVA

pour l'obtention du titre de

Docteur de l'Université de Lille

Discipline : Chimie organique, minérale, industrielle

Structure moléculaire et équilibres ioniques des colorants fluorogènes dans les solvants aprotiques polaires

Date de soutenance : 02 Mars 2023

Sophie	Fourmentin-Lamotte <i>Professeur, Université du Littoral-Côte d'Opale (ULCO)</i>	Rapporteur
Oksana	Tananaiko <i>Professeur associé, Université nationale Taras Shevchenko de Kyiv (Ukraine)</i>	Rapporteur
Mykola	Mchedlov-Petrosyan <i>Professeur, Université nationale de Kharkiv V. N. Karazine (Ukraine)</i>	Directeur de thèse
François-Alexandre	Miannay <i>Maître de conférences, Université de Lille</i>	Co-directeur de thèse
Bertrand	Chazallon <i>Professeur, Université de Lille</i>	Président
Minh-Huong	Ha-Thi <i>Maîtresse de conférences, Université Paris-Saclay</i>	Examineur
Alexander	Ishchenko <i>Professeur, Institut de chimie organique, NAS d'Ukraine (Ukraine)</i>	Examineur
Abdenacer	Idrissi <i>Professeur, Université de Lille</i>	Examineur

Acknowledgments

I would like to express my sincere gratitude to my supervisors, Prof. M.O. Mchedlov-Petrosyan and Prof. Francois-Alexandre Miannay, for their wisdom, patience, and scientific experience. Their motivation and strong support have been vital for my successful defence. I respect their personal sacrifices and the extra time that they have spent on this work. I appreciate Prof. Abdenacer Idrissi and Prof. Oleg Kalugin for their guidance and valuable advice during my PhD.

I am grateful to the referees of this thesis Prof. Sophie Fourmentin-Lamotte and Dr. Oksana Tananaiko, and the members of the jury Prof. Chazallon Bertrand, Dr. Minh-Huong Ha-Thi and Prof. Alexander Ishchenko for their time and effort to read this thesis

I also wish to thank my alma mater, V.N. Karazin Kharkiv National University, and my native department of Physical Chemistry, for playing a significant role in shaping my academic carrier. My research would not have been possible without the support of the Ukrainian government, which provided me with basic scholarships.

I would like to express my gratitude to my colleagues at V. N. Karazin Kharkiv National University in Ukraine for their contributions during the first part of the work. Specifically, I extend my appreciation to Mr. Sergey V. Shekhovtsov for the synthesis of the nitrofluorescein dyes and related compounds, to Prof. Andrey O. Doroshenko for the discussion of the ¹³C NMR spectra, and to Prof. Alexander D. Roshal for his help in the fluorescence studies, and to Dr. Tetiana Cheipesh for the discussions during the processing of some spectrophotometric data. I am also grateful to Dr. Iryna Omelchenko, Institute for Single Crystals, National Academy of Sciences of Ukraine, Kharkiv, Ukraine, for the X-ray analysis, to Prof. Vitaliy Kalchenko for providing access to the NMR measurements in Institute for Organic Chemistry, National Academy of Sciences of Ukraine, Kyiv. I would like to give special thanks to Oryna V. Mosharenkova and Kirylo I. Ostrovskiy, students of the Department of Physical Chemistry at V. N. Karazin Kharkiv National University, for their invaluable assistance in the experimental portion of this research.

The second part of the work was performed at the University of Lille, Laboratory of Infrared and Raman Spectrochemistry (LASIR UMR 8516). I would like to express my appreciation to the institution and its director, Dr. Hervé Vezin, for the possibility to pursue PhD studies. I am also grateful to the University of Lille and the PAUSE program for the scholarship.

Finally, I cannot forget to express my heartfelt thanks to my friends Anastasiia Kharchenko, Daria Stepaniuk, Anna Lahuta, and my beloved Dima Dudariev, who provided me with unwavering support throughout my work. And last but not least, my deepest gratitude is given to my family for their unconditional love and unwavering strength.

Abstract

Fluorescein dyes are widely used in different branches of chemistry and related sciences, first of all owing to their unique fluorescent properties. Among these compounds, nitro derivatives are much less explored. This work aimed to disclose the main protolytic and spectral properties of these dyes in non-aqueous solutions.

A series of nitrofluoresceins and several amino derivatives, 22 compounds in total, was studied in detail mainly by spectroscopic methods.

The behavior of these compounds differs significantly from that of other fluorescein dyes, e.g., very popular halogen derivatives. The tautomeric equilibrium of the neutral forms of the dyes is pronouncedly shifted toward the lactone. The peculiar feature of the dyes bearing four NO₂ groups in the xanthenes portion of the molecule is the formation of anionic lactones, caused by the pulling electron density away from the nodal carbon atom. Another feature is the ease of the rupture of the pyran ring in highly alkaline solutions.

The p*K*_a values of the dyes were determined by the spectrophotometric method in buffer solutions in DMSO and in several cases in acetonitrile that contains 4 mass % DMSO, at 25 °C. Interpreting the p*K*_a values requires an understanding of the state of tautomeric equilibria. For instance, the difference between the p*K*_a values of stepwise dissociation of the dyes, p*K*_{a2} – p*K*_{a1}, in DMSO varies from 1.2 for 5'-nitrofluorescein to 7.6 to 4,5-dinitro-2,7-dibromofluorescein. The analysis of the absorption spectra in the visible region allows identifying the molecular and ionic structures of the dyes. The evaluation of the fractions of the tautomers made it possible to calculate the so-called microscopic equilibrium constants, describing the dissociation of single tautomers. The last-named coincide with those of model compounds: esters, ether, and sulfo analogues.

A special study was devoted to revealing the transmittance of the electronic effects in the fluorescein molecule by examining the influence of NO₂ and NH₂ substituents in the phthalic acid residue on the p*K*_a s of the OH groups in the xanthenes part.

The introduction of a nitro group in the phthalic part of fluorescein quenches the emission. Surprisingly, the dyes with four NO₂ groups in the xanthenes part exhibit bright fluorescence in DMSO and other aprotic solvents. As result, a new pH-independent fluorescent indicator, methyl ester of 2,4,5,7-tetranitrofluorescein, very sensitive to the ability of the solvent to hydrogen bonding, is proposed. Also, the conditions of single- and double-charged anions of 5'-aminofluorescein in solutions of different natures are elucidated.

The study of a mixture of aprotic and hydrogen bond donor solvents with model compounds (BODIPY) will allow us to further study in more detail the mechanism of the effect of hydrogen bonds on fluorescein derivatives.

Keywords: fluorogenic dyes, nitrofluorescein, tautomeric constant, BODIPY, dipolar aprotic solvents, H-bonding interactions, fluorescence

Résumé

Les colorants à base de fluorescéine sont largement utilisés dans différentes branches de la chimie et des sciences connexes, d'abord en raison de leurs propriétés fluorescentes uniques. Parmi ces composés, les dérivés nitrés sont beaucoup moins étudiés. Ce travail a pour objectif d'étudier les principales propriétés protéolytiques et spectrales de ces colorants dans des solutions tampons non aqueuses.

Une série de nitrofluorescéines et de plusieurs dérivés aminés, soit un total de 22 composés, a été étudiée en détail principalement par des méthodes spectroscopiques.

Le comportement de ces composés diffère significativement de celui d'autres colorants à base de fluorescéine, par exemple des dérivés halogénés très populaires. Le déplacement de l'équilibre tautomère des formes neutres des colorants est déplacé vers la lactone. La particularité de ces colorants, portant quatre groupes NO_2 dans leur partie xanthène, est la formation de lactones anioniques, provoquée par l'éloignement de la densité électronique de l'atome de carbone nodal. Une autre de leurs caractéristiques est la facilité de rupture du cycle pyrane dans des solutions fortement alcalines.

Les valeurs des pK_a des colorants ont été déterminées par la méthode spectrophotométrique dans des solutions tampons dans du DMSO et dans plusieurs cas dans de l'acétonitrile contenant 4 % en masse de DMSO, à 25 °C. L'interprétation des valeurs des pK_a nécessite une compréhension de l'état des équilibres tautomères. Par exemple, la différence entre les constantes de dissociation par étapes des colorants, pK_a , dans le DMSO, varie de 1,2 pour la 5'-nitrofluorescéine à 7,6 pour la 4,5-dinitro-2,7-dibromofluorescéine. L'analyse des spectres d'absorption UV-visible permet d'identifier les structures moléculaires et ioniques des colorants. L'évaluation des fractions des tautomères a permis de calculer les constantes d'équilibre, dites microscopiques, décrivant la dissociation des tautomères simples. Ces derniers coïncident avec ceux des composés modèles : les esters, l'éther et un analogue sulfo.

De plus, une expérience visant à révéler la transmission des effets électroniques dans la molécule de fluorescéine en examinant l'influence des substituants nitro et amino dans le résidu d'acide phtalique sur le pK_a des groupes OH dans la partie xanthène des systèmes a aussi été effectuée.

L'introduction d'un groupe nitro dans la partie phtalique de la fluorescéine éteint l'émission. Étonnamment, les colorants avec quatre groupes NO_2 dans la partie xanthènes présentent une fluorescence plus intense dans le DMSO et dans les solvants aprotiques. En conséquence, un nouvel indicateur fluorescent indépendant du pH est proposé : l'ester méthylique de la 2,4,5,7-tétranitrofluorescéine, très sensible à la capacité du solvant à former des liaisons hydrogène. En outre, les propriétés photophysiques des anions à charge simple et double de la 5'-aminofluorescéine dans des solutions de nature différente sont présentées.

L'étude d'un mélange de solvants aprotiques et donneurs de liaisons hydrogène avec des composés modèles (BODIPY) nous permettra d'étudier plus en détail le mécanisme de l'effet des liaisons hydrogène sur les dérivés de la fluorescéine.

Mots clés: colorants fluorogènes, nitrofluorescéine, constante tautomère, BODIPY, solvants dipolaires aprotiques, interactions de liaison hydrogène, fluorescence.

Contents

Introduction	9
Chapter 1 Derivatives of fluorescein in solution.....	13
1.1 Introduction	14
1.2 Ionic equilibria and tautomerism	15
1.3 Hydroxyxanthene dyes that form anions-lactones: Amino- and nitrofluoresceins	19
1.4 Conclusions	22
Chapter 2 Equilibrium and Spectral Studies: Research Setting	29
2.1 Introduction	30
2.2 Materials	30
2.2.1 Dyes	30
2.2.2 Solvents.....	33
2.2.3 Other chemicals	33
2.3 Apparatus.....	34
2.4 Primary characterization of the dyes in solid state and solution	34
2.4.1 Lactones of 2,4,5,7,4'-pentanitrofluorescein and 2,4,5,7,5'-pentanitrofluorescein: Structural description via X-ray analysis	35
2.4.2 ¹³ C NMR study in DMSO solutions	39
2.4.3 Absorption spectra in solution	42
2.5 Approach to the p <i>K</i> _a determination	45
2.5.1 The acidity scale in DMSO.....	45
2.5.2 The acidity scale in acetonitrile-DMSO 96:4 mass	46
2.5.3 The principles of p <i>K</i> _a determination.....	47
Chapter 3 Nitro derivatives of fluorescein in solution: Towards understanding of stepwise acid- base dissociation in systems inclined to tautomerism	53
3.1 Introduction	54
3.2 The 4,5-dinitrofluorescein series in DMSO	56
3.3 The tetranitrofluorescein series	60
3.3.1 The tetranitrofluorescein series in DMSO	60
3.3.2 Rupture of the pyran ring and transformations in aqueous media	63

3.3.3 Ionic equilibria in acetonitrile with 4 mass % DMSO	66
3.4 Special cases of 4,5-dinitro-2,7-dibromofluorescein and 5'-nitrofluorescein in DMSO	71
3.5 4,5-Dinitrofluorescein: Detailed scheme of the protolytic equilibrium	76
3.6 Dyes that form anionic lactones: Dissociation and tautomerism of tetra- and pentanitro fluoresceins in DMSO	79
3.7 Tautomerism in acetonitrile with 4 mass % DMSO	82
3.8 Detailed scheme of protolytic equilibrium of 5'-nitrofluorescein	83
3.9 Explanation of the K_{a1} / K_{a2} ratio in DMSO	84
3.10 Conclusions	86
Chapter 4 Transmittance of the electronic effects in the fluorescein molecule: Nitro and amino groups in the phthalic acid residue	90
4.1 Introduction	91
4.2 Results and Discussion	98
4.3 Conclusions	101
Chapter 5 Fluorescent properties of amino and nitro derivatives of fluorescein in aprotic solvents	105
5.1 Introduction	106
5.2 Quantum yields of nitro and amino derivatives of fluorescein	108
5.3 Fluorescence of 4'-nitrofluorescein in solvents of different nature: low quantum yields	110
5.3 The peculiarity of aminofluoresceins fluorescence	113
5.4 2,4,5,7-Tetranitrofluorescein methyl ester: A new pH-independent indicator, sensitive to hydrogen binding	117
5.5 Conclusions	120
Chapter 6 Conformational effect on the photophysics of two BODIPY dyes in a mixture of butanol and acetonitrile	125
6.1 Introduction	126
6.2 Experimental section	128
6.2.1 Chemicals	128
6.2.2 Steady-state Spectroscopy	128
6.2.3 Time-resolved fluorescence	129
6.3 Result and Discussion	130
6.3.1 Steady-state Absorption and Fluorescence Spectra	130
6.3.2 Fluorescence quantum yield	133
6.3.3 TCSPC measurements	134

6.3.4 DFT calculation	138
6.4 Conclusion.....	140
Conclusions and perspectives.....	146
Appendices	149

List of abbreviations

e – elementary charge, C;

N_a – Avogadro number, mol^{-1} ; N_A

R – universal gas constant, $\text{J}\cdot\text{mol}^{-1}\cdot\text{K}^{-1}$;

T – temperature, K;

ε_0 – permittivity of free space, $8.854\times 10^{-12} \text{ C}^2 \text{ J}^{-1} \text{ m}^{-1}$;

ε_r – relative permittivity of the solvent;

ε_{eff} – effective relative permittivity of the space permeated by the electric field lines;

r – distance between the dissociating group and the negatively charged substituent, nm;

E_T^N – normalized Reichardt's parameter of polarity;

n – refractive index of solvent;

η – viscosity, $\text{mPa}\cdot\text{s}$;

$[i]$ – equilibrium concentration of the i -th particle;

α_b – mole fraction of the corresponding form of substance b , %;

M – $\text{mol}\cdot\text{l}^{-1}$;

pH – index of the hydrogen ion activity;

$\text{pH}_c = -\log[\text{H}^+]$ – index of hydrogen ion concentration

$\text{p}a_{\text{H}^+}^*$ – index of the activity of H^+ ions, referred to the standard state of the solvent;

f_z – ionic activity coefficients;

I – ionic strength, M;

z – charge of the ion;

$K_{a,i}$ – thermodynamic constant of the i -th stage of dissociation;

K_T – tautomeric equilibrium constants;

k_i – “microscopic” ionization constant characterizing the i -th equilibrium between individual tautomers;

K_b^f – formation constants characterizing the homoassociation process of corresponding form of substance b ;

c_b – analytical concentration of the corresponding form of substance b , M;

ε – molar extinction coefficient, $\text{cm}^{-1}\text{M}^{-1}$;

ε_{max} - molar extinction coefficient at the maximum of the spectrum, $\text{cm}^{-1}\text{M}^{-1}$;
 ε_b - molar extinction coefficient of solution under complete conversion of the dye into the corresponding form b ; $\text{cm}^{-1}\text{M}^{-1}$;
 ν - wavenumber, nm^{-1} ;
 ν_{max} - wavenumber at the maximum of the spectrum, cm^{-1} ;
 λ - wavelength, nm;
 λ_{max} - wavelength at the maximum of the spectrum, cm;
 $\Delta\nu_{Stokes}$ - Stokes shift, cm^{-1} ;
 A - absorbance at a current $\text{p}a_{\text{H}^+}^*$ value;
 A_b - absorbance of solution under complete conversion of the dye into the corresponding form b ;
 φ - fluorescence quantum yield, % (Φ_{sample}^{fluo}) ;
 φ_{st} - fluorescence quantum yield of a standard(reference) substance (Φ_{ref}^{fluo});
 I_{sample}^{fluo} - fluorescence intensity investigated solution;
 I_{ref}^{fluo} - fluorescence intensity of a standard(reference) substance;
 $k_{A \rightarrow B}$ - $A \rightarrow B$ rate constant, s^{-1} ;
 k_{rad} and k_{nonrad} - radiative and nonradiative rate constants;
 $IRF(t')$ - instrument response function;
 t - time, s;
 τ_i - lifetimes of i -th exponential component, ps;
 H_mR^l - ionic and molecular forms of dyes (m is the number of protons capable of participating in acid-base transformations, l is the particle charge);
 H_2L - lactone;
 H_2Q - quinone;
 H_2Z^\pm - zwitter-ion;
 DBU - diazabicyclo[5.4.0]undec-7-ene;
 $p\text{-TSA}$ - p -Toluenesulfonic acid;
 DMSO - dimethyl sulfoxide;
 AN - acetonitrile;
 BuOH - butanol-1;
 BODIPY - boron-dipyrromethene (4,4-difluoro-4-bora-3a,4a-diaza-s-indacene.

Introduction

Fluorescein, the progenitor of one of the most popular classes of organic dyes, has been synthesized as early as 1871 by Adolf Baeyer [1–3]. The excellent fluorescence of this compound and its numerous derivatives and analogues is considered in detail [4–7]. In the 1920s, some studies aimed to understand the structure in solution [8] and absorption spectra in the visible region [9] appeared. The history of the issue can be found in ref. [10].

More recent research of the molecular structure in solid state [11] and solutions [12–14] allowed clarifying the principal features of the dyes, whereas new studies of the dyes' fluorescence [15–17] demonstrated the rich possibilities and promise of this class of compounds.

Of course, the above-cited publications are only typical examples from a much larger body of literature. Some important papers are also considered in Chapter 1.

Though the first representative of nitrofluoresceins, 2,4,5,7-tetranitrofluorescein, was already prepared by Baeyer [2], this branch of the fluorescein family was much less studied. The sole exception is the so-called eosin bluish, the dinitrodibromo derivative of fluorescein. A paper devoted to the synthesis of several new nitrofluoresceins was published in 1999 [18]. This publication was followed by studies of the spectral and acid-base properties of the synthesized compounds [19, 20]. Some of them turned out to be fluorescent in non-aqueous media [20].

Therefore, the present study aimed to disclose the main parameters of absorption and fluorescence as well as the protolytic (acid-base and tautomeric) properties of a series of nitrofluorescein dyes. As it was shown recently [21], aminofluoresceins bearing the NH_2 group in the phthalic acid residue also exhibit bright emission in some organic solvents, such as dimethylsulfoxide (DMSO) and acetonitrile (AN), though previously they were considered as extremely weak luminophores basing on the data in water and alcohols. Therefore, some of the aminofluoresceins were also involved in this study.

The study of a mixture of aprotic and hydrogen bond donor solvents with model compounds (BODIPY) will allow us to further study in more detail the mechanism of the effect of hydrogen bonds on fluorescein derivatives.

Organization of the thesis

This thesis presents an investigation of the main parameters of absorption, fluorescence, and protolytic (acid-base and tautomeric) properties of a series of nitrofluorescein dyes in aprotic solvents and their mixtures. It is organized in the following way.

A short literature review of stepwise acid-base dissociation of nitro derivatives of fluorescein in solution is presented in Chapter 1. The problem about anions with a lactone structure of amino and nitro derivatives is described in this chapter. In Chapter 2, we present the objects of the study, and their main characterizations, and justify the choice of research methodology. First of all, the origin of the dye samples and the synthesis of new compounds are presented, as well as solvents and other materials. The equipment used in the study is also specified.

The pK_a values of the dyes were determined in Chapter 3 by the spectrophotometric method in buffer solutions in DMSO and acetonitrile-DMSO mixtures. Interpreting the pK_a values requires an understanding of the state of tautomeric equilibria. The analysis of the absorption spectra in the visible region and evaluation of the tautomerization constants made it possible to calculate the so-called microscopic equilibrium constants of the stepwise dissociation.

In Chapter 4 we examined the influence of the substituents in the phthalic residue on the dissociation of the hydroxy group of the compound. This can shed some light on the transmittance of the electronic effects between the two parts of the fluorescein molecule.

The fluorescent properties of amino and nitro derivatives of fluorescein in aprotic solvents were described in Chapter 5. This finding seems to be important for understanding the emission processes in fluorescein series in the case of the introduction of electron-donating groups, such as NH_2 , and acceptor groups, such as NO_2 , in the phthalic residue. Based on the results of the previous chapters and comparing fluorescence data with literature value for alcohol and water solutions and DFT calculation it is possible to put forward an assumption about the effect of hydrogen bonds on the fluorescence of nitro- and aminoderivatives of fluorescein.

The effect of mixture compositions of aprotic (or hydrogen bond donor) solvent on the steady-state properties like absorption and emission maxima, Stokes shift and relative quantum yield of BODIPY dyes is described in Chapter 6. Analysis of the influence of the mixture on the model compounds will help to further interpret the results for the nitro- and amino derivatives of fluorescein. Finally, conclusions, summarizing the key findings of the work, and future perspectives are outlined.

Bibliography

1. Baeyer, A.: Ueber eine neue Klasse von Farbstoffen. Berichte der deutschen chemischen Gesellschaft. 4, 555–558 (1871). <https://doi.org/10.1002/CBER.18710040209>
2. Baeyer, A.: Ueber die Verbindungen der Phtalsäure mit den Phenolen. Justus Liebigs Ann Chem. 202, 36–49 (1880). <https://doi.org/10.1002/JLAC.18802020105>
3. Lamberts, J.J.M., Neckers, D.C.: Rose Bengal and Non-Polar Derivatives: The Birth of Dye Sensitizers for Photooxidation+. Zeitschrift für Naturforschung - Section B Journal of Chemical Sciences. 39, 474–484 (1984). <https://doi.org/10.1515/ZNB-1984-0412>
4. Krasovitskii, B.M., Bolotin, B.M.: Organic luminescent materials. VCH, New York (1988)
5. Valeur, B.: Molecular Fluorescence: Principles and Applications. Wiley-VCH Verlag GmbH (2001)
6. Haugland, R.P.: Handbook of fluorescent probes and research products. Molecular Probes, Inc, Eugene, Or (2002)
7. Han, J., Burgess, K.: Fluorescent indicators for intracellular pH. Chem Rev. 110, 2709–2728 (2010). <https://doi.org/10.1021/CR900249Z>
8. Orndorff, W.R., Gibbs, R.C., Shapiro, C. v.: The absorption spectra of fluorescein, fluoran and some related compounds. J Am Chem Soc. 50, 819–828 (1928). https://doi.org/10.1021/JA01390A029/ASSET/JA01390A029.FP.PNG_V03
9. Moir, J.: Colour and chemical constitution. Transactions of the Royal Society of South Africa. 10, 159–164 (1922). <https://doi.org/10.1080/00359192209519277>
10. Mchedlov-Petrosyan, N.O.: Fluorescein dyes in solutions: well studied systems? . Kharkov Univ. Bull. . 626, 221–312 (2004)
11. Markuszewski, R., Diehl, H.: The infrared spectra and structures of the three solid forms of fluorescein and related compounds. Talanta. 27, 937–946 (1980). [https://doi.org/10.1016/0039-9140\(80\)80125-1](https://doi.org/10.1016/0039-9140(80)80125-1)
12. Fompeydie, D., Levillain, P.: Équilibre entre formes structurales de l'éosine et de la fluorescéine moléculaires. Bull. Soc. Chim, Fr. 11–12, 459–465 (1980)
13. Amat-Guerri, F., López-González, M.M.C., Sastre, R., late R. Martinez-Utrilla, the: Spectrophotometric determination of ionization and isomerization constants of Rose Bengal,

eosin Y and some derivatives. *Dyes and Pigments*. 13, 219–232 (1990). [https://doi.org/10.1016/0143-7208\(90\)80021-G](https://doi.org/10.1016/0143-7208(90)80021-G)

14. Mchedlov-Petrosyan, N.O., Kukhtik, V.I., Bezugliy, V.D.: Dissociation, tautomerism and electroreduction of xanthene and sulfonaphthalein dyes in N,N-dimethylformamide and other solvents. *J Phys Org Chem*. 16, 380–397 (2003). <https://doi.org/10.1002/POC.654>

15. Urano, Y., Kamiya, M., Kanda, K., Ueno, T., Hirose, K., Nagano, T.: Evolution of fluorescein as a platform for finely tunable fluorescence probes. *J Am Chem Soc*. 127, 4888–4894 (2005). <https://doi.org/10.1021/JA043919H/ASSET/IMAGES/MEDIUM/JA043919HN00001.GIF>

16. Grimm, J.B., Gruber, T.D., Ortiz, G., Brown, T.A., Lavis, L.D.: Virginia Orange: A Versatile, Red-Shifted Fluorescein Scaffold for Single- And Dual-Input Fluorogenic Probes. *Bioconjug Chem*. 27, 474–480 (2016). https://doi.org/10.1021/ACS.BIOCONJCHEM.5B00566/ASSET/IMAGES/LARGE/BC-2015-00566D_0006.JPEG

17. Zhou, P., Tang, Z., Li, P., Liu, J.: Unraveling the Mechanism for Tuning the Fluorescence of Fluorescein Derivatives: The Role of the Conical Intersection and $n\pi^*$ State. *Journal of Physical Chemistry Letters*. 12, 6478–6485 (2021). https://doi.org/10.1021/ACS.JPCLETT.1C01774/SUPPL_FILE/JZ1C01774_SI_001.PDF

18. Samoilov, D. V., Martynova, V.P., El'tsov, A. V.: Nitro derivatives of fluorescein. *Russ J Gen Chem*. 69, 1450–1460 (1999)

19. Mchedlov-Petrosyan, N.O., Vodolazkaya, N., Martynova, V.F., Samoylov, D., El'tsov, A.: Protolytic Equilibria in Nitro Derivatives of Fluorescein. *Russ J Gen Chem*. 70, 1259–1271 (2000)

20. Mchedlov-Petrosyan, N.O., Vodolazkaya, N.A., Surov, Y.N., Samoylov, D.V.: 2,4,5,7-Tetranitrofluorescein in solutions: novel type of tautomerism in hydroxyxanthene series as detected by various spectral methods. *Spectrochim Acta A Mol Biomol Spectrosc*. 61, 2747–2760 (2005). <https://doi.org/10.1016/J.SAA.2004.09.030>

21. Mchedlov-Petrosyan, N.O., Cheipesh, T.A., Roshal, A.D., Doroshenko, A.O., Vodolazkaya, N.A.: Fluorescence of aminofluoresceins as an indicative process allowing one to distinguish between micelles of cationic surfactants and micelle-like aggregates. *Methods Appl Fluoresc*. 4, (2016). <https://doi.org/10.1088/2050-6120/4/3/034002>

Chapter 1

Derivatives of fluorescein in solution

Nowadays, fluorescein dyes are widely used in different branches of chemistry and related sciences, first of all owing to their unique fluorescent properties. The general dissociation and tautomerization scheme is well developed and works well for fluorescein and its numerous derivatives and analogous, first of all, the halogen derivatives. Among these compounds, nitro derivatives are much less explored. However, new compounds of this family exhibit new types of behavior in solution.

This chapter reviews the tautomeric form of the most studied fluorescein derivatives. Analysis of the literature convincingly shows that, despite the presence of a series of publications, a general picture of the nitrofluoresceins equilibrium in solution is still absent. Compounds containing nitro groups in the xanthene part of the molecule are of particular interest. This requires additional thorough study.

1.1 Introduction

The hydroxyxanthene compounds of the fluorescein family belong to the oldest, most studied, and widely used organic dyes [1]. Nevertheless, the investigation of the various properties of these important compounds is continuously ongoing [2–5]. For example, now they are used in microscale thermophoresis [6], for creating functionalized luminescent materials [7] and studying surfactant micelles of different types [8, 9]. Fluorescein is used as a platform for finely tunable fluorescence probes [10], whereas many fluorescein dyes are applied as fluorescent indicators for intracellular pH [11], chromogenic and fluorogenic probes [12], for manufacturing sensors in marine systems [13], as biological probes [14], etc.

Recently, photoinduced proton transfer [15], oxygen- and pH-dependent photophysics [16], and mechanism for tuning of fluorescence [17] is explored for the dyes of fluorescein series. Of special interest is new research on the anions of fluorescein dyes in the gas phase [18]. However, the protolytic equilibria in liquid media have been studied in detail mainly for common representatives of this group of fluorophores, first of all for the mother compound [19–23] and halogen derivatives [19, 20, 24–26].

In Figure 1.1, the molecular formulas of the neutral and anionic forms of fluorescein are demonstrated.

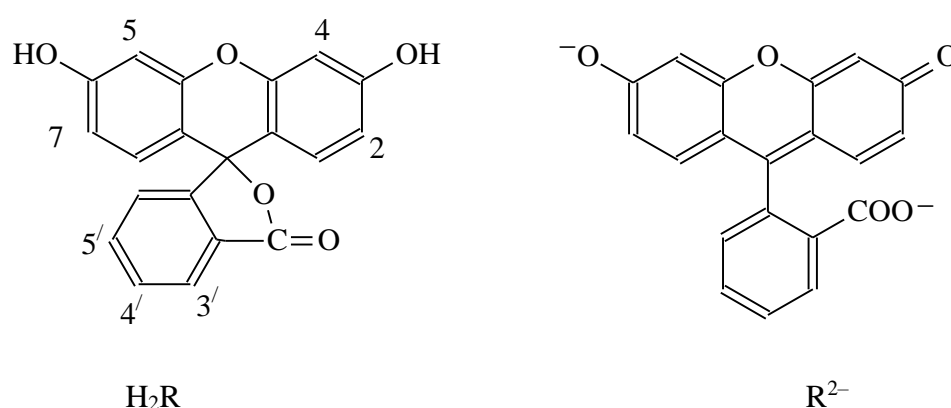


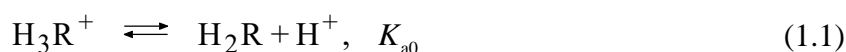
Figure 1.1: Molecular structures of neutral and dianionic forms of fluorescein.

In the xanthenes portion of the R^{2-} , the oxygen atoms are in an equal state, whereas the manner of the accepted representation is conventional.

The study of the protolytic equilibria of dibenzofluorescein show that the pK_a values in water somewhat deviate from those of fluorescein [27]. It was also demonstrated that the introduction of the ethyl group in the 2 and 7 positions of fluorescein shifts the pK_{a2} value toward the physiological pH region [28]. Recently, interesting properties of the new fluorescent probes – silicon-substituted fluorescein were reported [29]. The excited state proton transfer reactions in the hydroxyxanthene series were also studied [30, 31]. A detailed study of ionization and tautomerism of a series of fluorescein dyes in cetyltrimethylammonium chloride micellar solutions at a high ionic strength of the bulk phase was published recently [32].

1.2 Ionic equilibria and tautomerism

Fluorescein dyes are dibasic acids, which can also add a proton in solutions.



The cationic form can be represented as a carbenium cation:

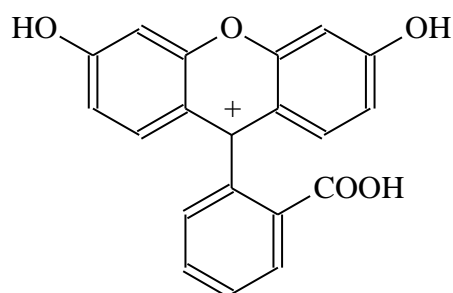


Figure 1.2: Molecular structure of fluorescein cation, H_3Z^+ .

The neutral form of fluorescein is represented by the following structures: lactone, H_2L , quinone, H_2Q , and zwitterion, H_2Z^\pm (Figure 1.3).

Chapter 1

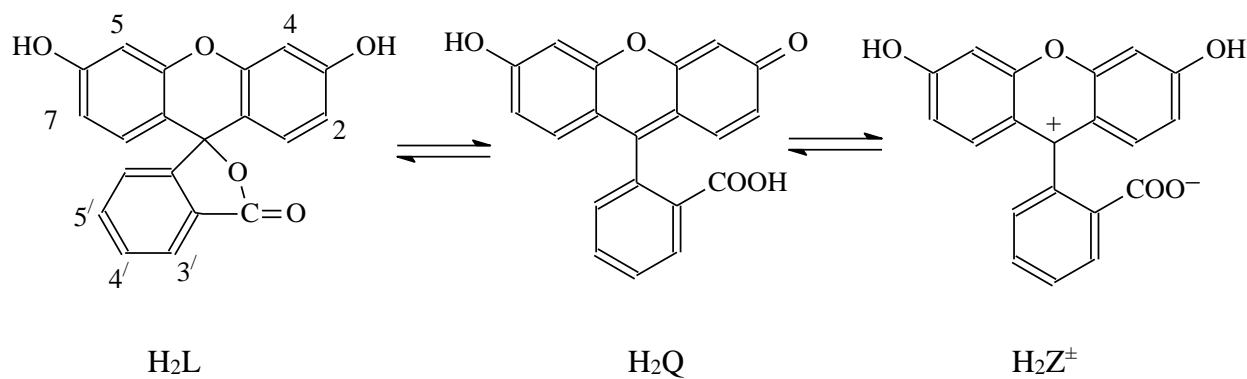


Figure 1.3: Molecular structures of the neutral form of fluorescein.

While the lactone H₂L is colorless, the other two tautomers absorb in the visible region. The fractions of these tautomers in water are 0.67, 0.11, and 0.22, respectively [20].

The single-charged anion, or monoanion, of fluorescein has the HQ⁻ structure in solution:

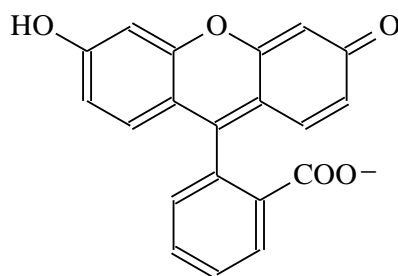


Figure 1.4: Fluorescein monoanion, HQ⁻.

The spectra of the ionic forms of fluorescein are presented in Figure 1.5 (where ϵ - the molar extinction coefficient, cm⁻¹M⁻¹).

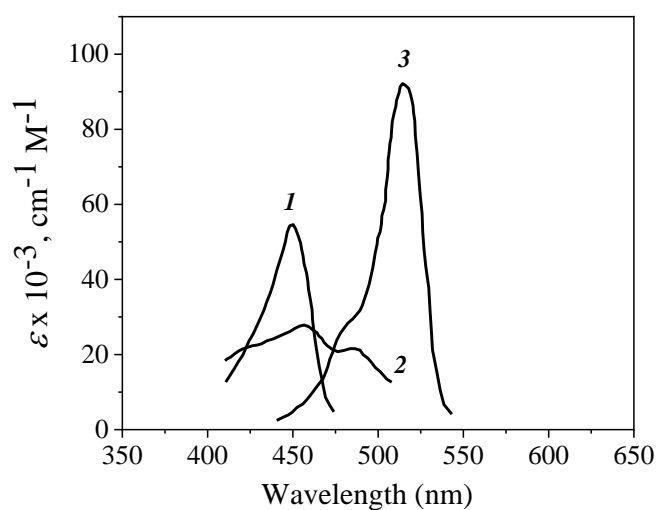


Figure 1.5: Spectra of fluorescein ionic forms in 91 mass % aqueous dimethyl sulfoxide (DMSO): H₃R⁺ (1); HR⁻ (2); R²⁻ (3) [20].

It is firmly proved that the absorption bands of the H_2Q and H_2Z^\pm tautomers in the visible are analogous to those of the ions HQ^- and H_3Z^+ , respectively. However, in the case of an ionized carboxylic group, the absorption maximum is somewhat bathochromically shifted [19, 20, 24, 26, 32]. This shift is also in agreement with quantum-chemical calculations [33].

The situation is different in the case of 2,4,5,7-tetrabromo and tetraiodo derivatives. Here, the monoanion appears as a “phenolate” tautomer, HX^- , owing to the pronounced strengthening of the hydroxyl group acidity, Figure 1.6. The bathochromic shift of the HX^- with respect to that of the quinonoidal dianion (Figure 1.1), designated as X^{2-} , is also in line with the abovementioned theoretical calculations [33].

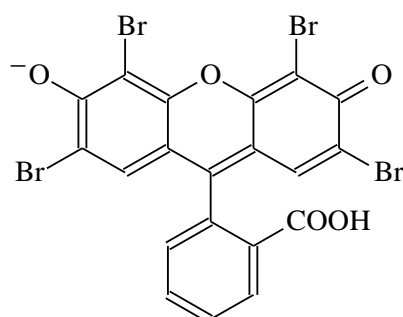


Figure 1.6: The molecular structure of the eosin monoanion, HX^- .

This is also the reason for the negligible fraction of the zwitterions in the case of eosin and similar dyes. But even for fluorescein, this tautomer, H_2Z^\pm , is observed only in water, not in organic solvents [19, 20, 22, 26, 32].

The spectra of several halogen derivatives of fluorescein in 90 mass % aqueous acetone are exemplified in Figure 1.7.

It is clearly seen, that the HR^- ions of dyes with halogen substitution in the phthalic acid residue have the structure of HQ^- type. For dyes with only two halogen atoms in the xanthene part, e.g., 2,7-dichlorofluorescein and 4,5-dibromofluorescein, the fractions of the HR^- tautomer can be commensurable, depending of the solvent nature [20, 26, 32].

The molar extinction coefficient of the R^{2-} anions are rather high (for example, see Figure 1.7); in water, for fluorescein, eosin, and erythrosin they are 88.0×10^3 , 96.7×10^3 , and $94.6 \times 10^3 \text{ M}^{-1}\text{cm}^{-1}$ at $\lambda_{\text{max}} = 490, 515, \text{ and } 525 \text{ nm}$, respectively.

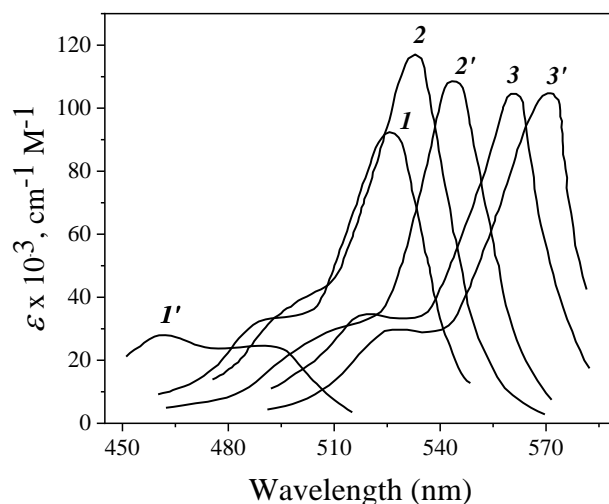


Figure 1.7: Absorption spectra of R^{2-} (1–3) and HR^{-} (1'–3') of 3',4',5',6'-tetrachlorofluorescein (1, 1'), 2,4,5,7-tetraiodofluorescein (erythrosin) (2, 2'), and 2,4,5,7-tetraiodo-3',4',5',6'-tetrachlorofluorescein (rose Bengal B) (3, 3') in 90 mass % aqueous acetone [34].

Taking into account the above information about tautomerism, the detailed scheme of protolytic equilibrium can be represented in Figure 1.8 for the simplest case, i.e., for fluorescein and eosin.

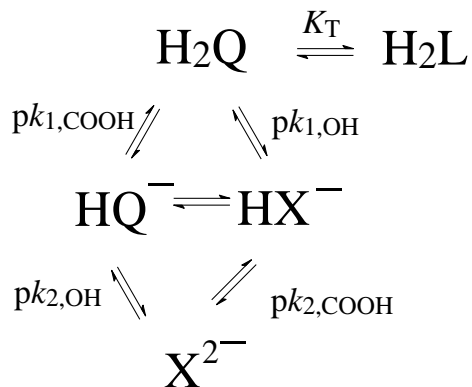


Figure 1.8: Detailed scheme of protolytic equilibrium of hydroxyxanthene dyes in solution.

From this scheme, the connection between the dissociation constants, K_a , and the so-called microscopic constants, k , can be derived.

For fluorescein:

$$pK_{a1} = pk_{1,COOH} + \log(1 + K_T) \quad (1.4)$$

$$pK_{a2} = pk_{2,OH} \quad (1.5)$$

For eosin:

$$pK_{a1} = pk_{1,OH} + \log(1 + K_T) \quad (1.6)$$

$$pK_{a2} = pk_{2,COOH} \quad (1.7)$$

These equations were used for the interpretation of the pK_{as} of dyes in different solvents [19, 20, 22, 26, 32]. An equation of the same type was used for the pK_{a0} value (see equation 1.1).

When the fluorescein dyes bear additional ionizing groups, e.g., COOH groups, the scheme of acid-base and tautomeric equilibria becomes much more complicated [35]. The same refers to the aminofluorescein dyes, which are often used in chemistry and related sciences. Two aminofluorescein dyes, namely, 4'- and 5'-aminofluorescein, were recently studied in water, aqueous ethanol [36], and in entire DMSO [37] (Figure 1.9).

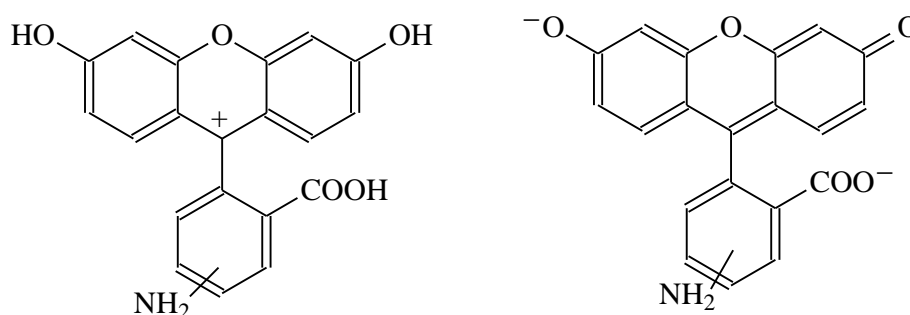


Figure 1.9: The structure of 4'- and 5'-aminofluoresceins in their cation and dianion forms.

Here, the amino groups can add a proton, and for each dye four dissociation constants in water and aqueous ethanol were reported [36]. Whereas for fluorescein and eosin in water, the pK_{a0} , pK_{a1} , and pK_{a2} values are 2.14; 4.45; 6.80, and -2.0 ; 2.81; 3.75, respectively [20], for 4'- and 5'-aminofluoresceins the $pK_{a(-1)}$, pK_{a0} , pK_{a1} , and pK_{a2} values were reported as 1.63; 2.46; 4.48; 6.84 and 1.27; 1.93; 5.67; 6.60 [36].

1.3 Hydroxyxanthene dyes that form anions-lactones: Amino- and nitrofluoresceins

The above-detailed scheme of protolytic equilibria (Figure 1.6) acquires distinctive features in the case of dyes prone to the formation of lactone anions. For example, the monoanion HR^- of 5'-aminofluorescein in DMSO (but not in water or aqueous ethanol) exists mainly as a lactone HL^- [37], while the double-charged anion R^{2-} of 2,4,5,7-

Chapter 1

tetranitrofluorescein in all solvent systems examined up now is present mainly as a lactone L^{2-} (Figure 1.10). Contrary to other species of the lactoid type, this dianion is yellow due to the typical absorption of the nitrophenolate portions. These results are in line with quantum-chemical calculations [38].

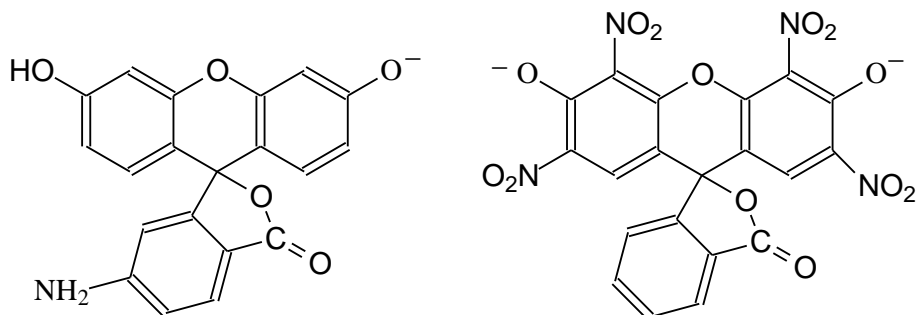


Figure 1.10: Examples of anions with lactonic structure: HL^- of 5'-aminofluorescein and L^{2-} of 2,4,5,7-tetranitrofluorescein.

It should be taken into account, that on going from solutions to the gas phase, some properties of the dyes can change cardinally. For example, fluorescein monoanion in the gas phase appears as the HX^- tautomer [39–41]. Therefore, the above-mentioned quantum-chemical calculations were performed in vacuo, water, and DMSO [38].

Analysis of the literature convincingly shows that, despite the presence of a series of publications, a general picture of the nitrofluoresceins equilibrium in solution is still absent. Compounds containing nitro groups in the xanthene part of the molecule are of particular interest. A set of such dyes was synthesized by Samoylov et al. [42]; shortly after, their acid-base and tautomeric equilibria were studied in 50 mass % aqueous ethanol [43, 44]. The behavior of 2,4,5,7-tetranitrofluorescein in different solvents [25, 45, 46] and surfactant micelles [32] was investigated in subsequent studies, which also utilized various techniques such as X-ray analyses, electrospray spectroscopy, and NMR [45, 46]. In addition, a new dye 4,5-dinitrosulfofluorescein was synthesized and its interaction with lysozyme was studied [47, 48]. A dye 4,5-dibromo-2,7-dinitrofluorescein was studied at the water/air interface [49]; recently, a theoretical study of the structure of this dye was published [50]. A synthesis of 2,4,5,7,4'-pentanitrofluorescein was reported by Negishi et al. [51].

Therefore, it is necessary to systematically investigate the nitrofluoresceins bearing the NO_2 group in the xanthene and phthalic portions of the fluorescein molecule. As a solvent, DMSO is worthwhile to use since it reveals molecular structures that are invisible in water and water-rich mixed solvents. For example, the HL^- tautomer of 5'-aminofluorescein [37] and HX^- tautomer of fluorescein [52] were observed just in DMSO.

The data concerning the dissociation constants of other fluorescein dyes available in the literature are given in Table 1.1.

Table 1.1: Indices of the thermodynamic dissociation constants of dyes in DMSO [37]

Compound	pK_{a1}	pK_{a2}
Fluorescein methyl ether	13.7 ± 0.1	—
Sulfonefluorescein	3.8 ± 0.1	12.3 ± 0.1
Fluorescein	13.1 ± 0.1	12.0 ± 0.1
5'-Aminofluorescein	11.0 ± 0.2	13.9 ± 0.3
Erythrosin	5.6 ± 0.1	10.6 ± 0.2

Data in DMSO-rich water–DMSO systems are also few [53, 54]. The choice of DMSO is also caused by the high acidity of nitrofluoresceins; the pK_a s are very low. Therefore, the quantitative study of the two-step dissociation was undertaken in entire dimethyl sulfoxide (DMSO).

The fluorescence of the nitro and amino derivatives is another interesting issue. Whereas the beautiful bright emission of fluorescein is observed in any solvent, for 4'- and 5'-aminofluoresceins it is possible only in aprotic solvents [55]. On the other hand, 2,4,5,7-tetranitrofluorescein exhibits bright fluorescence only in the form of a single-charged anion, which, however, exists in a narrow pH range [45]. The double-charged anion, contrary to the behavior of other fluoresceins, forms a non-fluorescent lactone.

Previously, an attempt was made to obtain a stable, pH-independent fluorescent 2,4,5,7-tetranitrosubstituted hydroxyxanthene by replacing the 2'-carboxylic group with the SO_3H group [48]. Although the xanthene part remained the same, the resulting dianion was unable to close into a lactone-like, i.e., sultone ring. Surprisingly, no fluorescence was observed, presumably due to the specific influence of the SO_3^- group. Therefore, a part of our work aimed to obtain a fluorescent 2,4,5,7-tetranitrofluorescein anion that would be stable within a wide pH range. This was done, and the fluorescence of the dye appeared to be dependent on the hydrogen bonding ability of the solvents.

Chapter 1

1.4 Conclusions

1. Though fluorescein dyes belong to the oldest and most used and investigated dyes, new representatives with interesting properties permanently appear. First of all, this refers to dyes with wonderful fluorescent properties.
2. The general dissociation and tautomerization scheme is well developed and works good for fluorescein and its numerous derivatives and analogous, first of all, the halogen derivatives. However, new compounds of this family exhibit new types of behavior in solution. This requires additional thorough study.
3. First of all, it deals with anions with a lactonic structure. This is already observed for amino and nitro derivatives. However, many features are still unexplored here.
4. Therefore, the present study is devoted to this problem. As the main solvent, the highly polar dimethyl sulfoxide (DMSO) is chosen. In this solvent, some quantitative results have already been published in the literature.
5. Also, the fluorescence properties of these dyes are an interesting issue. Many of them emit weakly. However, some of the compounds exhibit intensive fluorescence, depending on the solvent. Relevant research should also be the subject of this dissertation.

Bibliography

1. Lamberts, J.J.M., Neckers, D.C.: Rose Bengal and Non-polar Derivatives: The Birth of Dye Sensitizers for Photooxidation. *Zeitschrift für Naturforschung*. 39b, 474–484 (1984). <https://doi.org/10.1515/znb-1984-0412>
2. Slyusareva, E., Gerasimova, M., Plotnikov, A., Sizykh, A.: Spectral study of fluorone dyes adsorption on chitosan-based polyelectrolyte complexes. *J Colloid Interface Sci.* 417, 80–87 (2014). <https://doi.org/10.1016/J.JCIS.2013.11.016>
3. Zhou, P., Liu, J., Yang, S., Chen, J., Han, K., He, G.: The invalidity of the photo-induced electron transfer mechanism for fluorescein derivatives. *Physical Chemistry Chemical Physics*. 14, 15191–15198 (2012). <https://doi.org/10.1039/c2cp42167d>
4. Slyusareva, E., Gerasimova, M., Slabko, V., Abuzova, N., Plotnikov, A., Eychmüller, A.: Synthesis and Characterization of Chitosan-Based Polyelectrolyte Complexes Doped with Xanthene Dyes. *ChemPhysChem*. 16, 3997–4003 (2015). <https://doi.org/10.1002/CPHC.201500634>
5. Martins Estevão, B., Cucinotta, F., Hioka, N., Cossi, M., Argeri, M., Paul, G., Marchese, L., Gianotti, E.: Rose Bengal incorporated in mesostructured silica nanoparticles: structural characterization, theoretical modeling and singlet oxygen delivery. *Physical Chemistry Chemical Physics*. 17, 26804–26812 (2015). <https://doi.org/10.1039/C5CP03564C>
6. Nowak, P.M., Woźniakiewicz, M.: The Acid-Base/Deprotonation Equilibrium Can Be Studied with a MicroScale Thermophoresis (MST). *Molecules*. 27, (2022). <https://doi.org/10.3390/MOLECULES27030685>
7. Zdończyk, M., Potaniec, B., Skoreński, M., Cybińska, J.: Development of Efficient One-Pot Methods for the Synthesis of Luminescent Dyes and Sol-Gel Hybrid Materials. *Materials (Basel)*. 15, (2021). <https://doi.org/10.3390/MA15010203>
8. de Freitas, C.F., Vanzin, D., Braga, T.L., Pellosi, D.S., Batistela, V.R., Caetano, W., Hioka, N.: Multivariate analysis of protolytic and tautomeric equilibria of Erythrosine B and its ester derivatives in ionic and non-ionic micelles. *J Mol Liq.* 313, 113320 (2020). <https://doi.org/10.1016/J.MOLLIQ.2020.113320>
9. de Freitas, C.F., Estevão, B.M., Pellosi, D.S., Scarminio, I.S., Caetano, W., Hioka, N., Batistela, V.R.: Chemical equilibria of Eosin Y and its synthetic ester derivatives in non-ionic and ionic micellar environments. *J Mol Liq.* 327, 114794 (2021). <https://doi.org/10.1016/J.MOLLIQ.2020.114794>

Chapter 1

10. Urano, Y., Kamiya, M., Kanda, K., Ueno, T., Hirose, K., Nagano, T.: Evolution of fluorescein as a platform for finely tunable fluorescence probes. *J Am Chem Soc.* 127, 4888–4894 (2005).
<https://doi.org/10.1021/JA043919H/ASSET/IMAGES/MEDIUM/JA043919HN00001.GIF>
11. Han, J., Burgess, K.: Fluorescent indicators for intracellular pH. *Chem Rev.* 110, 2709–2728 (2010). https://doi.org/10.1021/CR900249Z/ASSET/CR900249Z.FP.PNG_V03
12. Li, X., Gao, X., Shi, W., Ma, H.: Design strategies for water-soluble small molecular chromogenic and fluorogenic probes. *Chem Rev.* 114, 590–659 (2014).
https://doi.org/10.1021/CR300508P/ASSET/IMAGES/CR300508P.SOCIAL.JPEG_V03
13. Schröder, C.R., Weidgans, B.M., Klimant, I.: pH fluorosensors for use in marine systems. *Analyst.* 130, 907–916 (2005). <https://doi.org/10.1039/B501306B>
14. Lavis, L.D.: Teaching Old Dyes New Tricks: Biological Probes Built from Fluoresceins and Rhodamines. *Annu Rev Biochem.* 86, 825–843 (2017).
<https://doi.org/10.1146/ANNUREV-BIOCHEM-061516-044839>
15. Gerasimova, M.A., Tomilin, F.N., Malyar, E.Y., Varganov, S.A., Fedorov, D.G., Ovchinnikov, S.G., Slyusareva, E.A.: Fluorescence and photoinduced proton transfer in the protolytic forms of fluorescein: Experimental and computational study. *Dyes and Pigments.* 173, 107851 (2020). <https://doi.org/10.1016/J.DYEPIG.2019.107851>
16. McLoughlin, C.K., Kotroni, E., Bregnhøj, M., Rotas, G., Vougioukalakis, G.C., Ogilby, P.R.: Oxygen- and pH-Dependent Photophysics of Fluorinated Fluorescein Derivatives: Non-Symmetrical vs. Symmetrical Fluorination. *Sensors (Basel).* 20, 1–19 (2020).
<https://doi.org/10.3390/S20185172>
17. Zhou, P., Tang, Z., Li, P., Liu, J.: Unraveling the Mechanism for Tuning the Fluorescence of Fluorescein Derivatives: The Role of the Conical Intersection and $n\pi^*$ State. *Journal of Physical Chemistry Letters.* 12, 6478–6485 (2021).
https://doi.org/10.1021/ACS.JPCLETT.1C01774/SUPPL_FILE/JZ1C01774_SI_001.PDF
18. Veenstra, A.P.: Zeit- und winkelaufgelöste Photoelektronenspektroskopie an massenselektierten Anionen in der Gasphase, (2022)
19. Mchedlov-Petrossyan, N.O., Kukhtik, V.I., Bezugliy, V.D.: Dissociation, tautomerism and electroreduction of xanthene and sulfonephthalein dyes in N,N-dimethylformamide and other solvents. *J Phys Org Chem.* 16, 380–397 (2003). <https://doi.org/10.1002/POC.654>
20. Mchedlov-Petrossyan, N.O.: Fluorescein dyes in solutions: well-studied systems? . *Kharkov Univ. Bull.* . 626, 221–312 (2004)
21. Niazi, A., Yazdanipour, A., Ghasemi, J., Kubista, M., Sheyda, A., Alikhah, M.: Spectrophotometric Determination of the Dissociation Constants of Fluorescein in Micellar Media. *Croat. Chem. Acta.* 82, 753–759 (2009)

22. Bogdanova, L.N., Mchedlov-Petrossyan, N.O., Vodolazkaya, N.A., Lebed, A. V.: The influence of β -cyclodextrin on acid–base and tautomeric equilibrium of fluorescein dyes in aqueous solution. *Carbohydr Res.* 345, 1882–1890 (2010). <https://doi.org/10.1016/J.CARRES.2010.07.002>
23. Batistela, V.R., da Costa Cedran, J., Moisés de Oliveira, H.P., Scarminio, I.S., Ueno, L.T., Eduardo da Hora Machado, A., Hioka, N.: Protolytic fluorescein species evaluated using chemometry and DFT studies. *Dyes and Pigments.* 86, 15–24 (2010). <https://doi.org/10.1016/J.DYEPIG.2009.11.002>
24. Amat-Guerri, F., López-González, M.M.C., Sastre, R., late R. Martinez-Utrilla, the: Spectrophotometric determination of ionization and isomerization constants of Rose Bengal, eosin Y and some derivatives. *Dyes and Pigments.* 13, 219–232 (1990). [https://doi.org/10.1016/0143-7208\(90\)80021-G](https://doi.org/10.1016/0143-7208(90)80021-G)
25. Batistela, V.R., Pellosi, D.S., de Souza, F.D., da Costa, W.F., de Oliveira Santin, S.M., de Souza, V.R., Caetano, W., de Oliveira, H.P.M., Scarminio, I.S., Hioka, N.: pKa determinations of xanthene derivates in aqueous solutions by multivariate analysis applied to UV–Vis spectrophotometric data. *Spectrochim Acta A Mol Biomol Spectrosc.* 79, 889–897 (2011). <https://doi.org/10.1016/J.SAA.2011.03.027>
26. Mchedlov-Petrossyan, N.O., Vodolazkaya, N.A., Gurina, Y.A., Sun, W.C., Gee, K.R.: Medium effects on the prototropic equilibria of fluorescein fluoro derivatives in true and organized solution. *Journal of Physical Chemistry B.* 114, 4551–4564 (2010). https://doi.org/10.1021/JP909854S/SUPPL_FILE/JP909854S_SI_001.PDF
27. Zhang, X.F., Liu, Q., Wang, H., Zhang, F., Zhao, F.: Prototropic equilibria, tautomerization and electronic absorption properties of dibenzofluorescein in aqueous solution related to its capability as a fluorescence probe. *Photochemical & Photobiological Sciences.* 7, 1079–1084 (2008). <https://doi.org/10.1039/B801883A>
28. Lavis, L.D., Raines, R.T.: Bright ideas for chemical biology. *ACS Chem Biol.* 3, 142–155 (2008). https://doi.org/10.1021/CB700248M/SUPPL_FILE/CB700248M-FILE007.PDF
29. Hirabayashi, K., Hanaoka, K., Takayanagi, T., Toki, Y., Egawa, T., Kamiya, M., Komatsu, T., Ueno, T., Terai, T., Yoshida, K., Uchiyama, M., Nagano, T., Urano, Y.: Analysis of Chemical Equilibrium of Silicon-Substituted Fluorescein and Its Application to Develop a Scaffold for Red Fluorescent Probes. *Anal Chem.* 87, 9061–9069 (2015). https://doi.org/10.1021/ACS.ANALCHEM.5B02331/SUPPL_FILE/AC5B02331_SI_001.PDF
30. Paredes, J.M., Crovetto, L., Rios, R., Orte, A., Alvarez-Pez, J.M., Talavera, E.M.: Tuned lifetime, at the ensemble and single molecule level, of a xanthenic fluorescent dye by means of a buffer-mediated excited-state proton exchange reaction. *Physical Chemistry Chemical Physics.* 11, 5400–5407 (2009). <https://doi.org/10.1039/B820742A>

Chapter 1

31. Paredes, J.M., Crovetto, L., Orte, A., Alvarez-Pez, J.M., Talavera, E.M.: Influence of the solvent on the ground- and excited-state buffer-mediated proton-transfer reactions of a xanthenic dye. *Physical Chemistry Chemical Physics*. 13, 1685–1694 (2011). <https://doi.org/10.1039/C0CP01232G>
32. Mchedlov-Petrossyan, N.O., Vodolazkaya, N.A.: Protolytic Equilibria in Organized Solutions: Ionization and Tautomerism of Fluorescein Dyes and Related Indicators in Cetyltrimethylammonium Chloride Micellar Solutions at High Ionic Strength of the Bulk Phase. *Liquids* 2021, Vol. 1, Pages 1-24. 1, 1–24 (2021). <https://doi.org/10.3390/LIQUIDS1010001>
33. Mchedlov-Petrossyan, N.O., Ivanov, V. V.: Effect of the solvent on the absorption spectra and protonation of fluorescein dye anions. *Russian Journal of Physical Chemistry* 2007 81:1. 81, 112–115 (2007). <https://doi.org/10.1134/S0036024407010219>
34. Mtschedlow-Petrossjan, N.O., Arias, K.E., Schapowalow, S.A., Rappoport, I.V., Egorowa, S.I.: Zur Frage der Struktur der einwertiger Fluoresceinfarbstoffanionen. *Zeitschrift für Chemie*. 30, 442–443 (1990)
35. Aschi, M., D'Archivio, A.A., Fontana, A., Formiglio, A.: Physicochemical properties of fluorescent probes: Experimental and computational determination of the overlapping pKa values of carboxyfluorescein. *Journal of Organic Chemistry*. 73, 3411–3417 (2008). https://doi.org/10.1021/JO800036Z/SUPPL_FILE/JO800036Z-FILE002.PDF
36. Mchedlov-Petrossyan, N.O., Cheipesh, T.A., Vodolazkaya, N.A.: Acid-base dissociation and tautomerism of two aminofluorescein dyes in solution. *J Mol Liq*. 225, 696–705 (2017). <https://doi.org/10.1016/J.MOLLIQ.2016.10.121>
37. Mchedlov-Petrossyan, N.O., Cheipesh, T.A., Shekhovtsov, S. V., Ushakova, E. V., Roshal, A.D., Omelchenko, I. V.: Aminofluoresceins Versus Fluorescein: Ascertained New Unusual Features of Tautomerism and Dissociation of Hydroxyxanthene Dyes in Solution. *Journal of Physical Chemistry A*. 123, 8845–8859 (2019). https://doi.org/10.1021/ACS.JPCA.9B05810/SUPPL_FILE/JP9B05810_SI_001.PDF
38. Lebed, A. V., Biryukov, A. V., Mchedlov-Petrossyan, N.O.: A quantum-chemical study of tautomeric equilibria of fluorescein dyes in DmsO. *Chem Heterocycl Compd (N Y)*. 50, 336–348 (2014). <https://doi.org/10.1007/S10593-014-1481-8/TABLES/5>
39. Yao, H., Jockusch, R.A.: Fluorescence and electronic action spectroscopy of mass-selected gas-phase fluorescein, 2',7'-dichlorofluorescein, and 2',7'- difluorofluorescein ions. *Journal of Physical Chemistry A*. 117, 1351–1359 (2013). https://doi.org/10.1021/JP309767F/SUPPL_FILE/JP309767F_SI_001.PDF
40. Tanabe, T., Saito, M., Noda, K., Starikov, E.B.: Molecular structure conversion of fluorescein monoanions in an electrostatic storage ring. *The European Physical Journal D* 2012 66:6. 66, 1–8 (2012). <https://doi.org/10.1140/EPJD/E2012-20763-7>

41. Horke, D.A., Chatterley, A.S., Bull, J.N., Verlet, J.R.R.: Time-resolved photodetachment anisotropy: Gas-phase rotational and vibrational dynamics of the fluorescein anion. *Journal of Physical Chemistry Letters*. 6,189–194 (2015).
https://doi.org/10.1021/JZ5022526/SUPPL_FILE/JZ5022526_SI_001.PDF
42. Samoilov, D. V, Martynova, V.P., El'tsov, A. V: Nitro derivatives of fluorescein. *Russ J Gen Chem*. 69, 1450–1460 (1999)
43. Mchedlov-Petrossyan, N.O., Vodolazkaya, N.A., Martynova, V.F., Samoylov, D., El'tsov, A.V.: Protolytic Equilibria in Nitro Derivatives of Fluorescein. *Russ J Gen Chem*. 70, 1259–1271 (2000)
44. Mchedlov-Petrossyan, N.O., Vodolazkaya, N.A., Martynova, V.F., Samoylov, D.V., El'tsov, A. V.: Protolytic Properties of Thiofluorescein and Its Derivatives. *Russ J Gen Chem*. 72, 785–792 (2002). <https://doi.org/10.1023/a:1019524722318>
45. Mchedlov-Petrossyan, N.O., Vodolazkaya, N.A., Surov, Y.N., Samoylov, D. V.: 2,4,5,7-Tetranitrofluorescein in solutions: novel type of tautomerism in hydroxyxanthene series as detected by various spectral methods. *Spectrochim Acta A Mol Biomol Spectrosc*. 61, 2747–2760 (2005). <https://doi.org/10.1016/J.SAA.2004.09.030>
46. Mchedlov-Petrossyan, N.O., Steinbach, K., Vodolazkaya, N.A., Samoylov, D. V., Shekhovtsov, S. V., Omelchenko, I. V., Shishkin, O. V.: The molecular structure of anionic species of 2,4,5,7-tetranitrofluorescein as studied by electrospray ionisation, nuclear magnetic resonance and X-ray techniques. *Coloration Technology*. 134, 390–399 (2018).
<https://doi.org/10.1111/COTE.12351>
47. Kriklya, N.N., Gromovoy, T.Y., Mchedlov-Petrossyan, N.O.: 4,5-Dinitrosulfonefluorescein and related dyes: Kinetics of reversible rupture of the pyran ring and their interaction with lysozyme. *Coloration Technology*. 137, 658–667 (2021).
<https://doi.org/10.1111/COTE.12565>
48. Shekhovtsov, S. V, Mchedlov-Petrossyan, N.O., Kamneva, N.N., Gromovoy, T.Y.: New orange dyes: Nitroderivatives of sulfonefluorescein. *Kharkov Univ. Bull*. 24, 7–18 (2014)
49. Tamburello-Luca, A.A., Hébert, P., Antoine, R., Brevet, P.F., Girault, H.H.: Optical Surface Second Harmonic Generation Study of the Two Acid/Base Equilibria of Eosin B at the Air/Water Interface. *Langmuir*. 13, 4428–4434 (1997). <https://doi.org/10.1021/LA9621271>
50. Fankam, J.B., Ejuh, G.W., Tchangnwa Nya, F., Ndjaka, J.M.B.: Theoretical investigation of the molecular structure, vibrational spectra, thermodynamic and nonlinear optical properties of 4, 5-dibromo-2, 7dinitro- fluorescein. *Opt Quantum Electron*. 52, 1–23 (2020). <https://doi.org/10.1007/S11082-020-02396-4/FIGURES/9>
51. Negishi, Y., Kawarada, A., Suzuki, T.: Synthesis of novel acid-base indicators by nitration of phenolphthalein and fluorescein. *J. College Educ., Yokohama Nat. Univ. The Natural Sciences*. 1, 20–31 (2018)

Chapter 1

52. Mchedlov-Petrosyan, N.O., Vodolazkaya, N.A., Salamanova, N. V, Roshal, A.D., Filatov, D.Yu.: In Search for the “Phenolate” Monoanion of Fluorescein in Solution. *Chem Lett.* 39, 30–31 (2009). <https://doi.org/10.1246/cl.2010.30>
53. Mchedlov-Petrosyan, N.O., Mayorga, R.S.: Extraordinary character of the solvent influence on protolytic equilibria: inversion of the fluorescein ionization constants in H₂O–DMSO mixtures. *Journal of the Chemical Society, Faraday Transactions.* 88, 3025–3032 (1992). <https://doi.org/10.1039/FT9928803025>
54. Vanzin, D., Freitas, C.F., Pellosi, D.S., Batistela, V.R., Machado, A.E.H., Pontes, R.M., Caetano, W., Hioka, N.: Experimental and computational studies of protolytic and tautomeric equilibria of Erythrosin B and Eosin Y in water/DMSO. *RSC Adv.* 6, 110312–110328 (2016). <https://doi.org/10.1039/C6RA12198E>
55. Mchedlov-Petrosyan, N.O., Cheipesh, T.A., Roshal, A.D., Doroshenko, A.O., Vodolazkaya, N.A.: Fluorescence of aminofluoresceins as an indicative process allowing one to distinguish between micelles of cationic surfactants and micelle-like aggregates. *Methods Appl Fluoresc.* 4, (2016). <https://doi.org/10.1088/2050-6120/4/3/034002>

Chapter 2

Equilibrium and Spectral Studies: Research Setting

The results of this Chapter are partly published in:

E. G. Moskaeva, K. I. Ostrovskiy, S.V. Shekhovtsov, N.O. Mchedlov-Petrosyan. Transmittance of electronic effects in the fluorescein molecule: Nitro and amino groups in the phthalic acid residue. *Kharkiv University Bull. Ser. Chem.* 36 (59), P. 24-32., (2021)

E.G. Moskaeva, A.V. Mosharenkova, S.V. Shekhovtsov, N.O. Mchedlov-Petrosyan. Protolytic equilibrium of tetra- and pentanitrofluoresceins in a binary solvent acetonitrile – dimethyl sulfoxide (mass ratio 96 : 4). *Ukrainian Chem J.* V. 87. No. 5., P. 25–37, (2021)

N. O. Mchedlov-Petrosyan, S. V. Shekhovtsov, E. G. Moskaeva, I. V. Omelchenko, A. D. Roshal, A. O. Doroshenko. New fluorescein dyes with unusual properties: Tetra- and pentanitrofluoresceins. *J. Mol. Liquids.* 367, 120541, (2022)

Chapter 2

2.1 Introduction

In this Chapter, we present the objects of the study, their main characterizations, and justify the choice of research methodology. First of all, the origin of the dye samples and the synthesis of new compounds are presented, as well as solvents and other materials. The equipment used in the study is also specified.

Then, the primary characterization of the dyes in a solid state and solution is presented. The X-ray analysis of two pentanitrofluoresceins discloses some features of their structure. On the other hand, the analysis of the ^{13}C NMR spectra proves the structure of the other two new tetranitrofluorescein compounds in the solution.

The next part of this Chapter presents the primary overview of the absorption spectra of the anionic forms of the dyes of interest in the visible region. In this case, the aim is to understand the concentration region of the further working solutions. Then, the procedure of the $\text{p}K_{\text{a}}$ determination in DMSO and acetonitrile with 4 mass % DMSO is described. One of the problems is the homoassociation of the components of the buffer systems.

2.2 Materials

2.2.1 Dyes

The samples of 4,5-dinitrofluorescein, 2,4,5,7-tetranitrofluorescein, and 4,5-dinitro-2,7-dibromofluorescein were kindly put to our disposal by Dr. Denis Samoylov, Saint-Petersburg State University of Technology and Design, Russia. Some properties of these dyes were already studied [1–5]. 4,5-Dinitrosulfofluorescein and 4,5-dinitrofluorescein methyl ether were synthesized by S. V. Shekhovtsov; the details, including identification of the compound, have been published [6–8]. The isomers 4'- and 5'-aminofluorescein (98% main compound) were purchased from Sigma-Aldrich and were used as received. 5'-Nitrofluorescein was synthesized according to the recently published procedure [9] and purified by the accepted method using diacetate [10, 11]. The methyl ester of 4,5-dinitrofluorescein was prepared and described previously [12].

The synthesis of 2,4,5,7,4'-pentanitrofluorescein was described by Negishi et al.[13]; here, another procedure was used. The syntheses given below were made by S. V. Shekhovtsov and included in the paper mentioned above.

2,4,5,7,4'-pentanitrofluorescein, 3',6'-dihydroxy-2',4',5,5',7'-pentanitro-3H-spiro[isobenzofuran-1,9'-xanthen]-3-one. To **2,4,5,7-tetranitrofluorescein** (5.12 g, 10 mmol) 50 mL of 95% sulphuric acid was added. The mixture was heated to 80 °C and stirred until a clear solution. After cooling to +10 °C, fuming nitric acid (2 mL, 48 mmol) was added dropwise. The reaction mixture was heated to 60 °C for 2 hours and then poured onto 150 g of cracked ice. The crude nitration product was filtered and washed with 25 mL of 10% HCl. The cake was removed, refluxed for several minutes with 50 ml of acetic acid, cooled, and filtered. The precipitate was dissolved by heating in a mixture of 30 mL acetic acid and 200 mL acetonitrile. The solution was filtered and evaporated until the beginning of crystallization (total volume 50–60 mL). After 2 hours, the precipitate was filtered off and dried at 110 °C and 60 mmHg for 2 hours. The yield was 3.05 g (55%) of a yellow powder. ¹H NMR (400 MHz, DMSO-*d*₆), δ/ppm: 8.84 (1H, d, *J* = 2.0 Hz, **3'**), 8.68 (1H, dd, *J* = 8.4 Hz, 2.0 Hz, **5'**), 7.80 (1H, d, *J* = 8.4 Hz, **6'**), 7.62 (2H, s, **1, 8**). X-Ray data are given below.

2,4,5,7,5'-pentanitrofluorescein, 3',6'-dihydroxy-2',4',5',6,7'-pentanitro-3H-spiro[isobenzofuran-1,9'-xanthen]-3-one. To **5'-nitrofluorescein** (1.00 g, 2.65 mmol) 15 mL of 95% sulphuric acid was added. The mixture was heated to 90 °C and stirred until a clear solution. After cooling to +5 °C, a nitrating mixture of fuming nitric acid (2 g, 31.7 mmol) with of 95% sulfuric acid (2 mL) was added dropwise. The reaction mixture was heated to 60 °C for 1 hour and then poured onto 150 g of cracked ice. The crude nitration product was filtered and washed with 20 ml of 10% HCl. The cake was removed, refluxed for several minutes with 30 ml of acetic acid and cooled. The crystals were filtered off, washed with 3 mL of acetic acid, and dried at 110 °C and 60 mmHg for 2 hours. The yield was 1.18 g (80%) of a yellow powder. For recrystallization, the product was dissolved in 20-30 mL acetonitrile, filtered, and evaporated to 10 mL. Then 20 mL of hot acetic acid was added, and the solution was evaporated until precipitation began. ¹H NMR (400 MHz, DMSO-*d*₆), δ/ppm: 8.57 (1H, d, *J* = 8.6 Hz, **3'**), 8.41 (1H, d, *J* = 8.6 Hz, **4'**), 8.39 (1H, s, **6'**), 7.63 (2H, s, **1, 8**).

Methyl ester of 2,4,5,7-tetranitrofluorescein, 3',6'-dihydroxy-2',4',5',7'-tetranitro-3H-spiro[isobenzofuran-1,9'-xanthen]-3-one. To a stirred mixture of **2,4,5,7-tetranitrofluorescein** (0.200 g, 0.39 mmol) with 10 mL of anhydrous methanol, thionyl chloride (1.0 ml, 13.76 mmol) was added under ice-cooling. The mixture was refluxed for 4 hours. After 60 minutes, 2,4,5,7-tetranitrofluorescein dissolved and a precipitate of **methyl ester of 2,4,5,7-tetranitrofluorescein** was observed. Then the solution was cooled and 3 mL

Chapter 2

of 90 % aqueous methanol was added. The crystals were filtered off and washed with 3 ml of methanol and dried at 110 °C and 60 mmHg for 2 hours. The yield was 0.10 g (49%) of orange crystals. ¹H NMR (400 MHz, DMSO-*d*₆), δ/ppm: 8.27 (1H, d, *J* = 7.7 Hz, **3'**), 7.92 (1H, t, *J* = 7.7 Hz, **5'**), 7.84 (1H, t, *J* = 7.7 Hz, **4'**), 7.54 (1H, d, *J* = 7.7 Hz, **6'**), 7.50 (2H, s, **1, 8**), 3.69 (3H, s, **COOCH**₃).

2,4,5,7-tetranitrofluorescein with opened pyran ring, 3,3-bis(2',4'-dihydroxy-3',5'-dinitrophenyl)-2-benzofuran-1(3H)-one. **2,4,5,7-tetranitrofluorescein** (0.51 g, 1 mmol) was dissolved in 10 mL aqueous solution of 0.60 g NaOH. The solution was heated to boiling, immediately cooled, and acidified with 5 % HCl. The precipitate was filtered off, washed with 30 mL 1% HCl and dried at 110 °C for 2 h. The substance was dissolved by heating in 10 mL toluene with a few drops of acetone and 0.05 g of activated charcoal was added. The hot solution was filtered, and the filtrate was left for a day at 6°C. The precipitate was recrystallized from 7 mL toluene with a few drops of acetone and dried at 110 °C and 60 mmHg for 1 hour. The yield was 0.35 g (56.6 %) of bright-yellow crystals. The substance contains toluene in a molar ratio of 1 : 0.25. ¹H-NMR (400 MHz, DMSO-*d*₆), δ/ppm: 8.06(1H, d, *J*=7.8 Hz, **3'**), 7.89(1H, d, *J*=7.8 Hz, **6'**), 7.83(2H, s, **1,8**), 7.80(1H, t, *J*=7.8 Hz, **5'**), 7.65(1H, t, *J*=7.8 Hz, **4'**).

The methyl esters of 3'-nitrofluorescein, 4'-nitrofluorescein, and 3'-aminofluorescein, ethyl esters of 4'-nitrofluorescein, 5'-nitrofluorescein, 4'-aminofluorescein, and 5'-aminofluorescein, and methyl ester of eosin described in publication [14] and Chapter 4, were synthesized and identified by S. V. Shekhovtsov; the procedures will be published elsewhere.

Methyl ester of eosin (methyl 2-(2,4,5,7-tetrabromo-6-hydroxy-3-oxo-3H-xanthen-9-yl)benzoate). To a stirred mixture of **2,4,5,7-tetrabromofluorescein** (0.324 g, 0.500 mmol) with 30 mL of anhydrous methanol, thionyl chloride (1.5 ml, 20.64 mmol) was added under ice-cooling. The mixture was refluxed for 30 minutes. After several minutes, **2,4,5,7-tetrabromofluorescein** dissolved and a precipitate of **methyl ester of 2,4,5,7-tetrabromofluorescein** was observed. Then the solution was cooled, the crystals were filtered off and washed with 7 ml of methanol. The yield was 0.315 g (95%) of red crystals. Eosin used in this synthesis was obtained by saponification of a sample of ethyl eosin (ca. 95 % purity), recrystallized in the form of a monoacetate, and its purity was checked by TLC.

The ¹H and ¹³C NMR spectra of the synthesized dyes are collected in Appendix A. They were recorded in Institute for Organic Chemistry, National Academy of Science of Ukraine, Kyiv.

2.2.2 Solvents

Dimethyl sulfoxide was purified by freezing and distilled under vacuum; water content 0.016 to 0.06 % as determined by the coulometric Karl Fischer method. Acetonitrile was stored for several days over P_4O_{10} and distilled over dehydrated K_2CO_3 . Water content was 0.007 to 0.015 %. Benzene was purified from water by P_4O_{10} and distilled; water content was below 0.01 %. Methyl *iso*-butyl ketone (Merck, for synthesis or for extraction analysis) was twice-distilled, and the fraction at 114.2 to 114.8 °C (99.7 kPa) was used. Dimethyl formamide was used as freshly purified with Al_2O_3 and distilled under a vacuum. 1-Octanol, *n*-octane, and cyclohexane were purified via distillation. Dichloromethane and acetone were commercial samples. 1-Butanol and methanol were dehydrated and distilled. Aqueous 96 % ethanol of high purity was purified by distillation.

2.2.3 Other chemicals

Benzoic and salicylic acids were purified by sublimation. Potassium benzoate and sodium hydrosalicylate were purified by re-crystallization. Picric acid was twice re-crystallized from ethanol and dried as described previously [15]. *p*-Toluenesulfonic acid (TSA) monohydrate was re-crystallized from acetonitrile. Triflic acid, CF_3SO_3H , was kindly donated by Professor Yu. L. Yagupolski. Sulfuric acid 98% aqueous sulfuric acid was of analytical grade. Diazabicyclo [5.4.0] undec-7-ene (DBU) (Merck) was used as obtained; the content of the main component was equal to 95 mass %, as determined by titration of its aqueous solutions with HCl. 2,4-dinitrophenol was re-crystallized from the benzene–cyclohexane mixture (1 : 1 by volume). The synthesis and purification of tetramethylammonium 2,4-dinitrophenolate was described previously [15]. The purity of 2,6-dinitrophenol, analytical grade, melting point 64 °C. Sodium 2,6-dinitrophenolate was prepared through the following procedure. 4.00 g of 2,6-dinitrophenol was solved under heating in 50 % aqueous ethanol, which contained 2.00 g sodium hydroxide. The hot solution was filtrated through a syringe membrane filter and cooled to +6 °C. On the next day, the deposit of the sodium salt of the 2,6-dinitrophenol was filtered, washed with 10 mL of 50 % aqueous ethanol and dried. The mass of the dried salt was 4.28 g. After re-crystallization from 50 mL of 50 % aqueous ethanol the mass of the dry salt was 3.74 g (yield 83.5%). In several experiments in aqueous solutions, standard buffers (potassium hydrophthalate, potassium dihydrophosphate + sodium hydrophosphate, borax), sodium hydroxide and diluted HCl were used to maintain the appropriate pH values.

Chapter 2

2.3 Apparatus

Absorption spectra of the dyes were run on a Hitachi U-2000 and an Agilent Cary 3500 UV-Vis spectrophotometers, against the solvent blanks at 25 °C.

Steady-state fluorescence spectra were obtained with either Hitachi F4010 or Hitachi 830 spectrofluorimeter and treated using Spectra Data Lab Software [16]. The fluorescence quantum yields were measured at 25 °C with reference to fluorescent standards, fluorescein solution at pH = 12 (NaOH) or fluorescein in aqueous carbonate buffer at pH = 9.93, excitation 490 nm, quantum yield 92.5, and an allowance for the difference in the refractive indices of solvents [17]. Fluorescence lifetimes and time-resolved spectra were measured on a subnanosecond kinetic spectrometer, consisting of an MDR-12 monochromator (LOMO, Russia), a TimeHarp 200 TCSPC device, a PLS 340–10 ps LED driven by a PDL 800-B device (PicoQuant GmbH, Germany), and a Hamamatsu H5783P PMT (Hamamatsu, Japan). Time-resolved spectra (TRS) were obtained in the case of species participating in excited state transformations when bi-exponential fluorescence decays were observed. The procedures of TRS measurements, as well as the determination of excited-state kinetic characteristics, were carried out as described in the literature [18–20].

The ^1H and ^{13}C NMR spectra were recorded on Varian VNMRs-400 Spectrometer (^1H : 400 MHz; ^{13}C : 100 MHz). NMR chemical shifts (δ) are reported in ppm downfield from tetramethylsilane as internal reference.

X-ray diffraction studies of isomeric pentanitrofluorescein were performed at room temperature on an «Xcalibur-3» diffractometer (MoK α radiation, CCD-detector, graphite monochromator, ω -scanning, $2\theta_{\text{max}} = 52^\circ$). Both structures were solved by direct methods and refined against F^2 within anisotropic approximation for all non-hydrogen atoms by full-matrix least-squares procedure using OLEX2 program package [21] with SHELXT and SHELXL modules [22]. All H atoms were placed in idealized positions (C–H = 0.93 – 0.96 Å, O–H = 0.82 Å) and constrained to ride on their parent atoms, with $U_{\text{iso}} = 1.2U_{\text{eq}}$ (1.5 U_{eq} for OH groups). Atom coordinates and crystallographic parameters have been deposited to the Cambridge Crystallographic Data Centre; The data can be obtained free of charge from the Cambridge Crystallographic Data Centre via www.ccdc.cam.ac.uk/data_request/cif/.

2.4 Primary characterization of the dyes in solid state and solution

In this section, we present the structural studies of four new dyes in solid and dissolved states. First, 2,4,5,7,4'-pentanitrofluorescein and 2,4,5,7,5'-pentanitrofluorescein were studied

by the X-ray method. Second, two derivatives of 2,4,5,7-tetranitrofluorescein were studied in DMSO via the ^{13}C NMR spectroscopy, namely, the methyl ester and a compound with opened pyran ring.

On the other hand, we examined the absorption spectra of the dyes in the visible region in DMSO solutions, to evaluate the absorption maxima and molar extinction coefficient. Finally, the procedure of the study of the acid-base equilibria is formulated, taking into account the specific features of DMSO as a solvent.

2.4.1 Lactones of 2,4,5,7,4'-pentanitrofluorescein and 2,4,5,7,5'-pentanitrofluorescein: Structural description via X-ray analysis

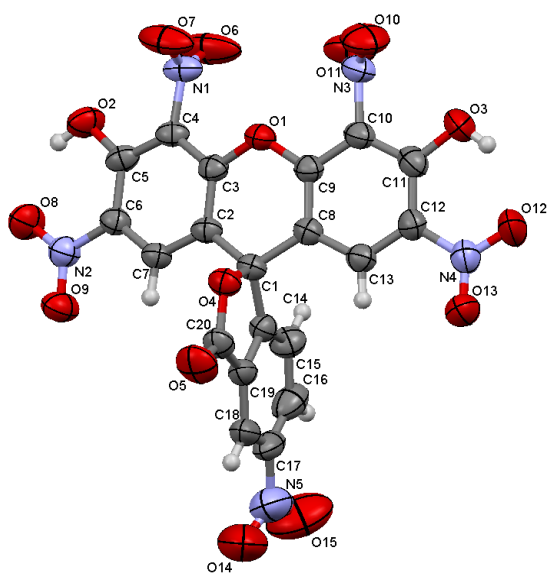
Details of the data collection and processing, structure solving and refinement, and CCDC numbers are summarized in Table 2.1.

Table 2.1: Crystallographic data and refinement parameters of 2,4,5,7,4'-pentanitrofluorescein (1) and 2,4,5,7,5'-pentanitrofluorescein (2).

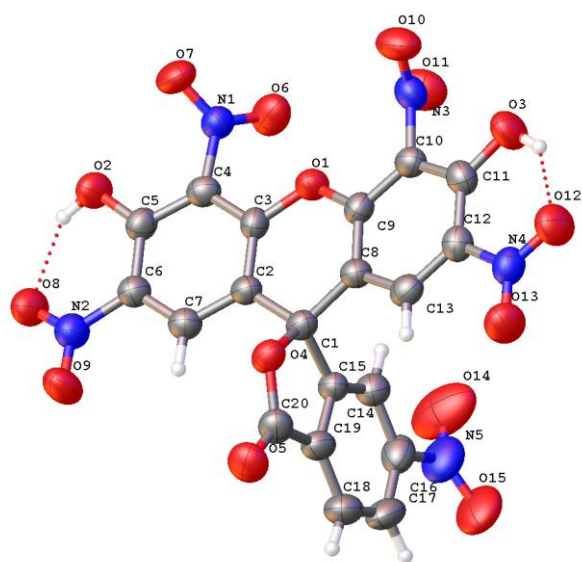
	1	2
Formula	$\text{C}_{20}\text{H}_7\text{N}_5\text{O}_{15}$	$\text{C}_{20}\text{H}_7\text{N}_5\text{O}_{15}$
M	557.31	557.31
Crystal system	monoclinic	monoclinic
Space group	$\text{P}2_1/\text{n}$	$\text{P}2_1/\text{c}$
a (Å)	13.4699(5)	18.6869(15)
b (Å)	12.1802(4)	6.3609(4)
c (Å)	13.6641(8)	19.3340(15)
$\alpha, ^\circ$	90	90
$\beta, ^\circ$	110.742(5)	115.770(9)
$\gamma, ^\circ$	90	90
V (Å ³)	2096.51(17)	2069.6(3)
Z	4	4
D _{calcd.} (g cm ⁻³)	1.766	1.789
T (K)	298	298
μ (mm ⁻¹)	0.156	0.158
F(000)	1128	1128
Reflections collected/unique	15783 / 5475	10034 / 5318
R _{int}	0.067	0.077
Reflections with I > 2 σ (I)	2396	2219
R1 [I > 2 σ (I)]	0.0721	0.0750
wR ² (all data)	0.2439	0.2341
GOF on F ²	0.969	0.965
CCDC	1848208	2124651

Chapter 2

Molecular structures of both isomeric pentanitrofluoresceins possess a lot of similar features. Xanthene moieties reveal a “butterfly” type distortion from planarity: fold angles between two benzene rings in xanthenes are $14.1(1)^\circ$ and $11.8(2)^\circ$, respectively (while twist angles between these rings are less than 2° in both, so twist deformation isn't observed). However, the deformation direction is different: in 2,4,5,7,4'-pentanitrofluorescein, the outer side of xanthene “butterfly” is directed to the O atom of isobenzofurane, while in 2,4,5,7,5'-pentanitrofluorescein, the inner side is (see Figure 2.1). Xanthene and isobenzofurane moieties are almost perpendicular as it is commonly observed for fluoresceins – twist angles between mean planes are close to 90° in both structures ($89.0(1)$ and $88.4(1)^\circ$, respectively). At the time, fold angles are slightly different ($16.0(1)^\circ$ in 2,4,5,7,4'-pentanitrofluorescein and $8.0(2)^\circ$ in 2,4,5,7,5'-pentanitrofluorescein).



2,4,5,7,4'-pentanitrofluorescein



2,4,5,7,5'-pentanitrofluorescein

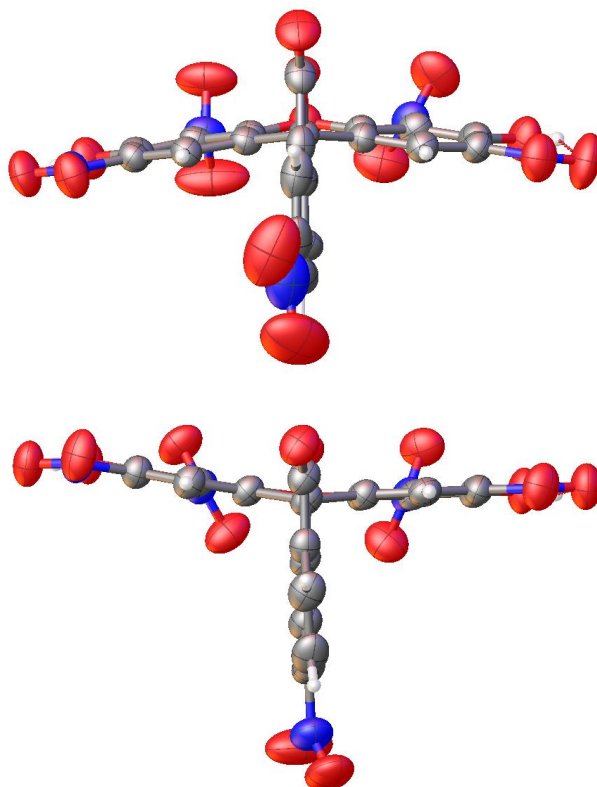


Figure 2.1: “Butterfly” distortion of xanthene moieties.

Those minor structural distortions do not affect conjugation in the pyran ring of xanthene: for both molecules, C-O_{pyran} distances lie in the range 1.358(4) – 1.370(4) Å, which is close to the mean value 1.377 Å [23]. Both rings reveal no pronounced alternation (as it was described for dinitro fluorescein methyl ether) [7]. Nitro groups at xanthene atoms C(4) and C(10) are rotated with respect to the ring plane (interplanar angles are 96.1(2)° and 63.1(2)° in 2,4,5,7,4'-pentanitrofluorescein and 52.1(3)° and 67.0(2)° in 2,4,5,7,5'-pentanitrofluorescein, respectively). Nitro groups at C(6) and C(12) atoms lie in the benzene ring plane due to intramolecular hydrogen bonding with hydroxyl groups (H...O 1.89 – 1.93 Å). Therefore C(4)-N(1) and C(10)-N(3) bonds (1.462(4) – 1.481(4) Å) are consistently longer than C(6)-N(2) and C(12)-N(4) bonds (1.440(3) to 1.452(4) Å). At the time, repulsion between O atoms of in-plane nitro groups and O atoms of hydroxyl groups cannot be fully compensated by H-bonding; it results in notable elongation of the C-C aromatic bond in O-C-C-N fragment (C(5)-C(6) and C(11)-C(12), distances lie in the range of 1.394(4) – 1.405(4) Å, while the typical value is 1.386 Å [7].

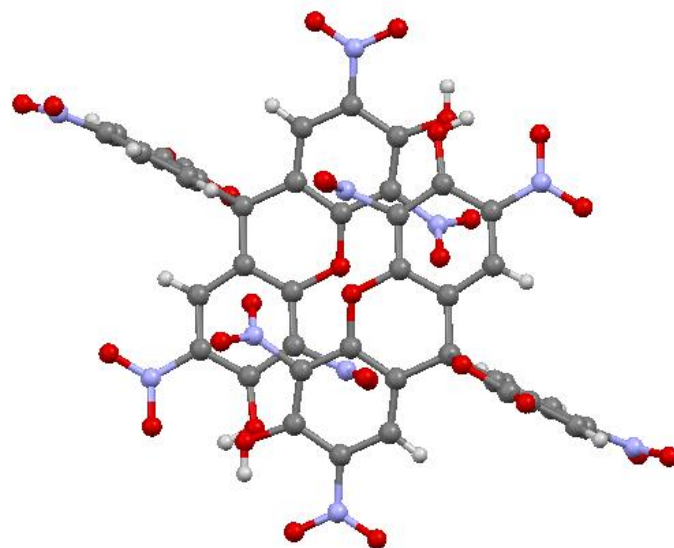


Figure 2.2: An example of “head-to-tail” stacking in 2,4,5,7,4'-pentanitrofluorescein.

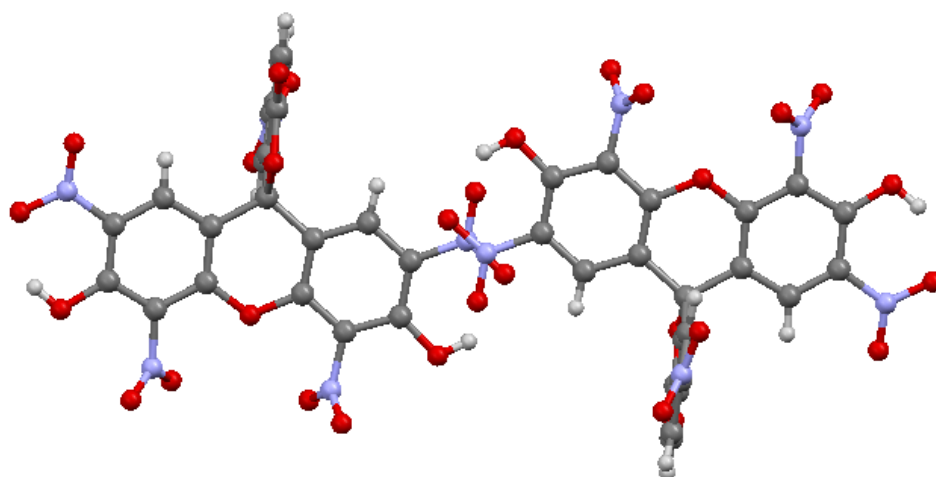


Figure 2.3: An example of “head-to-tail” stacking in 2,4,5,7,5'-pentanitrofluorescein.

In the crystals, both molecules form 3D structures based on stacking interactions that involve nitro groups. There are couple of different types of such stacking dimers, all sharing one structural feature – the “head-to-tail” orientation of molecules (Figures 2.2, 2.3), that indicates the dominant contribution of dipole-dipole interactions.

2.4.2 ^{13}C NMR study in DMSO solutions

Signals assignment in the ^{13}C NMR spectra was made analogously to the approach used in several papers [24, 25] – by comparison of the experimental spectrum with the theoretically calculated one. Theoretical calculations were conducted in the DFT scheme with *b3lyp* functional [26] in *cc-pvdz* orbital basis [27] in GIAO model [28] with the account of universal interactions with solvent only in PCM model [29] using Gaussian-09 program package [30]. Both data correlate well one with another among all the Carbon-13 chemical shifts scale covering carbonyl, aromatics and aliphatic regions. Examples of analogous successful ^{13}C NMR correlations can be found on the special website [31].

For 2,4,5,7-Tetranitrofluorescein with the cleaved pyran ring, the ^{13}C NMR spectrum in DMSO gives evidence for the lactonic structure. In Figure 2.4 and in Table 2.2, the numbering of carbon atoms is given for a triphenylmethane dye or phenolphthalein derivative.

The signal of the central carbon atom, 87.98 ppm, can be compared with those of H_2L and L^{2-} of 2,4,5,7-tetranitrofluorescein, 78.4 and 83.4 ppm, respectively [4]. The signal of the carbon atom of the C=O group of the lactone, 168.93 ppm, coincides with those of the neutral and dianionic lactones of the parent compound, 167–168 ppm [4].

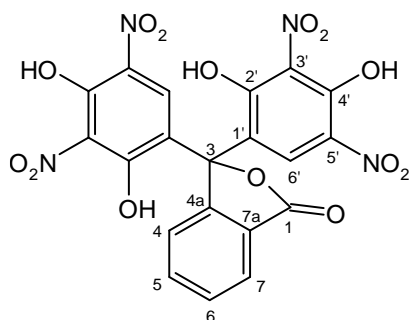


Figure 2.4: 2,4,5,7-Tetranitrofluorescein with the cleaved pyran ring in lactonic form.

Chapter 2

Table 2.2: ^{13}C NMR signals positions of the 2,4,5,7-tetranitrofluorescein with cleavage of pyran ring, 3,3-bis(2',4'-dihydroxy-3',5'-dinitrophenyl)-2-benzofuran-1(3H)-one, in DMSO- d_6 . For atoms numbering see Figure 2.4.

Atoms	^{13}C signal, ppm	Atoms	^{13}C signal, ppm	Atoms	^{13}C signal, ppm
1	168.93	7	124.92	3'	124.78
3	87.98	4a	149.35	4'	151.06
4	124.60	7a	123.38	5'	125.38
5	134.63	1'	121.67	6'	132.72
6	129.91	2'	161.21		

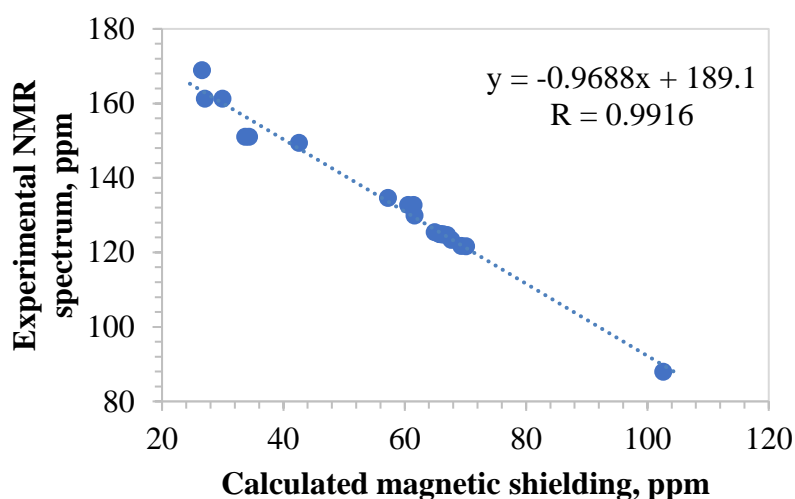


Figure 2.5: Correlation between the experimental and theoretical (*b3lyp/cc-pvdz/PCM*) ^{13}C NMR spectra of the 2,4,5,7-tetranitrofluorescein with the cleaved pyran ring, shown in Figure 2.4, in DMSO- d_6 .

The case of 2,4,5,7-tetranitrofluorescein methyl ester was special, because it exists in the DMSO- d_6 solution in the anionic form (Figure 2.6), for which one can expect less accurate theoretic predictions, than for neutral species.

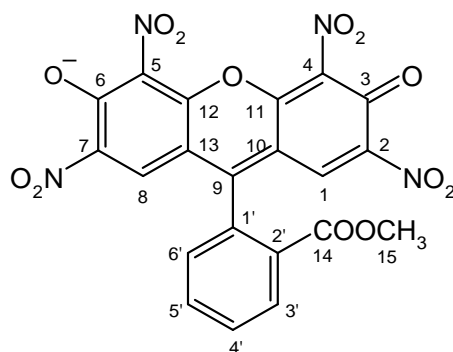


Figure 2.6: Anion of the methyl ester of 2,4,5,7-tetranitrofluorescein.

The calculated anionic form of this compound is characterized by planar xanthene moiety with practically orthogonal to its ester-substituted benzene ring. No steric repulsion between bulky ester group and xanthene tricycle is seemingly observed: distance between xanthene C₉ and carbonyl oxygen atoms in the most favorable conformation (≈ 0.27 nm) is comparable with the sum of their van der Waals radii. None of the four nitro groups is coplanar with xanthene moiety owing to steric effects of ionized hydroxy groups in its positions 3 and 6 (calculated torsional angles were $\sim 28^\circ$ and $\sim 61^\circ$ for nitro groups in positions 2,7 and 4,5 correspondently). The obtained correlation between the experimental NMR signals positions and calculated magnetic shielding of ^{13}C nucleus is presented in the numerical form in Table 2.3 and shown in Figure 2.7.

Table 2.3: ^{13}C NMR signals positions of the 2,4,5,7-tetranitrofluorescein methyl ester anion in DMSO- d_6 .

Atoms	^{13}C signal, ppm	Atoms	^{13}C signal, ppm	Atoms	^{13}C signal, ppm
1,8	129.18	10,13	105.64	4'	127.40
2,7	142.82	11,12	147.58	5'	131.78
3,6	161.63	1'	132.38	6'	127.40
4,5	133.39	2'	130.35	14	162.53
9	164.85	3'	131.03	15	52.60

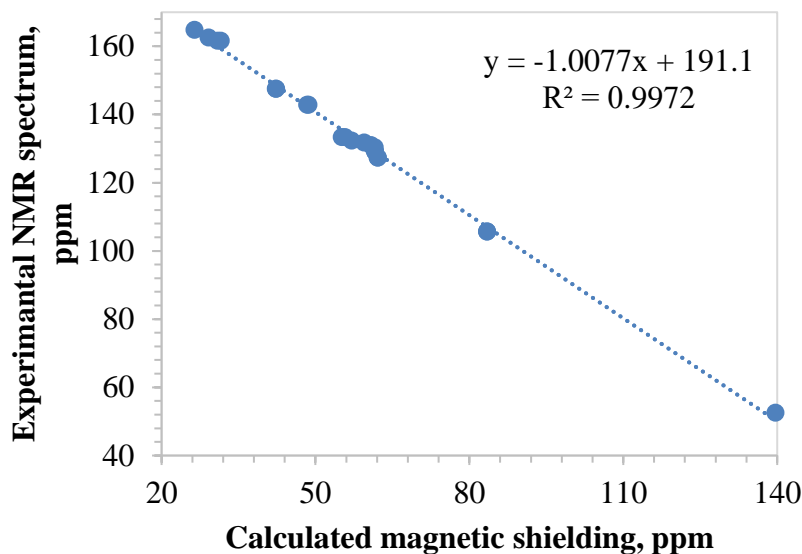


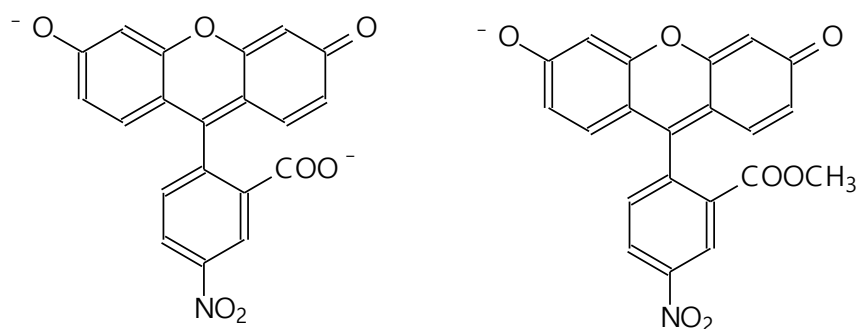
Figure 2.7: Correlation between the experimental and theoretical (*b3lyp/cc-pvdz/PCM*) ^{13}C NMR spectra of the anionic form of the 2,4,5,7-tetranitrofluorescein methyl ester in DMSO- d_6 .

The good linearity of the data can serve as an additional argument in favor of the anionic form of the 2,4,5,7-tetranitrofluorescein methyl ester in its concentrated solution in DMSO. Based on our correlation one can explain the reduced number of signals observed in the experimental ^{13}C NMR spectrum (14 instead of 15): the signals of two atoms in the side benzene ring (4' and 6') coincide owing to the current electron density redistribution in the anion form. The corresponding experimental signal was slightly broadened in comparison with the other ones.

2.4.3 Absorption spectra in solution

The spectral data of the dyes under study in their anionic forms are presented in Table 2.4. The molar extinction coefficient determined by us is high enough for studying the acid-base equilibria in the concentration range of about 10^{-5} M.

The absorption maxima of the esters of the dyes are 8–12 nm higher than those of the corresponding mother compounds; Figure 2.8.



λ_{\max} in DMSO: 526 nm 534 nm

Figure 2.8: 4'-Nitrofluorescein, R^{2-} , and 4'-nitrofluorescein methyl ester, R^- .

Table 2.4: Absorption maxima and molar extinction coefficient of the dye anions in the visible region; 25 °C.

No	Dye	In water ^a			In DMSO ^b	
		λ_{\max} , nm	λ_{\max} , nm	λ_{\max} , nm	$\epsilon_{\max} \times 10^{-3}$, M ⁻¹ cm ⁻¹	
1	4'-Nitrofluorescein, R^{2-} [7] ^c	493	526		97.83	
2	4'-Nitrofluorescein methyl ester, R^-	500	534		70.4	
3	4'-Nitrofluorescein ethyl ester, R^-	502	534		73.4	
4	5'-Nitrofluorescein, R^{2-}	494	528		95.8	
5	5'-Nitrofluorescein ethyl ester, R^-	501	535		87.8	
6	4'-Aminofluorescein, R^{2-} [7] ^c	488	518		131.0	
7	4'-Aminofluorescein ethyl ester, R^-	492	527		116.3	
8	5'-Aminofluorescein R^{2-} , [7] ^c	488	517		115.0	
9	4,5-Dinitrofluorescein, R^{2-}	481	510		82.2	
10	4,5-Dinitrofluorescein, methyl ester, R^-	489	521.5		87.1	
11	4,5-Dinitrosulfofluorescein, R^{2-}	492	520		85.75	
12	2,4,5,7-Tetranitrofluorescein, R^{2-} [3] ^c	400	441		19.0	
13	2,4,5,7-Tetranitrofluorescein, methyl ester, R^-	506	527		110.0	
14	2,4,5,7,4'-Pentanitrofluorescein, R^{2-}	402	429		17.7	
15	2,4,5,7,5'- Pentanitrofluorescein, R^{2-}	401	419		31.7	

Note. ^a In aqueous borate buffer solution, pH = 9.2. ^b With 0.02 M DBU. ^c References indicate the literature data for DMSO.

Chapter 2

This is typical for the xanthenes anions and was explained based on quantum-chemical calculations [32].

The λ_{\max} of anions of dyes bearing the nitro group in the phthalic acid residue are 7 to 10 nm higher as compared with those with the NH_2 group, while their ε_{\max} values are 1.2–1.6-fold lower, than for amino derivatives.

The bathochromic shifts of the anionic spectra on going from water to DMSO are within the range of 29–34 nm; for the 2,4,5,7-Tetranitrofluorescein, methyl ester it is with 21 nm somewhat lower.

A special case is the pentanitrofluoresceins. The absorption bands of the R^{2-} anions are close to the UV region, and the molar extinction coefficient is low (Table 2.4). The same is the picture in the case of the 2,4,5,7-tetranitrofluorescein, studied previously [3]; as it was indicated in Chapter 1, this is because of the lactonic structure of the R^{2-} anions. Despite the sp^3 -hybridization of the nodal carbon atom and contrary to the lactones of the neutral molecules, H_2R , these anions-lactones are not colorless, but yellow because of nitrophenolate absorption of the aromatic moieties.

The fluorescence of the considered dyes, if present, is weak. Only amino derivatives and the methyl ester of 2,4,5,7-tetranitrofluorescein emit substantially, but only in aprotic solvents. In the case of pentanitrofluoresceins, fluorescence was observed only in a narrow $\text{p}a_{\text{H}^+}^*$ range. The same behavior was described earlier for 2,4,5,7-tetranitrofluorescein and ascribed to the emission of the single-charged anion, HR^- [3]. Nonetheless, we decided to examine the above-mentioned cases of fluorescence in different solvents (see Chapter 5). First of all, the methyl ester of 2,4,5,7-tetranitrofluorescein is of interest because of the independence of its fluorescence on the $\text{p}a_{\text{H}^+}^*$ values.

The neutral molecular forms of the dyes of interest with free carboxylic group exist in DMSO almost in the colorless lactonic form. In the case of methyl and ethyl esters of the dyes, the decolorization was not observed within a wide acidity range.

The choice of a particular method of the spectrophotometric data processing depended on the character of the variations of the absorption spectra in solutions at different acidities. Preliminary experiments have shown that the quantitative study of the protolytic equilibria should be performed within $\text{p}a_{\text{H}^+}^*$ range from diluted strong enough acids to benzoate buffer solutions. {The designation $\text{p}a_{\text{H}^+}^*$ used hereafter means, according to Bates [33], that the standard state of the proton refers to the given non-aqueous solution.}

2.5 Approach to the pK_a determination

2.5.1 The acidity scale in DMSO

For this purpose, the $pa_{H^+}^*$ scale should be constructed [33]. The standard state is 1 M of lyonium ion with the properties of an infinitely diluted solution. The $pa_{H^+}^*$ values were obtained using either solution of strong enough acids or buffer mixtures of weak acids; pK_{HA} denotes the indices of the dissociation constants of the latter. The ionic activity coefficients were calculated according to the Debye–Hückel equation, second approach:

$$\log f_z = -\frac{1.12 z^2 \sqrt{I}}{1 + 2.13 \sqrt{I}} \quad (2.1)$$

Here I is the ionic strength, z is the charge of the ion. The activity coefficients of neutral species were equated to unity. Triflic acid was considered as completely dissociated in DMSO [34]. The same applies to the TSA [35] and to picric acid; according to Kolthoff et al., for the picric acid $pK_{HA} \approx -1$ [36]. The equilibrium concentration of the lyonium ion, $[H^+]$, was equated to the working concentrations of these acids. Hence, the $pa_{H^+}^*$ values were calculated as:

$$pa_{H^+}^* = -\log a_{H^+}^* = -\log[H^+] - \log f_1 \quad (2.2)$$

Here f_1 stands for the activity coefficient of the solvated proton. If necessary, the account of the protons originating from the dye dissociation was made.

In buffer solutions of sodium salicylate and potassium benzoate, the complete dissociation of all the salts is presumed. Here, $[H^+] \ll [K^+]$ and $[H^+] \ll [Na^+]$. The I value was equated to the salt concentration, which was usually 0.005 M. The pK_{HA} values of 6.8 and 11.1 for salicylic and benzoic acids, respectively, were reported by Kolthoff et al. [36]. Also, the

Chapter 2

homoassociation process was taken into account; the values of the so-called formation constants, $K_{\text{HA}_2}^f$, for these acids are 30 and 60 M^{-1} , respectively [37]. The equation proposed by Kolthoff et al. [38] was used in this case:

$$(a_{\text{H}^+}^*)^2 f_1^2 c_s - a_{\text{H}^+}^* f_1 K_a [c_a + c_s + K_{\text{HA}_2}^f (c_a - c_s)^2] + K_a^2 c_a = 0 \quad (2.3)$$

Here c_a and c_s are the molar concentrations of the acid and salt, respectively. Normally, the c_s value was fixed, while that of c_a was variable. As result, at $c_a > c_s$ thus estimated $\text{p}a_{\text{H}^+}^*$ values were lower than those calculated without taking into account the homoassociation process. The results were opposite at $c_a < c_s$. The homoassociation process is discussed in detail in Chapter 4.

2.5.2 The acidity scale in acetonitrile-DMSO 96:4 mass

A series of experiments was performed in acetonitrile, which contains 4 mass % DMSO. In a polar weakly basic solvent acetonitrile, even traces of water can distort the results obtained with this solvent. In order to avoid this interfering factor, a new binary solvent was proposed recently, namely, acetonitrile with 4 mass % DMSO [15]. The relative permittivity of the binary solvent is 36.95 at 25 °C.

In this solvent, the acidity scale ($\text{p}a_{\text{H}^+}^*$) was established, and a set of buffer solutions was proposed. It was shown that the proton is associated with the molecules of the protophilic dimethyl sulfoxide, while other ionic and molecular species are solvated mainly by acetonitrile. Hence, this binary solvent can be regarded, as a first approximation, as acetonitrile with lyonium ion $\text{H}(\text{DMSO})_2^+$ [15]. The acidity scale in this solvent was established recently [15]. In this case, the second approach of the Debye–Hückel equation is as follows:

$$\log f_z = -\frac{1.64z^2\sqrt{I}}{1+2.40\sqrt{I}} \quad (2.4)$$

The pK_{HA} values of salicylic and benzoic acids are 9.61 and 13.98, respectively. The $K_{\text{HA}_2}^f$ values for salicylic and benzoic acids are 2.5×10^2 and $2.2 \times 10^3 \text{ M}^{-1}$, respectively. Besides the homoassociation, the incomplete salt dissociation should be taken into account; the dissociation constants of sodium hydrosalicylate and tetraethylammonium benzoate are 5.0×10^{-3} and $3.5 \times 10^{-4} \text{ M}$, respectively [15]. For picric acid, 2,4-dinitrophenol, and 2,6-dinitrophenol, $pK_{\text{HA}} = 3.30, 8.68,$ and 8.73 , respectively. The dissociation constants of sodium salts of 2,4- and 2,6-dinitrophenol 1.4×10^{-3} and $3.5 \times 10^{-4} \text{ M}$ [15].

2.5.3 The principles of pK_a determination

The pK_a values of the dyes were obtained by processing the absorption spectra at different $pa_{\text{H}^+}^*$ values. The dye concentrations were two orders of magnitude lower than those of buffer components, if not otherwise specified. For the determination of the spectra of the limiting basic forms, the DBU solutions were used. High acidities were created by triflic, sulfuric, and *p*-toluenesulfonic acids. The working solutions were prepared in volumetric flasks by adding the aliquots of dye and buffer components, either as aliquots of their stock solutions or as weighted amounts. All salts were considered as completely dissociated. The possibility of heteroassociation between the dyes and buffer compounds was ignored.

The pK_a values of the dyes were obtained by processing the absorption spectra at different $pa_{\text{H}^+}^*$ values. The dye concentrations were two orders of magnitude lower than those of buffer components, if not otherwise specified. For the determination of the spectra of the limiting basic forms, the DBU solutions were used. High acidities were created by triflic,

Chapter 2

sulfuric, and *p*-toluenesulfonic acids. The working solutions were prepared in volumetric flasks by adding the aliquots of dye and buffer components, either as aliquots of their stock solutions or as weighted amounts. All salts were considered as completely dissociated. The possibility of heteroassociation between the dyes and buffer compounds was ignored at this stage of research.

Bibliography

1. Samoylov, D.V, Mchedlov-Petrosyan, N.O., Martynova, V.F., El'tsov, A. V: Protolytic equilibria of fluorescein nitro derivatives. *Russ J Gen Chem.* 70, 1259–1271 (2000)
2. Mchedlov-Petrosyan, N.O., Vodolazkaya, N.A., Martynova, V.F., Samoylov, D.V., El'tsov, A. V: Protolytic Properties of Thiofluorescein and Its Derivatives. *Russ J Gen Chem.* 72, 785–792 (2002). <https://doi.org/10.1023/a:1019524722318>
3. Mchedlov-Petrosyan, N.O., Vodolazkaya, N.A., Surov, Y.N., Samoylov, D. V.: 2,4,5,7-Tetranitrofluorescein in solutions: novel type of tautomerism in hydroxyxanthene series as detected by various spectral methods. *Spectrochim Acta A Mol Biomol Spectrosc.* 61, 2747–2760 (2005). <https://doi.org/10.1016/J.SAA.2004.09.030>
4. Mchedlov-Petrosyan, N.O., Steinbach, K., Vodolazkaya, N.A., Samoylov, D.V., Shekhovtsov, S.V., Omelchenko, I.V., Shishkin, O.V.: The molecular structure of anionic species of 2,4,5,7-tetranitrofluorescein as studied by electrospray ionisation, nuclear magnetic resonance and X-ray techniques. *Coloration Technology.* 134, 390–399 (2018). <https://doi.org/10.1111/COTE.12351>
5. Mchedlov-Petrosyan, N.O., Vodolazkaya, N.A.: Protolytic Equilibria in Organized Solutions: Ionization and Tautomerism of Fluorescein Dyes and Related Indicators in Cetyltrimethylammonium Chloride Micellar Solutions at High Ionic Strength of the Bulk Phase. *Liquids* 2021, Vol. 1, Pages 1-24. 1, 1–24 (2021). <https://doi.org/10.3390/LIQUIDS1010001>
6. Shekhovtsov, S. V, Mchedlov-Petrosyan, N.O., Kamneva, N.N., Gromovoy, T.Y.: New orange dyes: Nitroderivatives of sulfonefluorescein. *Kharkov Univ. Bull.* 24, 7–18 (2014)
7. Mchedlov-Petrosyan, N.O., Cheipesh, T.A., Shekhovtsov, S. V., Ushakova, E. V., Roshal, A.D., Omelchenko, I.V.: Aminofluoresceins Versus Fluorescein: Ascertained New Unusual Features of Tautomerism and Dissociation of Hydroxyxanthene Dyes in Solution. *Journal of Physical Chemistry A.* 123, 8845–8859 (2019). https://doi.org/10.1021/ACS.JPCA.9B05810/SUPPL_FILE/JP9B05810_SI_001.PDF
8. Kriklya, N.N., Gromovoy, T.Y., Mchedlov-Petrosyan, N.O.: 4,5-Dinitrosulfonefluorescein and related dyes: Kinetics of reversible rupture of the pyran ring and their interaction with lysozyme. *Coloration Technology.* 137, 658–667 (2021). <https://doi.org/10.1111/COTE.12565>
9. Glushko, V.N., Blokhina, L.I., Sadovskaya, N.Y.: Studies on the synthesis of fluorescein-5-isothiocyanate: A fluorescent nanomarker for biosensors. *Russian Journal*

Chapter 2

of General Chemistry 2015 85:10. 85, 2458–2464 (2015).

<https://doi.org/10.1134/S1070363215100412>

10. Coons, A.H., Kaplan, M.H.: Localization of antigen in tissue cells; improvements in a method for the detection of antigen by means of fluorescent antibody. *J Exp Med.* 91, 1–13 (1950). <https://doi.org/10.1084/JEM.91.1.1>
11. Sigmund, H., Pfeleiderer, W.: Nucleotides. Part LXXI. A New Type of Labelling of Nucleosides and Nucleotides. *Helv Chim Acta.* 86, 2299–2334 (2003). <https://doi.org/10.1002/HLCA.200390186>
12. Shekhovtsov, S. V., Shvets, E.H., Kolosov, M.A., Omelchenko, I. V., Batrak, A.S., Mchedlov-Petrosyan, N.O.: Peculiarities of the 4,5-dinitrofluorescein esters synthesis: formation of reduced species. *Coloration Technology.* 138, 192–200 (2022). <https://doi.org/10.1111/COTE.12582>
13. Negishi, Y., Kawarada, A., Suzuki, T.: Synthesis of novel acid-base indicators by nitration of phenolphthalein and fluorescein. *J. College Educ., Yokohama Nat. Univ. The Natural Sciences.* 1, 20–31 (2018)
14. Moskaeva, E.G., Ostrovskiy, K.I., Shekhovtsov, S.V., Mchedlov-Petrosyan, N.O.: Transmittance of electronic effects in the fluorescein molecule: nitro and amino groups in the phthalic acid residue. *Kharkiv University Bulletin. Chemical Series.* 24–32 (2021). <https://doi.org/10.26565/2220-637X-2021-36-05>
15. Gensh, K. V., Zevatskii, Y.E., Samoylov, D. V., Shekhovtsov, S. V., Lebed, A. V., Goga, S.T., Mchedlov-Petrosyan, N.O.: Ionic equilibrium in mixtures of polar protophobic and protophilic non-hydrogen bond donor solvents: Acids, salts, and indicators in acetonitrile with 4 mass % dimethylsulfoxide. *J Mol Liq.* 322, 114560 (2021). <https://doi.org/10.1016/J.MOLLIQ.2020.114560>
16. Doroshenko, A.O.: *Spectral Data Lab Software*, (1999)
17. Rabek, J.: *Experimental methods in photochemistry and photophysics.* Wiley–Blackwell (1982)
18. Doroshenko, A.O., Posokhov, E.A.: Mechanisms of Photoinduced Protolytic Interactions of 2,5-Diphenyloxazole ortho-Hydroxy Derivatives in Media of Various Acidities. Original Russian Text Copyright. 34, 124–132 (2000)
19. Doroshenko, A.O., Kirichenko, A. V., Mitina, V.G., Ponomaryov, O.A.: Spectral properties and dynamics of the excited state structural relaxation of the ortho analogues of POPOP — Effective abnormally large Stokes shift luminophores. *J Photochem Photobiol A Chem.* 94, 15–26 (1996). [https://doi.org/10.1016/1010-6030\(95\)04203-2](https://doi.org/10.1016/1010-6030(95)04203-2)
20. Serdiuk, I.E., Roshal, A.D.: 7-Hydroxyflavone Revisited. 2. Substitution Effect on Spectral and Acid-Base Properties in the Ground and Excited States. *Journal of*

Physical Chemistry A. 119, 12672–12685 (2015).

https://doi.org/10.1021/ACS.JPCA.5B09185/SUPPL_FILE/JP5B09185_SI_001.PDF

21. Dolomanov, O. V., Bourhis, L.J., Gildea, R.J., Howard, J.A.K., Puschmann, H.: OLEX2: a complete structure solution, refinement and analysis program. *J. Appl. Cryst.* 42, 339–341 (2009). <https://doi.org/10.1107/S0021889808042726>

22. Sheldrick, G.M., IUCr: SHELXT – Integrated space-group and crystal-structure determination. *Acta Cryst.* 71, 3–8 (2015). <https://doi.org/10.1107/S2053273314026370>

23. Groom, C.R., Allen, F.H.: The Cambridge Structural Database in retrospect and prospect. *Angew Chem Int Ed Engl.* 53, 662–671 (2014). <https://doi.org/10.1002/ANIE.201306438>

24. Kolos, N.N., Nazarenko, N. V., Shishkina, S. V., Doroshenko, A.O., Shvets, E.G., Kolosov, M.A., Yaremenko, F.G.: Synthesis, study of the structure, and modification of the products of the reaction of 4-aryl-4-oxobut-2-enoic acids with thiourea. *Chem Heterocycl Compd (N Y)*. 56, 1202–1209 (2020). <https://doi.org/10.1007/S10593-020-02798-Y/FIGURES/4>

25. Obukhova, O.M., Mchedlov-Petrosyan, N.O., Vodolazkaya, N.A., Patsenker, L.D., Doroshenko, A.O.: Stability of Rhodamine Lactone Cycle in Solutions: Chain‐Ring Tautomerism, Acid‐Base Equilibria, Interaction with Lewis Acids, and Fluorescence. *Colorants* 2022, Vol. 1, Pages 58-90. 1, 58–90 (2022). <https://doi.org/10.3390/COLORANTS1010006>

26. Becke, A.D.: Density-functional thermochemistry. III. The role of exact exchange. *J Chem Phys.* 98, 5648 (1998). <https://doi.org/10.1063/1.464913>

27. Woon, D.E., Dunning, T.H.: Gaussian basis sets for use in correlated molecular calculations. III. The atoms aluminum through argon. *J Chem Phys.* 98, 1358 (1998). <https://doi.org/10.1063/1.464303>

28. Wolinski, K., Hinton, J.F., Pulay, P.: Efficient Implementation of the Gauge-Independent Atomic Orbital Method for NMR Chemical Shift Calculations. *J Am Chem Soc.* 112, 8251–8260 (1990). https://doi.org/10.1021/JA00179A005/ASSET/JA00179A005.FP.PNG_V03

29. Tomasi, J., Mennucci, B., Cammi, R.: Quantum mechanical continuum solvation models. *Chem Rev.* 105, 2999–3093 (2005). https://doi.org/10.1021/CR9904009/ASSET/CR9904009.FP.PNG_V03

30. Frisch, M.J., Trucks, G.W., Schlegel, H.B., Scuseria, G.E., Robb, M.A., Cheeseman, J.R., Scalmani, G., Barone, V., Mennucci, B., Petersson, G.A., Nakatsuji, H., Caricato, M., Li, X., Hratchian, H.P., Izmaylov, A.F., Bloino, J., Zheng, G., Sonnenberg, J.L., Hada, M., Ehara, M., Toyota, K., Fukuda, R., Hasegawa, J., Ishida, M., Nakajima, T., Honda, Y., Kitao, O., Nakai, H., Vreven, T., Montgomery, J.A., Peralta, J.E., Ogliaro, F., Bearpark, M., Heyd, J.J.,

Chapter 2

Brothers, E., Kudin, K.N., Staroverov, V.N., Kobayashi, R., Normand, J., Raghavachari, K., Rendell, A., Burant, J.C., Iyengar, S.S., Tomasi, J., Cossi, M., Rega, N., Millam, J.M., Klene, M., Knox, J.E., Cross, J.B., Bakken, V., Adamo, C., Jaramillo, J., Gomperts, R., Stratmann, R.E., Yazyev, O., Austin, A.J., Cammi, R., Pomelli, C., Ochterski, J.W., Martin, R.L., Morokuma, K., Zakrzewski, V.G., Voth, G.A., Salvador, P., Dannenberg, J.J., Dapprich, S., Daniels, A.D., Farkas, Ö., Foresman, J.B., Ortiz, J. v, Cioslowski, J., Fox, D.J.: Gaussian 09 Revision B.1, (2016)

31. CHESHIRE Chemical Shift Repository, <http://cheshirenmr.info/index.htm>
32. Mchedlov-Petrossyan, N.O., Ivanov, V. V.: Effect of the solvent on the absorption spectra and protonation of fluorescein dye anions. *Russian Journal of Physical Chemistry* 2007 81:1. 81, 112–115 (2007). <https://doi.org/10.1134/S0036024407010219>
33. Bates, R.G.: Determination of pH, Theory and Practice. 2nd Edition. John Wiley & Sons, Ltd (1973)
34. Fujinaga, T., Sakamoto, I.: Electrochemical characteristics of trifluoromethanesulphonic acid and its salts in nonaqueous solvents. *Pure and Applied Chemistry*. 52, 1387–1396 (1980). <https://doi.org/10.1351/PAC198052051387>
35. Alía, J.M., Edwards, H.G.M., Kiernan, B.M.: Raman spectroscopy of benzenesulfonic and 4-toluenesulfonic acids dissolved in dimethylsulfoxide. *Spectrochim Acta A Mol Biomol Spectrosc.* 60, 1533–1542 (2004). <https://doi.org/10.1016/J.SAA.2003.08.016>
36. Kolthoff, I.M., Chantooni, M.K., Bhowmik, S.: Dissociation constants of uncharged and monovalent cation acids in dimethyl sulfoxide. *J Am Chem Soc.* 90, 23–28 (1968). https://doi.org/10.1021/JA01003A005/ASSET/JA01003A005.FP.PNG_V03
37. Kolthoff, I.M.: Acid-Base Equilibria in Dipolar Aprotic Solvents. *Anal Chem.* 46, 1992–2003 (1974). https://doi.org/10.1021/AC60349A005/ASSET/AC60349A005.FP.PNG_V03
38. Kolthoff, I.M., Chantooni, M.K.: Calibration of the Glass Electrode in Acetonitrile. Shape of Potentiometric Titration Curves. Dissociation Constant of Picric Acid. *J Am Chem Soc.* 87, 4428–4436 (1965). https://doi.org/10.1021/JA00948A004/ASSET/JA00948A004.FP.PNG_V03

Chapter 3

Nitro derivatives of fluorescein in solution: Towards understanding of stepwise acid-base dissociation in systems inclined to tautomerism

The results of this chapter are partly published in:

E.G. Moskaeva, A.V. Mosharenkova, S.V. Shekhovtsov, N.O. Mchedlov-Petrosyan. Protolytic equilibrium of tetra- and pentanitrofluoresceins in a binary solvent acetonitrile – dimethyl sulfoxide (mass ratio 96 : 4). Ukrainian Chem J. V. 87. No. 5., P. 25–37, (2021)

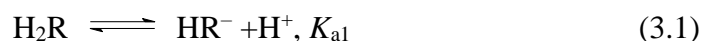
N. O. Mchedlov-Petrosyan, S. V. Shekhovtsov, E. G. Moskaeva, I. V. Omelchenko, A. D. Roshal, A. O. Doroshenko. New fluorescein dyes with unusual properties: Tetra- and pentanitrofluoresceins. J. Mol. Liquids. 367, 120541, (2022)

In this chapter, we are going to discuss acid-base dissociation and tautomeric equilibrium of nitroderivatives of fluorescein in buffered solutions in aprotic solvents. In the previous chapter electronic spectroscopy in dimethyl sulfoxide, DMSO, proves that doubly charged anions of several compounds, R^{2-} , exist in solution in the form of lactone structures, which is not characteristic of other fluorescein dyes. These lactones are yellow ($\lambda_{max} = 420\text{--}430\text{ nm}$) due to the nitrophenolate absorption. On the contrary, singly charged anions are represented predominantly by fluorescent and intensely colored particles. So, the next step is to calculate the pK_a values from spectrophotometric data. Interpreting this constant requires an understanding of the state of tautomeric equilibria. The analysis of the absorption spectra in the visible region and evaluation of the tautomerization constants made it possible to calculate the so-called microscopic equilibrium constants of the stepwise dissociation.

Of particular interest is the methyl ester of 2,4,5,7-tetranitrofluorescein. The esterification of the carboxyl group avoids lactonization. In contrast to the initial dye, this compound exists as a stable singly charged anion in a wide pH range in all solvents except nonpolar ones.

3.1 Introduction

The thermodynamic pK_a values were determined using the spectrophotometric method in buffered solutions.



The study was conducted with a twofold purpose. First, because preliminary experiments demonstrate new features of this important family of dyes, it seemed worth exploring them in detail. Second, the analysis of the dissociation constants and absorption spectra of twelve newly considered and six earlier studied dyes showed that this series in DMSO gives excellent examples of dramatic differences in the K_{a1} / K_{a2} ratio, from 8×10^2 for 4,5-dinitrofluorescein to 4.0×10^7 for 4,5-dinitro-2,7-dibromofluorescein. This and many other effects were explained in terms of tautomerism and microscopic dissociation constants. The explanation was confirmed using the pK_a s of the model compounds with blocked hydroxylic or carboxylic groups, OCH_3 , $COOCH_3$ and $COOC_2H_5$, or with SO_3H group instead of $COOH$.

For a two-step dissociation (4,5-dinitro-; 2,4,5,7-tetranitro-; 2,4,5,7,4'- and 2,4,5,7,5'-pentanitro-; and 4,5-dinitro-2,7-dibromofluorescein) a general equation for a fixed wavelength, dye concentration, and ionic strength is as follows:

$$A = \frac{A_{HR^-} a_{H^+}^* K_{a1} f_1^{-1} + A_{R^{2-}} K_{a1} K_{a2} f_2^{-1}}{(a_{H^+}^*)^2 + a_{H^+}^* K_{a1} f_1^{-1} + K_{a1} K_{a2} f_2^{-1}} \quad (3.3)$$

Here, A is the absorbance at a current $pa_{H^+}^*$ value, A_{HR^-} and $A_{R^{2-}}$ are absorbances of solutions under complete conversion of the dye into the corresponding form. While the last one can be determined directly at high enough $pa_{H^+}^*$ values, the A_{HR^-} value is unavailable when the dissociation constants are close. This equation can be represented in three forms for the calculation of both dissociation constants and the A_{HR^-} value:

$$K_{a1}^{-1} = \frac{A_{HR^-} - A}{A} f_1^{-1} (a_{H^+}^*)^{-1} + \frac{A_{R^{2-}} - A}{A} K_{a2} f_1 f_2^{-1} (a_{H^+}^*)^{-2} \quad (3.4)$$

$$K_{a2} = \frac{A_{HR^-} - A}{A - A_{R^{2-}}} f_2 f_1^{-1} a_{H^+}^* - \frac{A}{A - A_{R^{2-}}} K_{a1}^{-1} f_2 (a_{H^+}^*)^2 \quad (3.5)$$

$$A_{HR^-} = A \{ a_{H^+}^* K_{a1}^{-1} f_1 + 1 + K_{a2} f_1 f_2^{-1} (a_{H^+}^*)^{-1} \} - A_{R^{2-}} K_{a2} f_1 f_2^{-1} (a_{H^+}^*)^{-1} \quad (3.6)$$

($A_{H_2R} \approx 0$). Here, K_a are thermodynamic constants.

In a simple case of one-step dissociation (ether and esters of the dyes), the equation is trivial:

$$pK_{a1} = pa_{H^+}^* + \log \frac{A_{R^-} - A}{A - A_{HR}} - \log f_1 \quad (3.7)$$

For 4,5-dinitrosulfofluorescein, the first dissociation step occurs at much higher acidity, and the second dissociation step can be studied as isolated:

$$pK_{a2} = pa_{H^+}^* + \log \frac{A_{R^{2-}} - A}{A - A_{HR^-}} - \log f_2 + \log f_1 \quad (3.8)$$

The $pa_{H^+}^*$ values of the buffer solutions in DMSO were calculated taking into account the homoassociation equilibrium, as described in Chapter 2. In buffer solutions, the ionic strength was as a rule 0.005 M (equal to the buffer salt concentration; the concentrations of the buffer acid were variable). The $pa_{H^+}^*$ values in the acidic region were created using *p*-toluenesulfonic or triflic acids, and in the case of tetra- and pentanitrofluoresceins, picric acid was also used. In the acidic region, the ionic strength was equal to the “strong” acid concentration.

In acetonitrile with 4 mass % DMSO, the $pa_{H^+}^*$ values were calculated using the set of equilibrium data for the buffers [1].

3.2 The 4,5-dinitrofluorescein series in DMSO

The absorption spectra at different $p\alpha_{\text{H}^+}^*$ are presented in Figures 3.1 and 3.2. Therein, the values of the used buffer solutions are indicated. For pK_a calculations, several wavelengths around the λ_{max} values of the dissociated forms are used as analytical positions.

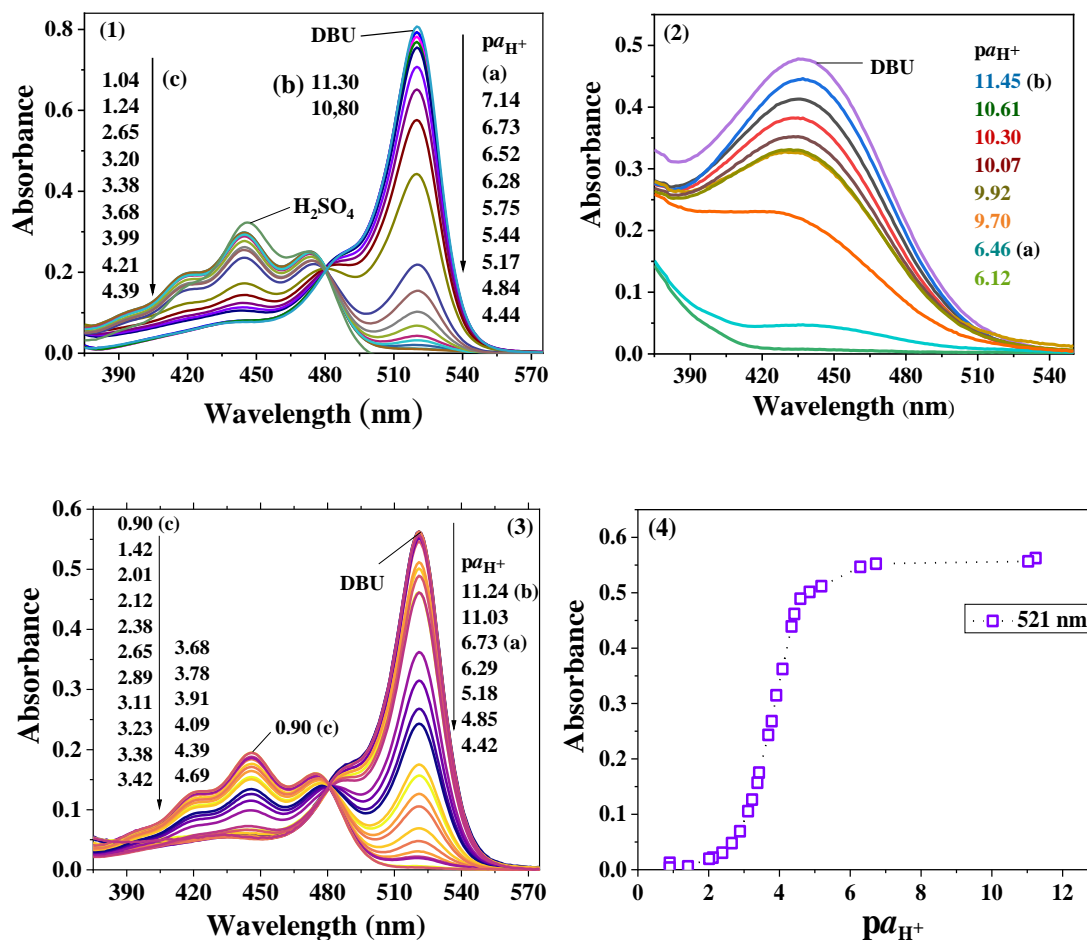


Figure 3.1: Steady-state absorption spectra in DMSO at different $p\alpha_{\text{H}^+}^*$ values: 4,5-dinitrosulfofluorescein (1); 4,5-dinitrofluorescein methyl ether (2); 4,5-dinitrofluorescein methyl ester (3); and dependence of 4,5-dinitrofluorescein methyl ester absorbance at 522 nm on $p\alpha_{\text{H}^+}^*$ (4) in DMSO at different $p\alpha_{\text{H}^+}^*$: in salicylate (a) and benzoate (b) buffer solutions and in *p*-toluenesulfonic acid solutions (c).

The obtained pK_a s are collected in Table 3.1. The molar extinction coefficients are given in Table 3.2. The most complicated case is the 4,5-dinitrofluorescein. In Figure 3.3, the dependence of absorbance vs. $pa_{H^+}^*$ at $\lambda = 520$ nm is exemplified. The K_{a1} , K_{a2} , and A_{HR^-} values were jointly calculated using the chemometric CLINP method [2]. Absorbance from $\lambda = 500$ to 535 nm in one nanometer was used for 24 working solutions, at ionic strength 0.005 M. Table 3.1: The thermodynamic pK_a values of the nitrofluorescein dyes in DMSO; 25 °C.

No.	Compound	pK_{a1}	pK_{a2}	$pK_{a2} - pK_{a1}$
1	4,5-Dinitrosulfofluorescein	n.d.	4.88 ± 0.11	–
2	4,5-Dinitrofluorescein methyl ester	3.79 ± 0.03	–	–
3	4,5-Dinitrofluorescein methyl ether	9.6 ± 0.2	–	–
4	4,5-Dinitrofluorescein	7.0 ± 0.1	9.9 ± 0.2	2.9
5	4,5-Dinitro-2,7-dibromofluorescein	1.34 ± 0.1	8.9 ± 0.1	7.6
6	2,4,5,7-Tetranitrofluorescein {from ref. [3]}	1.3 ± 0.17	4.4 ± 0.13	3.1
7	2,4,5,7-Tetranitrofluorescein methyl ester	below 0	—	—
8	2,4,5,7,4'-Pentanitrofluorescein	0.59 ± 0.03	4.42 ± 0.04	3.8
9	2,4,5,7,5'-Pentanitrofluorescein	0.63 ± 0.03	4.45 ± 0.03	3.8
10	5'-Nitrofluorescein	10.6 ± 0.1	11.8 ± 0.1	1.2

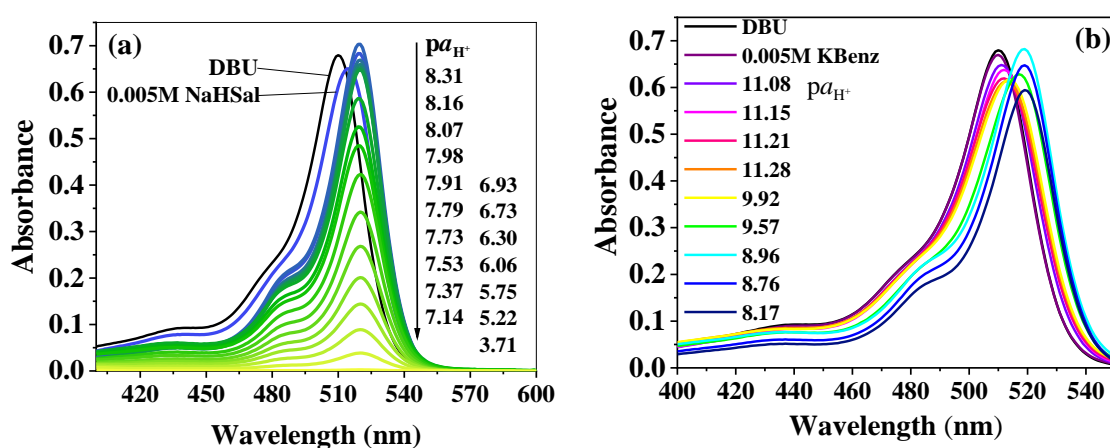


Figure 3.2. Steady-state absorption spectra of 4,5-dinitrofluorescein in DMSO at different $pa_{H^+}^*$ values in salicylate (a) and benzoate (b) buffer solutions.

Chapter 3

Table 3.2: Characterization of the absorption spectra of the dyes in DMSO, 25 °C

Compound	λ_{\max} , nm ($\epsilon_{\max} \times 10^{-3}$, M ⁻¹ cm ⁻¹)		
	Neutral	Monoanion	Dianion
4,5-Dinitrofluorescein	445.5 (0.037); 474 (0.031)	520 (86.8)	510 (82.2)
4,5-Dinitrofluorescein methyl ester	424 (20.2); 446 (30.1); 474 (24.8)	521.5 (87.1)	—
4,5-Dinitrofluorescein methyl ether	almost colorless	437 (2.49)	—
4,5-Dinitrosulfofluorescein	n.d.	424 (21.7); 445 (31.6); 474 (26.6)	520 (85.8)
4,5-Dinitro-2,7-dibromofluorescein	almost colorless	525 (96.2)	513 (30.6)
2,4,5,7,4'-Pentanitrofluorescein	almost colorless	525 (98.6)	429 (17.7)
2,4,5,7,5'-Pentanitrofluorescein	almost colorless	525 (99.8)	419 (31.7)
2,4,5,7-Tetranitrofluorescein	almost colorless	525 (62.0)	441 (19.0)
2,4,5,7-Tetranitrofluorescein methyl ester	452 (37.9) ^a	527 (110.0)	—
5'-Nitrofluorescein	437 (0.048), 461 (0.054), 492 (0.039)	435 (22.4) 461 (30.3) 490 (21.9)	528 (95.8)

^a In benzene with the addition of 0.1 M sulfuric acid.

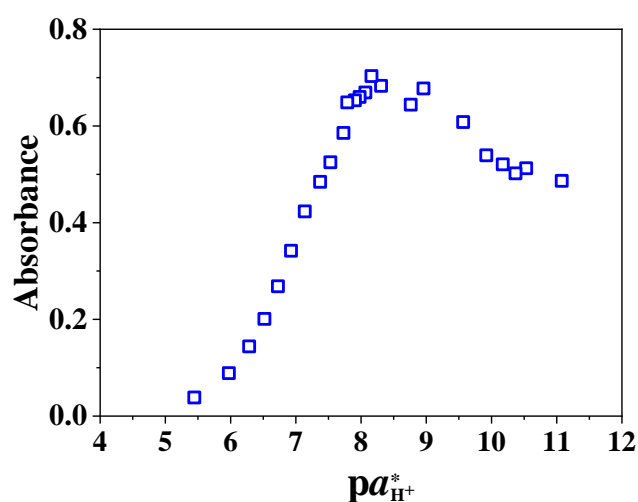


Figure 3.3: The dependence of absorbance of 4,5-dinitrofluorescein at $\lambda = 520$ nm on $p\alpha_{\text{H}^+}^*$ in DMSO; ionic strength 0.005 M.

Finally, the values $\text{p}K_{a1} - \log f_1 = 6.88 \pm 0.10$ and $\text{p}K_{a2} - \log f_2 + \log f_1 = 9.71 \pm 0.20$ were obtained. The spectrum of the HR^- ion (Figure 3.4) was singled out using thus obtained $\text{p}K_a$ values, Equation (3.6).

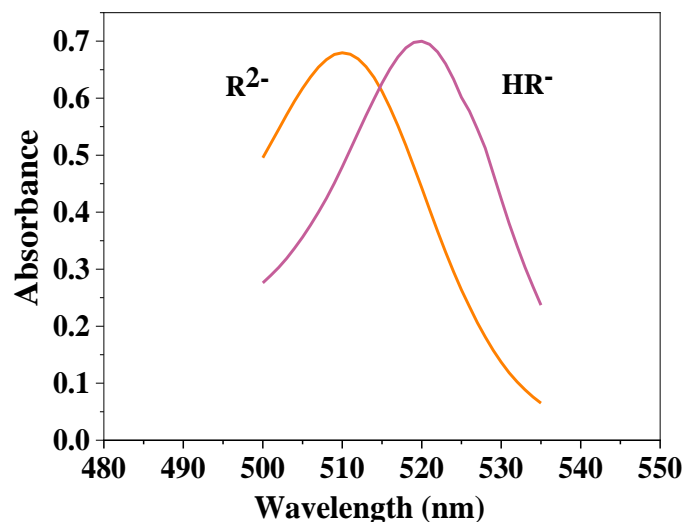


Figure 3.4: Steady-state absorption spectra of the anions of 4,5-dinitrofluorescein in DMSO at ionic strength of 0.005 M; the HR^- spectrum was singled out using the calculated $\text{p}K_a$ values.

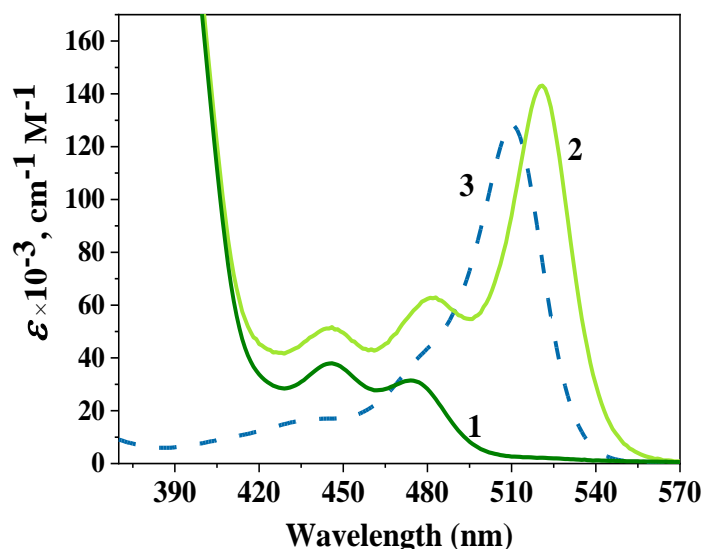


Figure 3.5: The molar extinction coefficient of 4,5-dinitrofluorescein: 1 – neutral form H_2R in the presence of 0.05 M *p*-toluenesulfonic acid; 2 – the spectrum in the presence of 0.001 M of *p*-toluenesulfonic acid; 3 – absorption of the R^{2-} dianion in the presence of 0.02 M DBU (in this case, the E values were divided by 650). The spectra 1 and 2 were obtained at dye concentrations of 3.7×10^{-3} and 7.5×10^{-4} M.

It is clearly seen that for 4,5-dinitrofluorescein the monoanion belongs to the HX^- type, like that of eosin, erythrosin, etc. (see Chapter 1).

Chapter 3

The spectrum of the neutral form of 4,5-dinitrofluorescein in DMSO is available in acidic solutions, e.g., in 0.05 M *p*-toluenesulfonic acid. In Figure 3.5, the corresponding data are represented. In 0.001 M acid solution, the appearance of the HR^- anion is evident (curve 2).

The spectrum of the R^{2-} ion is presented for comparison (curve 3, dotted line); the ϵ values are divided by 650. It should be noted that the molecular spectrum (curve 1) contains a substantial absorbance in the UV portion. The reason is the specificity of the spectrum of the lactone. The presence of a nitro group causes the slight yellow color of nitrophenol; analogous effect is observed for the 4,5-dinitrofluorescein lactone. The bands at 446 and 474 nm resemble by shape those of the methyl ester of 4,5-dinitrofluorescein (Figure 3.1, c; Table 3.2), whereas the short-wavelength band, probably around 424 nm, is overlapped by the absorption of the lactonic tautomer.

3.3 The tetranitrofluorescein series

3.3.1 The tetranitrofluorescein series in DMSO

The absorption spectra are exemplified in Figures 3.6 and 3.7. The results obtained with the picric and triflic acids and *p*-TSA coincide. In solutions with a low concentration of picric acid, the contribution of the dye concentration to the material balance was taken into account. Measurements were made against the solvent blanks, which is of special importance in the case of picric acid. Therefore, in Figure 3.6 the short-wavelength portion of the spectra in picric acid solutions was cut off because of too high absorbance of the blank solutions. The picture is in outline similar to that reported by us earlier for 2,4,5,7-tetranitrofluorescein [3]. Because the $\text{p}K_{\text{a1}}$ values are rather low, the traces of colored anionic species disappear only at high concentrations of acids (sulfuric, *p*-toluenesulfonic, or triflate). Hence, the molecular forms, H_2R , are colorless and exist in form of lactones, H_2L (see Chapters 1 and 2), which are in line with those considered above in the solid state.

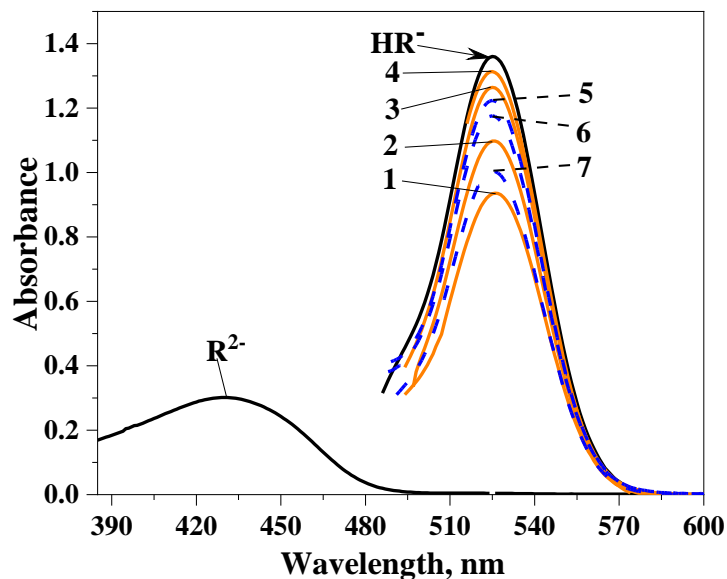


Figure 3.6: Steady-state absorption spectra of 2,4,5,7,4'-pentanitrofluorescein, 1.40×10^{-5} M, in DMSO. The spectrum of the dianion R^{2-} was measured in 0.02 M DBU solution; the same spectrum was obtained in benzoate buffer solutions. The values for the picric acid solutions in the concentration scale, $\text{pH}_c = -\log[\text{H}^+]$, and in the activity scale $\{ \text{p}a_{\text{H}^+}^* \}$ are as follows: 0.35 {0.66} (1); 0.66 {0.93} (2); 1.27 {1.44} (3); 1.81 {1.92} (4); 3.38 {3.40} (5); 3.51 {3.53} (6); 3.98 {3.99} (7); the spectrum within the range of 1.84 {1.92} to 3.08 {3.11} are almost invariable and correspond to the single-charged anion, HR^- . This is a representative set of points from a much larger body of data (see Figure 3.8).

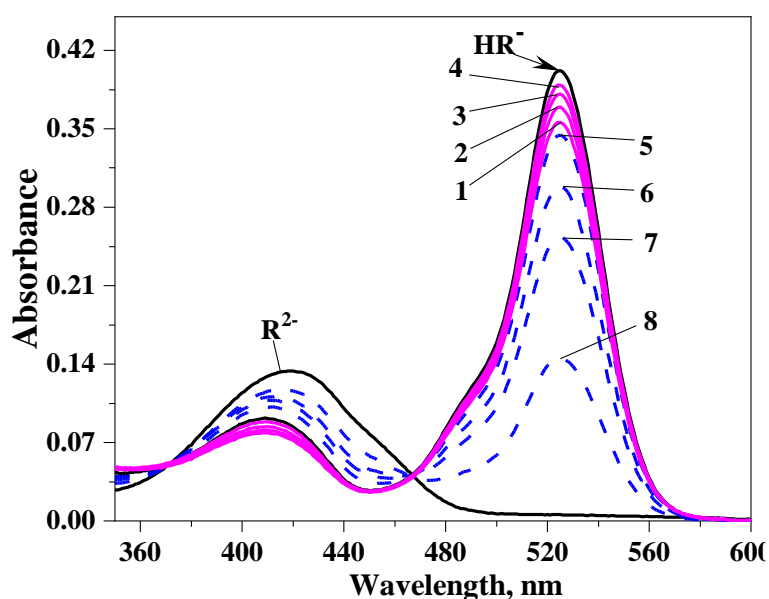


Figure 3.7: Steady-state absorption spectra of 2,4,5,7,5'-pentanitrofluorescein, 4.17×10^{-6} M, in DMSO. The spectrum of the dianion R^{2-} was measured in 0.02 M DBU solution; the same

Chapter 3

spectrum was obtained in the benzoate buffer solution. The values in the concentration scale, $\text{pH}_c = -\log[\text{H}^+]$, and in the activity scale $\{ \text{p}a_{\text{H}^+}^* \}$ are as follows: 1.05 {1.26} (1); 1.22 {1.40} (2); 1.40 {1.55} (3); 1.70 {1.82} (4); 3.70 {3.71} (5); 4.00 {4.01} (6); 4.22 {4.23} (7); 4.70 {4.70} (8); the spectrum within the range of 1.70 {1.82} to 3.52 {3.54} are almost invariable and correspond to the single-charged anion, HR^- . In the acidic region, *p*-TSA, picric, and triflic acids were used. This is a representative set of points from a much larger body of data (see Figure 3.8).

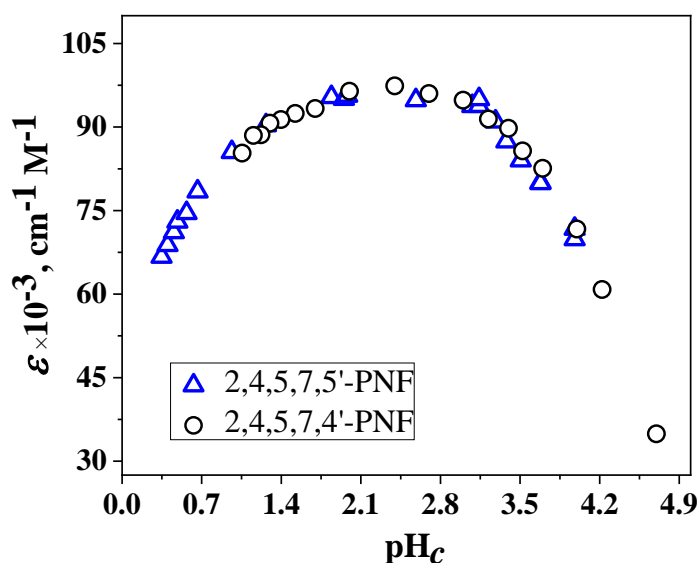


Figure 3.8: Dependence of the molar extinction coefficient at λ_{max} on $\text{pH}_c = -\log[\text{H}^+]$ in DMSO; 2,4,5,7,4'-pentanitrofluorescein (triangles); 2,4,5,7,5'-pentanitrofluorescein (circles).

The absorbance in the middle of the plateau and the $\text{p}a_{\text{H}^+}^*$ value that corresponds to the middle of the right branch of the dependence were taken as the first approximation of A_{HR^-} and $\text{p}K_{\text{a}2}$, respectively. Thus calculated $K_{\text{a}1}^{-1}$ value (Equation 3.4) was used in the calculation of $K_{\text{a}2}$ (Equation 3.5), and both constants were used to obtain the refined A_{HR^-} value (Equation 3.6). Then the procedure was repeated. The second iteration leads to the same results. The results are presented in Tables 3.1 and 3.2.

Because previous experiments demonstrated the pronounced tendency to alkaline rupturing the pyran cycle in the case of sulfofluorescein nitroderivatives [4, 5], it was necessary to shed light upon this problem for the dyes under study as well.

3.3.2 Rupture of the pyran ring and transformations in aqueous media

It was shown and firmly proved, that in the case of nitro derivatives, the rupture of the pyran ring in the fluorescein molecule occurs at a lower alkali concentration than for the unsubstituted dye or its halogen derivatives [4–7]. In these cases, new bands in the visible appear which correspond to the anions of triphenylmethine dyes formed after pyran ring rupture. It concerns compounds with two nitro groups in the xanthenes part [4, 5, 7]. In our previous work, two examples of the above cycle cleavage are demonstrated for the 2,4,5,7-tetranitrofluorescein [6]. First, the electrospray ionization spectroscopy revealed a four-charged anion with three Na^+ ions, using a NaOH solution in aqueous acetonitrile. X-ray analysis of crystals obtained from concentrated aqueous KOH solution proved a five-charged anion of carbinolic type. Both structures are shown in Figure 3.9.

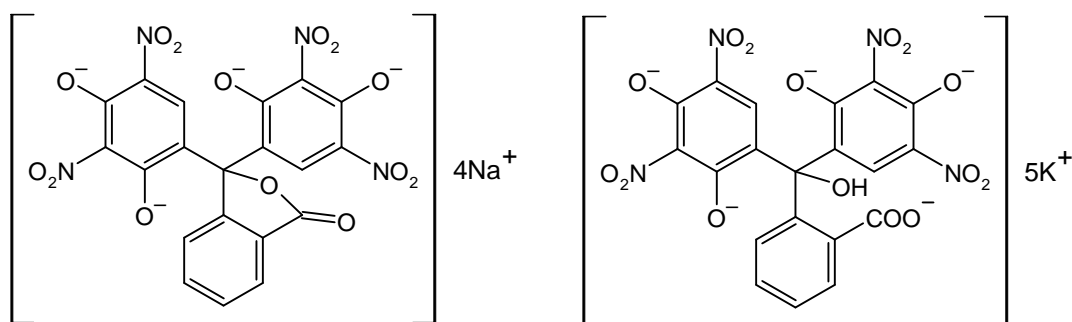


Figure 3.9: Highly charged anions of 2,4,5,7-tetranitrofluorescein with ruptured pyran ring identified using electrospray spectroscopy (left) and X-ray analysis of crystals (right) [6].

Now we made some experiments in order to additionally clarify this issue. In DMSO at high concentrations of DBU, no new absorption bands in the visible spectrum appear. On the other hand, we synthesized the corresponding compound with cleaved pyran ring (see Chapter 2).

Thus, the prepared compound (Figure 3.10) is a neutral form that corresponds to the four-charged anion revealed in the solution (Figure 3.9, left).

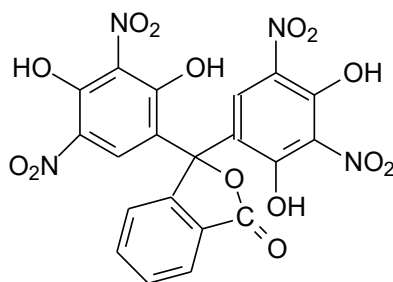


Figure 3.10: The molecular structure of the 2,4,5,7-tetranitrofluorescein with ruptured pyran ring (see also Chapter 2)

Concluding, the tendency to lactone formation is so pronounced in the case of 2,4,5,7-tetranitro derivatives of fluorescein, that the new band corresponding to the deeply colored triphenylmethine anion with sp^2 -hybridization cannot appear, in contrary to the 4,5-dinitrofluorescein [7] and 4,5-dinitrosulfonefluorescein [4, 5]. Note that the dianion of tetranitrophenolphthalein exists predominantly as a lactonic yellowish colored tautomer [8]. Somewhat different is the behavior of the 2,4,5,7-tetranitrosulfonefluorescein, which is unable to form a stable inner ester, a so-called sultone five-member cycle, under alkaline conditions 4 [6]. In this case, after the pyran ring rupture the nucleophilic attack of the HO^- ion leads to a carbinol formation [4, 6]. For 2,4,5,7-tetranitrofluorescein this takes place only in extremely high alkali concentrations (Figure 3.9, right).

This allows us to explain the absence of new bands either in DMSO with DBU additions or in aqueous NaOH solutions. Obviously, the tendency to lactone formation in the presence of four nitro groups in the xanthenes part is so pronounced that the anion that appears in alkaline media retains the lactonic structure.

Negishi et al. [9] reported the color transitions of 2,4,5,7,4'-pentanitrofluorescein in water within a wide pH range from 1 to 14. The scheme of the protolytic equilibrium proposed by the authors is clear, despite some discrepancies between the data presented in the abstract and the main text. Though the detailed quantitative study of the equilibria in aqueous solutions was beyond the shape of our work, we reproduced these experiments by determination of the absorption spectra within the same acidity range and observed similar color changes for both dyes. The spectra are typified in Figure 3.11.

However, taking into account the low pK_a values of the dyes and judging by the absorption spectra, we guess that the single-charged anion, HR^- , appears at $pH \leq 3$. For the 2,4,5,7,5'-pentanitrofluorescein, $\lambda_{max} = 396$ and 513 nm. Along with pH decreasing, the fraction

of the colorless neutral lactonic form increases, resulting in an intensity drop. On the other hand, at higher pH, the dianion R^{2-} predominates and the spectrum stays unchanged within the pH range from 4 to 9; $\lambda_{\max} = 398\text{--}401$ and 512 nm. The last band was not observed with the R^{2-} spectrum in DMSO.

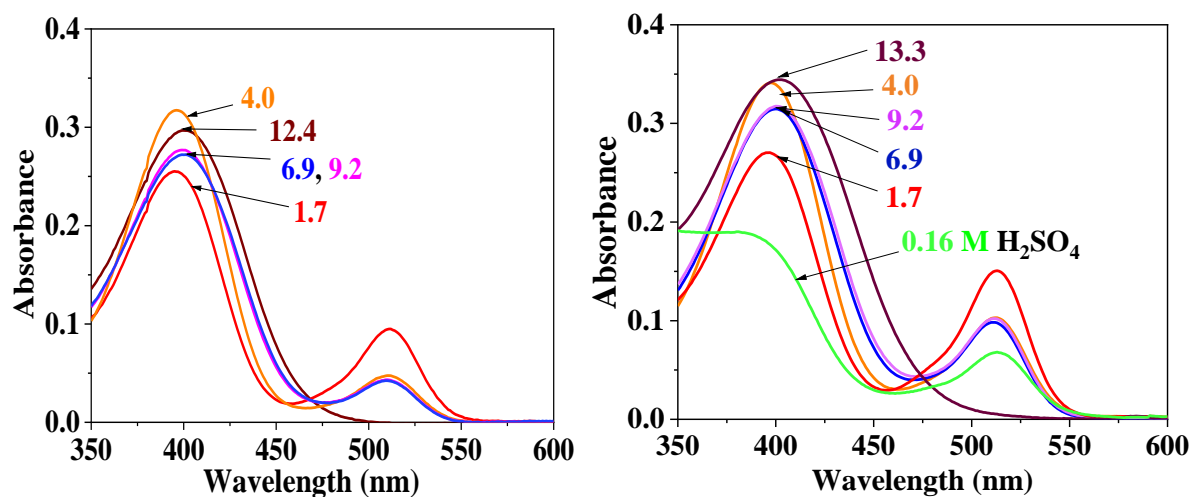


Figure 3.11: Steady-state absorption spectra of 2,4,5,7,4'- and 2,4,5,7,5'-pentanitrofluorescein in water with 1 vol % DMSO; the numbers denote the pH values; dye concentrations: 1.01×10^{-5} and 1.57×10^{-5} M, respectively.

For a very similar dye, 2,4,5,7-tetranitrofluorescein, the dianion not only absorbs around 400 nm in an aqueous medium, but a less intense band at ≈ 505 nm is also observed [7, 10]. The last should be ascribed to the small fraction of the quinonoidal X^{2-} dianion, which is the predominating tautomer in the case of fluorescein and its halogen derivatives [10–13]. In organic solvents, however, such absorption was not observed [3, 7, 8]. Hence, for pentanitrofluoresceins the picture is similar, and at pH 4–9 in water, the deeply colored quinonoidal tautomer of the dianion, X^{2-} , is also present as an admixture to the L^{2-} tautomer.

Batistella et al [10] determined the $pK_{a1} = 0.38$ and $pK_{a2} = 2.48$ values of 2,4,5,7-tetranitrofluorescein in water. Similar values should be expected for both pentanitrofluoresceins. The disappearance of the absorption near 510–512 nm at higher pH of 12.4–13.3 (Figure 3.11) should be explained by the disappearance of the X^{2-} ion, which indicates the conversion of the dianion into another species. The most probable is the rupture of the pyran ring at substantial NaOH concentrations. It cannot be firmly proved by the visible spectra. Indeed, as was demonstrated above, the dye with a ruptured pyran ring has a lactonic structure in neutral form and either lactonic or carbinolic structures in anionic forms (Figure 3.9).

3.3.3 Ionic equilibria in acetonitrile with 4 mass % DMSO

Fluorescein dyes bearing NO₂ groups in the xanthenes portion are relatively strong acids. Therefore, their investigation in terms of pK_a values should be conducted in a polar weakly basic solvent, e.g., in acetonitrile. However, even traces of water can distort the results obtained with this solvent. In order to avoid this interfering factor, a new binary solvent was proposed recently, namely, acetonitrile with 4 mass % dimethyl sulfoxide [1,8]. In this solvent, the acidity scale ($pa_{H^+}^*$) was established, and a set of buffer solutions was proposed. It was shown that the proton is associated with the molecules of the protophilic dimethyl sulfoxide, while other ionic and molecular species are solvated mainly by acetonitrile. Hence, this binary solvent can be regarded, as a first approximation, as acetonitrile with lyonium ion $H(DMSO)_2^+$ [1,8].

In the case of the 2,4,5,7-tetranitrofluorescein methyl ester, the dissociation of the HR form takes place at very low $pa_{H^+}^*$ values. The molecular spectrum was available only in benzene with small H₂SO₄ addition. Higher concentrations of the sulfuric acid and additions of the *p*-toluenesulfonic acid led to decolorization, obviously due to hydrolysis of the ester group and turning to the mother compound. The appearance of the R⁻ ion in pure benzene may be caused by small traces of water. The aprotic solvent acetonitrile with 4 mass % dimethyl sulfoxide is a good choice for obtaining the value of the ionization constant of this methyl ester [8].

The pK_a values of the dyes were re-calculated to the thermodynamic ones using the activity coefficients f_1 and f_2 for single and double-charged anions. The value of the ionic strength was calculated for each working solution. It did not exceed 0.005 M in buffer solutions and diluted picric acid.

The neutral HR and anionic R⁻ forms of the methyl ester of 2,4,5,7-tetranitrofluorescein exists as colored quinonoidal structures HQ and X⁻, respectively (Figure 3.12).

Three wavelengths around the absorption maximum were used as analytical positions. Here, the absorption of the molecular form HR is small. The thermodynamic value $pK_{a1} = 1.95 \pm 0.19$ was obtained from measurements with 8 different $pa_{H^+}^*$ values, from 1.45 to 2.35. Here, the utilization of the Debye–Hückel equation is conventional. Note that in this binary solvent and entire DMSO, the anion R⁻ exhibits bright fluorescence.

Much more diluted solutions of picric acid were used in the case of 2,4,5,7-tetranitrofluorescein (Figure 3.14, a). Here, the neutral form H_2R is almost colorless due to the predominance of the lactonic tautomer, as in other solvents [3, 6, 14, 15]

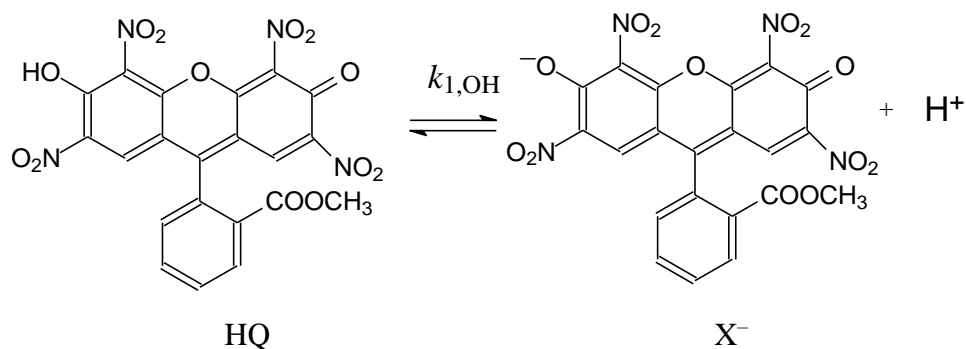


Figure 3.12: Dissociation equilibrium of 2,4,5,7-tetranitrofluorescein methyl ester

The absorption spectra of 2,4,5,7-tetranitrofluorescein methyl ester at different concentrations of the picric acid are given in Figure 3.13.

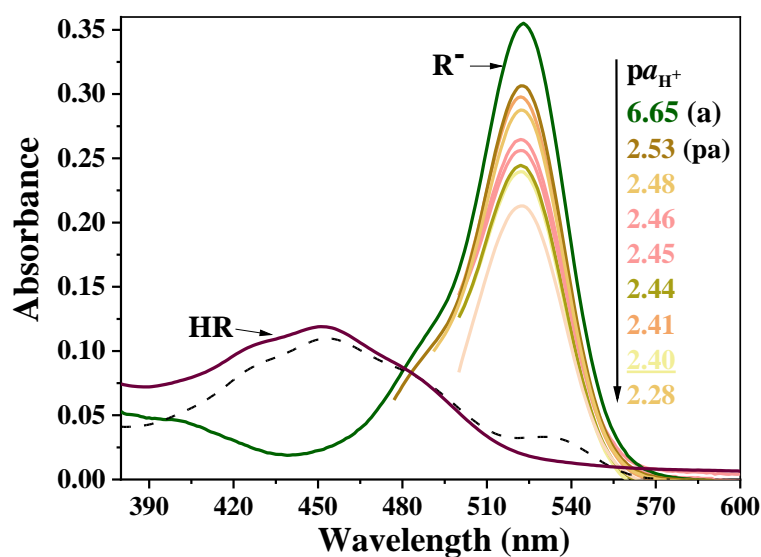


Figure 3.13: Steady-state absorption spectra of 2,4,5,7-tetranitrofluorescein methyl ester (3.1×10^{-6} M) in the binary solvent at different picric acid solutions (pa). The spectrum of the anionic form R^- was obtained in a salicylate buffer solution (a). The spectrum of the entire HR form was measured in benzene with 0.1 M sulfuric acid; without such acidifying, some amounts of the anion R^- are present in the solution (dotted curve).

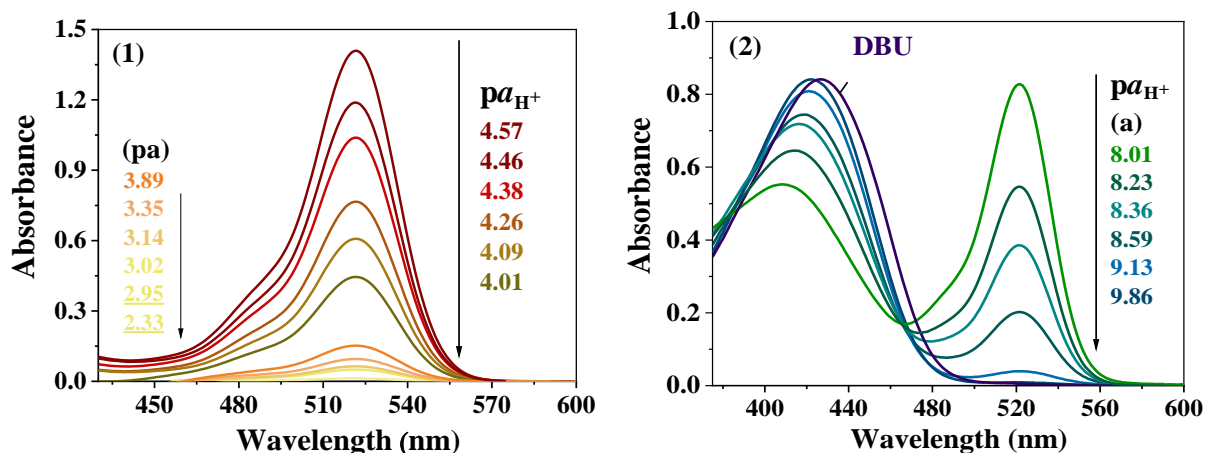


Figure 3.14: Steady-state absorption spectra of 2,4,5,7-tetranitrofluorescein (4.2×10^{-5} M) in diluted picric acid (pa) (1) and in the salicylate buffer solutions (a) (2). The R^{2-} spectrum was obtained in 0.02 M DBU solution.

The spectrum of the dianion R^{2-} of the dye is obtained in the DBU solution (Figure 3.14). This absorption band is shifted to some extent as compared with the spectra in salicylate buffers. This can be explained by the specific interaction of this double-charged anion with either $DBUH^+$ cation or salicylic acid molecules. Such interactions may also somewhat contribute to the main equilibrium. The dependence of absorbance at 522 nm is given in Figure 3.15.

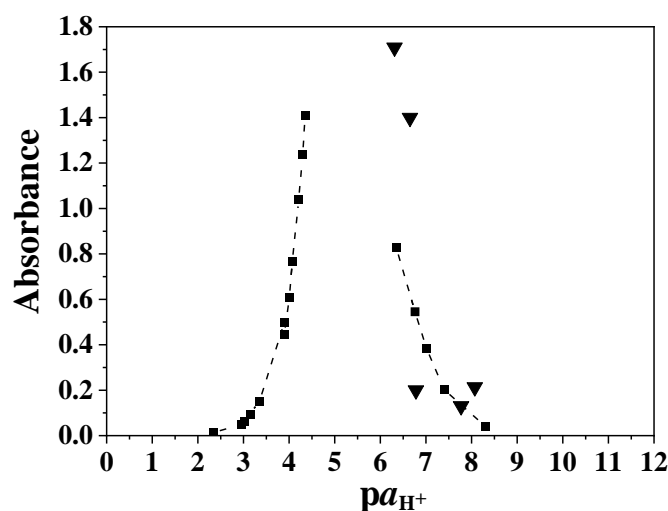


Figure 3.15: Absorption of 2,4,5,7-tetranitrofluorescein (4.2×10^{-5} M) at 522 nm vs. pK_{a^*} . Picric acid solutions (left-hand side) and salicylate buffers (right-hand side); 2,6-dinitrophenolate buffer solutions are shown with a triangle.

If the difference between the dissociation constants is big enough, the A_{HR^-} value can be determined directly and only the first items on the right-hand side of Equations 3.4 and 3.5 can be used for the calculation of the constants. But if the yield of the single-charged anion, HR^- , does not reach 100 % at any $\text{pa}_{\text{H}^+}^*$ value, then an iterative procedure should be used. The method of calculations was as follows. As the first approximation, A_{HR^-} was equated to the maximal absorption in Figure 3.14. The dissociation constants were calculated under the assumption that stepwise equilibria are isolated. Then the A_{HR^-} value was refined using Equation 3.6, and the values were successively improved via Equations 3.4 and 3.5.

In dilute picric acid solution, the $[\text{HR}^-]$ values were determined from the absorption spectra. The $a_{\text{H}^+}^*$ values were calculated using Equation 3.9, which is derived using the equations of mass action law for the picric acid, mass balance, and electroneutrality.

$$(a_{\text{H}^+}^*)^2 + a_{\text{H}^+}^* \{K_{\text{HPic}} f_1^{-1} - [\text{HR}^-] f_1\} - K_{\text{HPic}} \{c_{\text{HPic}} - [\text{HR}^-]\} = 0 \quad (3.9)$$

First, the f_1 value was equated to unity. Then, the ionic strength was approximately equated to $a_{\text{H}^+}^*$, and after evaluation of the f_1 value the calculations were repeated. Finally, knowing $a_{\text{H}^+}^*$, $[\text{HR}^-]$, and f_1 , the K_{a1} value was obtained. After five iterations, the results became stable. The $\text{pa}_{\text{H}^+}^*$ values indicated in Figures 2a and 3 are obtained as a result of the first iteration.

The calculations of the $\text{pa}_{\text{H}^+}^*$ values and ionic strengths of the buffer mixtures were performed using the values of the dissociation constants of the buffer acid and buffer salts (see Appendix B). However, the data obtained with the two dinitrophenolate buffer systems were considered only as supporting information. As a rule, three wavelengths around the absorption maximum of the HR^- anion were used. For instance, the final A_{HR^-} value at 522 nm (Figure 3.14) was 2.455. This value was used to calculate the molar extinction coefficient of the single-charged anion.

Spectrophotometric data for the two pentanitrofluoresceins (Figures 3.16 and 3.17) were processed in the same way.

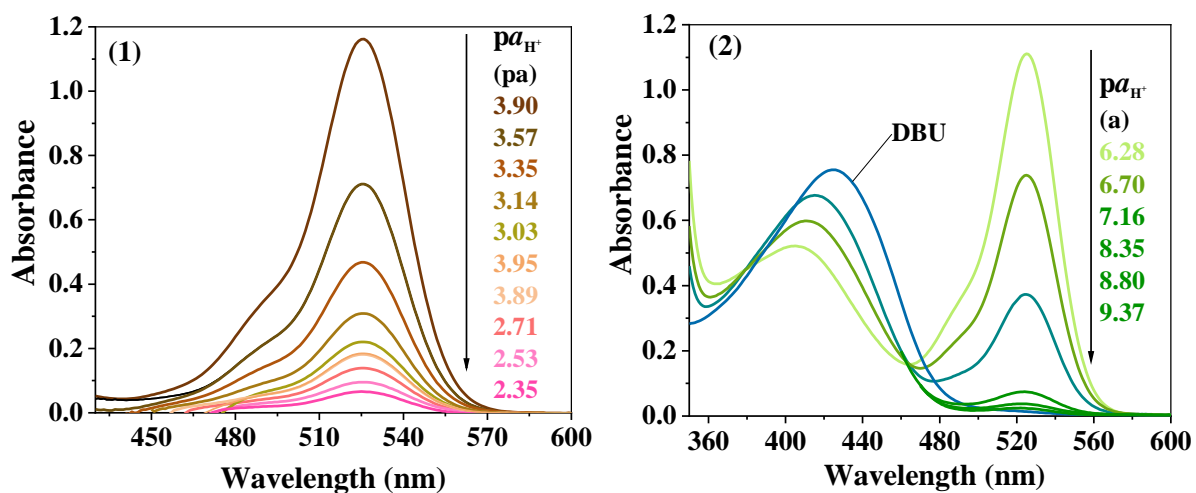


Figure 3.16: Steady-state absorption spectra of 2,4,5,7,4'-pentanitrofluorescein (4.7×10^{-5} M) in diluted solutions of the picric acid (pa) (1) and in the salicylate buffer solutions (a) (2). The R^{2-} spectrum was obtained in 0.02 M DBU solution.

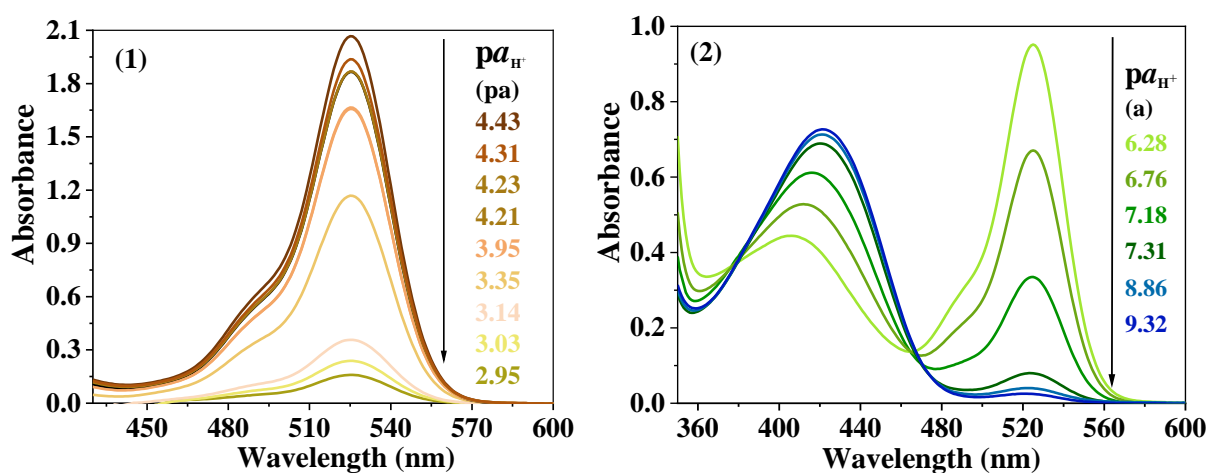


Figure 3.17: Steady-state absorption spectra of 2,4,5,7,5'-pentanitrofluorescein (4.4×10^{-5} M) in diluted solutions of the picric acid (pa) (1) and in the salicylate buffer solutions (a) (2). The R^{2-} spectrum was obtained in 0.02 M DBU solution.

The numerical results are collected in Tables 3.3 and 3.4.

Table 3.3: Molar extinction coefficient of the dyes in acetonitrile – DMSO binary solvent (96 : 4 by mass), 25 °C

Dye	λ_{\max} , nm ($\varepsilon_{\max} \times 10^{-3}, \text{M}^{-1} \text{cm}^{-1}$)		
	Neutral	Monoanion	Dianion
2,4,5,7-Tetranitrofluorescein methyl ester	452 (37.9) ^a	523 (112.0)	—
2,4,5,7-Tetranitrofluorescein	— ^b	522 (58.4) ^c	422 (20.0)
2,4,5,7,4'-Pentanitrofluorescein	— ^b	526 (49.2) ^c	425 (16.1)
2,4,5,7,5'-Pentanitrofluorescein	— ^b	525 (64.0) ^c	421 (16.5)

Note. ^a In benzene with 0.1 M sulfuric acid. ^b Almost colorless. ^c Calculated from the equilibrium data jointly with the dissociation constants.

Table 3.4: Indices of the thermodynamic dissociation constants of the dyes in acetonitrile – DMSO binary solvent (96 : 4 by mass), 25 °C

Dye	$\text{p}K_{\text{a}1}$	$\text{p}K_{\text{a}2}$	$\text{p}K_{\text{a}2} - \text{p}K_{\text{a}1}$
2,4,5,7-Tetranitrofluorescein methyl ester	1.95 ± 0.19	—	—
2,4,5,7-Tetranitrofluorescein	4.49 ± 0.08	6.48 ± 0.17	1.99
2,4,5,7,4'-Pentanitrofluorescein	4.02 ± 0.03	6.58 ± 0.10	2.56
2,4,5,7,5'-Pentanitrofluorescein	4.11 ± 0.08	6.5 ± 0.4	2.4

3.4 Special cases of 4,5-dinitro-2,7-dibromofluorescein and 5'-nitrofluorescein in DMSO

The dye 4,5-dinitro-2,7-dibromofluorescein reflects to some extent the aforesaid features of tetra- and pentanitrofluoresceins. The destabilization of the deeply colored tautomers of the R^{2-} form is expressed but not complete (Figure 3.18, 2). The values of $\text{p}K_{\text{a}1}$ and $\text{p}K_{\text{a}2}$ were easily determined separately in *p*-TSA solutions and benzoate buffers, respectively (Figure 3.19), and added to Table 3.1. In the $\text{p}a_{\text{H}^+}$ range equal 10÷12 the increase of absorbance was observed. Further study of this phenomenon was impossible due to the small amount of the dye.

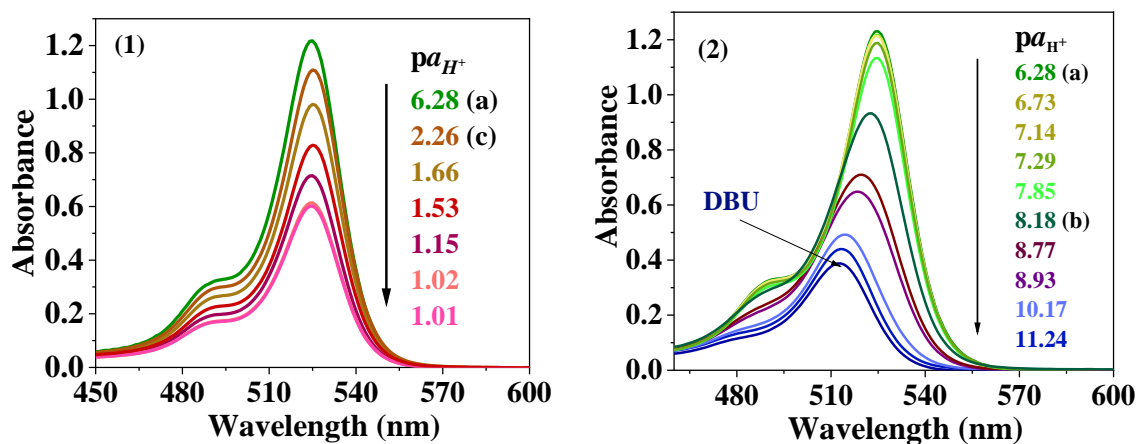


Figure 3.18: Steady-state absorption spectra of 4,5-dinitro-2,7-dibromofluorescein in DMSO at different pK_a^* : in *p*-toluenesulfonic acid solutions (c) and salicylate (a) and benzoate (b) buffer solutions.

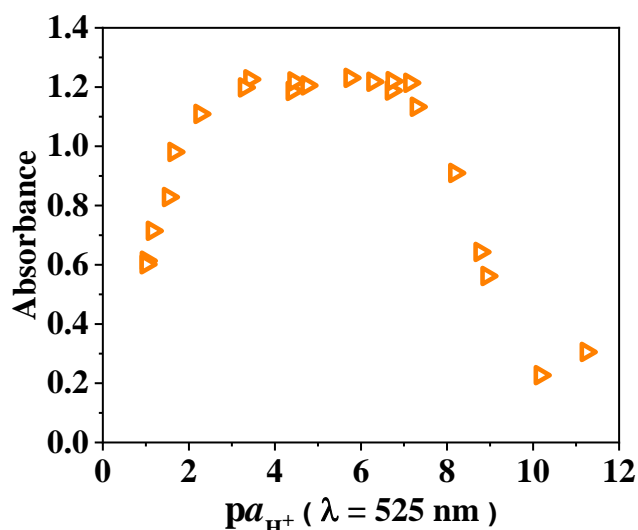


Figure 3.19: Dependence of absorption of 4,5-dinitro-2,7-dibromofluorescein in DMSO at $\lambda = 525$ nm on pK_a^* .

Having the pK_a s for all the dyes, the absorption spectra of the HR^- ion can be obtained using Equation 3.6. However, in the case of 4,5-dinitro-2,7-dibromofluorescein, this ion predominates within a wide pK_a^* range, and its spectrum was determined directly. The molar extinction coefficients of the molecular and ionic forms are gathered in Table 3.2.

The spectra of 5'-nitrofluorescein at different pK_a^* values in DMSO are presented in Figures 3.20 – 3.23. The gradual decrease of the intensive band of the R^{2-} form occurs along with pK_a^* decreasing. Here, the HR^- spectrum is difficult to identify, because the expressed

decolorization of the dye gives evidence for the presence of substantial fractions of the neutral form, H_2R , which exist mainly as a colorless lactone.

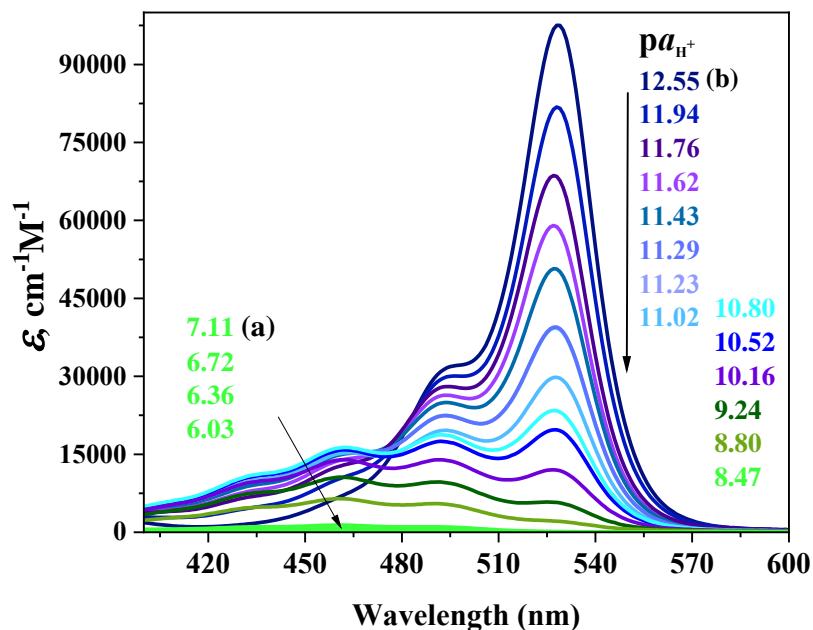


Figure 3.20: Steady-state absorption spectra of 5'-nitrofluorescein at different $pK_{aH^+}^*$ values in DMSO: salicylate (a) and benzoate (b) buffer solutions.

In Figure 3.21, the spectra in the lower $pK_{aH^+}^*$ region are presented in a more obvious manner. Here, the absorption of HR^- is clearly seen. The band at 528 nm is still present, but at $pK_{aH^+}^* \leq 9.2$ it disappears.

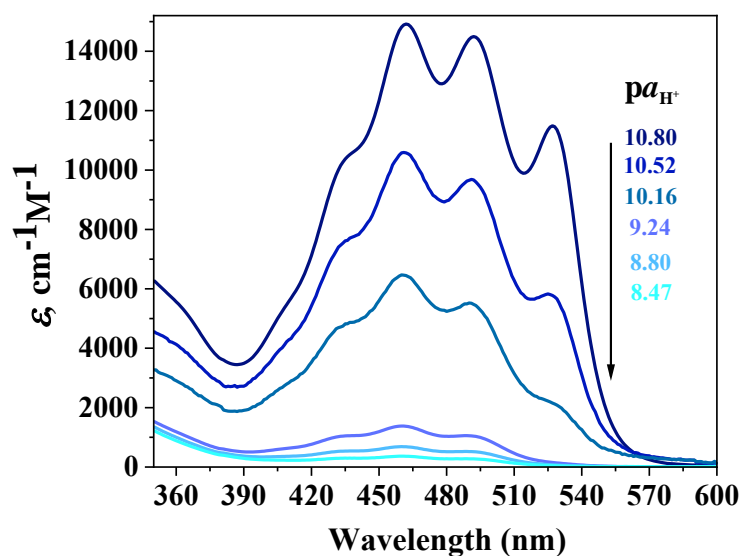


Figure 3.21: Absorption of 5'-nitrofluorescein in the acidic range of the benzoate buffer solutions in DMSO.

Chapter 3

On the other hand, the spectrum of the neutral form, H₂R, exhibits much lower intensity (Figure 3.22). Therefore, within a $pa_{\text{H}^+}^*$ range from ≈ 8 to ≈ 9 , the $pK_{\text{a}1}$ value can be determined by Equation 3.10.

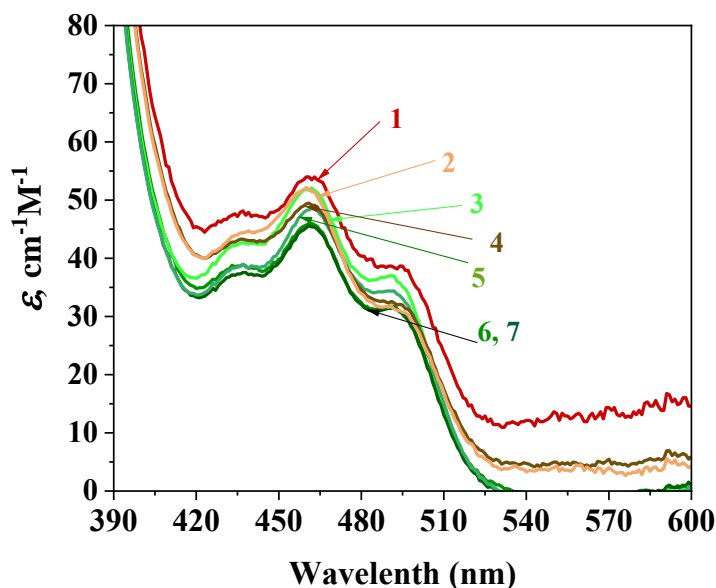


Figure 3.22: Absorption of 5'-nitrofluorescein around the spectra of the neutral form, H₂R. The values in the activity scale $pa_{\text{H}^+}^*$ are as follows: 4.12 (1); 3.60 (2); 7.11 (3); 3.90 (4); 6.72 (5); 6.36 (6); 6.03 (7); *p*-TSA and salicylic buffer solution were used.

$$pK_{\text{a}1} = pa_{\text{H}^+}^* + \log \frac{\varepsilon_{\text{HR}^-} - \varepsilon}{\varepsilon - \varepsilon_{\text{H}_2\text{R}}} - \log f_1 \quad (3.10)$$

At 460 nm, the ε_{max} value of the molecular form is $47.3 \text{ M}^{-1} \text{ cm}^{-1}$. As the absorptivity of the HR⁻ ion, unavailable by direct determination, the $\varepsilon_{\text{HR}^-}$ value of the ethyl ester of 5'-nitrofluorescein, $25.8 \times 10^3 \text{ M}^{-1} \text{ cm}^{-1}$ (see Chapter 4). In benzoate and salicylate buffer solutions, $pK_{\text{a}1} = 10.6 \pm 0.1$. Then, the $pK_{\text{a}2}$ value was determined using a set of benzoate buffers with $pa_{\text{H}^+}^*$ from 12.55 to 10.80, using the wavelengths around λ_{max} of the R²⁻ ion (Figure 3.20). Calculations were performed using Equation 3.5: $pK_{\text{a}2} = 11.8 \pm 0.1$. The HR⁻ spectrum was refined using Equation 3.6 and the above obtained $pK_{\text{a}1}$ and $pK_{\text{a}2}$ values (Figure 3.23).

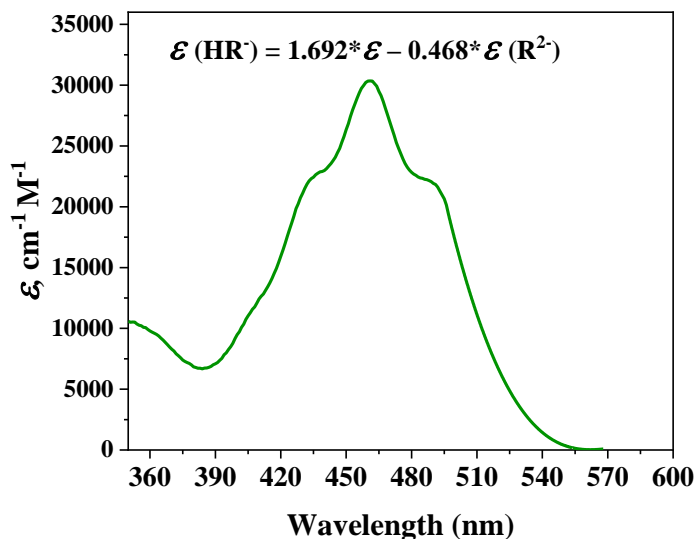


Figure 3.23: The spectrum of the single-charged anion of 5'-nitrofluorescein, HR^- , in DMSO.

In this work, we do not consider the formation of dye cations, because, for the nitrofluoresceins bearing the NO_2 groups in the xanthenes part, the corresponding $\text{p}K_{\text{a}0}$ values (see Equation 1.1) are substantially negative. However, in the case of 5'-nitrofluorescein the dissociation constant of the cation, H_3R^+ , can be obtained in diluted solutions of *p*-TSA (Figure 3.24). As the ϵ_{max} value of the cation, the corresponding value of the 5'-nitrofluorescein ester cation, $58.5 \times 10^3 \text{ M}^{-1} \text{ cm}^{-1}$ (see Chapter 4) was used. The acid concentration was from 0.0025 to 0.0423 M; $\text{p}K_{\text{a}0} = -0.28 \pm 0.03$.

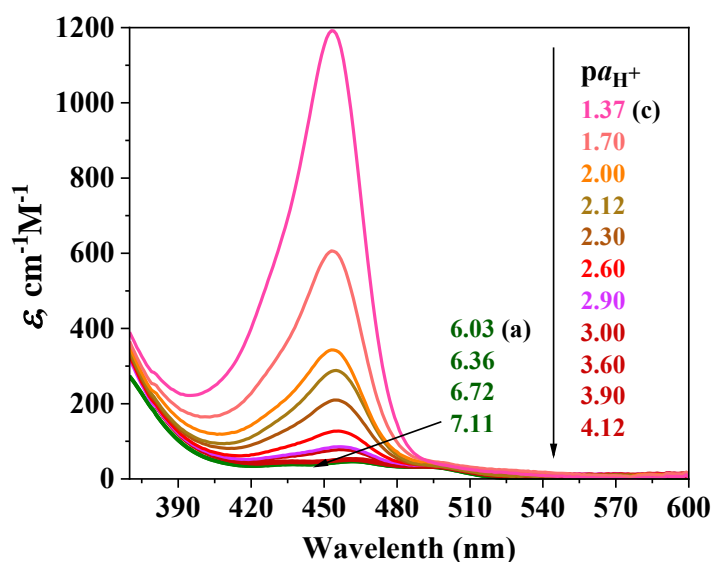


Figure 3.24: Absorption spectra of 5'-nitrofluorescein in DMSO in the acidic region (*p*-toluenesulfonic acid solutions (c) and in salicylate (a) buffer solutions).

Chapter 3

It can be stated that this dye belongs to the “fluorescein type”; the monoanion exists in solution as the HQ^- tautomer. This is the only exception to the series of nitrofluoresceins discussed above.

Finally, in Figure 3.25, several spectra of 4'-nitrofluorescein in DMSO are presented.

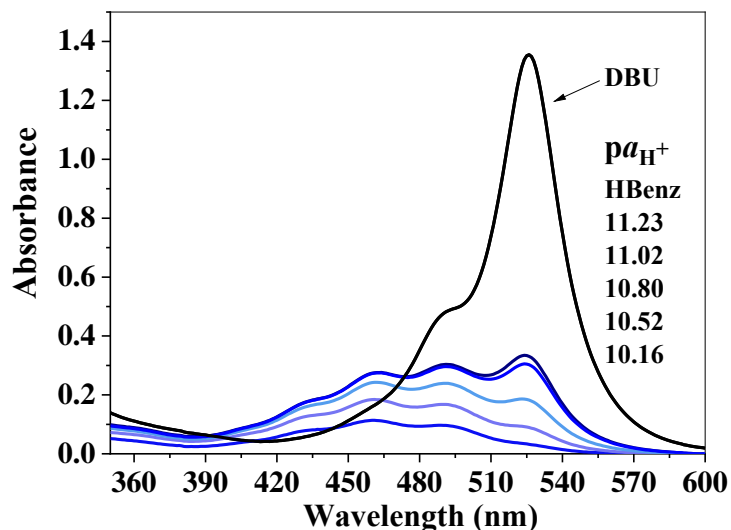
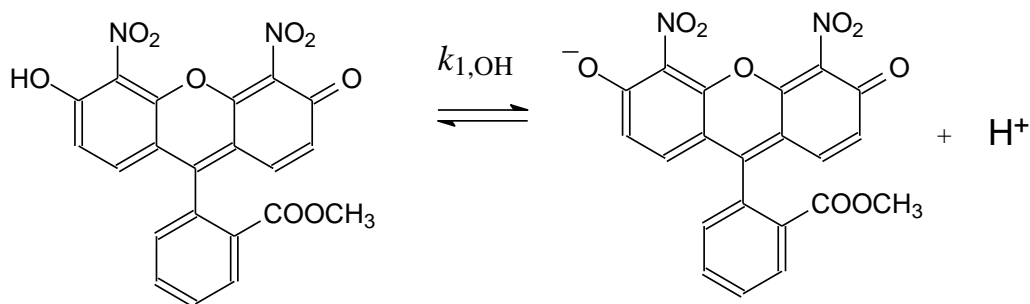


Figure 3.25: Steady-state absorption spectra of 4'-nitrofluorescein in DMSO in benzoate buffer solutions

This dye was not studied in a more detailed manner, but the general picture is similar to that observed for the 4'-isomer.

3.5 4,5-Dinitrofluorescein: Detailed scheme of the protolytic equilibrium

First, let us compare the pK_{a1} value of 4,5-dinitrofluorescein methyl ester with the pK_{a2} of 4,5-dinitrosulfonephthalein: 3.79 and 4.88, respectively. The difference is obviously caused by the additional negative charge in the second case, which hinders the release of the H^+ ion.



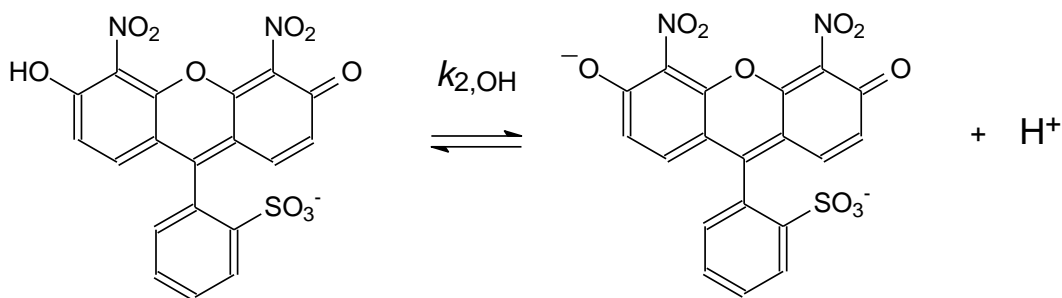


Figure 3.26: The dissociation of methyl ester of 4,5-dinitrofluorescein (top panel) and 4,5-dinitrosulfofluorescein (bottom panel).

The effect can be explained by the Bjerrum – Kirkwood – Westheimer equation:

$$pk_{2,\text{OH}} - pk_{1,\text{OH}} = \frac{e^2 N_A}{2.303RT \times 4\pi\epsilon_0\epsilon_{\text{eff}} r} = \frac{24.7}{\epsilon_{\text{eff}} r} \quad (3.11)$$

Here, R , T , and ϵ_0 have their usual meanings, ϵ_{eff} is the effective relative permittivity of the space permeated by the electric field lines, r is the distance (in nm) between the dissociating group and the negatively charged substituent [16]. For more details, see the book by Vereshchagin [17].

Now let us compare the pK_{a1} ($=pk_{1,\text{OH}}$) of ethyl ester of fluorescein is 10.91; the difference is 7.1; for sulfonefluorescein, pK_{a2} ($=pk_{2,\text{OH}}$) is 12.3, and the difference is 7.4. This reflects the influence of two nitro groups. At the first glance, the difference between the pK_{a1} values of fluorescein methyl ether (13.7) and its 4,5-dinitro analog (9.61) does not confirm this regularity, being equal to 4.1. However, as it was proved in a previous paper [18], the predominating tautomers of the anions of these dyes are different:

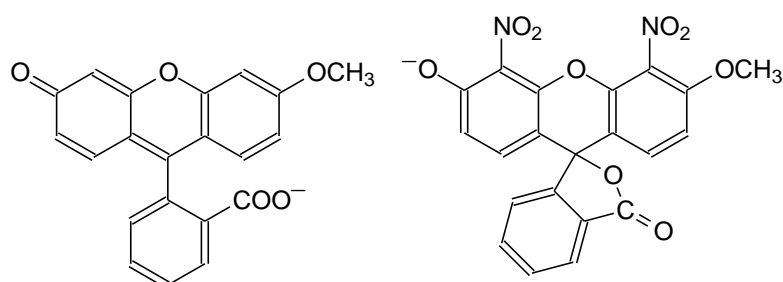


Figure 3.27: The structures of the single-charged anions of methyl ethers of fluorescein (left) and 4,5-dinitrofluorescein (right).

As it is shown above, see Figure 3.4, the monoanion HR^- of 4,5-dinitrofluorescein is represented by the tautomer of the HX^- type. The neutral form, H_2R , is an equilibrium mixture

Chapter 3

of the lactonic and quinonoidal tautomers, H₂L and H₂Q, respectively (see Figure 3.5 and Chapter 1, a scheme in Figure 1.8). Hence, the dissociation of 4,5-dinitrofluorescein occurs like that of 2,4,5,7-tetrabromo- and iodofluoresceins [3, 5, 16, 18] Equations 1.6 and 1.7, or 3.12 and 3.13, respectively, give the connection between the experimental K_a values and microscopic dissociation constants.

$$pK_{a1} = pk_{1,OH} + \log(1 + K_T) = pk_{1,OH} - \log \alpha_{H_2Q} \quad (3.12)$$

$$pK_{a2} = pk_{2,COOH} \quad (3.13)$$

The $pK_{a2} = pk_{2,COOH}$ value is equal to 9.9 (Table 3.1). The same value for 2,4,5,7-tetraiodofluorescein (erythrosin) is equal to 10.6 [18]. This value was determined in benzoate buffer solutions; recalculations taking into account the heteroassociation of the benzoic acid resulted in a value of 10.1. The difference of 0.2 pK_a units can be ascribed to the influence of the nitro groups; the transmittance of the electronic effects in the fluorescein system is considered in Chapter 4.

The estimation of the α_{H_2Q} value can be made using Equation 3.14.

$$\alpha_{H_2Q} = \frac{\varepsilon_{\max}(H_2R)}{\varepsilon_{\max}(HR_{\text{ester}})} \quad (3.14)$$

The shape of the spectrum of the ester of the dye (Figure 3.1, c) is similar to that of the mother dye (Figure 3.5). The specificity of the nitro derivatives consists in the yellowish color of the lactones (Figure 3.5), whereas for fluorescein and the halogen derivatives, the absorption of the lactone exhibits no contribution to the visible portion of the spectrum. However, the ratio of the molar extinction coefficients at 446 to 474 nm is 1.21 and 1.19 for the ester and mother dye, respectively (Table 3.2). This allows expecting that at 446 nm and even more so at 474 nm, the influence of the lactone is negligible. As result, a value $\alpha_{H_2Q} = 1.25 \times 10^{-3}$ is estimated using the wavelength 474 nm; $\log \alpha_{H_2Q} = -2.90$. Hence, $pk_{1,OH} = 4.1$, which is close to the $pk_{1,OH} = 3.8$ value of the ester (Table 3.1). The last-named serves as a model compound. For esters of eosin (Chapter 4), $pk_{1,OH} = 2.8-2.9$.

Concluding, the proposed “eosin-like” dissociation scheme is valid for 4,5-dinitrofluorescein.

3.6 Dyes that form anionic lactones: Dissociation and tautomerism of tetra- and pentanitro fluoresceins in DMSO

Whereas in the case of the neutral forms, H_2R , and dianions, R^{2-} , the lactonic tautomers H_2L and L^{2-} , respectively, predominate, the monoanionic form HR^- is intensively colored (Table 3.2). At the same time, the maximal molar extinction coefficient of the HR^- ions are ca. 10% lower than that of the methyl ester of 2,4,5,7-tetranitrofluorescein (Figure 3.12). Therefore, the fraction of the tautomer HX^- can be calculated by Equation 3.15.

$$\alpha_{HX^-} = \frac{\varepsilon_{\max}(HR^-)}{\varepsilon_{\max}(R_{\text{ester}}^-)} \quad (3.15)$$

The results are presented in Table 3.5.

Table 3.5: Fractions of tautomers and the indices of the microscopic dissociation constants

Dye	α_{HX^-}	α_{HL^-}	$pK_{1,L}$	$pK_{2,L}$	$pK_{2,L} - pK_{1,L}$	ε_{eff}
2,4,5,7-Tetranitrofluorescein	0.56	0.44	1.66	4.04	2.4	14.5
2,4,5,7,4'-Pentanitrofluorescein	0.90	0.10	1.59	3.42	1.8	21.2
2,4,5,7,5'-Pentanitrofluorescein	0.91	0.09	1.72	3.40	1.7	23.7

Knowing these values, the so-called microscopic dissociation constants, k , can be estimated. From the detailed dissociation scheme (Figure 3.28), equations (3.16)–(3.18) can be derived.

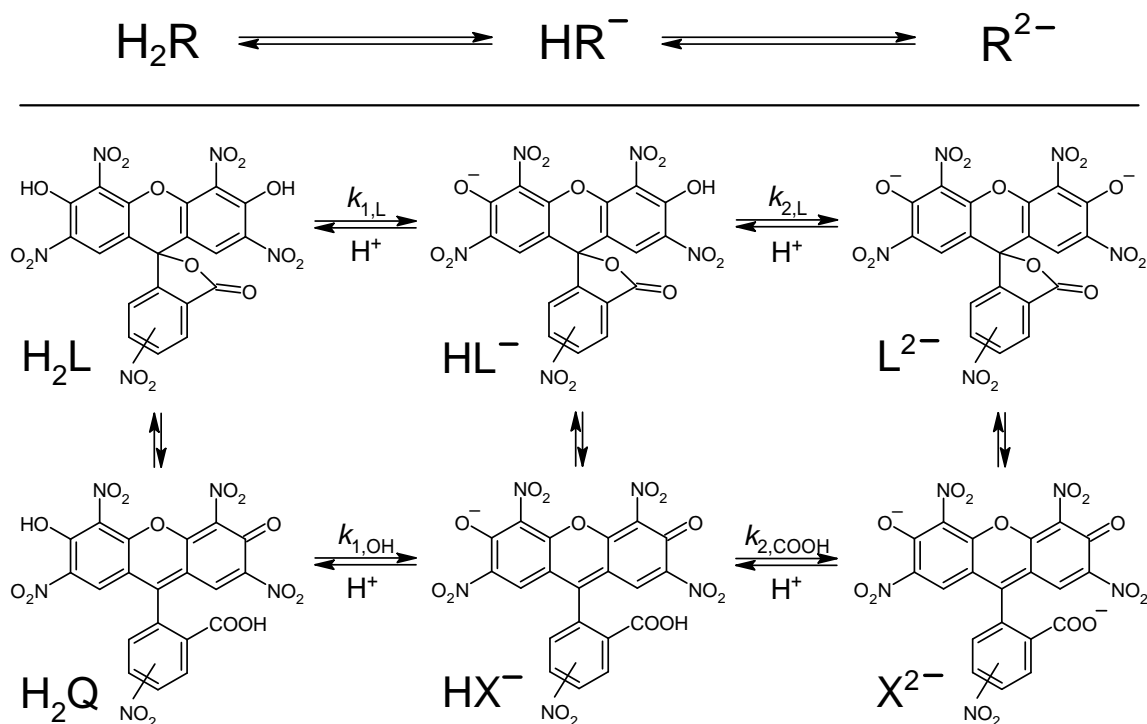


Figure 3.28: Detailed scheme of protolytic equilibrium of the nitro derivatives of fluorescein.

$$pk_{2,\text{L}} = pK_{a2} + \log \alpha_{\text{HL}^-} \quad (3.16)$$

$$pk_{1,\text{L}} = pK_{a1} + \log \alpha_{\text{H}_2\text{L}} - \log \alpha_{\text{HL}^-} \quad (3.17)$$

$$pk_{1,\text{OH}} = pK_{a1} + \log \alpha_{\text{H}_2\text{Q}} - \log \alpha_{\text{HX}^-} \quad (3.18)$$

Thus obtained $pk_{1,\text{L}}$ and $pk_{2,\text{L}}$ values allow us to evaluate the difference between the stepwise dissociation of the OH groups of the lactone H_2L , $pk_{2,\text{L}} - pk_{1,\text{L}}$ (Table 3.5). The effect can be explained by the Bjerrum – Kirkwood – Westheimer equation (3.19), where the term $\log 4$ reflects the statistical factor [16, 17].

$$pk_{2,\text{L}} - pk_{1,\text{L}} = \log 4 + \frac{e^2 N_A}{2.303RT \times 4\pi\epsilon_0\epsilon_{\text{eff}}r} = 0.602 + \frac{24.7}{\epsilon_{\text{eff}}r} \quad (3.19)$$

The $r = 0.95$ nm value for these dyes was estimated by Dr. V. S. Farafonov in this Department. Thus estimated ϵ_{eff} values are presented in Table 3.5. The average value is 20,

while the relative permittivity of the solvent equals 46.5. This allows concluding that the influence of charged group occurs both through the aromatic molecule and through the solvent.

Finally, the reasons for the strongly pronounced lactonization of molecules and dianions, on the one hand, and commensurable concentrations of HL^- and HX^- tautomers should be explained. Electro-deficient nitro groups reduce the electron density on the nodal carbon atom thus favoring the intramolecular acid-base reaction, i.e., lactone formation. This leads to lactonization even in the case of dianions. On the other hand, the structure HL^- is an asymmetrical one. In contrast, the negatively charged chromophore system of the quinonoidal structure HX^- is symmetrical, because the image is conventional and both oxygen atoms are equal. Therefore, the equipotential charge distribution favors the stability of the structure. In addition, the presence of DMSO molecules, which are hydrogen bond acceptors, stabilizes the COOH groups.

The expressed stability of the lactones in the case of fluorescein dyes bearing nitro groups in the xanthenes moiety is obviously connected with the electrophilicity of the NO_2 groups, which enhances the effective positive charge on the nodal carbon atom C_9 . The quantum-chemical calculations confirm this statement [19].

Returning to the 4,5-dinitrofluorescein dye, a rough estimate of the fraction of the lactonic monoanion can be made, as it was shown previously, the single-charged anion R^- of the methyl ether of 4,5-dinitrofluorescein (Figure 3.21) exists in DMSO as a lactone L^- [18]; see also section 3.5. If we use the following equation for 4,5-dinitrofluorescein:

$$\text{p}K_{\text{a1}} = \text{p}k_{1,\text{L}} - \log \alpha_{\text{H}_2\text{L}} + \log \alpha_{\text{HL}^-} \quad (3.20)$$

and assume that $\alpha_{\text{H}_2\text{L}} \rightarrow 1$ and that instead of $\text{p}k_{1,\text{L}}$ the $\text{p}K_{\text{a1}}$ value of the dye ether (= 9.6) can be used, we obtain the value $\alpha_{\text{HL}^-} \approx 3 \times 10^{-3}$. Hence, the lactonic tautomer of the 4,5-dinitrofluorescein monoanion, HL^- , should be excluded from the consideration. Hence, the tautomer HX^- predominates.

A special case is 4,5-dinitro-2,7-dibromofluorescein. In the case of this dye, the drop of the molar absorptivity of R^{2-} is very expressed. Whereas the rather high maximal molar absorptivity of the single-charged HR^- form equals $96.2 \times 10^3 \text{ M}^{-1} \text{ cm}^{-1}$ (Table 3.2) and does not give reason to assume the presence of a high fraction of HL^- tautomer, the $\epsilon_{\text{max}} = 30.6 \times 10^3 \text{ M}^{-1} \text{ cm}^{-1}$ value for the R^{2-} ion leaves no doubt about the presence of the L^{2-} lactones besides the deeply colored X^{2-} tautomer. Then $\alpha_{\text{X}^{2-}} = 30.6/96.2 = 0.32$, $\alpha_{\text{L}^{2-}} = 0.68$. Thus, the dissociation

Chapter 3

should be described as the first approximation by the scheme: $\text{HX}^- \rightarrow (\text{X}^{2-} \rightleftharpoons \text{L}^{2-})$. Therefore, the $\text{p}k_{2,\text{COOH}}$ value can be estimated as $\text{p}K_{\text{a}2} - \log \alpha_{\text{X}^{2-}} = 9.4$. This value is lower than those for erythrosin, and 4,5-dinitrofluorescein (see above). This allows assuming that the nitro groups in concert with the bromine substituents affect the carboxyl group, despite the almost complete absence of conjugation between the two parts of the molecule.

3.7 Tautomerism in acetonitrile with 4 mass % DMSO

The main difference between the behavior of the tetra- and pentanitro fluoresceins in DMSO and acetonitrile with 4 mass % DMSO is the pronounced decrease in the HR^- molar absorptivity in this above binary solvent. The results of calculations of the monoanionic tautomers fractions are presented in Table 3.6. The data allows us to assume that the HR^- forms consist of a commensurable concentration of intensively colored HX^- tautomer and a lactonic anion HL^- . Note that the single-charged anions are fluorescent owing to the presence of the HX^- tautomer.

Table 3.6: Fractions of tautomers and the indices of the microscopic dissociation constants in acetonitrile with 4 mass % DMSO

Dye	α_{HX^-}	α_{HL^-}	$\text{p}k_{1,\text{L}}$	$\text{p}k_{2,\text{L}}$	$\text{p}k_{2,\text{L}} - \text{p}k_{1,\text{L}}$	ϵ_{eff}
2,4,5,7-Tetranitrofluorescein	0.52	0.48	4.8	6.2	1.4	32
2,4,5,7,4'-Pentanitrofluorescein	0.44	0.56	4.3	6.3	2.0	18
2,4,5,7,5'-Pentanitrofluorescein	0.57	0.43	4.5	6.2	1.7	24

The $\text{p}k_{1,\text{L}}$ value can be calculated by taking $\alpha_{\text{H}_2\text{L}}$ close to unity. The results are collected in Table 6. The tautomerization constants of the $\text{HX}^- \rightleftharpoons \text{HL}^-$ equilibrium are 0.92, 1.27, and 0.75, respectively. Also, the fractions of the tautomer H_2Q may be estimated. For example, if the $\text{p}k_{1,\text{OH}}$ value of 2,4,5,7-tetranitrofluorescein is equated to that of its methyl ester, a $\alpha_{\text{H}_2\text{Q}}$ value of 1.5×10^{-3} follows from equation (3.17). Hence, the negligible content of this tautomer is confirmed in such an indirect way.

The ϵ_{eff} values (Table 3.6) were calculated via Equation 3.18, as it was shown above for solutions in the entire DMSO. The average value is 25, while the relative permittivity of the solvent equals 36.95. Hence, in this case, the influence of charged group again occurs both through the aromatic molecule and through the solvent.

3.8 Detailed scheme of protolytic equilibrium of 5'-nitrofluorescein

Judging from the absorption spectra, first of all, in Figure 3.23, the monoanion HR^- exists as the quinoidal tautomer, HQ^- (see Chapter 1). Here, Equations 3.21 and 3.22 are valid.

$$pK_{a1} = pk_{1,\text{COOH}} - \log \alpha_{\text{H}_2\text{Q}} \quad (3.21)$$

$$pK_{a0} = pk_{0,\text{OH}} + \log \alpha_{\text{H}_2\text{Q}} \quad (3.22)$$

Here, the pK_{a0} value refers to the dissociation of a cation H_3R^+ (Equation 1.1). The absorption in the visible region of the molecular forms of 5'-nitrofluorescein (Figure 3.22) and of ester of this dye (see Chapter 4), and of the 5'-nitrofluorescein anion HR^- (Figure 3.23) exhibit analogous shapes. The fraction of the H_2Q tautomer, $\alpha_{\text{H}_2\text{Q}}$, can be estimated using the spectrum of the ethyl ester of the same dye, Equation 3.23.

$$\alpha_{\text{H}_2\text{Q}} = \frac{\varepsilon_{\max}(\text{H}_2\text{R})}{\varepsilon_{\max}(\text{HR}_{\text{ester}})} \quad (3.23)$$

The corresponding molar absorptivities are 47 and $25.8 \times 10^3 \text{ M}^{-1} \text{ cm}^{-1}$, respectively, and $\alpha_{\text{H}_2\text{Q}} = 2.1 \times 10^{-3}$. The $pk_{0,\text{OH}}$ value of 5'-nitrofluorescein corresponds to the dissociation of the cation with the formation of the H_2Q tautomer (Figure 3.29).

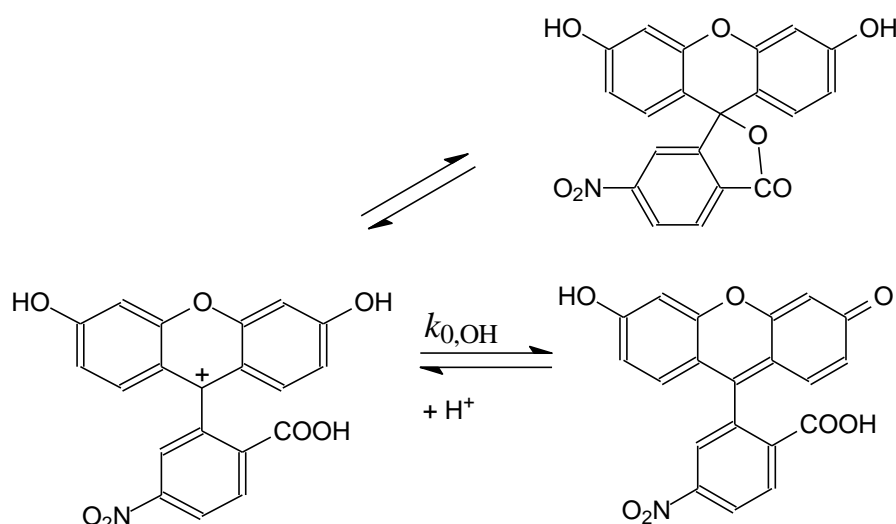


Figure 3.29: The dissociation scheme of the 5'-nitrofluorescein cation with the formation of the H_2L and H_2Q tautomers.

The dissociation of the ester cation is shown in Figure 3.30.

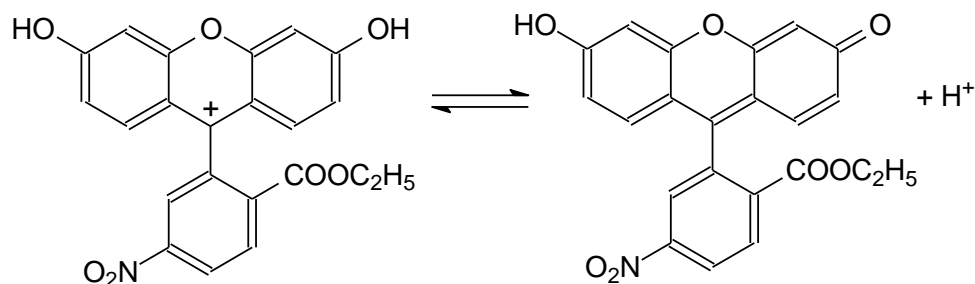


Figure 3.30: The dissociation scheme of the 5'-nitrofluorescein cation.

For 5'-nitrofluorescein in DMSO, $\log \alpha_{\text{H}_2\text{Q}} = -2.68$. Hence, $\text{p}k_{1,\text{COOH}} = 7.9$ and $\text{p}k_{0,\text{OH}} = 2.4$. The first value is substantially lower than that of fluorescein ($\text{p}k_{1,\text{COOH}} = 10.7$) [18], because of the strong influence of the nitro group. Indeed, the Hammett σ_p value for the NO_2 group is $+0.78$, whereas the ρ constant in DMSO is much higher as compared with that in water. The second value is in good agreement with the value $\text{p}K_{\text{a}0} = 2.44$ (Chapter 4).

There is another point that allows us to distinguish between fluorescein and its 5'-nitro derivative. In the case of fluorescein in DMSO, acetonitrile, and acetone, a small fraction of the HR^- anion converts into the HX^- tautomer, which is not typical for this compound in alcohols and water-organic solvents [18]. The reason is the pronounced increase in the $k_{1,\text{OH}}/k_{1,\text{COOH}}$ ratio in the entire aprotic solvents [18]. However, in the case of 5'-nitrofluorescein, the increase in the $\text{p}k_{1,\text{COOH}}$ value due to the nitro group prevents the formation of the “phenolate” tautomer HX^- .

3.9 Explanation of the $K_{\text{a}1}/K_{\text{a}2}$ ratio in DMSO

The difference between a series of nitrofluoresceins in DMSO is in some cases very different (Table 3.1). This allows disclosing the ratio between the stepwise dissociation constants in systems that are inclined to tautomerism.

For 2,4,5,7-tetranitro-, 2,4,5,7,4'-pentanitro-, and 2,4,5,7,5'-pentanitrofluoresceins, the following equation describes the $K_{\text{a}1}/K_{\text{a}2}$ ratio:

$$\text{p}K_{\text{a}2} - \text{p}K_{\text{a}1} = \text{p}k_{2,\text{L}} - \text{p}k_{1,\text{L}} - 2\log \alpha_{\text{HL}^-} . \quad (3.24)$$

The difference between the $pk_{2,L}$ and $pk_{1,L}$ is within the range of 1.7–2.0 in both solvents under study, and the $pK_{a2} - pK_{a1}$ difference is governed by the state of the equilibrium between HX^- and HL^- . The shift of this tautomeric equilibrium toward the deeply colored HX^- ion favors the resolution of the first and second steps of dissociation.

4,5-Dinitrofluorescein belongs to the “eosin (erythrosin) type” (see Chapter 1). Here, Equation 3.25 is valid:

$$pK_{a2} - pK_{a1} = pk_{2,COOH} - pk_{1,OH} + \log \alpha_{H_2Q} \quad (3.25)$$

The difference $pk_{2,COOH} - pk_{1,OH}$ equals $9.9 - 4.1 = 5.8$. Therefore, it is the extremely low α_{H_2Q} value that decreases the $pK_{a2} - pK_{a1}$ value to 2.9 (Table 3.1).

For erythrosin, the fraction of the quinonoid tautomer, H_2Q , is higher as compared to fluorescein, and the influence of the negative item $\log \alpha_{H_2Q}$ is less pronounced. Though the dissociation constants of the OH and COOH groups approach each other for the unsubstituted dye, the 2, 4, 5, and 7-substitution substantially increase the above difference (Table 1.1). However, in the case of 4,5-dinitrofluorescein, the decrease is substantial, and the $pK_{a2} - pK_{a1}$ value decreases to about 3 units.

The case of 4,5-dinitro-2,7-dibromofluorescein is of special interest. Here, the difference $pK_{a2} - pK_{a1}$ reaches an extremely high value of 7.6. From the equilibrium scheme, the following equation can be deduced:

$$pK_{a2} - pK_{a1} = pk_{2,COOH} - pk_{1,OH} + \log \alpha_{H_2Q} - \log \alpha_{HX^-} + \log \alpha_{X^{2-}} \quad (3.26)$$

If the above estimates (section 3.6) are correct and $\alpha_{X^{2-}} = 0.32$, $\alpha_{HX^-} \approx 1$, and $pk_{2,COOH}$ is about 10, then $pk_{1,OH} - \log \alpha_{H_2Q} = 1.9$. For the dyes in this series, the α_{H_2Q} value is very low: 1.25×10^{-3} for 4,5-dinitrofluorescein and below 1×10^{-3} for tetra- and pentanitro fluoresceins. Therefore, the $pk_{1,OH}$ value should be equal to -1 or even lower.

Quite different is the picture 5'-nitrofluorescein. Taking into account the character of the tautomeric equilibrium, the following equation is appropriate for the dyes of the “fluorescein type”:

Chapter 3

$$pK_{a2} - pK_{a1} = pk_{2,OH} - pk_{1,COOH} + \log \alpha_{H_2Q} \quad (3.27)$$

While the difference $pk_{2,OH} - pk_{1,COOH}$ is equal to 3.9 (see above), the $\log \alpha_{H_2Q} = -2.74$ value diminishes the $pK_{a2} - pK_{a1}$ difference to a very small value of 1.2.

At the same time, the $pK_{a1} - pK_{a0}$ difference is 10.9 and can be expressed as follows:

$$pK_{a1} - pK_{a0} = pk_{1,COOH} - pk_{0,OH} - 2\log \alpha_{H_2Q} \quad (3.28)$$

The first two items on the right side gave 5.44, while the quantity $-2\log \alpha_{H_2Q}$ is with 5.36 ca. the same, and the resolution of the K_{a0} / K_{a1} ratio is pronounced, ca. 10^{11} .

The considered examples explain the discord of the K_{a1} / K_{a2} ratio within the series of nitrofluorescein compounds.

3.10 Conclusions

1. The pK_a values and molar absorptivities of a series of nitrofluorescein dyes are determined in DMSO; several dyes are studied in binary solvent acetonitrile – DMSO (96 : 4 by mass).
2. Interpreting the pK_a values requires an understanding of the state of tautomeric equilibria. The analysis of the absorption spectra in the visible region and evaluation of the tautomerization constants made it possible to calculate the so-called microscopic equilibrium constants of the stepwise dissociation.
3. The behavior of these compounds differs significantly from that of other fluorescein dyes, e.g., halogen derivatives. The shift of the tautomeric equilibrium of the neutral forms of the dyes, H_2R , is shifted toward the lactone, H_2L . The fraction of the quinonoid tautomer, H_2Q , for 4,5-dinitrofluorescein in DMSO, is $\alpha_{H_2Q} = 1.25 \times 10^{-3}$, and for the 2,4,5,7-tetranitro derivatives is even lower.
4. The structures of the mono- and dianions of 4,5-dinitrofluorescein in DMSO are of “eosin”, or “erythrosin” type, with no signs of anionic lactones. The estimated microscopic dissociation constants are in line with the pK_a s of the model compounds: 4,5-dinitrofluorescein ester, ether, and 4,5-dinitrosulfofluorescein.

5. The dyes of the 2,4,5,7-tetranitrofluorescein group, including two pentanitrofluoresceins and 4,5-dinitro-2,7-dibromofluorescein, exhibit principally different behavior. The dyes of this group are inclined to form anionic lactones. The fractions of the anions-lactones, HL^- and L^{2-} are estimated.
6. In the case of tetra- and pentanitrofluoresceins, the R^{2-} ions in DMSO and CH_3CN with 4 mass % DMSO is completely transformed to the L^{2-} tautomer. In water, some fractions of the X^{2-} tautomer are observed.
7. In highly alkaline solutions, the rupture of the pyran ring can occur.
8. The influence of a negative charge of a single-charged anion on the dissociation of the second acidic group is in line with the Bjerrum – Kirkwood – Westheimer equation. This also allowed for estimating the effective relative permittivity of the space between the ionizing groups.
9. The behavior of the 5'-nitrofluorescein is quite different. This is the sole case in this series, where the dissociation of the COOH group takes place before that of the OH group.
10. It is demonstrated that the ratio of K_{a1} / K_{a2} , or the difference $pK_{a2} - pK_{a1}$ is governed by the state of the tautomeric equilibrium of molecules and anions.

Bibliography

1. Gensh, K. V., Zevatskii, Y.E., Samoylov, D. V., Shekhovtsov, S. V., Lebed, A. V., Goga, S.T., Mchedlov-Petrosyan, N.O.: Ionic equilibrium in mixtures of polar protophobic and protophilic non-hydrogen bond donor solvents: Acids, salts, and indicators in acetonitrile with 4 mass % dimethylsulfoxide. *J Mol Liq.* 322, 114560 (2021). <https://doi.org/10.1016/J.MOLLIQ.2020.114560>
2. Konyaev, D., Myerniy, S., Kholin, Y.: CLINP Program, <http://chemo.univer.kharkov.ua/kholin/clinp.html>
3. Mchedlov-Petrosyan, N.O., Vodolazkaya, N.A., Surov, Y.N., Samoylov, D. V.: 2,4,5,7-Tetranitrofluorescein in solutions: novel type of tautomerism in hydroxyxanthene series as detected by various spectral methods. *Spectrochim Acta A Mol Biomol Spectrosc.* 61, 2747–2760 (2005). <https://doi.org/10.1016/J.SAA.2004.09.030>
4. Shekhovtsov, S. V, Mchedlov-Petrosyan, N.O., Kamneva, N.N., Gromovoy, T.Y.: New orange dyes: Nitroderivatives of sulfonefluorescein. *Kharkov Univ. Bull.* 24, 7–18 (2014)
5. Kriklya, N.N., Gromovoy, T.Y., Mchedlov-Petrosyan, N.O.: 4,5-Dinitrosulfonefluorescein and related dyes: Kinetics of reversible rupture of the pyran ring and their interaction with lysozyme. *Coloration Technology.* 137, 658–667 (2021). <https://doi.org/10.1111/COTE.12565>
6. Mchedlov-Petrosyan, N.O., Steinbach, K., Vodolazkaya, N.A., Samoylov, D. V., Shekhovtsov, S. V., Omelchenko, I. V., Shishkin, O. V: The molecular structure of anionic species of 2,4,5,7-tetranitrofluorescein as studied by electrospray ionisation, nuclear magnetic resonance and X-ray techniques. *Coloration Technology.* 134, 390–399 (2018). <https://doi.org/10.1111/COTE.12351>
7. El'tsov, A.V., Samoylov, D.V., Mchedlov-Petrosyan, N.O.: Contribution to the knowledge about colouristic properties of some xanthene dyes. *Kharkiv Univ. Bull.* 5, 75–87 (2000)
8. Moskaeva, E.G., Mosharenkova, A. V, Shekhovtsov, S. V, Mchedlov-Petrosyan, N.O., Karazin, V.N.: Protolytic equilibrium of tetra- and pentanitrofluoresceins in a binary solvent acetonitrile – dimethyl sulfoxide (mass ratio 96 : 4). *Ukrainian Chemistry Journal.* 87, 25–37 (2021). <https://doi.org/10.33609/2708-129X.87.05.2021.25-37>
9. Negishi, Y., Kawarada, A., Suzuki, T.: Synthesis of novel acid-base indicators by nitration of phenolphthalein and fluorescein. *J. College Educ., Yokohama Nat. Univ. The Natural Sciences.* 1, 20–31 (2018).

10. Batistela, V.R., Pellosi, D.S., de Souza, F.D., da Costa, W.F., de Oliveira Santin, S.M., de Souza, V.R., Caetano, W., de Oliveira, H.P.M., Scarminio, I.S., Hioka, N.: pKa determinations of xanthene derivates in aqueous solutions by multivariate analysis applied to UV–Vis spectrophotometric data. *Spectrochim Acta A Mol Biomol Spectrosc.* 79, 889–897 (2011). <https://doi.org/10.1016/J.SAA.2011.03.027>
11. de Freitas, C.F., Vanzin, D., Braga, T.L., Pellosi, D.S., Batistela, V.R., Caetano, W., Hioka, N.: Multivariate analysis of protolytic and tautomeric equilibria of Erythrosine B and its ester derivatives in ionic and non-ionic micelles. *J Mol Liq.* 313, 113320 (2020). <https://doi.org/10.1016/J.MOLLIQ.2020.113320>
12. de Freitas, C.F., Estevão, B.M., Pellosi, D.S., Scarminio, I.S., Caetano, W., Hioka, N., Batistela, V.R.: Chemical equilibria of Eosin Y and its synthetic ester derivatives in non-ionic and ionic micellar environments. *J Mol Liq.* 327, 114794 (2021). <https://doi.org/10.1016/J.MOLLIQ.2020.114794>
13. Snigur, D., Fizer, M., Chebotarev, A., Lukianova, O., Zhukovetska, O.: Spectroscopic and computational studies of erythrosine food dye protonation in aqueous solution. *Dyes and Pigments.* 198, 110028 (2022). <https://doi.org/10.1016/J.DYEPIG.2021.110028>
14. Mchedlov-Petrossyan, N.O., Vodolazkaya, N.A.: Protolytic Equilibria in Organized Solutions: Ionization and Tautomerism of Fluorescein Dyes and Related Indicators in Cetyltrimethylammonium Chloride Micellar Solutions at High Ionic Strength of the Bulk Phase. *Liquids* 2021, Vol. 1, Pages 1-24. 1, 1–24 (2021). <https://doi.org/10.3390/LIQUIDS1010001>
15. Samoylov, D.V., Mchedlov-Petrossyan, N.O., Martynova, V.F., El'tsov, A. V.: Protolytic equilibria of fluorescein nitro derivatives. *Russ J Gen Chem.* 70, 1259–1271 (2000)
16. Mchedlov-Petrossyan, N.O., Kukhtik, V.I., Bezugliy, V.D.: Dissociation, tautomerism and electroreduction of xanthene and sulfonephthalein dyes in N,N-dimethylformamide and other solvents. *J Phys Org Chem.* 16, 380–397 (2003). <https://doi.org/10.1002/POC.654>
17. Vereshchagin, A.N.: *Induktivnyi effekt (Inductive Effect)*. Nauka, Moscow (1987)
18. Mchedlov-Petrossyan, N.O., Cheipesh, T.A., Shekhovtsov, S. V., Ushakova, E. V., Roshal, A.D., Omelchenko, I. V.: Aminofluoresceins Versus Fluorescein: Ascertained New Unusual Features of Tautomerism and Dissociation of Hydroxyxanthene Dyes in Solution. *Journal of Physical Chemistry A.* 123, 8845–8859 (2019). https://doi.org/10.1021/ACS.JPCA.9B05810/SUPPL_FILE/JP9B05810_SI_001.PDF
19. Lebed, A. V., Biryukov, A. V., Mchedlov-Petrossyan, N.O.: A quantum-chemical study of tautomeric equilibria of fluorescein dyes in DmsO. *Chem Heterocycl Compd (N Y).* 50, 336–348 (2014). <https://doi.org/10.1007/S10593-014-1481-8/TABLES/5>

Chapter 4

Transmittance of the electronic effects in the fluorescein molecule: Nitro and amino groups in the phthalic acid residue

The chapter is the basis of the paper titled:

Moskaeva, E.G., Ostrovskiy, K.I., Shekhovtsov, S.V., Mchedlov-Petrosyan, N.O.: Transmittance of electronic effects in the fluorescein molecule: nitro and amino groups in the phthalic acid residue, Kharkiv University Bull. Ser. Chem., 24–32, (2021).

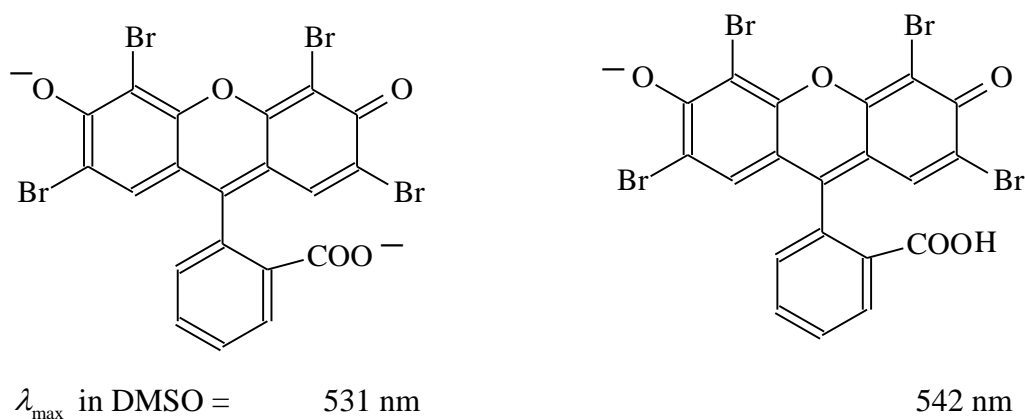
This chapter aims to examine the influence of the substituents in the phthalic residue on the dissociation of the hydroxy group of the compound. This can shed some light on the transmittance of the electronic effects between the two parts of the fluorescein molecule.

Despite the almost orthogonal orientation of the latter concerning the rest of the molecule, some influence of substituents in this 9-aryl ring on the dissociation of the hydroxyl group of the hydroxyxanthene cannot be ruled out. In order to reveal this (possible) effect, we blocked the carboxylic group via esterification. The previous chapter mostly discussed the influence of the nitro group amount in the xanthene part on acid-based properties. This chapter explores the changes in protolytic properties when the nitro group is introduced in the phthalic residue.

In addition, the pK_a values of methyl and ethyl esters of eosin (2,4,5,7-tetrabromofluorescein) were determined in order to clarify the influence of the alkyl group.

4.1 Introduction

Fluorescein and its derivatives belong to the most popular organic dyes in many fields of chemistry and related sciences [1–7]. Despite the huge number of publications devoted to these compounds, there are still many unsolved problems. One of such problem is the influence of the substituents in the arene cycle on the xanthene portion. It is generally known that this cycle, i.e., the residue of the phthalic acid, is rotated by 60–90 ° relative to the xanthene plane [8, 9]. Hence, relatively small electronic interactions between these parts of the molecule should be expected. However, it is firmly proved that the protonation of the COO⁻ group in the dianion of eosin (2,4,5,7-tetrabromofluorescein) and other dyes of this type leads to a bathochromic shift, as it is exemplified in Scheme 4.1.



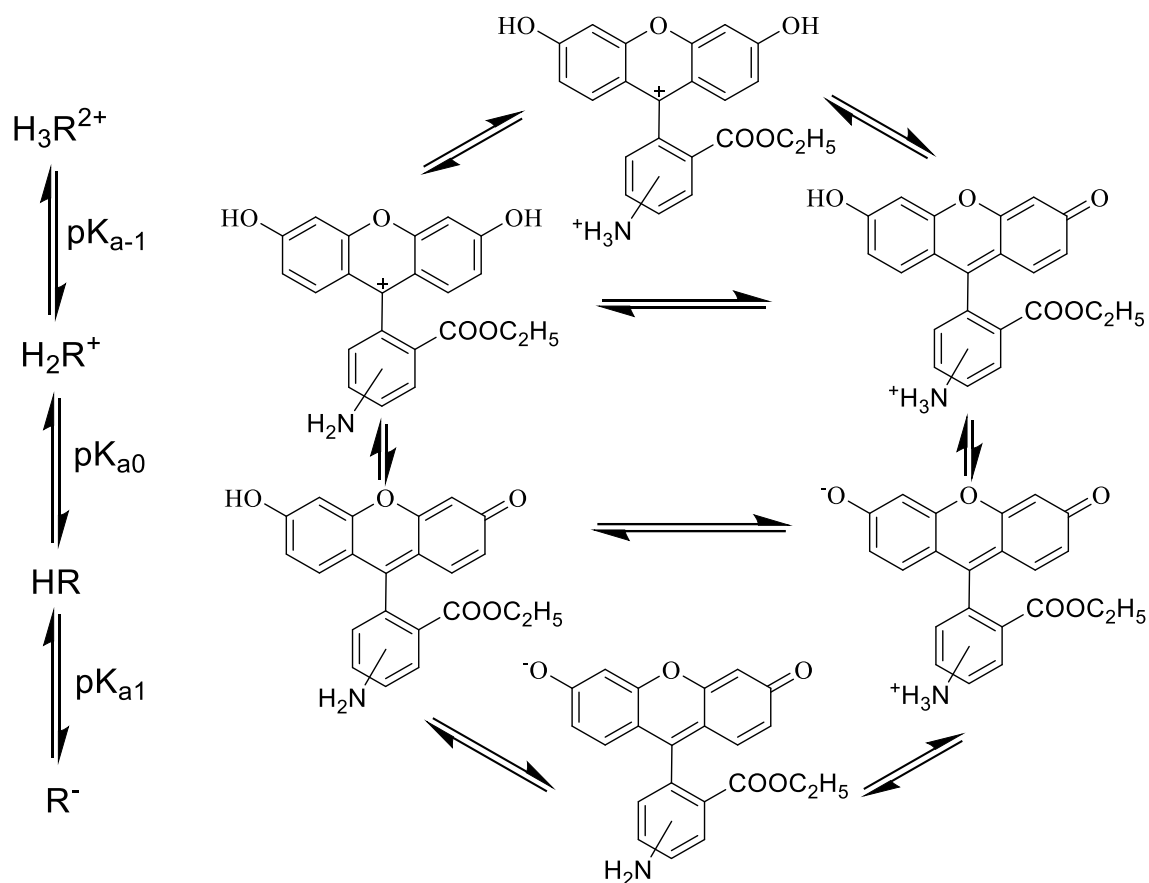
Scheme 4.1: Ions R²⁻ and HR⁻ anions of eosin

In this chapter, we examined the influence of the substituents in the phthalic residue on the dissociation of the hydroxy group of the compound. This can shed some light on the transmittance of the electronic effects between the two parts of the fluorescein molecule.

A number of works are devoted to the study of lactone tautomeric structures [10–12], which are formed by the intramolecular attachment of a deprotonated carboxyl group to a "nodal" electrophilic carbon atom. This leads to a change of the π -electron system in the xanthene fragment and in the electronic absorption spectra of the corresponding forms (hypochromic shift and hypsochromic effect are observed). In addition, different forms differ significantly in terms of luminescence parameters. The highest quantum yields are typical for solutions of deprotonated resorcinol rings of xanthene dyes in not hydrogen donor bond (aprotic) solvents [13].

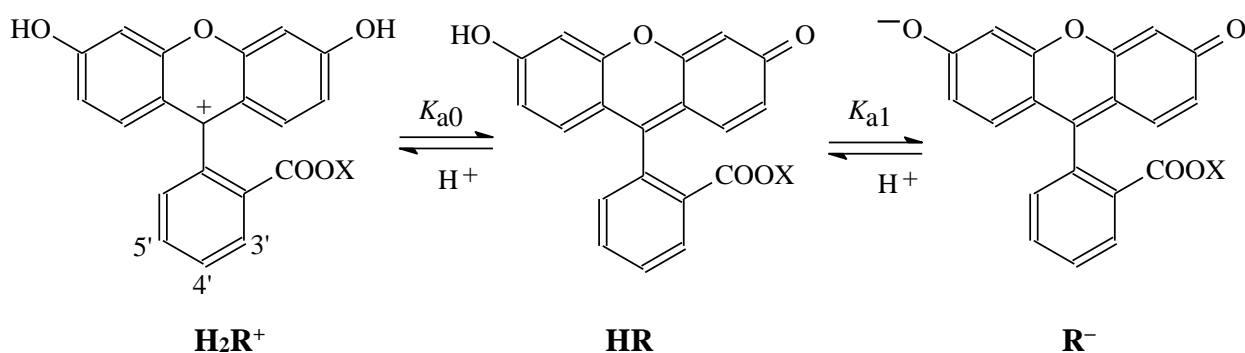
Chapter 4

During the esterification of the carboxyl group, the processes of both its ionization and the formation of lactone and zwitterionic structures become impossible. Therefore, if there is an alkoxy-carbonyl substituent instead of a COOH group, the scheme of protolytic equilibria of fluorescein derivatives is significantly simplified (Scheme 4.2).



Scheme 4.2: Scheme of equilibria of amino-substituted fluorescein esters.

In order to avoid difficulties connected with the interpretation of lactone formation and complicated overlapping equilibria, we decided to examine the methyl (ethyl) esters of fluorescein, Scheme 4.3.



Scheme 4.3: Stepwise dissociation of the esters of nitro and amino fluoresceins; X = CH₃ or C₂H₅. The NO₂ or NH₂ groups occupy positions 3', 4', or 5'.

As substituents that are known to display opposite electronic effects, the nitro and amino groups were chosen. The Hammett σ_{para} constants are +0.78 and -0.57, whereas the σ_{meta} values are +0.71 and -0.09, respectively [14]. In the case of the fluorescein series, the 4-substituents are in the *para* position to the nodal C₉ atom. As a solvent appropriate for the declared goal, dimethyl sulfoxide (DMSO) was used. In this solvent, the Hammett ρ constant for phenols is 4.29, while in water $\rho = 2.11$ [15]. The pK_{a1} values were obtained for all the dyes under study, while those of pK_{a0} were determined only for nitro derivatives because, in the case of the amino fluoresceins, the protonation of the NH₂ group should also be taken into account.

The pK_a values of the fluorescein derivatives were determined in DMSO at 25 °C using spectrometric measurements. The acidity of the solvents in buffer solutions was characterized by the $pa_{H^+}^*$ values. These values were calculated using the pK_{HA} values of the buffer acids and the formation constants of the HA₂⁻ ions, $K_{HA_2}^f$ [16] (Equation 2.2, Chapter 2).

The pK_{HA} values of the salicylic and benzoic acids used in the calculations are 6.80 and 11.10, respectively, $K_{HA_2}^f = 30 \text{ M}^{-1}$ and 60 M^{-1} , respectively [17]. All salts were considered completely dissociated. The f_1 values were calculated using the Debye-Hückel second approach law. The possibility of heteroassociation between the dyes and buffer compounds was ignored. High acidities were created by the *p*-toluenesulfonic acid.

The pK_a values of the dyes were obtained by processing the absorption spectra at different $pa_{H^+}^*$ values. The dye concentrations were two orders of magnitude lower than those of buffer components. The spectra of the forms R⁻ and H₂R⁺ were measured in 0.02 M DBU solution and *p*-toluenesulfonic acid solutions at concentration of 0.2 M, respectively. The spectra that coincide in salicylate buffer solution at $pa_{H^+}^* = 5.93$, in pure salicylic and benzoic acids with concentrations of 0.02 and 0.21 M, respectively can be considered as the first approximation as the spectra of the HR forms. The problem of the HR spectra will be discussed below.

The absorption spectra are typified in Figures 4.1–4.3 at different $pa_{H^+}^*$: in salicylate (a) and benzoate (b) buffer solutions and in *p*-toluenesulfonic acid solutions (c). The remaining spectra are presented in Appendix C.

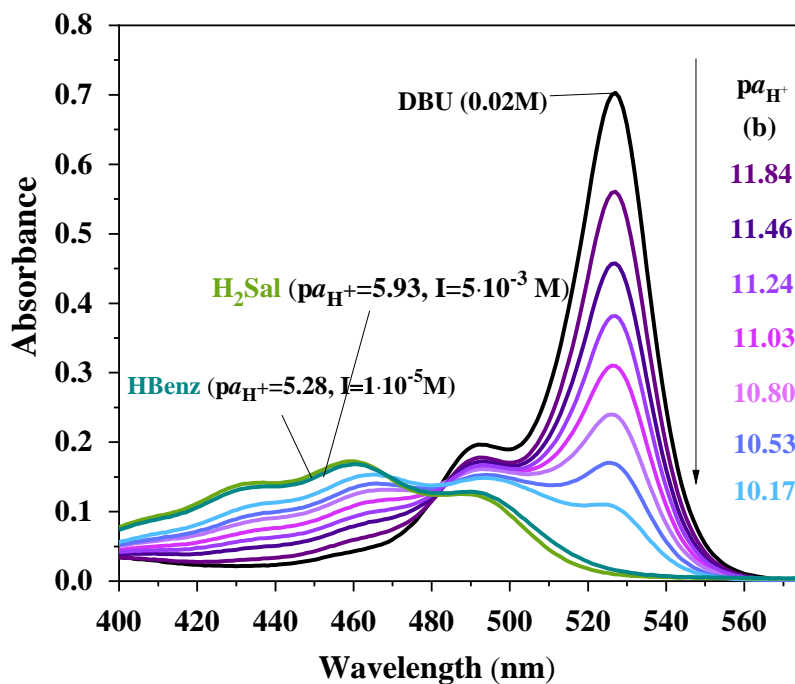


Figure 4.1: Steady-state absorption spectra of ethyl ester of 4'-aminofluorescein in DMSO at different pH values where H_2Sal – salicylic acid, $HBenz$ – benzoic acid, salicylate (a) and benzoate (b) buffer solutions and in *p*-toluenesulfonic acid solutions (c).

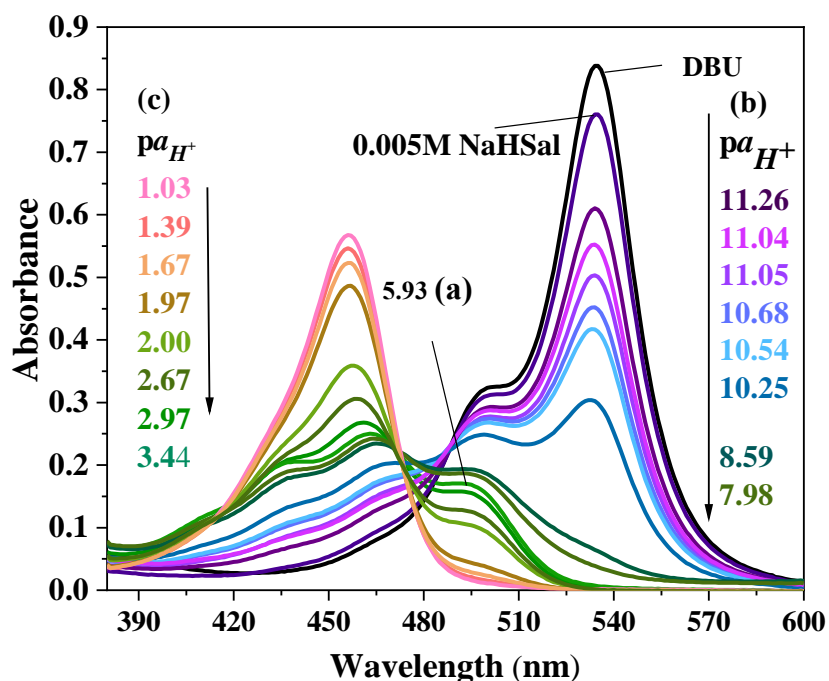


Figure 4.2: Steady-state absorption spectra of ethyl ester of 5'-nitrofluorescein in DMSO at different pH values where salicylate (a) and benzoate (b) buffer solutions and in *p*-toluenesulfonic acid solutions (c).

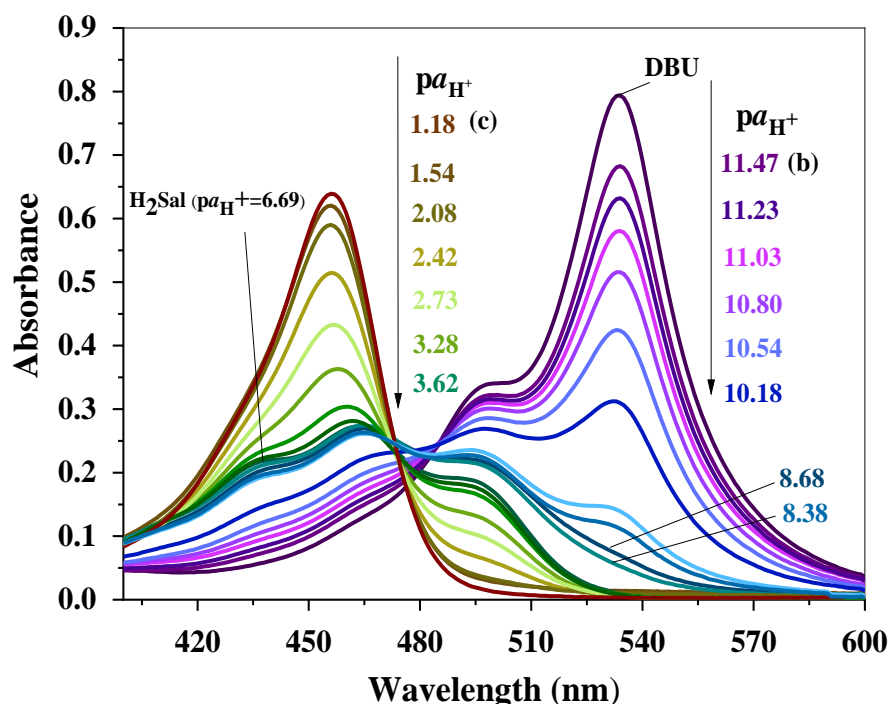


Figure 4.3: Steady-state absorption spectra of ethyl ester of 4'-nitrofluorescein in DMSO at different $pa_{H^+}^*$ values where H_2Sal – salicylic acid, salicylate (a) and benzoate (b) buffer solutions and in *p*-toluenesulfonic acid solutions (c).

The thermodynamic pK_{a1} values were calculated using Equation 4.1 at a fixed wavelength, optical path length, and constant dye concentration:

$$pK_{a1} = pa_{H^+}^* + \log \frac{A_{R^-} - A}{A - A_{HR}} - \log f_1 \quad (4.1)$$

Here A_{R^-} and A_{HR} are absorbances of the solution under complete transformation into the corresponding form, A is the absorbance at the current $pa_{H^+}^*$ value. The wavelengths around the R^- ion were used as analytical positions. The wavelengths within the range of 450–460 nm were used for the determination of the thermodynamic pK_{a0} values in solutions of *p*-toluenesulfonic acid (Equation 4.2). The latter was considered completely dissociated; c_{H^+} is equated to the analytical concentration of the acid.

$$pK_{a0} = -\log c_{H^+} + \log \frac{A_{HR} - A}{A - A_{H_2R^+}} \quad (4.2)$$

In the case of the eosin esters (Figures 4.4 and 4.5), the pK_{a1} values are substantially lower and were also determined in the *p*-toluenesulfonic acid solutions, Equation 4.1.

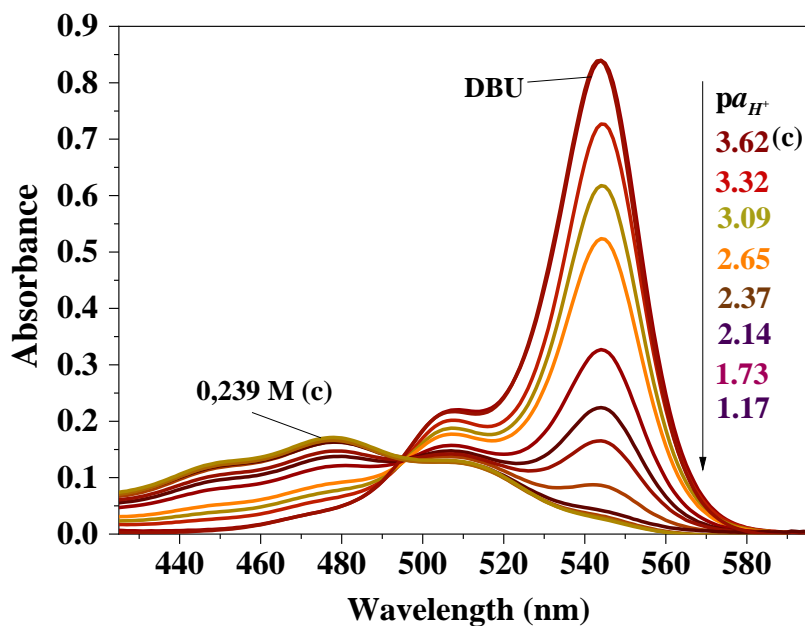


Figure 4.4: Steady-state absorption spectra of methyl ester of eosin in DMSO at different concentrations of *p*-toluenesulfonic acid (c); $pa_{H^+}^* = -\log c_{H^+} - \log f_1$. The values below $pa_{H^+}^*$ should be considered conventional ones because of relatively high ionic strength. The spectra in 0.239 M acid and 0.02 M DBU correspond to the neutral form, HR, and the anion, R^- , respectively.

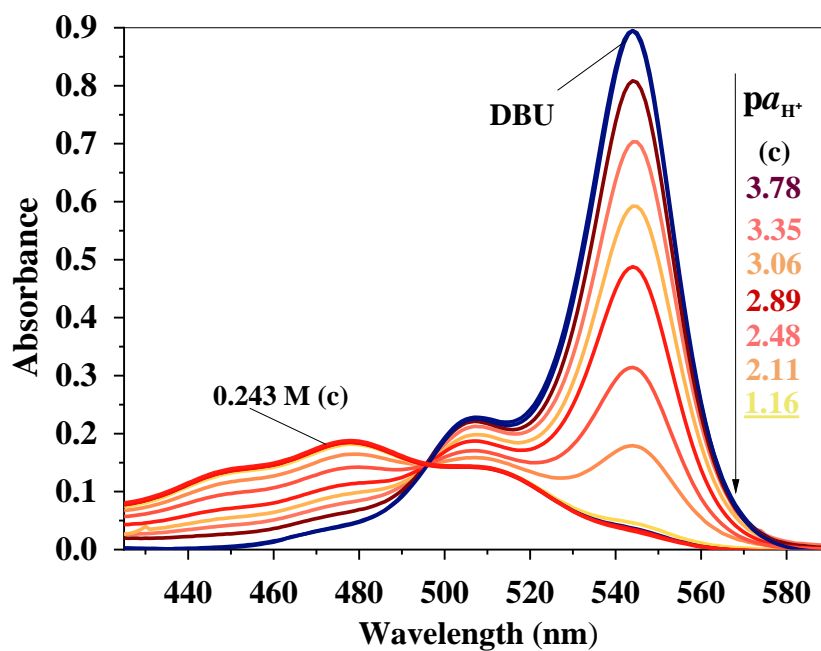


Figure 4.5: Steady-state absorption spectra of methyl ester of eosin in DMSO at different concentrations of *p*-toluenesulfonic acid (c); $pa_{H^+}^* = -\log c_{H^+} - \log f_1$. The values below $pa_{H^+}^*$

should be considered conventional ones because of relatively high ionic strength. The spectra in 0.243 M acid and 0.02 M DBU correspond to the neutral form, HR, and the anion, R⁻, respectively.

The isosbestic point is well expressed in the spectra of eosin esters; the same is the case with the equilibrium of 3'-, 4'-, and 5'-substituted fluorescein esters in the acidic region. On the contrary, this point is clearly blurred when moving from benzoate buffers to the HR absorption curve. The reason can be the heteroassociation of the HR molecules with the benzoate ions. As a result, the molecular spectrum of the given dye in the presence of the C₆H₅COO⁻ ions somewhat differs from that in benzoic and salicylic acids and salicylate buffer solutions. At the lowest $p a_{H^+}^*$ in the benzoate buffers, the A⁻ ions are almost completely transformed to the complex HA₂⁻; the latter is much less pronounced H-bonds acceptor. Therefore, the absorption curve does not cross the isosbestic point.

Note, that for the sulfonefluorescein, a dye with the SO₃⁻ group instead of COOC₂H₅, the spectrum of the monoanion, HR⁻, in DMSO also does not cross the isosbestic point in the spectra in *p*-aminobenzoate buffer solutions, where the equilibrium between the anions HR⁻ and R²⁻ takes place [18]. At the same time, in 50 mass % aqueous ethanol, where the heteroassociation processes are improbable, the spectra of the fluorescein ethyl ester are well expressed [19].

Two experiments were made to confirm our above explanation. The measurements with benzoate buffers in DMSO in the presence of 1 and 10 vol % of water were performed. Whereas the introduction of 1 vol % displays practically no influence on the spectra, in the presence of 10 vol % a distinct isosbestic point is observed (Figure 4.6).

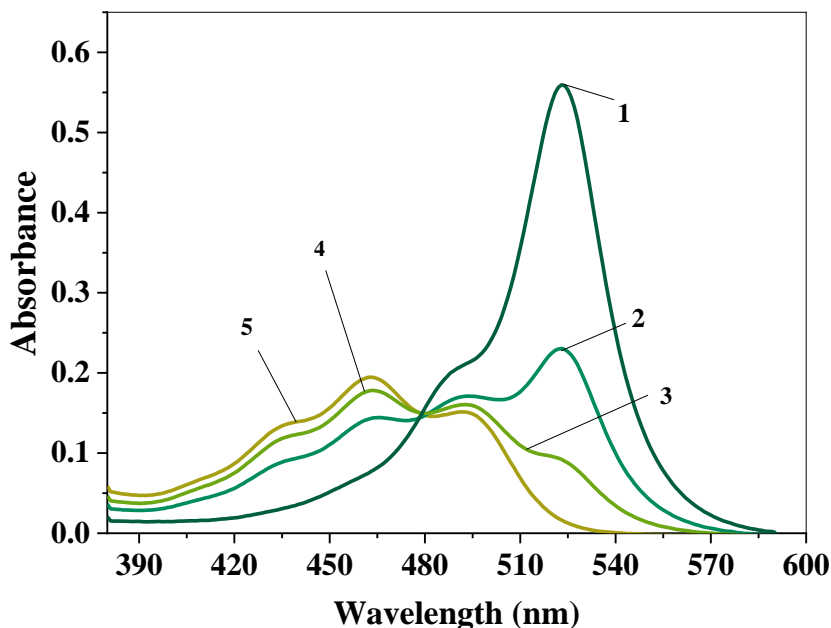


Figure 4.6: Steady-state absorption of 4'-Nitrofluorescein methyl ester in benzoate and salicylate buffer solutions in DMSO with 20 vol % water: 0.005M KBenz (1), 0.005M HBenz +0.005M KBenz (2), 0.0075 M HBenz +0.005M KBenz (3), 0.020 M HBenz +0.005M KBenz (4), 0.001 M H2Sal +0.005M NaHSal (5).

In any case, the absorption of the neutral form of the anion is negligible even if the spectrum in the salicylate buffer solution is displaced to cross the isosbestic point in benzoate buffers. Variation in the absorbance of HR at an absorption maximum of R^- results in pK_a changes of approximately about 0.04 units. Ultimately, one must take into account that the pK_a value of the benzoic acid in DMSO (11.1) is determined with an uncertainty of ± 0.1 . Additional digits in the pK_{a1} values in Table 4.1 primarily reflect the accuracy of the spectral data.

4.2 Results and Discussion

The results are presented in Tables 4.1 and 4.2. The bathochromic (4 to 9 nm) and hypsochromic (2 to 3 nm) shifts of the absorption bands of the nitro and amino derivatives, respectively, with respect to those of the unsubstituted compound give additional evidence of the small but distinct influence of the NO_2 groups.

Table 4.1: Absorption spectra maxima and dissociation constant indices of the esters of nitro and amino fluoresceins in DMSO

Dye	λ_{\max} , nm/		pK_{a0}	pK_{a1}	ΔpK_{a1}
	$\varepsilon_{\max} \times 10^{-3}, M^{-1} \text{ cm}^{-1}$				
	cation	anion			
Fluorescein ethyl ester	451/48.7	530/101.0	2.74±0.01	10.91±0.08	0
3'-Nitrofluorescein methyl ester	462/50.9	539/96.6	1.99±0.02	10.46±0.07	-0.4
4'-Nitrofluorescein ethyl ester	456/64.1	535/73.4	2.39±0.05	10.63±0.09	-0.3
4'-Nitrofluorescein methyl ester	456/53.3	534/70.4	2.35±0.04	10.57±0.09	-0.3
5'-Nitrofluorescein ethyl ester	457/58.5	534/87.8	2.44±0.08	10.74±0.12	-0.2
3'-Aminofluorescein methyl ester	n.d.	528/109.9	n.d.	11.12±0.07	+0.2
4'-Aminofluorescein ethyl ester	n.d.	527/116.3	n.d.	11.22±0.07	+0.3
5'-Aminofluorescein ethyl ester	n.d.	527/110.8	n.d.	11.10±0.11	+0.2

It can be concluded that the nitro group in the phthalic acid residue displays pK_{a1} shifts up to 0.4 units. The molecular absorption band of the esters is broad and triple-humped; the maxima positions and molar absorptivities are collected in Table 4.2.

Table 4.2: Absorption spectra maxima of the neutral forms of the esters of nitro and amino fluoresceins in DMSO

Compound	λ_{\max} , nm ($\varepsilon_{\max} \times 10^{-3}, M^{-1} \text{ cm}^{-1}$)		
Fluorescein ethyl ester	437 (17.5)	460 (21.9)	488 (14.9)
3'-Nitrofluorescein methyl ester	442 (18.0)	464 (22.2)	492 (14.6)
4'-Nitrofluorescein ethyl ester	440 (20.2)	463 (25.3)	490 (17.9)
4'-Nitrofluorescein methyl ester	441 (18.4)	463 (22.8)	489 (16.0)
5'-Nitrofluorescein ethyl ester	440 (21.2)	463 (25.8)	491 (17.6)

Chapter 4

3'-Aminofluorescein methyl ester	436 (23.6)	459 (29.4)	487 (20.7)
4'-Aminofluorescein ethyl ester	433 (23.8)	459 (29.2)	489 (21.2)
5'-Aminofluorescein ethyl ester	434 (21.6)	458 (27.2)	485 (19.3)
Eosin methyl ester	453 (17.3)	478 (22.8)	504 (17.4)
Eosin ethyl ester	452 (17.2)	478 (22.9)	504 (17.6)

Table 4.3 additionally demonstrates the similarity of the pK_{a1} values and spectral parameters of the hydroxyxanthene dyes with COOCH_3 and COOC_2H_5 groups in the 2' position.

Table 4.3: Absorption spectra maxima and dissociation constant indices of the eosin esters in DMSO

Dye	pK_{a1}	$\lambda_{\text{max}} (\text{R}^-)$, nm	$\epsilon_{\text{max}} (\text{R}^-) \times 10^{-3}, \text{M}^{-1} \text{cm}^{-1}$
Eosin methyl ester	2.91 ± 0.04^a	544	112.0
Eosin ethyl ester	2.85 ± 0.04^b	544	108.5

Note. ^a For calculations, the data at $p\alpha_{\text{H}^+}^* = 3.32, 3.09, 2.65,$ and 2.37 were used. ^b For calculations, the data at $p\alpha_{\text{H}^+}^* = 3.78, 3.35, 3.06,$ and 2.89 were used.

The pK_{a0} values of the nitro derivatives are 0.30–0.75 units lower than that of ethyl fluorescein. The NO_2 group in position 4' displays a somewhat larger effect, 0.35–0.39 units, as compared with the pK_{a0} shift of 0.30 in the case of 5'-nitrofluorescein ethyl ester. This is in line with the relation between the constants of the nitro group. Here, the terms *para* and *meta* indicate the position of the substituents with respect to the nodal carbon atom C_9 . The last is in direct polar conjugation with both quinone and OH groups. The distinct difference between the influence of the substitution in the positions 3' and 5', 0.75 and 0.30 units, respectively, reflects the specificity of the *ortho*-effect in the respect to the carbalkoxy group.

Similar effects are observed for the pK_{a1} of 3', 4', and 5' nitro derivatives: $\Delta pK_{a1} = -0.4$; -0.30 ; and -0.2 , respectively (Table 4.1). In contrast, the ΔpK_{a1} values of the corresponding amino derivatives are equal to $+0.2$; $+0.3$; and $+0.2$, respectively. Therefore, the *para* and *meta* effects are approximately 17 and 5 times lower as predicted by the $\rho\sigma$ product for corresponding phenols. Of course, such estimates are only conventional, because it deals with the OH group as the xanthene part.

On the other hand, the corresponding effects in the aqueous solution should be predicted to be $4.29/2.11 = 2.03$ times lower than those determined in the present work in DMSO.

Since the pK_{a1} values are somewhat distorted by heteroassociation and their accuracy is limited by that the pK_{HA} of the benzoic acid, we additionally compared the spectrophotometric data for different dyes at the same $pa_{H^+}^*$ values. In Table 4.4, the ratio of the absorbance of the anion and that at the given $pa_{H^+}^*$ value is presented.

Table 4.4: Ratios of absorbances at a given $pa_{H^+}^*$ and of the anion

Compound	A/ A (R ⁻) at λ_{max} of the anion	
	$pa_{H^+}^* = 11.04 \pm 0.01$	$pa_{H^+}^* = 10.54 \pm 0.01$
3'-Nitrofluorescein methyl ester	0.805	0.615
4'-Nitrofluorescein methyl ester	0.731	0.534
4'-Nitrofluorescein ethyl ester	0.731	0.533
5'-Nitrofluorescein ethyl ester	0.659	0.498
Fluorescein ethyl ester	<u>0.601</u>	<u>0.378</u>
3'-Aminofluorescein methyl ester	0.491	0.290
4'-Aminofluorescein ethyl ester	0.443	0.243
5'-Aminofluorescein ethyl ester	0.494	0.283

An inspection of Table 4.4 confirms the above observations: the 4'-substitution has a somewhat stronger effect than the influence of the 5'-derivatives. The introduction of the NO₂ group in the 3' position reduces pK_{a1} even more.

4.3 Conclusions

The introduction of nitro and amino groups into the phthalic acid residue affects the protolytic properties of the functional groups in the xanthene part of the fluorescein molecule in DMSO. The decrease in the pK_a caused by the NO₂ group and increase with the introduction of the NH₂ group is somewhat more pronounced with the substitution at the 4'- compared to the

Chapter 4

5'-position. For the nitro derivatives, the decrease in the pK_{a0} value is more pronounced than that in the case of pK_{a1} . Here the impact sequence is as follows: $3' > 4' > 5'$.

Although the variations in the pK_a values in DMSO are only in the range of 0.2–0.8, they convincingly prove the transmission of the electronic effects despite the almost perpendicular orientation of the phthalic residue to the xanthenes fragment. In water, the effects are expectedly less.

Bibliography

1. Zhou, P., Tang, Z., Li, P., Liu, J.: Unraveling the Mechanism for Tuning the Fluorescence of Fluorescein Derivatives: The Role of the Conical Intersection and $n\pi^*$ State. *Journal of Physical Chemistry Letters*. 12, 6478–6485 (2021). https://doi.org/10.1021/ACS.JPCLETT.1C01774/SUPPL_FILE/JZ1C01774_SI_001.PDF
2. Nowak, P.M., Woźniakiewicz, M.: The Acid-Base/Deprotonation Equilibrium Can Be Studied with a MicroScale Thermophoresis (MST). *Molecules*. 27, (2022). <https://doi.org/10.3390/MOLECULES27030685>
3. Zdończyk, M., Potaniec, B., Skoreński, M., Cybińska, J.: Development of Efficient One-Pot Methods for the Synthesis of Luminescent Dyes and Sol-Gel Hybrid Materials. *Materials (Basel)*. 15, (2021). <https://doi.org/10.3390/MA15010203>
4. Oliveira, E., Bértolo, E., Núñez, C., Pilla, V., Santos, H.M., Fernández-Lodeiro, J., Fernández-Lodeiro, A., Djafari, J., Capelo, J.L., Lodeiro, C.: Green and Red Fluorescent Dyes for Translational Applications in Imaging and Sensing Analytes: A Dual-Color Flag. *ChemistryOpen*. 7, 9–52 (2018). <https://doi.org/10.1002/open.201700135>
5. Patterson, K.N., Romero-Reyes, M.A., Heemstra, J.M.: Fluorescence Quenching of Xanthene Dyes during Amide Bond Formation Using DMTMM. *ACS Omega*. 7, 33046–33053 (2022). <https://doi.org/10.1021/acsomega.2c03085>
6. Pilla, V., Gonçalves, A., dos Santos, A., Lodeiro, C.: Lifetime and Fluorescence Quantum Yield of Two Fluorescein-Amino Acid-Based Compounds in Different Organic Solvents and Gold Colloidal Suspensions. *Chemosensors*. 6, 26 (2018). <https://doi.org/10.3390/chemosensors6030026>
7. Hwang, J., Lee, J.-Y., Cho, C.-W., Choi, W., Lee, Y., Shim, S., Hwang, G.: 5-Bromo-4',5'-bis(dimethylamino)fluorescein: Synthesis and Photophysical Studies. *Molecules*. 23, 219 (2018). <https://doi.org/10.3390/molecules23010219>
8. Tamulis, A., Tamuliene, J., Balevicius, M.L., Rinkevicius, Z., Tamulis, V.: Quantum Mechanical Studies of Intensity in Electronic Spectra of Fluorescein Dianion and Monoanion Forms. *Struct Chem*. 14, 643–648 (2003). <https://doi.org/10.1023/B:STUC.0000007575.53499.d0>
9. Slyusareva E.A., Tomilin F.N., Sizykh A.G., Tankevich E.Y., Kuzubov A.A., Ovchinnikov S.G.: The effect of halogen substitution on the structure and electronic spectra of fluorone dyes. *Opt Spectrosc*. 112, 671–678 (2012)

Chapter 4

10. Patterson, K.N., Romero-Reyes, M.A., Heemstra, J.M.: Fluorescence Quenching of Xanthene Dyes during Amide Bond Formation Using DMTMM. *ACS Omega*. 7, 33046–33053 (2022). <https://doi.org/10.1021/acsomega.2c03085>
11. Lebed, A. V., Biryukov, A. V., McHedlov-Petrosyan, N.O.: A quantum-chemical study of tautomeric equilibria of fluorescein dyes in DmsO. *Chem Heterocycl Compd (N Y)*. 50, 336–348 (2014). <https://doi.org/10.1007/S10593-014-1481-8/TABLES/5>
12. Bogdanova, L.N., McHedlov-Petrosyan, N.O., Vodolazkaya, N.A., Lebed, A. V.: The influence of β -cyclodextrin on acid–base and tautomeric equilibrium of fluorescein dyes in aqueous solution. *Carbohydr Res*. 345, 1882–1890 (2010). <https://doi.org/10.1016/J.CARRES.2010.07.002>
13. Mchedlov-Petrosyan, N.O.: Fluorescein dyes in solutions: well-studied systems? . *Kharkov Univ. Bull.* . 626, 221–312 (2004)
14. Reutov O.A., Kurts A.L., Butin K.P.: *Organic chemistry*. M.: Binom. *Laboratoriya znaniy V.4*, P.568, (2012)
15. Chantooni, M.K., Kolthoff, I.M.: Comparison of substituent effects on dissociation and conjugation of phenols with those of carboxylic acids in acetonitrile, N,N-dimethylformamide, and dimethyl sulfoxide. *J Phys Chem*. 80, 1306–1310 (1976). <https://doi.org/10.1021/j100553a009>
16. Kolthoff, I.M., Chantooni, M.K.: Calibration of the Glass Electrode in Acetonitrile. Shape of Potentiometric Titration Curves. Dissociation Constant of Picric Acid. *J Am Chem Soc*. 87, 4428–4436 (1965). https://doi.org/10.1021/JA00948A004/ASSET/JA00948A004.FP.PNG_V03
17. Kolthoff, I.M., Chantooni, M.K., Bhowmik, S.: Dissociation constants of uncharged and monovalent cation acids in dimethyl sulfoxide. *J Am Chem Soc*. 90, 23–28 (1968). https://doi.org/10.1021/JA01003A005/ASSET/JA01003A005.FP.PNG_V03
18. McHedlov-Petrosyan, N.O., Cheipesh, T.A., Shekhovtsov, S. V., Ushakova, E. V., Roshal, A.D., Omelchenko, I. V.: Aminofluoresceins Versus Fluorescein: Ascertained New Unusual Features of Tautomerism and Dissociation of Hydroxyxanthene Dyes in Solution. *Journal of Physical Chemistry A*. 123, 8845–8859 (2019). https://doi.org/10.1021/ACS.JPCA.9B05810/SUPPL_FILE/JP9B05810_SI_001.PDF
19. Mchedlov-Petrosyan, N.O., Cheipesh, T.A., Shekhovtsov, S. V, Redko, A.N., Rybachenko, V.I., Omelchenko, I. V, Shishkin, O. V: Ionization and tautomerism of methyl fluorescein and related dyes. *Spectrochim Acta A Mol Biomol Spectrosc*. 150, 151–161 (2015). <https://doi.org/10.1016/j.saa.2015.05.037>

Chapter 5

Fluorescent properties of amino and nitro derivatives of fluorescein in aprotic solvents

The material presented in this chapter forms the basis of publications:

Mchedlov-Petrosyan, N.O., Cheipesh, T.A., Roshal, A.D., Shekhovtsov, S.V., Moskaeva, E. G., Omelchenko, I.V., Aminofluoresceins vs Fluorescein: Peculiarity of Fluorescence, *J. Phys. Chem. A*, 123, 41, 8860–8870, (2019).

Mchedlov-Petrosyan, N.O., Shekhovtsov, S.V., Moskaeva, E. G., Omelchenko, I.V., Roshal, A.D., Doroshenko, A.O., New fluorescein dyes with unusual properties: Tetra- and pentanitrofluoresceins. *J. Mol. Liq.*, 367, B, 120541, (2022).

In this chapter, we examined the fluorescent properties of aminofluorescein and nitro derivative of fluorescein in a set of solvent systems. Fluorescence lifetimes, quantum yields, time-resolved and fluorescence spectra allowed clarifying the reasons for the emitting properties in this dye series.

The completely deprotonated form of unsubstituted fluorescein exhibits fluorescence with a quantum yield close to 1 in water, in aprotic solvents this value tends to 0.82 – 0.85. The presence of substituents on the xanthene fragment significantly affects the spectral properties of fluorescein dyes. Thus, in water, the dianions R^{2-} of aminofluoresceins are practically non-fluorescent; in alcohols the quantum yields are low. In DMSO, acetonitrile and other aprotic solvents, the bright fluorescence of R^{2-} ions is quenched either on adding small amounts of water which hydrate the carboxylate group or under conditions of protonation of this group ($COO^- \rightarrow COOH$). This part of the work aimed to consider in detail the problem of fluorescence of amino and nitro derivatives of fluorescein in different solvents, especially in DMSO. The information, obtained in the previous chapters, about tautomeric equilibria and the effect of substituents on the electron density of the xanthene fragment allows us to interpret presented fluorescent data.

5.1 Introduction

Fluorescein in its double-charged anionic form in solution exhibits strong fluorescence. Its structure is depicted in Figure 5.1 in a conventional manner; the oxygen atoms in the 3 and 6 positions in the xanthenes ring should be considered as equal. Numerous derivatives and analogs of fluorescein are widely used in different fields of chemistry and applied science. Besides, well-known chloro-, bromo-, and iodo derivatives, such as eosin, erythrosin, Rose Bengal, etc., fluorinated fluoresceins [1–4], silicon-substituted fluoresceins [5–9], dibenzofluorescein [10] and other dyes of this family are nowadays very popular. For example, a new valuable dye Tokyo Green [4, 11] bears the CH_3 instead of the carboxylic group. Substitution by ethyl groups in 2- and 7-positions of fluorescein shift the indices of dissociation of the OH group toward the physiological region [12].

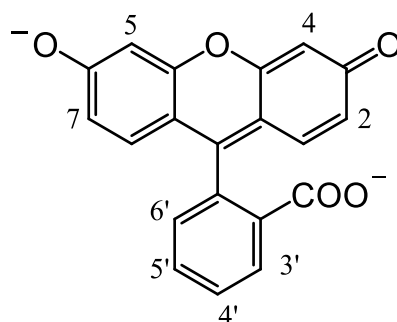


Figure 5.1: Fluorescein dianion R^{2-} .

The fluorescein dyes are utilized in biomedical research [1, 2, 4, 12], including nitric oxide determination [13–15], for monitoring in drug delivery [16], as fluorogenic protease substrates [17], as semisynthetic fluorescent pH sensors for imaging exocytosis and endocytosis [18]. Versatile substituents in the phthalic residue influence the fluorescence of the mother compound, including amino and nitro derivatives [19, 20].

Fluorescein dyes bearing one or two NH_2 groups in the phthalic acid residue as well as their derivatives are of special interest [13, 15, 17, 21, 22]. The double-charged anions of the above aminofluoresceins do not exhibit intense fluorescence [19, 20]. However, the emission is restored if the amino groups are involved in new covalent bonds [13]. Recently [23], we have demonstrated that the common idea of the non-fluorescent character of the double-charged anions (dianions, R^{2-}) of 4'- and 5'-aminofluoresceins with entire NH_2 groups may be

misleading as it rests upon the experiments exclusively in water [24]. In alcohols, the quantum yield, ϕ , is still rather low [19, 20], but in DMSO, acetone, and other aprotic solvents, the ϕ values approach that of bright-fluorescent fluorescein dianion [23]. However, these findings are still not entirely explained. First of all, it should be clarified what functional group of the dyes is responsible for such a decisive influence of H-bonding. It may be either the COO^- group, the xanthene part of the dye, or the NH_2 group.

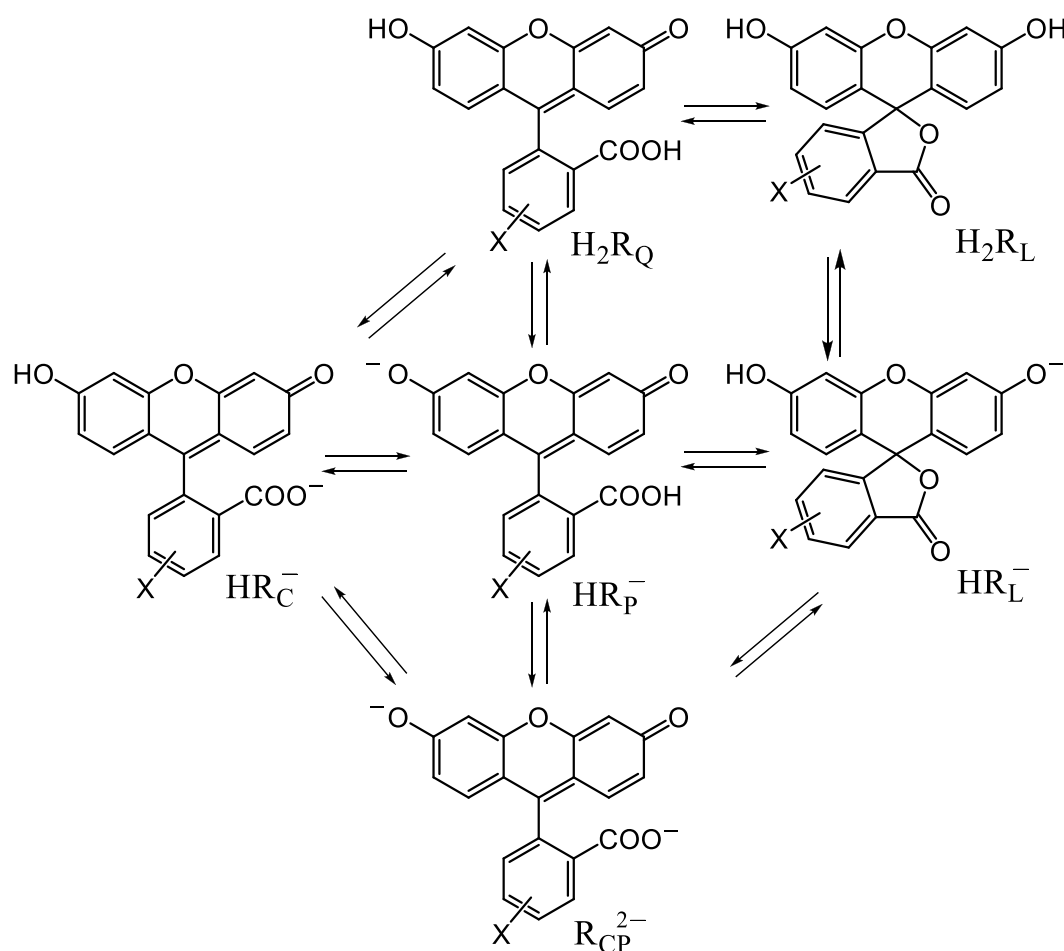
Fluorescein and its derivatives are diprotic acids, hereafter designated as H_2R . They ionize in solutions to form anions, HR^- and R^{2-} , equations (5.1) and (5.2). In acidic media, the formation of cations H_3R^+ (not shown here) takes place.



In the case of 4'- and 5'-aminofluoresceins, the presence of an additional basic group NH_2 makes the equilibria more complicated. In organic solvents, however, the formation of the NH_3^+ group takes place only in acidic enough media. For example, as it was shown, the dissociation of the carboxylic and hydroxyl groups of these two dyes in DMSO the amino groups stay unchanged [25]. The neutral form H_2R exists in DMSO as the lactone $\text{H}_2\text{R}_\text{L}$ with a small admixture of quinonoid tautomer $\text{H}_2\text{R}_\text{Q}$ (Scheme 5.1).

In DMSO, the single-charged anion HR^- of fluorescein exists as the carboxylate tautomer HR_C^- with a 20 % admixture of the 'phenolate' tautomer HR_P^- . For 4'-aminofluorescein, the tautomeric equilibrium of monoanion is similar, whereas, in the case of 5'-aminofluorescein in DMSO, the lactone HR_L^- predominates, with 1.2 % of phenolate tautomer HR_P^- . The dianion R^{2-} bares both groups in the ionized state, which is shown as a structure R_CP^{2-} in Scheme 5.1 [25].

This part of the work aimed to consider in detail the problem of fluorescence of amino and nitro derivatives of fluorescein in different solvents based on the above-mentioned findings in DMSO and using a set of other fluorescein dyes for comparison. This, in turn, should explain the origin of fluorescence quenching of R^{2-} species of fluorescein derivatives in water and alcohols.



Scheme 5.1: The detailed equilibrium of fluorescein and aminofluoresceins; X = H: fluorescein; X = 4'-NH₂: 4'-aminofluorescein; X = 5'-NH₂: 5'-aminofluorescein.

Quantum yields, fluorescence lifetimes, and time-resolved emission spectra should shed more light on the problem of xanthene dyes emission. Also, the dye 4'-nitrofluorescein was involved in the research, because it is known that the fluorescence of its R²⁻ anion is very poor [19, 20]. This was demonstrated, however, only in water and alcohols as solvents [19, 20], and thus it is worthwhile to examine the phenomenon in aprotic solvents.

5.2 Quantum yields of nitro and amino derivatives of fluorescein

The completely deprotonated form of unsubstituted fluorescein exhibits fluorescence with a quantum yield close to 1 in water, in aprotic solvents this value tends to 0.82 - 0.85. The presence of substituents on the xanthene fragment significantly affects the spectral properties of fluorescein dyes. Thus, according to the value from Table 5.1, the introduction of nitro groups into the xanthene fragment significantly reduces the value of the quantum yield of the dianion ($\phi < 0.1$). In the case of dinitrofluorescein, tetra- and pentanitrofluorescein, the dianion

is characterized by the formation of colorless lactones in dimethyl sulfoxide, which leads to a significant drop in fluorescence.

Table 5.1: Quantum yield values of dye anions R^{2-} (HR^-) in dimethyl sulfoxide (R^{2-} was obtained by the addition of DBU 0.02 M, Fluorescein in 9.93 carbonate aqueous buffer solution ($\Phi_{\text{fluo}} = 0.93$) was used as a standard [27])

	ϕ (%)	τ_1 (ns) / (τ_2)	λ_{max} , nm (abs/em)
Fluorescein, R^{2-}	85		521/540
4'-Aminofluorescein	74	3.94 ^e	518/534
5'-Aminofluorescein	67	3.41	517/534
4'-Nitrofluorescein	1.01	3.35	526/543
5'-Nitrofluorescein	0.062	n.d.	527/545
2,4,5,7,4'-Pentanitrofluorescein (HR^-) ^b	21,22	n.d.	525/564
2,4,5,7,4'-Pentanitrofluorescein	0,42	3.55 / (0.572)	429/560
2,4,5,7,5'-Pentanitrofluorescein	0,51	5.45 / (0.864)	419/560
2,4,5,7,-Tetranitrofluorescein	n.d.	5.11 / (0.915)	441 ^a
4,5-Dinitrofluorescein	0.09	4.31 / (0.788)	510/535
4,5-Dinitrosulfofluorescein	0.23	4.36 / (0.165)	520/549
4'-Aminofluorescein ethyl ester (R^-)	21.58	3.70	527 ^a
5'-Aminofluorescein ethyl ester (R^-)	18.75	3.39	524 ^a
4'-Nitrofluorescein ethyl ester (R^-)	0.70	4.26 / (0.361)	534 ^a
5'-Nitrofluorescein ethyl ester (R^-)	0.023	n.d.	535 ^a
2,4,5,7,-Tetranitrofluorescein Methyl ester (R^-)	80.2	n.d.	527/564

Note: n.d. – not determined, ^a currently no access to values

Modification of the phthalic fragment also affects the fluorescent properties of dyes. The nitro group into the 4' and 5' positions results in a decrease in the quantum yield to 1.01 and 0.06, respectively. For the amino group in the same positions, the reverse behavior is observed - fluorescence occurs more efficiently. Thus, significant quenching was observed for fluoresceins in water, both for nitro and for amino substituents in the phthalic fragment. The mechanism of this phenomenon requires a more detailed discussion, which is given below.

Chapter 5

It should be noted that the blocking of the carboxyl group with an ethyl residue leads to an increase in the quantum yield compared to unsubstituted nitro and aminofluoresceins. Further in the chapter, the mechanisms of the influence of substituents and the ethyl fragment on the fluorescent properties of dyes are reviewed in detail.

5.3 Fluorescence of 4'-nitrofluorescein in solvents of different nature: low quantum yields

In Figures 5.2–5.3, absorption and emission normalized spectra of 4' aminofluorescein, and 4' nitrofluorescein in different organic solvents are presented. Dyes with amino and nitro substituents in the 5' position do not differ from those in the 4' position, so the spectra for them are not shown. The dye concentrations were within the range of 10^{-5} – 10^{-6} M, as a rule, lower for emission measurements. Dichloromethane was chosen as a less polar solvent (at 25 °C, relative permittivity $\epsilon_r = 8.93$, normalized Reichardt's parameter of polarity $E_T^N = 0.309$)[26]. Acetonitrile ($\epsilon_r = 35.94$; $E_T^N = 0.460$) and DMSO ($\epsilon_r = 46.45$; $E_T^N = 0.444$) are typical aprotic solvents, sometimes called 'polar aprotic' ones. The λ_{max} values of both absorption and emission of dyes are as a rule higher in the case of the least polar solvent. In all these media, aminofluoresceins in their dianionic form, R^{2-} , exhibit bright fluorescence, whereas the emission of the nitro derivative is poor. This means that, contrary to aminofluoresceins, the dye 4' nitrofluorescein stays poorly emitting in aprotic solvents.

In Table 5.2, the quantum yields of fluorescence of aminofluorescein R^{2-} ions in a variety of solvents are presented. Both presently obtained and earlier reported data confirm the general regularity: in hydrogen bond-donor solvents such as water and alcohols, the ϕ values are substantially lower as compared with the values in aprotic (last lines in Table 5.2). The viscosity of the solvent displays but small influence; for instance, in viscous 1-butanol, and glycerol the ϕ values are higher than those in water, but the same is true for methyl alcohol, which is less viscous as compared with water [23].

In water, the dianions R^{2-} of aminofluoresceins are practically non-fluorescent; in alcohols the quantum yields are low. In DMSO, acetonitrile and other aprotic, the bright fluorescence of R^{2-} ions is quenched either on adding small amounts of water which hydrate the carboxylate group or under conditions of protonation of this group ($COO^- \rightarrow COOH$). By contrast, the R^{2-} anion of 4'-nitrofluorescein demonstrates spectral behavior different from that

of the amino derivatives. It practically does not emit in aprotic solvents, however, in alcohol or water media, its quantum yield increases to some extent.

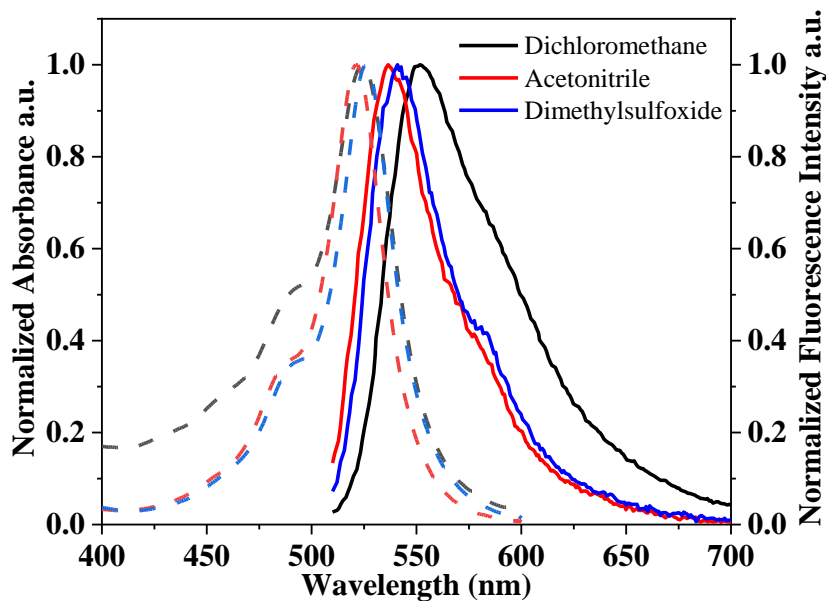


Figure 5.2: Normalized absorption (dash line) and fluorescence spectra of 4'-nitrofluorescein in dichloromethane (1; -----), acetonitrile (2; - - - - -), and dimethylsulfoxide (3; - - - - -); 0.02 M DBU in all solutions ensure complete conversion of the dye into the R^{2-} ion.

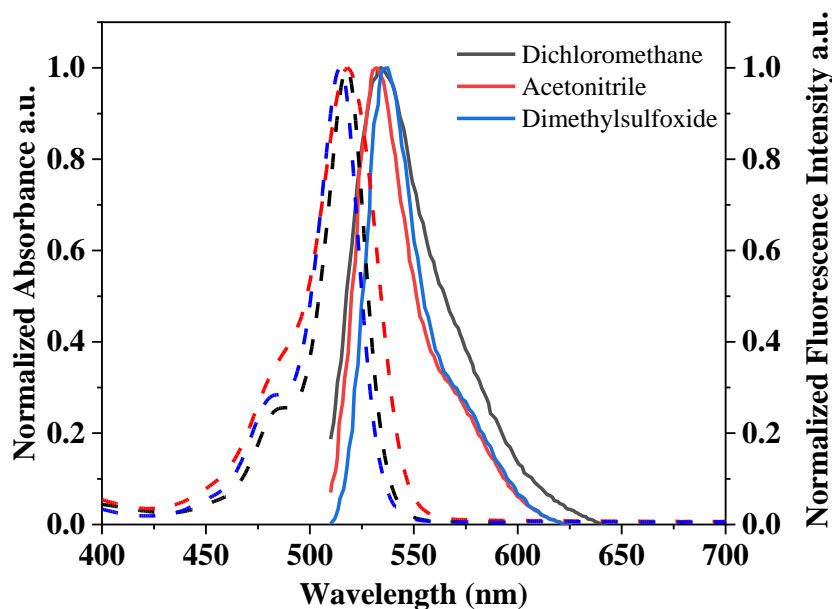


Figure 5.3: Normalized absorption (dash line) and fluorescence spectra of 4'-aminofluorescein in dichloromethane (1; -----), acetonitrile (2; - - - - -), and dimethylsulfoxide (3; - - - - -); 0.02 M DBU in all solutions ensure complete conversion of the dye into the R^{2-} ion.

Chapter 5

In Table 5.2, the values of fluorescence lifetimes are presented. As a rule, the measurements were made in the presence of 0.02 M DBU, in order to ensure the complete conversion of the dyes into the R^{2-} species, which actually exist in form of R_{CP}^{2-} (Scheme 5.1). In addition, some experiments with 5'-aminofluorescein in DMSO were performed using benzoate buffer solutions; the reason was to examine the emission of the single-charged ion HR^- of this dye.

Table 5.2: Quantum yield values and fluorescence lifetimes of amino and nitro R^{2-} anions in different solvents ^a

Solvent	τ (ns)	ϕ (%)	τ (ns)	ϕ (%)	τ (ns)	ϕ (%)
	4'-Aminofluorescein		5'-Aminofluorescein		4'-Nitrofluorescein	
Water ^b	0.12 (96 %); 3.78 ^c	0.6	0.12 (98 %); 3.89	0.8	3.32 ^d	1.60 ^h
Methanol				4.0		1.7 ^d
DMSO	3.94 ^e	74	3.41 ^f	67	3.35	1.01
Acetonitrile	3.93	59	3.98	60	3.19	0.38
Dichloromethane	3.58	77	3.84	84	2.89	0.40

^a In organic solvents, 0.02 M DBU was added if not otherwise specified. ^b From ref. 24. ^c In ref.[20]: $\tau = 0.22$; 2.39 ns ^d In ref.[20]: 1.69 and 4.08 ns. ^e The value is corrected using the deconvolution procedure; in ref.[24] $\tau = 3.26$ ns. ^f The value is corrected using the deconvolution procedure; in ref.[24], $\tau = 2.78$ ns. ^h In ref. [20] $\phi = 3$ %.

For un-substituted fluorescein, the τ values in DMSO, acetonitrile, and dichloromethane are 3.81, 3.99, and 3.97 ns, respectively (measured in 0.02 M DBU solutions). These values are somewhat lower as compared with those reported by Magde et al. for fluorescein R^{2-} in water (4.16 ns), methanol (4.28 ns), and ethanol (4.25 ns) [27]. However, as early as 1975 Martin [28] reported the $\tau = 3.6 \pm 0.2$ ns value for fluorescein dianion in DMSO, which is also lower than the corresponding values in methanol (4.1 ns) and ethanol (3.9 ns) [28]

According to DFT calculations for fluorescein dyes [25] dianions dihedral angles between xanthene and phenyl fragments in the ground and excited states are in the range of (85–90)°. Thus, these fragments are, in fact, orthogonal, and no π -conjugation between them could be. Under these conditions, the influence of substituents or specific solvation on the re-distribution of the charge between fragments can only be due to an inductive effect.

Since charged carboxylate and 'phenolate' groups are located in different not conjugated fragments of the dianions, the electronic density redistribution between these fragments is

hardly probable. The presence of substituents in the phenyl ring hinders the charge transfer between fragments which results in the equalization of charges on the fragments. The presence of electron-releasing groups in the side phenyl ring results in a weak decrease of this charge (not depending on the positions of these groups). In contrast, the electron-withdrawing NO_2 group increases the negative charge of the xanthene moiety.

5.3 The peculiarity of aminofluoresceins fluorescence

As the COO^- group is an expressed acceptor of H-bonds, a conclusion about the quenching mechanism can be deduced. Namely, the introduction of the amino group decreases the ϕ value if the charge of the anionic group in the 2' position is to some extent leveled by H-bonds with water or alcohol molecules. Contrary, if the carboxylate group is poorly solvated in DMSO, acetonitrile, etc., its localized negative charge prevents quenching. The data gathered in Tables 5.2 and 5.3 give evidence for this regularity.

Table 5.3. Quantum yield values of anions of fluorescein dyes in DMSO

Dye, condition	ϕ (%)	
	Water ^a	DMSO ^b
Fluorescein, R^{2-}	93	85 ^c
5'-Aminofluorescein, R^{2-} ^c	0.8	67
4'-Nitrofluorescein, R^{2-}	1.6	1.0
5'-Aminofluorescein, $\text{p}a_{\text{H}^+} = 12.0$ ^d	—	23
5'-Aminofluorescein, dye : DBU = 20 : 1 ^e	—	12
5'-Aminofluorescein, $\text{p}a_{\text{H}^+} = 10.1$ ^e	—	11
5'-Aminofluorescein, $\text{p}a_{\text{H}^+} \approx 6$ ^g	—	0.6

^a With the addition of diluted NaOH. ^b With 0.02 M DBU, if not otherwise specified. ^c From ref. [24]. ^d In benzoate buffer solutions. ^e Such concentration ratio allows observing the absorption spectrum of HR^- under conditions of the predominance of the molecular form H_2R . ^g In 0.10 M solution of benzoic acid.

The single-charged monoanion HR^- of this dye exists in DMSO mainly (98.8 %) as colorless and non-fluorescent lactone, HR_L^- , and the rest 1.2 % belong to the colored phenolate, HR_P^- , the fraction of the carboxylate, HR_C^- , is negligible [25]. Hence, it gives the possibility to directly observe the spectral properties of the tautomer HR_P^- and compare them with those of the R^{2-} ion (in Scheme 5.1), which has the same structure except the state of the

Chapter 5

carboxylic group (COO^- instead of COOH). It is reasonable to consider the maximal molar absorptivities of the species HR_p^- and $\text{R}_{\text{CP}}^{2-}$ approximately equal taking into account the values for fluorescein and its ethyl ester in DMSO, which are about $10^5 \text{ M}^{-1} \text{ cm}^{-1}$ [25]. Also, the maximal molar absorptivity of species of H_2R_Q type is within the range of $(22\text{--}27) \cdot 10^3 \text{ M}^{-1} \text{ cm}^{-1}$ [25].

Two benzoate buffers were used for the determination of the quantum yield and time-resolved emission spectra of 5'-aminofluorescein. One of them contained 0.01 M potassium benzoate and 0.001 M benzoic acid, whereas, in the second one, the salt and acid concentrations were 0.001 M and 0.01 M, respectively.

The TRS allows for gaining insight into the fluorescence mechanism in these dye series. When estimating 5'-aminofluorescein dianion lifetime values at different wavelengths, it was repeatedly found that the dianion exhibits bi-exponential fluorescence decays. It was also shown that, independently of the experimental conditions, in previous publications [20, 23] and our investigations, all the decay curves contain a long-living component with a lifetime higher than 2.4 ns. Pre-exponential coefficients of this component are higher in the short-wavelength spectral range. Hence, this form predominantly emits in the blue region. In the long-wavelength range, these pre-exponential coefficients are negative, thus indicating that the transformation of this form to another long-wavelength one occurs.

For understanding the composition of the solutions of 5'-aminofluorescein in DMSO in the ground state, the tautomerism of the single-charged anion should be taken into account. Indeed, at $\text{p}a_{\text{H}^+} = 12.0$ the HR^- ion predominates. However, the populations of the species HR_p^- and $\text{R}_{\text{CP}}^{2-}$ are equal to 1.1% and 2%, respectively. Contrary to it, despite the predominating of the almost colorless and non-emitting molecular form H_2R_L at $\text{p}a_{\text{H}^+} = 10.1$, the populations of the ions HR_p^- and $\text{R}_{\text{CP}}^{2-}$ are here 0.13 % and 0.002%, respectively. Hence, at this $\text{p}a_{\text{H}^+}$ we observe practically only the fluorescence of the phenolate monoanion, HR_p^- . (Note, that the monoanionic cyclic lactone belongs to non-emitting species and the emission of the neutral molecules is negligible, see the last line in Table 5.3)

To determine the spectral characteristics of the emitting forms and the kinetics of their transformations, the TRS of 5'-aminofluorescein in different media has been measured. Figure 5.4 shows the TRS in benzoate buffer solutions with $\text{p}a_{\text{H}^+}$ equal to 10.1 and 12.0. In the buffer of lower $\text{p}a_{\text{H}^+}$ (Figure 5.4a), no change in TRS was observed. This evidences the absence of any monoanion form transformations in the excited state.

In the buffer of higher $p\alpha_{\text{H}^+}$ value, the formation of a new long-wavelength emission band was detected (Figure 5.4b). The analysis of TRS showed that the formation of the new form in the excited state is an irreversible process. Fluorescence band maxima, lifetimes of the dianion, as well as rate constants of the new emitting form formation in the excited state, are listed in Table 5.4.

Figure 5.5 shows the TRS of 5'-aminofluorescein and non-substituted fluorescein dianions in the presence of 0.02 M DBU. It can be seen that the long-wavelength fluorescence appears only in the case of amino derivative and does not when the amino substituent is absent. Thus, it would be logical to conclude that the observed phenomenon is due to changing the charge distribution in the side phenyl ring in the excited state.

The data listed in Table 5.4 show that λ_{max} and lifetime values of the short-wavelength band weakly depend on the nature of an ionizing agent and correspond to those of 5'-aminofluorescein dianion. On the other hand, the form responsible for the long-wavelength fluorescence band demonstrates a very strong dependence on the ionic composition of the solution.

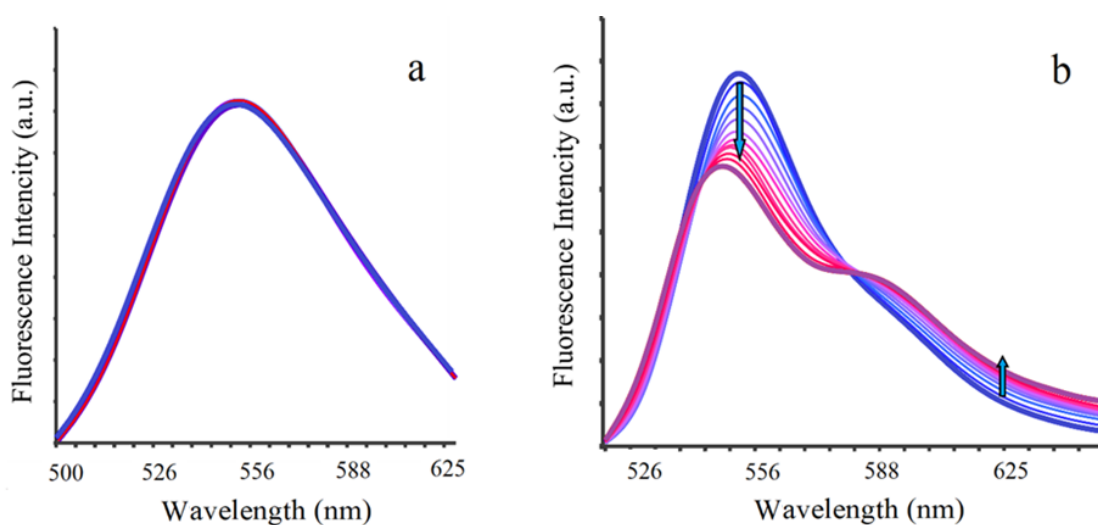


Figure 5.4: Time-resolved spectrum of 5'-aminofluorescein in DMSO at different $p\alpha_{\text{H}^+}$ values. a: monoanion spectrum at $p\alpha_{\text{H}^+} = 10.1$, benzoate buffer (a); spectrum at $p\alpha_{\text{H}^+} = 12.0$, benzoate buffer (b). Starting curve is approximately 0.3 ns after pulse, the final curve is for 3 ns delay; the time gap between neighboring spectral curves is 0.1 ns.

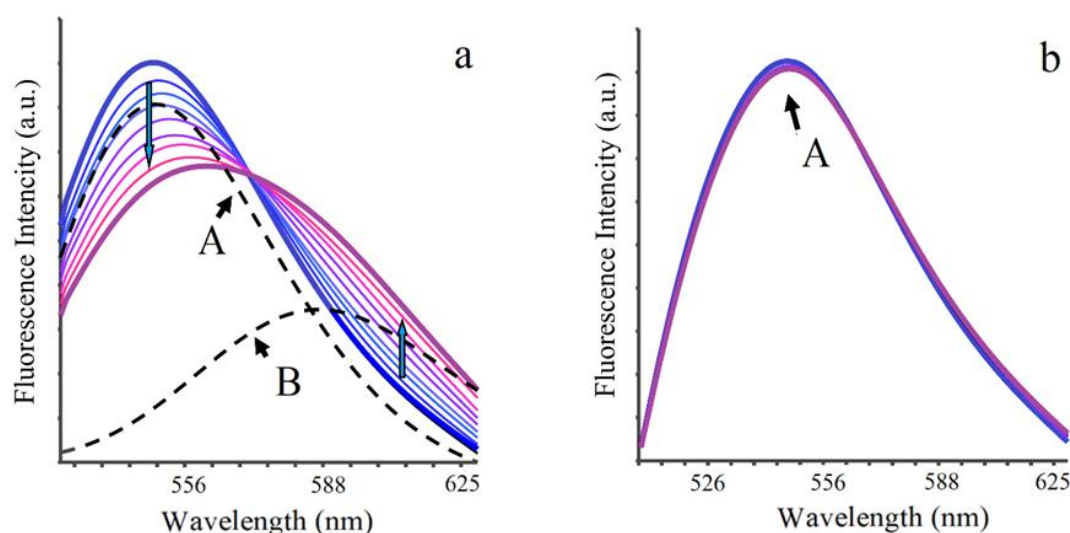


Figure 5.5: Time-resolved spectrum of 5'-aminofluorescein (*a*) and un-substituted fluorescein (*b*) in DMSO in the presence of 0.02 M DBU. Starting curve A is approximately 0.3 ns after pulse, the final curve is for 3 ns delay; the time gap between neighboring spectral curves is 0.1 ns. A: dianion emission band, B: new long-wavelength emission band.

Table 5.4: Spectral and kinetic characteristics of emitting forms of 5'-aminofluorescein in DMSO solutions obtained by TRS analysis

Medium	Short-wavelength band (A)		Long-wavelength band (B)		A→B rate constant, $k_{A\rightarrow B}, \text{ s}^{-1}$
	$\lambda_{\text{max}}, \text{ nm}$ ($\nu_{\text{max}}, \text{ cm}^{-1}$)	$\tau, \text{ ns}$	$\lambda_{\text{max}}, \text{ nm}$ ($\nu_{\text{max}}, \text{ cm}^{-1}$)	$\tau, \text{ ns}$	
Benzoate buffer, $\text{p}a_{\text{H}^+} = 12.0$	555 (18020)	2.3	615 (16280)	0.67	8.5×10^7
DBU solution, 0.02 M	550 (18220)	2.9	588 (17020)	4.31	4.2×10^7

Since the acidic dissociation of the amino group in the basic medium used seems to be hardly possible, the formation of the new form can be explained by the interaction between the carboxyl anion and a counter ion. In our opinion, it would be reasonable to attribute this form to excited-state ionic pairs stabilized by the electron-releasing effect of the amino group.

In the case of benzoate buffer (Figure 5.4b), the counter ion is K^+ . Its interaction with carboxylate anion results, in fact, in its partial neutralization, so, the structure obtained

approaches to some degree that of the monoanion. The ionic pair thus obtained has a low fluorescence intensity, short lifetime and the emission band shifted to the red region by 1740 cm^{-1} relative to that of the dianion.

In the case of DBU addition (Figure 5.5a), HDBU⁺ ions appear as a result of deprotonation of the dye ($\text{H}_2\text{R} \rightarrow \text{R}^{2-}$). We expect that these cations can form ionic pairs with the COO^- groups of dye anions in the excited state. The rate of such interaction is twice slower as in the case of K^+ counter ion because the concentration of the latter is three orders of magnitude higher as compared with that of HDBU⁺. On the other hand, the last-named cation may form a hydrogen bond with the carboxylate; thus, this ionic pair should be considered a tighter one, despite the well-known electron-donor ability of the DMSO molecules. Therefore, such either contact or solvent-shared ionic pair exhibits a much higher fluorescence lifetime than the (probably solvent-separated) ionic pair with the K^+ ion. In the DBU-containing solution, the emission band of the (probable) ionic pair is of higher intensity and less shifted to the red range (1200 cm^{-1}), and the lifetime is drastically longer. This phenomenon is absent in the case of the un-substituted fluorescein because of the lack of the NH_2 group, which increases the basicity of the carboxylate group.

5.4 2,4,5,7-Tetranitrofluorescein methyl ester: A new pH-independent indicator, sensitive to hydrogen binding

Single-charged anions HR^- exist in solutions within a narrow $\text{p}a_{\text{H}^+}^*$ range. However, it is well established that they exhibit bright light emission. For 2,4,5,7-tetranitrofluorescein, it was already demonstrated in 90 % aqueous acetone [29], entire acetone [30], and DMSO [29]. We determined the quantum yield for the monoanion of 2,4,5,7,4'-pentanitrofluorescein in DMSO (Figure 5.6), $\varphi = 21.2\%$. Obviously, the origin of the emission is the HX^- tautomer. Note, that the emission of solutions where the R^{2-} ions predominate is negligible: $\varphi = 0.4\text{--}0.5\%$ for both pentanitrofluoresceins.

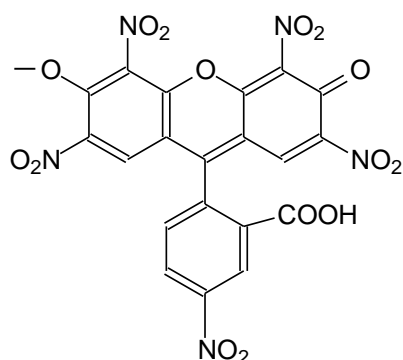


Figure 5.6: 2,4,5,7,4'-pentanitrofluorescein anion R^- .

The methyl ester of the 2,4,5,7-tetranitrofluorescein (Figure 5.7) is almost pH-independence in different solvents from DMSO to water. Even in benzene, some features of the anion are observed in the visible spectrum, though they may be caused by small traces of water. Only in alkaline media, the compound is unstable because of hydrolysis of the ester group followed by rupture of the pyran ring. Also, in concentrated acids, about 0.5–1 M, hydrolysis occurs, and the colorless lactone is formed.

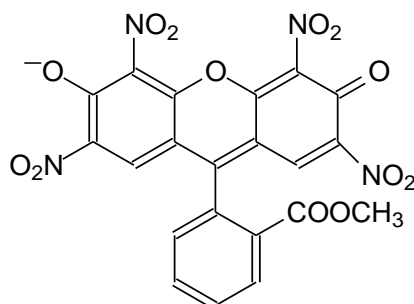


Figure 5.7: The methyl ester of the 2,4,5,7-tetranitrofluorescein anion R^- .

At the same time, this dye is highly fluorescent. Moreover, the dependence of the fluorescence on the hydrogen bond of the solvent is pronounced. Namely, the light emission in water is almost absent; while in acetonitrile the quantum yield is 86 % (Table 5.5). Normalized fluorescence spectra of the methyl ester of the 2,4,5,7-tetranitrofluorescein for several solvents are represented in Figure 5.8.

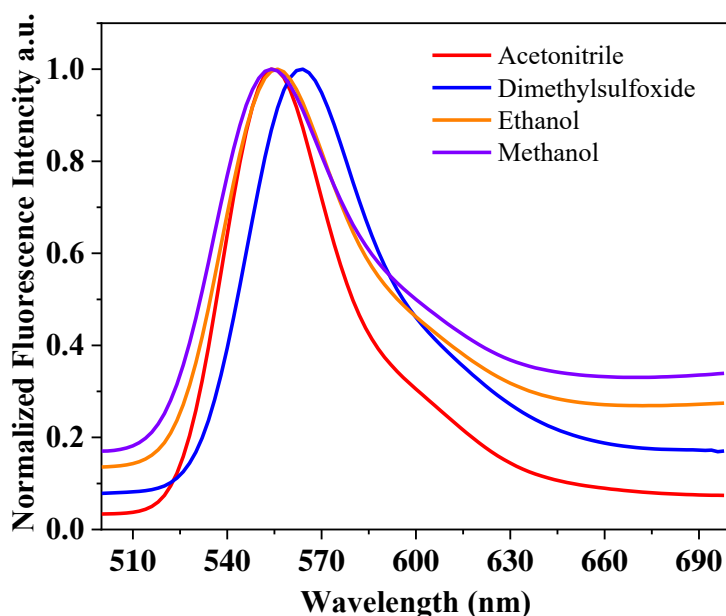


Figure 5.8: Normalized fluorescence spectra of the methyl ester of the 2,4,5,7-tetranitrofluorescein in methanol (-----), ethanol (-----), acetonitrile (2; -----), and dimethylsulfoxide (3; -----); 0,01 M NaOH and 0.02 M DBU in solutions ensure complete conversion of the dye into the R^- ion.

Table 5.5: Fluorescence parameters of the 2,4,5,7-tetranitrofluorescein methyl ester anion in different solvents

Solvent	ϵ_r	E_T^N	$\lambda_{\max}^{\text{abs}}$	$\lambda_{\max}^{\text{em}}$	$\phi, \%$
Acetonitrile	35.95	0.460	522	554	85.5
DMSO	46.5	0.444	527	563	80.2
96 % aqueous ethanol	25.9	0.861	523	555	65.9
Methanol	32.7	0.762	519	554	49.0
H ₂ O	78.4	1.000	506	—	0

The ϵ_r and E_T^N values are from ref. [26]; the ϵ_r and E_T^N values for aqueous ethanol are from ref. [31] and [32], respectively.

Chapter 5

The dye in DMSO solutions is chemically- and photo-stable. In the dark, no changes were observed within two weeks. After two days of exposure to normal laboratory lighting, the absorbance is reduced by 25%, while after 10 min illuminating by a standard deuterium lamp, no changes are registered. Only when exposed to direct sunlight on a bright sunny day, absorption decreases by a factor of three within an hour.

The lower ϕ value for the monoanion of 2,4,5,7,4'-pentanitrofluorescein in DMSO is clearly caused by the emission quenching by the nitro group in the case of 4'-nitrofluorescein [28]. Therefore, it is just the ester of 2,4,5,7-tetranitrofluorescein that can serve as a hydrogen bonds-sensitive fluorescent indicator. To obtain the neutral form in any of the polar solvents is impossible, only in benzene with small sulfuric acid addition. High acid concentrations lead to hydrolysis of the carbmethoxy group; in concentrated alkali, in addition to the hydrolysis, the rupture of the pyran cycle takes place. Accepting these extreme media, the anion predominates within the whole pH scale.

5.5 Conclusions

Dianions R^{2-} of 4'- and 5'-aminofluoresceins in DMSO, DMF, acetonitrile, ketones, and dichloromethane exhibit bright fluorescence with quantum yields of (59–84) %. However, contrary to the un-substituted fluorescein, the emission is strongly quenched in water and alcohols. This observation, in accord with titration of the dye solutions in DMSO and CH_3CN with water and time-resolved measurements, allows deducing that the reason for quenching is the hydration of the COO^- group in the phthalic residue of dye ion R^{2-} , solvation of it with H-bond donors such as alcohols, and protonation ($COO^- \rightarrow COOH$). The last conclusion was made based on the study of tautomerism of the single-charged ion HR^- of 5'-aminofluorescein, reported in the preceding paper.²⁶ Hence, the quenching influence of the NH_2 group on the emission of the xanthene fluorophore manifests itself only if the COO^- group in the 2' position is either involved in H-bonds (e.g., hydrated) or protonated. Otherwise, the negatively charged carboxylate, which is poorly solvated in aprotic solvents, prevents the above-mentioned influence of the amino group. This finding seems to be important for understanding the emission processes in fluorescein series in the case of the introduction of electron-donating groups, such as NH_2 , in the phthalic residue.

The lower ϕ value for the monoanion of 2,4,5,7,4'-pentanitrofluorescein in DMSO is clearly caused by the emission quenching by the nitro group in the case of 4'-nitrofluorescein.

Therefore, it is just the ester of 2,4,5,7-tetranitrofluorescein that can serve as a hydrogen bonds-sensitive fluorescent indicator.

Also, the above-mentioned ester is a useful tool for studying different liquid media. Owing to the extremely high acidity of the OH group, it exists in anionic form within a wide pH range. The quantum yield of fluorescence is strongly dependent on the hydrogen bond donor ability of the solvent, from $\phi = 85\%$ in acetonitrile to 49% in methanol; in water, $\phi = 0$. It is also important in the future to study step-by-step the effect of hydrogen bonds in mixtures of aprotic and hydrogen bond donor solvents.

Bibliography

1. Haugland, R.P.: Handbook of fluorescent probes and research products. Molecular Probes, Inc, Eugene, Or (2002).
2. Gee, K.R.: Novel fluorogenic substrates for acid phosphatase. *Bioorg Med Chem Lett.* 9, 1395–1396 (1999). [https://doi.org/10.1016/S0960-894X\(99\)00199-7](https://doi.org/10.1016/S0960-894X(99)00199-7)
3. Mottram, L.F., Boonyarattanakalin, S., Kovel, R.E., Peterson, B.R.: The Pennsylvania Green Fluorophore: A Hybrid of Oregon Green and Tokyo Green for the Construction of Hydrophobic and pH-Insensitive Molecular Probes. *Org Lett.* 8, 581–584 (2006). <https://doi.org/10.1021/ol052655g>
4. Ueno, T., Urano, Y., Setsukinai, K.I., Takakusa, H., Kojima, H., Kikuchi, K., Ohkubo, K., Fukuzumi, S., Nagano, T.: Rational principles for modulating fluorescence properties of fluorescein. *J Am Chem Soc.* 126, 14079–14085 (2004). <https://doi.org/10.1021/ja048241k>
5. Egawa, T., Koide, Y., Hanaoka, K., Komatsu, T., Terai, T., Nagano, T.: Development of a fluorescein analogue, TokyoMagenta, as a novel scaffold for fluorescence probes in red region. *Chemical Communications.* 47, 4162 (2011). <https://doi.org/10.1039/c1cc00078k>
6. Hirabayashi, K., Hanaoka, K., Takayanagi, T., Toki, Y., Egawa, T., Kamiya, M., Komatsu, T., Ueno, T., Terai, T., Yoshida, K., Uchiyama, M., Nagano, T., Urano, Y.: Analysis of Chemical Equilibrium of Silicon-Substituted Fluorescein and Its Application to Develop a Scaffold for Red Fluorescent Probes. *Anal Chem.* 87, 9061–9069 (2015). https://doi.org/10.1021/ACS.ANALCHEM.5B02331/SUPPL_FILE/AC5B02331_SI_001.PDF
7. Grimm, J.B., Sung, A.J., Legant, W.R., Hulamm, P., Matlosz, S.M., Betzig, E., Lavis, L.D.: Carbofluoresceins and Carborhodamines as Scaffolds for High-Contrast Fluorogenic Probes. *ACS Chem Biol.* 8, 1303–1310 (2013). <https://doi.org/10.1021/cb4000822>
8. Crovetto, L., Orte, A., Paredes, J.M., Resa, S., Valverde, J., Castello, F., Miguel, D., Cuerva, J.M., Talavera, E.M., Alvarez-Pez, J.M.: Photophysics of a Live-Cell-Marker, Red Silicon-Substituted Xanthene Dye. *J Phys Chem A.* 119, 10854–10862 (2015). <https://doi.org/10.1021/acs.jpca.5b07898>
9. Grimm, J.B., Gruber, T.D., Ortiz, G., Brown, T.A., Lavis, L.D.: Virginia Orange: A Versatile, Red-Shifted Fluorescein Scaffold for Single- And Dual-Input Fluorogenic Probes. *Bioconjug Chem.* 27, 474–480 (2016). https://doi.org/10.1021/ACS.BIOCONJCHEM.5B00566/ASSET/IMAGES/LARGE/BC-2015-00566D_0006.JPEG
10. Zhang, X.F., Liu, Q., Wang, H., Zhang, F., Zhao, F.: Prototropic equilibria, tautomerization and electronic absorption properties of dibenzofluorescein in aqueous solution related to its capability as a fluorescence probe. *Photochemical & Photobiological Sciences.* 7, 1079–1084 (2008). <https://doi.org/10.1039/B801883A>

11. Urano, Y., Kamiya, M., Kanda, K., Ueno, T., Hirose, K., Nagano, T.: Evolution of fluorescein as a platform for finely tunable fluorescence probes. *J Am Chem Soc.* 127, 4888–4894 (2005).
<https://doi.org/10.1021/JA043919H/ASSET/IMAGES/MEDIUM/JA043919HN00001.GIF>
12. Lavis, L.D., Rutkoski, T.J., Raines, R.T.: Tuning the pK_a of Fluorescein to Optimize Binding Assays. *Anal Chem.* 79, 6775–6782 (2007). <https://doi.org/10.1021/ac070907g>
13. Kojima, H., Urano, Y., Kikuchi, K., Higuchi, T., Hirata, Y., Nagano, T.: Fluorescent Indicators for Imaging Nitric Oxide Production. *Angewandte Chemie International Edition.* 38, 3209–3212 (1999). [https://doi.org/10.1002/\(SICI\)1521-3773\(19991102\)38:21<3209::AID-ANIE3209>3.0.CO;2-6](https://doi.org/10.1002/(SICI)1521-3773(19991102)38:21<3209::AID-ANIE3209>3.0.CO;2-6)
14. Nagano, T., Yoshimura, T.: Bioimaging of Nitric Oxide. *Chem Rev.* 102, 1235–1270 (2002). <https://doi.org/10.1021/cr010152s>
15. Fabregat, V., Izquierdo, M.Á., Burguete, M.I., Galindo, F., Luis, S. V.: Nitric oxide sensitive fluorescent polymeric hydrogels showing negligible interference by dehydroascorbic acid. *Eur Polym J.* 55, 108–113 (2014). <https://doi.org/10.1016/j.eurpolymj.2014.03.027>
16. Bazylevich, A., Patsenker, L.D., Gellerman, G.: Exploiting fluorescein based drug conjugates for fluorescent monitoring in drug delivery. *Dyes and Pigments.* 139, 460–472 (2017). <https://doi.org/10.1016/j.dyepig.2016.11.057>
17. Burchak, O.N., Mughherli, L., Chatelain, F., Balakirev, M.Y.: Fluorescein-based amino acids for solid phase synthesis of fluorogenic protease substrates. *Bioorg Med Chem.* 14, 2559–2568 (2006). <https://doi.org/10.1016/j.bmc.2005.11.037>
18. Martineau, M., Somasundaram, A., Grimm, J.B., Gruber, T.D., Choquet, D., Taraska, J.W., Lavis, L.D., Perrais, D.: Semisynthetic fluorescent pH sensors for imaging exocytosis and endocytosis. *Nat Commun.* 8, 1412 (2017). <https://doi.org/10.1038/s41467-017-01752-5>
19. Zhang, X.-F.: The effect of phenyl substitution on the fluorescence characteristics of fluorescein derivatives via intramolecular photoinduced electron transfer. *Photochemical & Photobiological Sciences.* 9, 1261 (2010). <https://doi.org/10.1039/c0pp00184h>
20. Zhang, X.-F., Zhang, J., Liu, L.: Fluorescence Properties of Twenty Fluorescein Derivatives: Lifetime, Quantum Yield, Absorption and Emission Spectra. *J Fluoresc.* 24, 819–826 (2014). <https://doi.org/10.1007/s10895-014-1356-5>
21. Ge, F., Yang, C., Cai, Z.: Fluorescence Sensor Performance of a New Fluorescein Derivate: [2-Morpholine-4-(6-chlorine-1,3,5-s-triazine)-aminofluorescein. *Bull Korean Chem Soc.* 36, 2703–2709 (2015). <https://doi.org/10.1002/bkcs.10551>
22. Liu, B., Fletcher, S., Avadisian, M., Gunning, P.T., Gradinaru, C.C.: A Photostable, pH-Invariant Fluorescein Derivative for Single-Molecule Microscopy. *J Fluoresc.* 19, 915–920 (2009). <https://doi.org/10.1007/s10895-009-0492-9>

Chapter 5

23. Mchedlov-Petrosyan, N.O., Cheipesh, T.A., Roshal, A.D., Doroshenko, A.O., Vodolazkaya, N.A.: Fluorescence of aminofluoresceins as an indicative process allowing one to distinguish between micelles of cationic surfactants and micelle-like aggregates. *Methods Appl Fluoresc.* 4, 034002 (2016). <https://doi.org/10.1088/2050-6120/4/3/034002>
24. Munkholm, C., Parkinson, D.R., Walt, D.R.: Intramolecular fluorescence self-quenching of fluoresceinamine. *J Am Chem Soc.* 112, 2608–2612 (1990). <https://doi.org/10.1021/ja00163a021>
25. Mchedlov-Petrosyan, N.O., Cheipesh, T.A., Shekhovtsov, S. V., Ushakova, E. V., Roshal, A.D., Omelchenko, I. V.: Aminofluoresceins Versus Fluorescein: Ascertained New Unusual Features of Tautomerism and Dissociation of Hydroxyxanthene Dyes in Solution. *Journal of Physical Chemistry A.* 123, 8845–8859 (2019). https://doi.org/10.1021/ACS.JPCA.9B05810/SUPPL_FILE/JP9B05810_SI_001.PDF
26. Reichardt, C. (Christian): *Solvents and solvent effects in organic chemistry.* Wiley-VCH (2003).
27. Magde, D., Wong, R., Seybold, P.G.: Fluorescence Quantum Yields and Their Relation to Lifetimes of Rhodamine 6G and Fluorescein in Nine Solvents: Improved Absolute Standards for Quantum Yields. *Photochem Photobiol.* 75, 327 (2002). [https://doi.org/10.1562/0031-8655\(2002\)075<0327:FQYATR>2.0.CO;2](https://doi.org/10.1562/0031-8655(2002)075<0327:FQYATR>2.0.CO;2)
28. Martin, M.M.: Hydrogen bond effects on radiationless electronic transitions in xanthene dyes. *Chem Phys Lett.* 35, 105–111 (1975). [https://doi.org/10.1016/0009-2614\(75\)85598-9](https://doi.org/10.1016/0009-2614(75)85598-9)
29. Mchedlov-Petrosyan, N.O., Vodolazkaya, N.A., Surov, Y.N., Samoylov, D. V.: 2,4,5,7-Tetranitrofluorescein in solutions: novel type of tautomerism in hydroxyxanthene series as detected by various spectral methods. *Spectrochim Acta A Mol Biomol Spectrosc.* 61, 2747–2760 (2005). <https://doi.org/10.1016/J.SAA.2004.09.030>
30. Mchedlov-Petrosyan, N.O., Steinbach, K., Vodolazkaya, N.A., Samoylov, D. V., Shekhovtsov, S. V., Omelchenko, I. V., Shishkin, O. V.: The molecular structure of anionic species of 2,4,5,7-tetranitrofluorescein as studied by electrospray ionisation, nuclear magnetic resonance and X-ray techniques. *Coloration Technology.* 134, 390–399 (2018). <https://doi.org/10.1111/COTE.12351>
31. Akerlof, G.: Dielectric constants of some organic solvent-water mixtures at various temperatures. *J Am Chem Soc.* 54, 4125–4139 (1932). <https://doi.org/10.1021/ja01350a001>
32. Krygowski, T.M., Wrona, P.K., Zielkowska, U., Reichardt, C.: Empirical parameters of lewis acidity and basicity for aqueous binary solvent mixtures. *Tetrahedron.* 41, 4519–4527 (1985). [https://doi.org/10.1016/S0040-4020\(01\)82346-2](https://doi.org/10.1016/S0040-4020(01)82346-2)

Chapter 6

Conformational effect on the photophysics of two BODIPY dyes in a mixture of butanol and acetonitrile

The chapter is the basis of the paper titled:

BODIPY dyes as molecular rotors for evaluating the viscosity of acetonitrile-butanol-1 mixtures Olena Moskaieva,¹ Maksim Lebedev,² Yevheniia Smortsova,³ Julien Dubois,³ Abdenacer Idrissi,^{3*} Oleg Kalugin,⁴ Francois-Alexandre Miannay.^{3*}

In the previous chapter, we made assumptions about the origin of fluorescence quenching of R^{2-} species of fluorescein derivatives in DMSO, water and alcohols based on fluorescence lifetimes, quantum yields, time-resolved, fluorescence spectra data and DFT calculation results.

All these data were obtained for pure solvents. There are a small number of articles that observed fluoresceins in solvent mixtures in the literature. It is promising to study the nitro- and aminoderivatives of fluorescein in a mixture of an aprotic solvent - a hydrogen bond donor solvent.

Such a study is complicated by the presence of various tautomeric forms of the dye, which complicates the interpretation of the results. Also, the choice of compounds that create a certain acidity of the medium is limited. For the first stage of the investigation, as the model compound was taken BODIPY derivatives with aryl, pyridine substituents in the meso position are similar to fluorescein, which has a xanthene fragment and a phenyl fragment perpendicular to it. The dyes chosen for the study do not dissociate upon dissolution and have stable fluorescence in these solvents. This allows observing the influence of solvent mixture on the photophysics of the investigated dyes with a change in the molar fraction of the solvent.

6.1 Introduction

Nowadays, boron-dipyrromethene (4,4-difluoro-4-bora-3a,4a-diaza-s-indacene, BODIPY), fluorescent dyes are one of the 30 most common and intensively studied classes of fluorophores [1]. BODIPY finds numerical applications as pH sensors for biological systems [2], measuring agents for solvents parameters [3–5], label for marking proteins and DNA [6–8], fluorescent indicators for selective detection of cations and anions [9–13], molecular rotors for the evaluation of the viscosity of microenvironment [14–17].

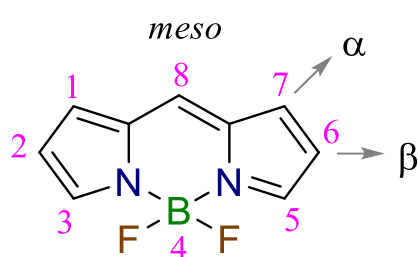


Figure 6.1: Structure of 4,4-difluoro-4-bora-3a,4a-diaza-s-indacene, BODIPY “core”.

The study of the literature indicates that the photophysical properties of the BODIPY is strongly dependent on the substituent on the different positions that are indicated in Fig. 1. Indeed, there is no significant difference between the absorption wavelength maxima for compounds with unsymmetrical or symmetrical methyl substituents in the β position, while the substituent in the α -position slightly affects the absorption maxima (7-10 nm shift) [18, 19]. However, there is a noticeable trend towards red-shifted absorption and emission maxima with an increase in substitution for symmetrically-tetra-, hexa-, and hepta-alkylated systems [18, 19]. The presence of substituents on the 2,6 positions of the pyrrole units (both are β -pyrrole positions) exerts some evident effects: for instance, the presence of alkyl groups or heavy atoms has a direct influence on the energy of the HOMO-LUMO orbitals [20, 21]. Alkylation or arylation at position 8 does not significantly affect the absorption and emission wavelengths (3-5 nm). However, the quantum yield of the mesophenyl compounds with 3,5 substituents is noticeably lower than that of the more substituted analogue. 1,7-substituents prevent the free rotation of the phenyl group, reducing energy loss from excited states. The introduction of ortho substituents into the phenyl ring is used to increase the quantum yield [18, 19, 22, 23]. Finally, 8-Phenyl substituted boron-dipyrromethene exhibits properties of the molecular rotor, especially long chain alkyl substituents, i.e., its fluorescent characteristics highly dependent on

the viscosity or rigidity of the microenvironment [16, 21]. This property allows us to measure viscosity on a microscopic scale [14].

The above-mentioned results on the effect of the photophysics of the BODIPY derivatives were rationalized in various neat solvents that mimic locale environment with specific polarity; viscosity and ability to form hydrogen bonds [2, 24–26]. However, very few works were dedicated to the effect of progressive changes of media properties (by varying solvent mixture molar fractions) on the photophysics of the BODIPY derivatives [5, 27, 28]. The advantage of this approach is to progressively change the BODIPY derivatives' local environment between two strongly different intermolecular interactions associated with the neat components of the solvent mixtures. The changes in the mixture composition allow to modulate gradually these interactions and as so the changes in the spectroscopic behaviour of the dye are not a linear combination between the two main interactions in the neat components but a synergetic effect may result in a particular behaviour of the photophysics of the BODIPY derivatives. One interesting mixture is that of butanol-1 (BuOH) and acetonitrile (AN), where the local environment is dominated by hydrogen bond and dipole-dipole interactions, respectively. More specifically, the experimental data shows that with increasing the BuOH content in the mixture, the density, viscosity, and index of refraction increase, while the dielectric constant and the conductivity decrease [29–31].

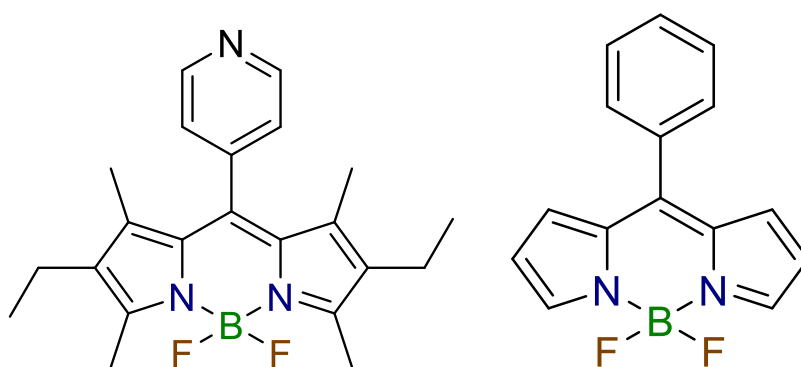


Figure 6.2: 1,3,5,7-tetramethyl-4,4-difluoro-2,6-diethyl-8-(4-pyridine)-4-boron-3a,4a-diaza-s-indacene – BDP1 (left) and 8-phenyl-4,4-difluoro-4-boron-3a,4a-diaza-s-indacene – BDP2 (right).

In this work, we present an investigation of the effects of the BuOH/AN mixture composition on the photophysics of two new BODIPY derivatives, with an aryl and pyridine substituent in the meso position and methyl (ethyl) in α,β -position (Figure 6.2), using steady-state spectroscopies (UV-Vis absorption spectra, fluorescence emission spectra, and fluorescence quantum yields), time-resolved fluorescence spectroscopy (Time-Correlated-

Chapter 6

Single-Photon-Counting) and theoretical calculations. By combining these three investigation techniques, we have been able to introduce an accessible explanation of how the molecular structure of BODIPY helps a fast photodeactivation of the molecule and to assess the possible use of these dyes as a viscosity probe of media.

6.2 Experimental section

6.2.1 Chemicals

The dyes (Figure 6.2) are synthesized at the Ivanovo State University of Chemistry and Technology. Acetonitrile (ACN, $\geq 99,9$ %, HPLC) and butanol-1 (BuOH, anhydrous, spectrophotometric grade, 99.8%) were purchased from Sigma Aldrich. The rhodamine 6G (99% pure) used as a reference for fluorescence quantum yields of BDP1 and BDP2 was purchased from ACORS Organics.

All the substances and solvents were stored in a glove box under an inert argon atmosphere. All solvent mixtures were prepared and kept inside an argon-atmosphere glovebox.

6.2.2 Steady-state Spectroscopy

The absorption and the fluorescence steady-state measurements were performed at room temperature (20°C air conditioning) using a Cary 100 spectrophotometer and a Cary-Eclipse spectrofluorometer (Varian) and a FLUOROMAX 3 spectrofluorometer (Jobin-Yvon-Horiba). The fluorescence spectra were acquired with 2 nm and 3 nm bandpass for the excitation and emission, respectively. Correction for the instrument wavelength-dependent response was applied. Quartz fluorescence cells 10 mm SUPRASIL from Hellma with screw cap and septum were used. All the fluorescence measurements have been performed with solutions with absorbance values lower than 0.1 at the excitation wavelength.

To determine the fluorescence quantum yields of BDP1 and BDP2, a solution of rhodamine 6G in ethanol was used as a reference with a known quantum yield ($\Phi_{\text{fluo}}=0.94$) [32]. This standard is chosen because it absorbs and emits light in the same spectral region as the BODIPY derivatives under study [33].

The quantum yield of the studied compound was calculated using the equation (6.1):

$$\Phi_{sample}^{fluo}(\lambda_{exc}) = \Phi_{ref}^{fluo}(\lambda_{exc}) \frac{\int_0^{\infty} I_{sample}^{fluo}(\lambda_{exc}; \lambda_{fluo}) d\lambda_{fluo}}{\int_0^{\infty} I_{ref}^{fluo}(\lambda_{exc}; \lambda_{fluo}) d\lambda_{fluo}} * \frac{1-10^{-A_{ref}(\lambda_{exc})}}{1-10^{-A_{sample}(\lambda_{exc})}} * \frac{n_{solve,sample}^2}{n_{solve,ref}^2} \quad (6.1)$$

6.2.3 Time-resolved fluorescence

Fluorescence decays of the various solutions of BDP1 and BDP2 were performed using the TCSPC technique. The TCSPC setup used was described elsewhere [34]. The excitation source is provided by a 467 nm PICOQUANT picosecond laser diode (LDH-P-C-470) at 4 MHz. The Poisson statistics of the count's distribution have been fulfilled during all the measurements. The FT-200 PicoQuant spectrometer was used to perform fluorescence signal acquisition. A HAMAMATSU cooled microchannel plate photomultiplier tube was used as the detector, with signals recorded by a PicoHarp 300 TCSPC card. A single-grated monochromator placed after the emission polarizer 0.5 mm slits provides 4 nm spectral resolution. The overall time resolution of the setup was characterized by the Instrument Response Function (IRF), measured by placing a LUDOX solution in the sample holder and recording the scattered excitation light to get the time profile of the excitation pulse. The IRF full-width half maximum (FWHM) was measured to be 80 ps. Temperature control of the sample was performed using a Peltier module. For all the measurements, the temperature of the sample holder was fixed at 20°C. All the system was checked before each experiment, recording the fluorescence decays of C153 in MeOH and ACN at 530 nm, giving both a mono-exponential decay ($\chi^2 = 1.01$) with times in good agreement with the literature, 4.03 ns and 5.62 ns respectively [35].

The radiative and non-radiative constants of the studied compound were calculated using the equation 6.2 and 6.3 [36]:

$$k_{rad} = \frac{\Phi_{sample}^{fluo}}{\tau_{fluo}} \quad (6.2)$$

$$k_{nonrad} = \frac{k_{rad} * (1 - \Phi_{sample}^{fluo})}{\Phi_{sample}^{fluo}} \quad (6.3)$$

The fluorescence decays were analyzed with multiexponential models (Equation 6.4) using FluoFit Picoquant software [27].

$$F(t) = \int_0^t IRF(t') \sum_{i=1}^n A_i \exp\left(-\frac{t-t'}{\tau_i}\right) dt' \quad (6.4)$$

Where $IRF(t')$ is the instrument response function, n is the number of exponential components, A_i and τ_i are the pre-exponential factors and lifetimes of the i -th exponential component. The iterative deconvolution procedure was followed, applying Poisson distribution weighing. The quality of the fits was estimated by visual inspection of the weighted residues and autocorrelation function $Res(\tau)$ of residues, as well as the reduced chi-squared value χ_{Red}^2 .

6.3 Result and Discussion

6.3.1 Steady-state Absorption and Fluorescence Spectra

UV-Vis absorption and emission spectra of BDP1 and BDP2 dyes were recorded in the whole mixture of acetonitrile-butanol-1 mixture. The compositions considered cover the entire composition range from neat BuOH to neat AN with a mole fraction grid of ~ 0.1 . Steady-state absorption and emission spectra of BDP1 and BDP2 in acetonitrile-butanol-1 mixtures are shown in Figure 6.3 and Figure 6.4.

There are no changes in the absorption spectra. In the fluorescence spectra, we observe a noticeable decrease in the fluorescence intensity for BDP1 and an increase for BDP2 with changing X_{BuOH} . We reported in Tables 6.1 and 6.2, the values of the maximum of both absorption and emission wavelengths (λ_{max} , in nm) of the two BODPY derivatives as a function of the mixture composition the behaviour of which is presented in Figure 6.5. It shows that increasing the BuOH content of the mixture, which means an increase of the viscosity, a decrease of the dielectric constant, a decrease of the ability to form a hydrogen bond, an increase of dipole–dipole interactions), the maxima of the absorption and fluorescence spectra are weakly dependent on the mixture composition and a slight bathochromic shift occurs (the shift never exceeds 2-4 nm).

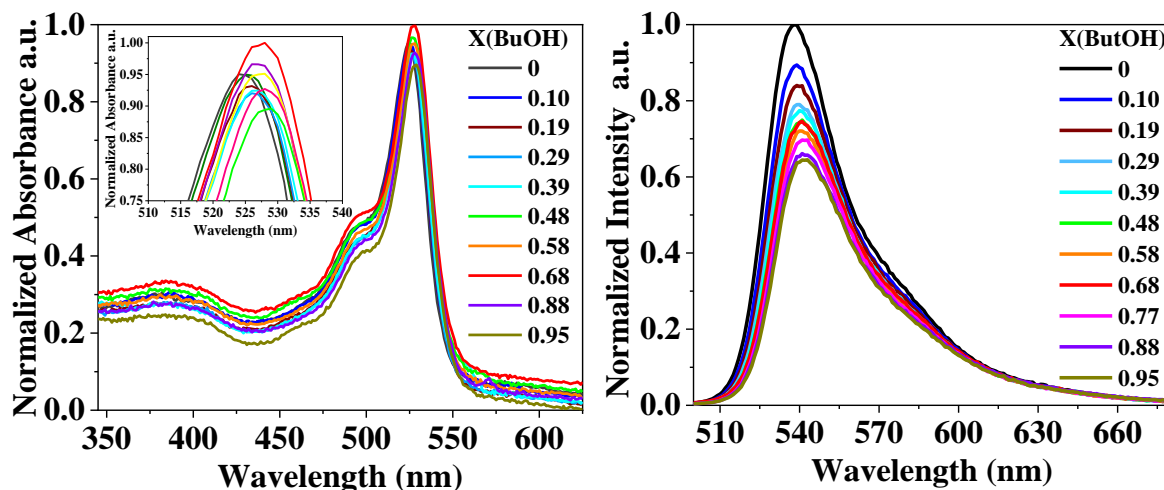


Figure 6.3: Normalized steady-state absorption (left) and emission (right) spectra of BDP1 in whole mixture composition of AN and BuOH ($\lambda_{\text{excitation}}=470$ nm). The absorption spectra at the maximum are shown in the inset.

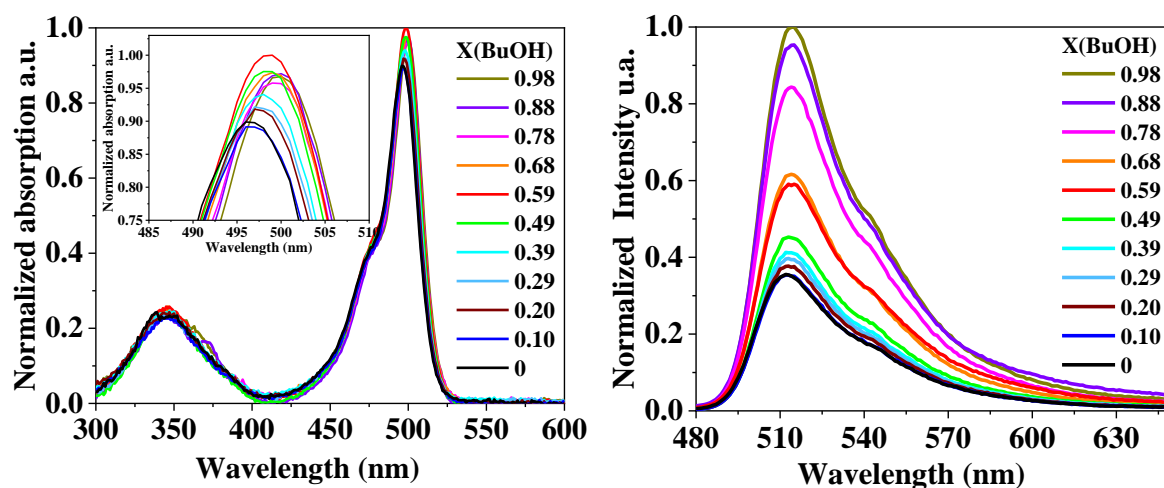


Figure 6.4: Normalized steady-state absorption (left) and emission (right) spectra of BDP2 in whole mixture composition of AN and BuOH ($\lambda_{\text{excitation}}=470$ nm). The absorption spectra at the maximum are shown in the inset.

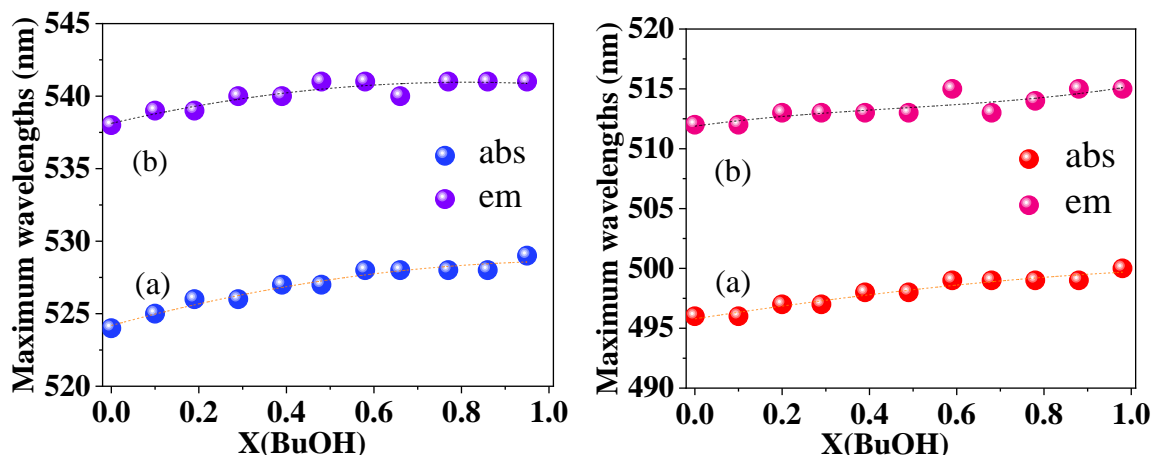


Figure 6.5: Maximum absorption (a) and emission (b) wavelengths for $S_0 \rightarrow S_1$ transition for BDP1(left) and BDP2 (right) as a function of the molar fraction of the BuOH.

Table 6.1: The spectroscopic properties of BDP1 in acetonitrile butanol-1 mixtures: maximum absorption and emission wavelengths (λ_{max} in nm). The average value of wavelengths ($\lambda_{average}$ in nm) and Stokes shift ($\Delta\nu_{Stokes}$ in cm^{-1}) are defined as the difference of maximum wavenumbers for absorption and emission. fluorescence quantum yield Φ_{fluo} (Rhodamine 6G in ethanol ($\Phi_{fluo} = 0.94$) was used as a standard); solvent properties: dielectric constant ϵ and viscosity η taken from [29]. The names of the solvents as well as their short names are listed this way: acetonitrile (ACN). butanol (BuOH).

X (BuO H)	ϵ	η . mPa*s	λ_{max}^{abs}	λ_{max}^{em}	$\Delta\nu_{Stokes}$. cm^{-1}	Φ_{fluo} . %
0.00	35.93	0.3326	524	538	531.09	0.1954
0.10	32.41	0.3599	525	539	494.74	0.1903
0.19	29.39	0.4087	526	539	527.12	0.1752
0.29	26.81	0.4754	526	540	492.89	0.1627
0.39	24.64	0.5602	527	540	491.04	0.1602
0.48	22.81	0.6674	527	541	527.12	0.1399
0.58	21.30	0.8047	528	541	455.11	0.1482
0.66	20.16	0.9638	528	540	455.11	0.1387
0.77	19.03	1.2190	528	541	523.19	0.1384
0.86	18.19	1.5296	528	541	523.19	0.1564
0.95	17.49	1.9357	529	541	453.41	0.1675

Table 6.2: The spectroscopic properties of BDP2 in acetonitrile butanol-1 mixtures: maximum absorption and emission wavelengths (λ_{max} , in nm). The average value of wavelengths ($\lambda_{average}$ in nm) and Stokes shift ($\Delta\nu_{Stokes}$, in cm^{-1}) are defined as the difference of maximum wavenumbers for absorption and emission. fluorescence quantum yield Φ_{fluo} (Rhodamine 6G in ethanol ($\Phi_{fluo} = 0.94$) was used as a standard); solvent properties: dielectric constant ε and viscosity η taken from [29].

X (BuOH)	ε	η , mPa*s	λ_{max}^{abs}	λ_{max}^{em}	$\Delta\nu_{Stokes}$, cm-1	Φ_{fluo} .%
0.00	35.93	0.3326	496	512	630.04	0.5141
0.10	32.31	0.3611	496	512	630.04	0.5552
0.20	29.21	0.4126	497	513	703.25	0.5785
0.29	26.81	0.4756	497	513	703.25	0.5940
0.39	24.55	0.5646	498	513	625.07	0.6222
0.49	22.66	0.6788	498	513	625.07	1.2049
0.59	21.10	0.8279	499	515	622.60	1.3753
0.68	19.94	1.004	499	513	622.60	2.3153
0.78	18.88	1.263	499	514	622.60	2.4504
0.88	18.02	1.612	499	515	622.60	2.9915
0.98	17.30	2.078	500	515	582.52	2.7299

6.3.2 Fluorescence quantum yield

The values of the fluorescence quantum yields of BDP1 and BDP2, calculated using Equation 6.1, are presented in Tables 6.1 and 6.2, respectively and their behavior as a function of the molar fraction of BuOH is built on Figure 6.6. This figure shows that in the mixtures, BDP2 exhibited always a higher fluorescence quantum yield than BDP1 whose values remain almost constant. Furthermore, the behaviour BDP2 can be divided into two stages in two stages: (i) in the first one which encompasses the low mole fraction range of values of X_{BuOH} from 0 to 0.48, where the viscosity values, η , change slightly, by about 0.33 units, the quantum yield values remain almost constant; (ii) for further increase of the BuOH content in the mixture, the viscosity increases by 1.27, and a significant increase of the quantum yield values are observed.

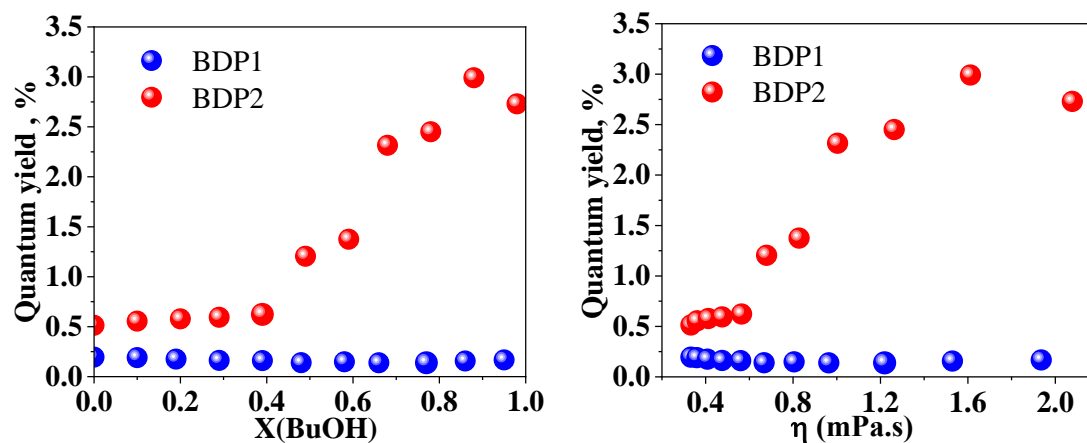


Figure 6.6: Fluorescence quantum yields of BDP1 (blue circle) and BDP2 (red circle) excited at 470 nm for various molar fractions of BuOH and viscosity. The reference used to measure the fluorescence quantum yields was rhodamine 6G in ethanol (excited at the same wavelength).

6.3.3 TCSPC measurements

The fluorescence intensity decays of the BDP1 and BDP2 were recorded varying the mixture composition of acetonitrile-butanol (Figures 6.7 and 6.8). The fitting parameters of the fluorescence decays of BDP1 using multiexponential functions: fluorescence lifetime components (τ_i , ps) and their relative contributions (A_i , normalized to the sum of positive components) are presented in the tables D1-D4(Appendix D).

Figures 6.7 and 6.8 show the fluorescence decays of BDP1 and BDP2, respectively, varying the BuOH molar fraction of the mixture. They clearly show that, in the whole mixture composition, the excited state relaxation process of BDP2 occurs in a shorter time than that of BDP1.

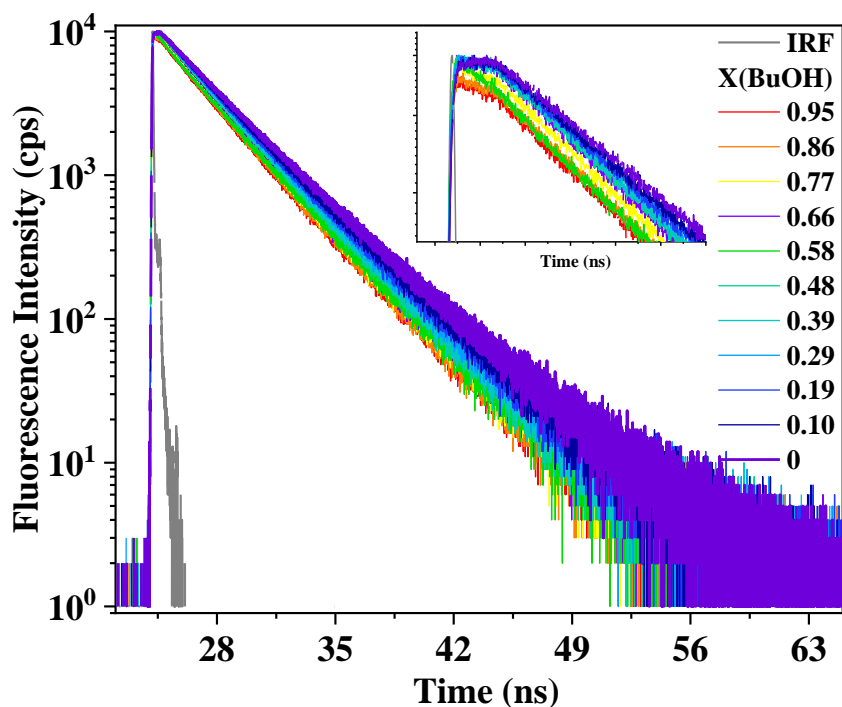


Figure 6.7: The fluorescence intensity decays of BDP1 in acetonitrile/butanol mixtures, pure ACN ($\lambda_{em}=538$ nm), X (BuOH) = 0.1 and 0.19 ($\lambda_{em}=539$ nm), X (BuOH) = 0.29 and 0.39 ($\lambda_{em}=540$ nm), X (BuOH) = from 0.48 to 0.95 ($\lambda_{em}=541$ nm), The instrument response function (IRF in grey) was recorded at 470 nm (FWHM = 80ps). The fluorescence intensity decays at the maximum are presented closer (inset).

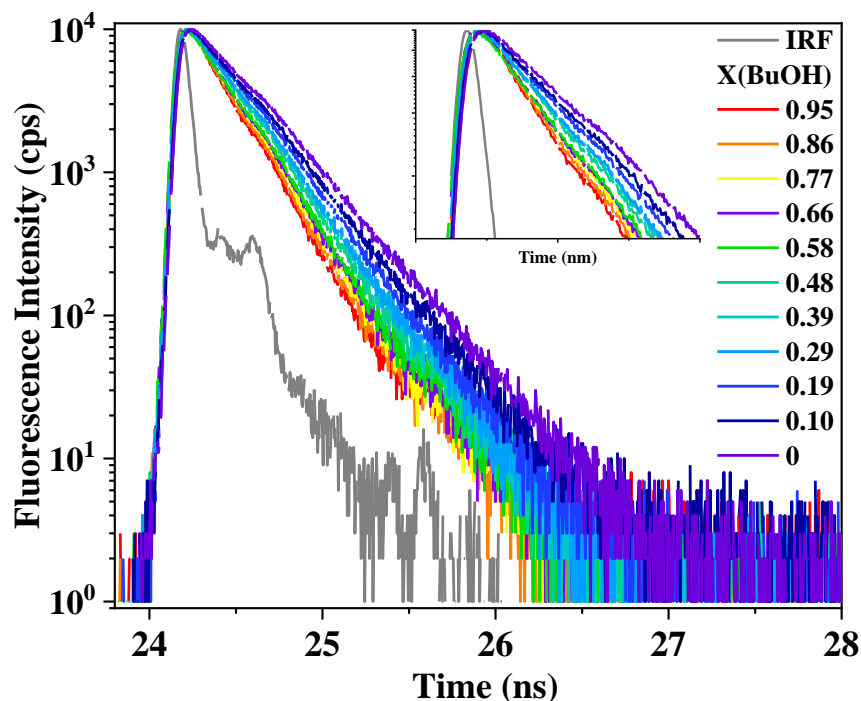


Figure 6.8: The fluorescence intensity decays of BDP2 in acetonitrile butanol mixtures, ($\lambda_{em}=513$ nm). The instrument response function (IRF in grey) was recorded at 470 nm (FWHM = 80ps). The fluorescence intensity decays at the maximum are presented closer (inset).

To quantify this relaxation process, we undertook a fluorescence intensity decay fitting (see 6.2 Experimental section). Depending on the composition of the mixture and the chosen BDP, one to two relaxation times were identified. Their evolution as a function of mixture composition is shown in Fig. 6.9. The two relaxation times that characterize the excited state of BDP1 (~ 4.4 ns and ~ 2.8 ns), show a slight dependence on the mixture composition. Of note is that the slower/faster of them increases/decreases slightly. The same trend is observed for the two relaxation times of BDP2 with a noticeable increase for the slower of them.

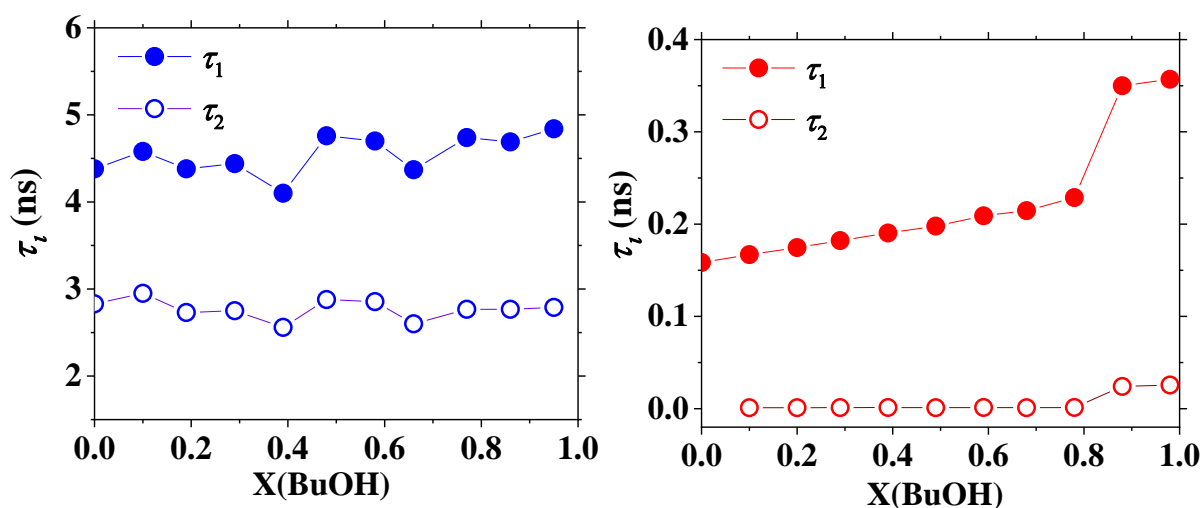


Figure 6.9: Evolution of the time components of BDP1(left) and BDP2 (right) fluorescence decay in acetonitrile/butanol mixtures in the function of the molar fraction of BuOH.

In order to get additional information on the relaxation process of the excited state, we calculated the fluorescence radiative and nonradiative rate constants of BDP1 and BDP2 in the mixture of ACN and BuOH. Their evolutions are illustrated in Figure 6.10.

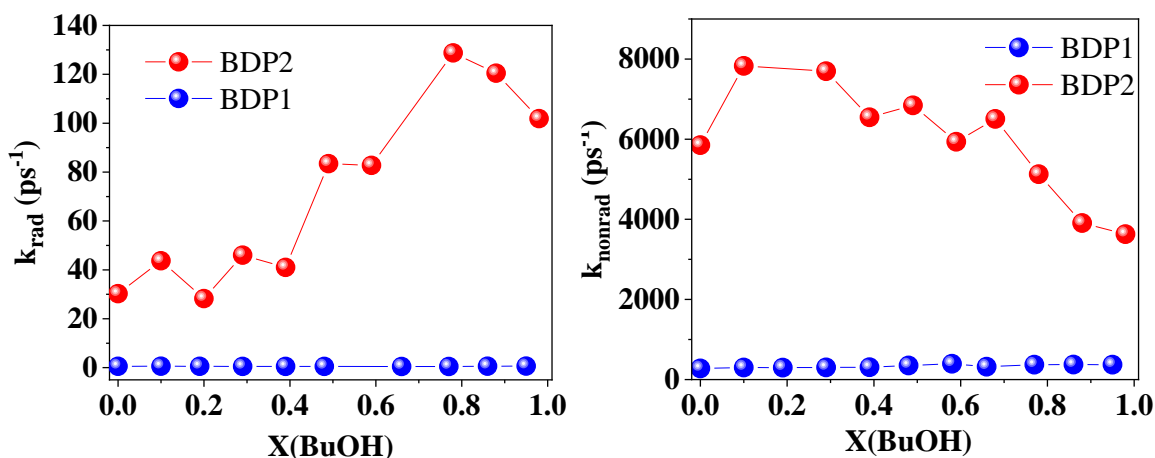


Figure 6.10: Evolution of fluorescence radiative and nonradiative rate constants of BDP1 and BDP2 in acetonitrile/butanol mixtures as a function of the molar fraction of the solvent.

In the whole mixture composition, the values of k_{rad} and k_{nonrad} relaxation constants for BDP2 are more than two orders of magnitude higher than those for BDP1, which values remain almost constant. The nonradiative relaxation constants values of BDP2 are higher compared to those of the nonradiative ones. Similarly to the fluorescence quantum yield evolution, BDP2's k_{rad} values are almost not affected by changing X_{BuOH} between 0 and 0.48, while they increase to reach a factor of 100 times that of BDP1. The rotation of the phenyl ring in BDP2 is stabilized by increasing the viscosity of the medium (by adding butanol). In the above-mentioned X_{BuOH} range values, k_{nonrad} remains constant in the first range and they decrease in the second range for X_{BuOH} over 0.48. All these results are in good agreement with the fact that while increasing X_{BuOH} in the mixture, the nonradiative deactivation pathways are less efficient for BDP2. For BDP1 changes in k_{nonrad} could not be considered as a significant trend.

The values of the quantum yield for the BDP1 change insignificantly, which affects the lower value of the quantum yield. That eliminates the effect of viscosity for this compound.

The behavior of the photophysical properties (quantum yield, relaxations times of the excited state, the radiative and nonradiative constants) as a function of the mixture composition points to its correlation with the rotation of the phenyl group of BDP2 as a channel of the excited state relaxation. The rotation of the pyridine ring in BDP1 is partially prevented by groups in position 1.7. and it is more difficult to turn to the best position that favours the fluorescence. The same properties have been already described for BODIPY dyes with ortho substituents in the pyridine(aryl) fragment [18–20, 22]. In such cases, additional groups will also hinder the rotation and a low quantum yield will be the consequence.

In the range of X_{BuOH} between 0 and 0.48, the values of the fluorescence quantum yields, the radiative and nonradiative constants of BDP2 remain stable. In this range, a slight increase of the viscosity by 0.3 MPa.s is observed. We hypothesise that in this range of mole fraction, the orientation/rotation of the phenyl group is not hindered and many configurations are then possible. Some of them favour the excited state energy to relax through the change of the orientation of the phenyl group with respect to the BODIPY core, however, still, the excited state relaxation can occur through the electron density delocalization. In the range of X_{BuOH} higher than 0.48, the viscosity values increase by 1.7 MPa.s which gradually hinders the rotation of the phenyl groups. The excited state energy relaxation through its rotation is then gradually reduced and so do the nonradiative constant. It seems that the BDP2 molecules adopt gradually configuration that favours the electronic density of the electron from the donor part to the accepted part decreases and then this results in an increase of the quantum yield. Furthermore, the difference in the excited state relaxation times of the BDP2 may be explained by the

Chapter 6

difference in their structures. Indeed, as it was mentioned previously, the rotation of the phenyl group is possible for BDP2 however in the case of BDP1, the methyl groups hinder this rotation. It is plausible then the excited state of BDP2 relaxes through the rotation of the phenyl group. This was confirmed by carrying out DFT quantum calculations, that shows that the optimal dihedral angle ($C_1-C_5-C_6-C_8$, α) between the BODIPY core and pyridine change from 90° in the ground state to 69.7° in the excited state; for phenyl part to 56.9° (51.4° - 52.7° for similar substitutes [23, 38]) in the excited state.

6.3.4 DFT calculation

We have performed quantum chemistry calculations to explore the energy surface of the two dyes. We ran a relaxed scan of the relevant dihedral angle describing the rotation of the phenyl group with respect to the core of the two dyes (Figure 6.11). The PES calculations have been performed in the range of the dihedral angle α for the ground and excited state

This angle affects the delocalization or aromaticity of the two dyes and then might have an important effect on the absorption and emission spectra. The relative energy (difference between the energy at a certain value of the dihedral angle and that corresponding to the minimum energy) as a function of the relaxed dihedral angle is shown in Figure 6.12. The horizontal line value is equal to the thermal energy (that defines the conformations that can be accessible thanks to the thermal kinetic energy).

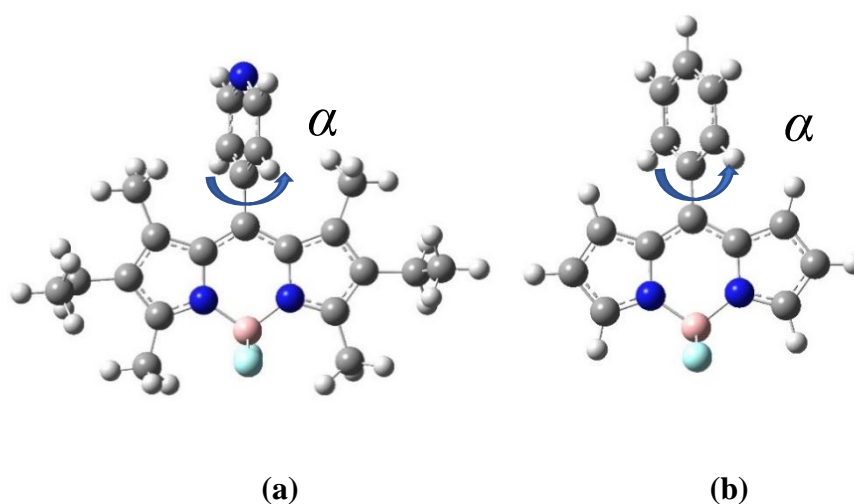


Figure 6.11: Structure of Molecular structures of BODIPYs under study: BDP1 (left) and BDP2 (right). α is the dihedral angle that defines the rotation of the phenyl group with respect to the pyridine BODIPY core.

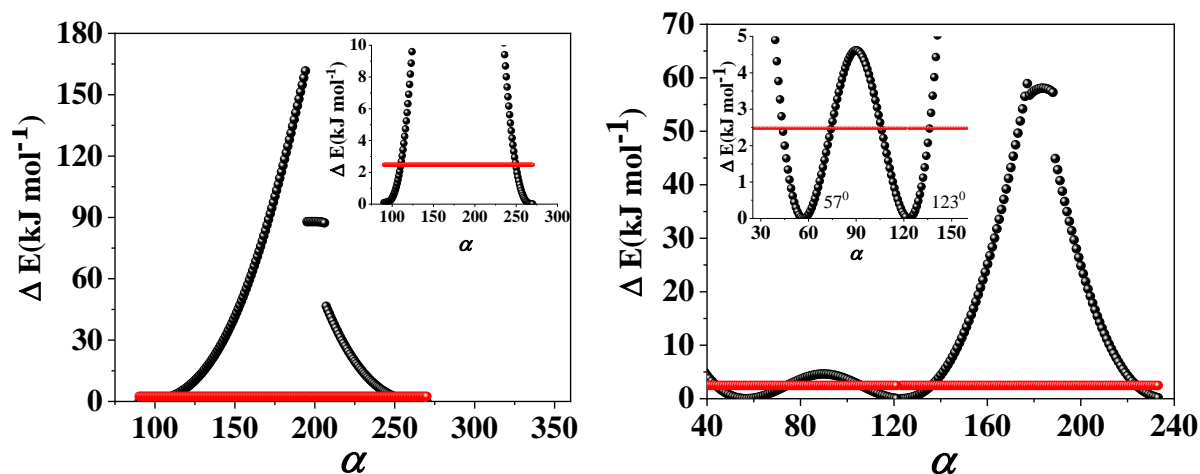


Figure 6.12: Potential energy profiles in the ground state for BDP1(left) and BDP2(right) along the dihedral angle ($C_1-C_5-C_6-C_7$, α) obtained with a hybrid functional cam-B3LYP at 6-311+G(d) basis set. The horizontal red line value is equal to the thermal energy $2.5 \text{ kJ}\cdot\text{mol}^{-1}$. The potential energy curve lower than $2.5 \text{ kJ}\cdot\text{mol}^{-1}$ is presented closer (inset).

Quantum chemical computations were carried out to further investigate the electronic properties of BDP1 and BDP2. The TD-DFT/cam-B3LYP method at 6-311+G(d) basis set has been used to determine the first low-lying excited states for investigating the UV-Vis absorption spectra of the title compound. The calculated results involving the vertical excitations energies, oscillator strength and wavelength are carried out and compared with the measured experimental wavelength (table 6.3).

In order to quantify the correlation between the conformation and the absorption and emission wavelength, we performed values of the dihedral angles, 57° (minimum energy), 44° , 74° and 90° (minimum energy), 70° , 110° , for BDP2 and BDP2 respectively, TD-DFT calculations to obtain the absorption and emission wavelengths as well as their corresponding oscillator strength. These values are gathered Tableble 6.3. We can observe red shifts in the absorption and fluorescence maximum wavelength for BDP2/BDP1, according to increasing/decreasing the value of oscillator strength. These values are in reasonable agreement with the experimental data.

Chapter 6

Table 6.3: Calculated absorption (fluorescence) wavelengths λ_{max} (in nm) and oscillator strengths with different dihedral angles, α . The structure of the dye with this angle has total energy lower than 2.5 kJ* mol^{-1} .

Dihedral Angle, α BDP1 / BDP2*	λ_{max} (abs), nm	Oscillator strength (abs)	λ_{max} (fluo), nm	Oscillator strength (fluo)
110°	488.7	0.875	509.5	0.822
90°	488.7	0.893	502.3	0.848
70°	489.5	0.870	509.1	0.824
44°*	459.3	0.725	474.3	0.617
57°*	457.4	0.743	471.6	0.715
74°*	457.7	0.760	471.7	0.732

At room temperature, the kinetic energy (2.5 kJ) allows the BDP2 to rotate to the conformation that corresponds to angle values between 44 °and 74° (the minimum energy – 57°). We suggest that with increasing the BuOH (viscosity increase) the rotation is hindered in the position of the dihedral angle (C₁-C₅-C₆-C₇) of the BDP2 in 74° , which has great influence on fluorescence.

6.4 Conclusion

In this work, we investigated the photophysical properties of two BDP derivatives by steady-state and Time-resolved fluorescence techniques and theoretical calculation.

We measured the fluorescence quantum yields and the fluorescence lifetimes of these dyes in acetonitrile – butanol-1 mixtures varying the BuOH molar fraction. Whatever in the mixtures, BDP2 exhibited always a higher fluorescence quantum yield than BDP1. While increasing the molar fraction of BuOH, the quantum yield of BDP2 is increasing after 0,48. The values of the quantum yield for the BDP1 change insignificantly.

The two relaxation times that characterize the excited state of BDP1 (~4.4 ns and ~2.8 ns), show a slight dependence on the mixture composition. Of note that the slower/faster of them increases/decreases slightly. The same trend is observed for the two relaxation times of

BDP2 with a noticeable increase for the slower of them and the values of both lifetimes for X_{BuOH} upper than 0.8 are higher than for average molar fractions than for lower values.

The value of radiative and nonradiative relaxation constants for BDP2 is higher than the ones for BDP1 in a whole range of molar fractions of butanol-1. For BDP1 changes in k_{nonrad} could not be considered as a significant trend. The radiative relaxation constants values are very small compared to those of the nonradiative ones for both dyes.

The rotation of the pyridine ring in BDP1 is partially prevented by groups in position 1,7, and it is more difficult to turn to the best position for fluorescence, which affects the lower value of the quantum yield and the long value of the time component.

The difference in the mixture composition of the photophysical properties of the two dyes may be explained by the difference in their structures. Indeed, the rotation of the phenyl group is possible for BDP2 and the excited state energy relaxation may occur through this rotation therefore the photophysical properties depend on how this rotation may be hindered. As a matter of fact, when the viscosity of the mixture is high enough to hinder this rotation (and this is possible for mole fractions of BuOH higher than 0.48), the fluorescence quantum yield and the radiative constant values increase, and consistently those of the nonradiative constant decrease.

This is confirmed by the results of DFT calculations. The BDP1 and BDP2 have many conformations in the range of dihedral angle between 70° - 110° (minimum potential energy – 90°) and 44° – 74° (the minimum energy – 57°) respectively. We suggest that with increasing the BuOH (viscosity increase) the rotation is hindered in the position of the dihedral angle (C₁-C₅-C₆-C₇) of the BDP2 in 74° and has great influence on fluorescence (according to the value of oscillator strength).

The behavior of the quantum yield, relaxations times of the excited state, the radiative and non-radiative constants as a function of the mixture composition points to its correlation with the rotation of the phenyl group of BDP2 as a channel of the excited state relaxation. Its fluorescent characteristics are highly dependent on the viscosity or rigidity of the microenvironment, as expected from literature data for pure alcohol solvents. These results suggest using BDP2 as molecular probe rotor of the viscosity for molecular systems which viscosity values are in the range between 0.5 and 3 MPas·s

Bibliography

1. Lavis, L.D., Raines, R.T.: Bright Ideas for Chemical Biology. *ACS Chem Biol.* 3, 142–155 (2008). <https://doi.org/10.1021/cb700248m>
2. Prasannan, D., Arunkumar, C.: A “turn-on-and-off” pH sensitive BODIPY fluorescent probe for imaging: *E. coli* cells. *New Journal of Chemistry.* 42, 3473–3482 (2018). <https://doi.org/10.1039/c7nj04313a>
3. Marfin, Y.S., Shipalova, M. v., Kurzin, V.O., Ksenofontova, K. v., Solomonov, A. v., Rumyantsev, E. v.: Fluorescent Properties of BODIPY Sensors Based on Photoinduced Electron Transfer. *J Fluoresc.* 26, 2105–2112 (2016). <https://doi.org/10.1007/s10895-016-1905-1>
4. Marfin, Y.S., Merkushev, D.A., Usoltsev, S.D., Shipalova, M. v, Rumyantsev, E. v: Fluorescent Properties of 8-Substituted BODIPY Dyes: Influence of Solvent Effects. *J Fluoresc.* 25, 1517–1526 (2015). <https://doi.org/10.1007/s10895-015-1643-9>
5. Marfin, Y.S., Merkushev, D.A., Levshanov, G.A., Rumyantsev, E. v: Fluorescent properties of 8-phenylbodipy in ethanol - Ethylene glycol mixed solutions. *J Fluoresc.* 24, 1613–1619 (2014). <https://doi.org/10.1007/s10895-014-1447-3>
6. Karolin, J., Johansson, L.B.-A., Strandberg, L., Ny, T.: Fluorescence and Absorption Spectroscopic Properties of Dipyrrometheneboron Difluoride (BODIPY) Derivatives in Liquids, Lipid Membranes, and Proteins. *J Am Chem Soc.* 116, 7801–7806 (1994). <https://doi.org/10.1021/ja00096a042>
7. Haugland, R.P.: Handbook of fluorescent probes and research products. Molecular Probes, Inc, Eugene, Or (2002)
8. Tan, K., Jaquinod, L., Paolesse, R., Nardis, S., di Natale, C., di Carlo, A., Prodi, L., Montalti, M., Zaccheroni, N., Smith, K.M.: Synthesis and characterization of β -fused porphyrin-BODIPY® dyads. *Tetrahedron.* 60, 1099–1106 (2004). <https://doi.org/10.1016/j.tet.2003.11.072>
9. Wang, L., Fang, G., Cao, D.: A novel phenol-based BODIPY chemosensor for selective detection Fe³⁺ with colorimetric and fluorometric dual-mode. *Sens Actuators B Chem.* 849–857 (2015). <https://doi.org/10.1016/j.snb.2014.10.110>

10. He, Y., Feng, R., Yi, Y., Liu, Z.: Recent Progress in the Research of Borondipyrrromethene-Based Fluorescent Ion Chemosensor. *Chinese Journal of Organic Chemistry*. 34, 2236 (2014). <https://doi.org/10.6023/cjoc201403066>
11. Shi, W.-J., Liu, J.-Y., Ng, D.K.P.: A Highly Selective Colorimetric and Fluorescent Probe for Cu²⁺ and Hg²⁺ Ions Based on a Distyryl BODIPY with Two Bis(1,2,3-triazole)amino Receptors. *Chem Asian J*. 7, 196–200 (2012). <https://doi.org/10.1002/asia.201100598>
12. Madhu, S., Kalaiyarasi, R., Basu, S.K., Jadhav, S., Ravikanth, M.: A boron-dipyrin–mercury(ii) complex as a fluorescence turn-on sensor for chloride and applications towards logic gates. *J Mater Chem C Mater*. 2, 2534 (2014). <https://doi.org/10.1039/c3tc32188f>
13. Liu, J., He, X., Zhang, J., He, T., Huang, L., Shen, J., Li, D., Qiu, H., Yin, S.: A BODIPY derivative for colorimetric and fluorometric sensing of fluoride ion and its logic gates behavior. *Sens Actuators B Chem*. 208, 538–545 (2015). <https://doi.org/10.1016/j.snb.2014.11.094>
14. Vu, T.T., Méallet-Renault, R., Clavier, G., Trofimov, B.A., Kuimova, M.K.: Tuning BODIPY molecular rotors into the red: Sensitivity to viscosity: Vs. temperature. *J Mater Chem C Mater*. 4, 2828–2833 (2016). <https://doi.org/10.1039/c5tc02954f>
15. Dziuba, D., Jurkiewicz, P., Cebecauer, M., Hof, M., Hocek, M.: A Rotational BODIPY Nucleotide: An Environment-Sensitive Fluorescence-Lifetime Probe for DNA Interactions and Applications in Live-Cell Microscopy. *Angewandte Chemie International Edition*. 55, 174–178 (2016). <https://doi.org/10.1002/anie.201507922>
16. Kuimova, M.K., Yahioğlu, G., Levitt, J.A., Suhling, K.: Molecular Rotor Measures Viscosity of Live Cells via Fluorescence Lifetime Imaging. *J Am Chem Soc*. 130, 6672–6673 (2008). <https://doi.org/10.1021/ja800570d>
17. Alamiry, M.A.H., Benniston, A.C., Copley, G., Elliott, K.J., Harriman, A., Stewart, B., Zhi, Y.-G.: A Molecular Rotor Based on an Unhindered Boron Dipyrromethene (Bodipy) Dye. *Chemistry of Materials*. 20, 4024–4032 (2008). <https://doi.org/10.1021/cm800702c>
18. Loudet, A., Burgess, K.: BODIPY dyes and their derivatives: Syntheses and spectroscopic properties, (2007)
19. Solomonov, A. v., Marfin, Y.S., Tesler, A.B., Merkushev, D.A., Bogatyreva, E.A., Antina, E. v., Rumyantsev, E. v., Shimanovich, U.: Spanning BODIPY fluorescence with self-assembled micellar clusters. *Colloids Surf B Biointerfaces*. 216, 112532 (2022). <https://doi.org/10.1016/j.colsurfb.2022.112532>

Chapter 6

20. Banfi, S., Nasini, G., Zaza, S., Caruso, E.: Synthesis and photo-physical properties of a series of BODIPY dyes. *Tetrahedron*. 69, 4845–4856 (2013). <https://doi.org/10.1016/j.tet.2013.04.064>
21. Dong, Y., Taddei, M., Doria, S., Bussotti, L., Zhao, J., Mazzone, G., di Donato, M.: Torsion-Induced Nonradiative Relaxation of the Singlet Excited State of *meso*-Thienyl Bodipy and Charge Separation, Charge Recombination-Induced Intersystem Crossing in Its Compact Electron Donor/Acceptor Dyads. *J Phys Chem B*. 125, 4779–4793 (2021). <https://doi.org/10.1021/acs.jpccb.1c00053>
22. Wang, D., Guo, X., Wu, H., Wu, Q., Wang, H., Zhang, X., Hao, E., Jiao, L.: Visible Light Excitation of BODIPYs Enables Dehydrogenative Enamination at Their α -Positions with Aliphatic Amines. *J Org Chem*. 85, 8360–8370 (2020). <https://doi.org/10.1021/acs.joc.0c00620>
23. Kee, H.L., Kirmaier, C., Yu, L., Thamyongkit, P., Youngblood, W.J., Calder, M.E., Ramos, L., Noll, B.C., Bocian, D.F., Scheldt, W.R., Birge, R.R., Lindsey, J.S., Holten, D.: Structural control of the photodynamics of boron-dipyrin complexes. *Journal of Physical Chemistry B*. 109, 20433–20443 (2005). <https://doi.org/10.1021/jp0525078>
24. Baruah, M., Qin, W., Flors, C., Hofkens, J., Vallée, R.A.L., Beljonne, D., van der Auweraer, M., de Borggraeve, W.M., Boens, N.: Solvent and pH Dependent Fluorescent Properties of a Dimethylaminostyryl Borondipyrromethene Dye in Solution. *J Phys Chem A*. 110, 5998–6009 (2006). <https://doi.org/10.1021/jp054878u>
25. Bartelmess, J., Weare, W.W., Latortue, N., Duong, C., Jones, D.S.: *Meso*-Pyridyl BODIPYs with tunable chemical, optical and electrochemical properties. *New Journal of Chemistry*. 37, 2663–2668 (2013). <https://doi.org/10.1039/c3nj00426k>
26. Feng, S., Qu, Z., Zhou, Z., Chen, J., Gai, L., Lu, H.: Si-Bridged annulated BODIPYs: synthesis, unique structure and photophysical properties. *Chemical Communications*. 57, 11689–11692 (2021). <https://doi.org/10.1039/D1CC04687J>
27. Marfin, Y.S., Banakova, E.A., Merkushev, D.A., Usoltsev, S.D., Churakov, A. v: Effects of Concentration on Aggregation of BODIPY-Based Fluorescent Dyes Solution. *J Fluoresc*. 30, 1611–1621 (2020). <https://doi.org/10.1007/s10895-020-02622-y>
28. Roacho, R.I., Metta-Magaña, A.J., Peña-Cabrera, E., Pannell, K.H.: Synthesis, structural characterization, and spectroscopic properties of the ortho, meta, and para isomers of 8-(HOCH₂-C₆H₄)-BODIPY and 8-(MeOC₆H₄)-BODIPY. *J Phys Org Chem*. 26, 345–351 (2013). <https://doi.org/10.1002/poc.3095>

29. Rahman, M.S., Chowdhury, F.I., Ahmed, M.S., Rocky, M.M.H., Akhtar, S.: Density and viscosity for the solutions of 1-butanol with nitromethane and acetonitrile at 303.15 to 323.15 K. *J Mol Liq.* 190, 208–214 (2014). <https://doi.org/10.1016/j.molliq.2013.11.011>
30. Jogdand, A.P., Corresponding, I.: Dielectric Behavior of Acetonitrile + N-Butyl Alcohol Binary Mixtures at Microwave Frequency at 10°C. *IOSR Journal of Applied Physics (IOSR-JAP.* 11, 40–49. <https://doi.org/10.9790/4861-1102014049>
31. Jogdand, A., Kadam, P.L.: Dielectric behavior of acetonitrile + methanol binary mixtures at microwave frequency. (2014)
32. Brouwer, A.M.: Standards for photoluminescence quantum yield measurements in solution (IUPAC technical report), (2011)
33. Kumagai, A., Ando, R., Miyatake, H., Greimel, P., Kobayashi, T., Hirabayashi, Y., Shimogori, T., Miyawaki, A.: A Bilirubin-Inducible Fluorescent Protein from Eel Muscle. *Cell.* 153, 1602–1611 (2013). <https://doi.org/10.1016/j.cell.2013.05.038>
34. Smortsova, Y., Miannay, F.-A., Oher, H., Marekha, B., Dubois, J., Sliwa, M., Kalugin, O., Idrissi, A.: Solvation dynamics and rotation of coumarin 153 in a new ionic liquid/molecular solvent mixture model: [BMIM][TFSI]/propylene carbonate. *J Mol Liq.* 226, 48–55 (2017). <https://doi.org/10.1016/j.molliq.2016.10.008>
35. Boens, N., Qin, W., Basarić, N., Hofkens, J., Ameloot, M., Pouget, J., Lefèvre, J.-P., Valeur, B., Gratton, E., vandeVen, M., Silva, N.D., Engelborghs, Y., Willaert, K., Sillen, A., Rumbles, G., Phillips, D., Visser, A.J.W.G., van Hoek, A., Lakowicz, J.R., Malak, H., Gryczynski, I., Szabo, A.G., Krajcarski, D.T., Tamai, N., Miura, A.: Fluorescence Lifetime Standards for Time and Frequency Domain Fluorescence Spectroscopy. *Anal Chem.* 79, 2137–2149 (2007). <https://doi.org/10.1021/ac062160k>
36. Valeur, B.: *Molecular Fluorescence: Principles and Applications.* Wiley-VCH Verlag GmbH (2001)
37. Version 4.1: User's Manual and Technical Data FluoFit Global Fluorescence Decay Data Analysis Software Contents.
38. Prasannan, D., Raghav, D., Sujatha, S., Hareendrakrishna kumar, H., Rathinasamy, K., Arunkumar, C.: Synthesis, structure, photophysical, electrochemical properties and antibacterial activity of brominated BODIPYs. *RSC Adv.* 6, 80808–80824 (2016). <https://doi.org/10.1039/C6RA12258B>

Conclusions and perspectives

In this work, a series of nitrofluoresceins and several amino derivatives, 22 compounds in total, are studied in solutions, first of all, in DMSO, using spectroscopic methods. The molar absorptivities and pK_a values of a series of nitrofluorescein dyes are determined; the spectra of the individual molecular and ionic forms are singled out. The obtained pK_a s of the dyes in DMSO cover the range from 0 to 12.

The results provide an understanding of the scheme of the protolytic equilibrium for this group of dyes in solution. Furthermore, they reveal that the properties of nitrofluoresceins differ significantly from those of other fluorescein dyes, such as the widely-used halogen derivatives.

The main reason is the high electrophilicity of the NO_2 groups, which leads to the pulling of electron density away from the nodal carbon atom, C_9 . This, in turn, strongly stabilizes the lactonic tautomers. The X-ray analysis shed light upon the structure of lactones of two pentanitrofluoresceins. While for the 4,5-dinitrofluorescein, this refers only to the neutral form, H_2R , for dyes of 2,4,5,7-tetranitro type, even the anions readily form lactones. It is even more pronounced in acetonitrile with 4 mass % DMSO. This is not typical for other branches of the fluorescein family.

Another consequence of the electron-attracting properties of the nitro group is the rupture of the pyran ring in highly alkaline solutions, which occurs much easier than for other fluorescein dyes; a product of such rupture is isolated and examined via the ^{13}C NMR spectroscopy in this work.

Secondly, the acidity of the OH groups of the dyes with nitro groups in the xanthenes part increases dramatically as compared to that of the unsubstituted fluorescein and substantially exceeds the acidity of the COOH group. This feature resembles the well-known influence of halogen substitutions and is numerously demonstrated for eosin, erythrosin, etc.

The analysis of the absorption spectra in the visible region and evaluation of the fractions of tautomers made it possible to calculate the so-called microscopic equilibrium constants of the stepwise dissociation of tautomers. For the 4,4-dinitrofluorescein, the estimated microscopic dissociation constants are in line with the pK_a s of the model compounds: 4,5-dinitrofluorescein ester, ether, and 4,5-dinitrosulfofluorescein.

The influence of a negative charge of a single-charged anion on the dissociation of the second acidic group is in line with the Bjerrum – Kirkwood – Westheimer equation. This allows for estimating the effective relative permittivity of the space between the ionizing groups and supports the proposed scheme of the protolytic equilibrium of nitrofluoresceins in solution.

As a kind of secondary result, the data can serve as an instructive illustration of the reasons governing the $pK_{a2} - pK_{a1}$ difference for a dibasic acid inclined to tautomerism. It is demonstrated that the ratio of K_{a1} / K_{a2} , or the difference $pK_{a2} - pK_{a1}$ is governed by the state of the tautomeric equilibrium of molecules and anions. For instance, the difference between the pK_a s of stepwise dissociation of the dyes, $pK_{a2} - pK_{a1}$, in DMSO varies from 1.1 for 5'-nitrofluorescein to 7.6 to 4,5-dinitro-2,7-dibromofluorescein. The H_2R forms are almost completely transformed into the lactonic tautomer in both cases. However, in the first case, the sequence of the functional group dissociation is as follows: (1) COOH and (2) OH. In the second case, the single-charged anion contains the COOH and O^- groups, while the double-charged anion is an equilibrium mixture of intensively coloured and colourless lactonic tautomers, 32 % and 68 %, respectively.

Another issue solved in the present work is the transmittance of the electronic effects in the fluorescein molecule between the phthalic acid residue and the xanthene moiety. Despite the almost orthogonal orientation of the latter with respect to the rest of the molecule, the pK_a in DMSO of the OH group in the xanthene part increases by 0.2–0.3 units in the case of amino derivatives in the phthalic part, while the nitro group decreases the pK_a s by 0.2–0.8.

Of course, these effects are much lower than the pK_a decrease of the same group when the substituents are introduced nearby (3.6–3.7 units pro one *ortho*-NO₂ group).

Interestingly, the influence on the emitting ability of fluorescein by nitro groups in these two parts of the molecule. Whereas the introduction of the NH₂ group in the 9-arene part decreases fluorescence only in water and alcohols, but not in DMSO and acetonitrile, the appearance of the NO₂ group results in fluorescence quenching. In contrast, the tetranitro substitution in the 2, 4, 5, and 7-position of the xanthenes part allowed to obtain an excellent fluorescent indicator, which is sensitive to the hydrogen bonding ability of the solvent (quantum yields from $\varphi = 80\text{--}86\%$ in DMSO and acetonitrile to $\varphi \approx 0$ in water. Hence, the introduction of the NH₂ group in the phthalic part and four NO₂ groups in the xanthenes portion of fluorescein led to similar consequences. The advantage of the nitro derivative is the

independence of the emission on pH, because of the highly pronounced stability of this anionic dye with respect to H⁺ addition.

Regarding the influence of the solvent mixture acetonitrile-butanol on the photophysics of dyes – the photophysical properties of BDP2 are strongly dependent on the mixture composition. This effect is mainly due to a change in the viscosity of the mixture, which affects the rotation of the two parts of the BODIPY relative to each other. Increasing the BuOH content of the mixture, which means an increase of the viscosity, decrease of the dielectric constant, decrease of the ability to form hydrogen bonds, an increase of dipole–dipole interactions, the maxima of the absorption and fluorescence spectra of BDP1 and BDP2 are weakly dependent on the mixture composition and a slight bathochromic shift occurs (the shift never exceeds 2-4 nm). So, we expect not strong changes in the spectra of fluorescein dyes, but strong changes in the ratios of dissociation constants due to the transition from an aprotic medium (acetonitrile) to a proton-binding medium (butanol).

In perspectives, this work can be the basis of the following developments:

- Study on the fluorescence quantum yield of the fluorogenic dyes in the polar protic and aprotic solvents (for example, acetonitrile, dimethyl sulfoxide, acetonitrile-butanol-1 mixtures) that has unextremely low values of quantum yields to minimize measurement error using nitrofluoresceins as the reference dye.
- The approach of using esters with a similar fluorescent moiety, as in the case of parent compounds, to determine the tautomeric composition can be used for the entire range of fluorescein derivatives.
- Finally, all the results in this thesis should be useful for further study of amino derivatives and mixed amino-nitro derivatives of fluorescein, which also represent the scientific interest and poorly studied in aprotic solvents.
- The ester of 2,4,5,7-tetranitrofluorescein can serve as a hydrogen bonds-sensitive fluorescent indicator and as a useful tool for studying different liquid media. It is also important in the future to study step-by-step the effect of hydrogen bonds in mixtures of aprotic and hydrogen bond donor solvents.

Appendices

Appendix A: NMR spectra of the dyes

Contents:

Figure A1: ^1H NMR spectrum of 4'-nitrofluorescein

Figure A2: ^{13}C NMR spectrum of 4'-nitrofluorescein

Figure A3: ^1H NMR spectrum of 5'-nitrofluorescein

Figure A4: ^{13}C NMR spectrum of 5'-nitrofluorescein

Figure A5: ^1H NMR spectrum of 4'-aminofluorescein

Figure A6: ^{13}C NMR spectrum of 4'-aminofluorescein

Figure A7: ^1H NMR spectrum of 5'-aminofluorescein

Figure A8: ^{13}C NMR spectrum of 5'-aminofluorescein

Figure A9: ^1H NMR spectrum of 4'-nitrofluorescein ethyl ester

Figure A10: ^{13}C NMR spectrum of 4'-nitrofluorescein ethyl ester

Figure A11: ^1H NMR spectrum of 5'-nitrofluorescein ethyl ester

Figure A12: ^{13}C NMR spectrum of 5'-nitrofluorescein ethyl ester

Figure A13: ^1H NMR spectrum of 2,4,5,7,4'-pentanitrofluorescein

Figure A14: ^1H - ^1H COSY NMR spectrum of 2,4,5,7,4'-pentanitrofluorescein

Figure A15: ^{13}C NMR spectrum of 2,4,5,7,4'-pentanitrofluorescein

Figure A16: ^1H NMR spectrum of 2,4,5,7,5'-pentanitrofluorescein

Figure A17: ^1H - ^1H COSY NMR spectrum of 2,4,5,7,5'-pentanitrofluorescein

Figure A18: ^{13}C NMR spectrum of 2,4,5,7,5'-pentanitrofluorescein

Figure A19: ^1H NMR spectrum of 2,4,5,7-tetranitrofluorescein with the cleaved pyran ring

Figure A20: ^{13}C NMR spectrum of 2,4,5,7-tetranitrofluorescein with the cleaved pyran ring

Figure A21: ^1H NMR spectrum of 2,4,5,7-tetranitrofluorescein methyl ester

Figure A22: ^{13}C NMR spectrum of 2,4,5,7-tetranitrofluorescein methyl ester

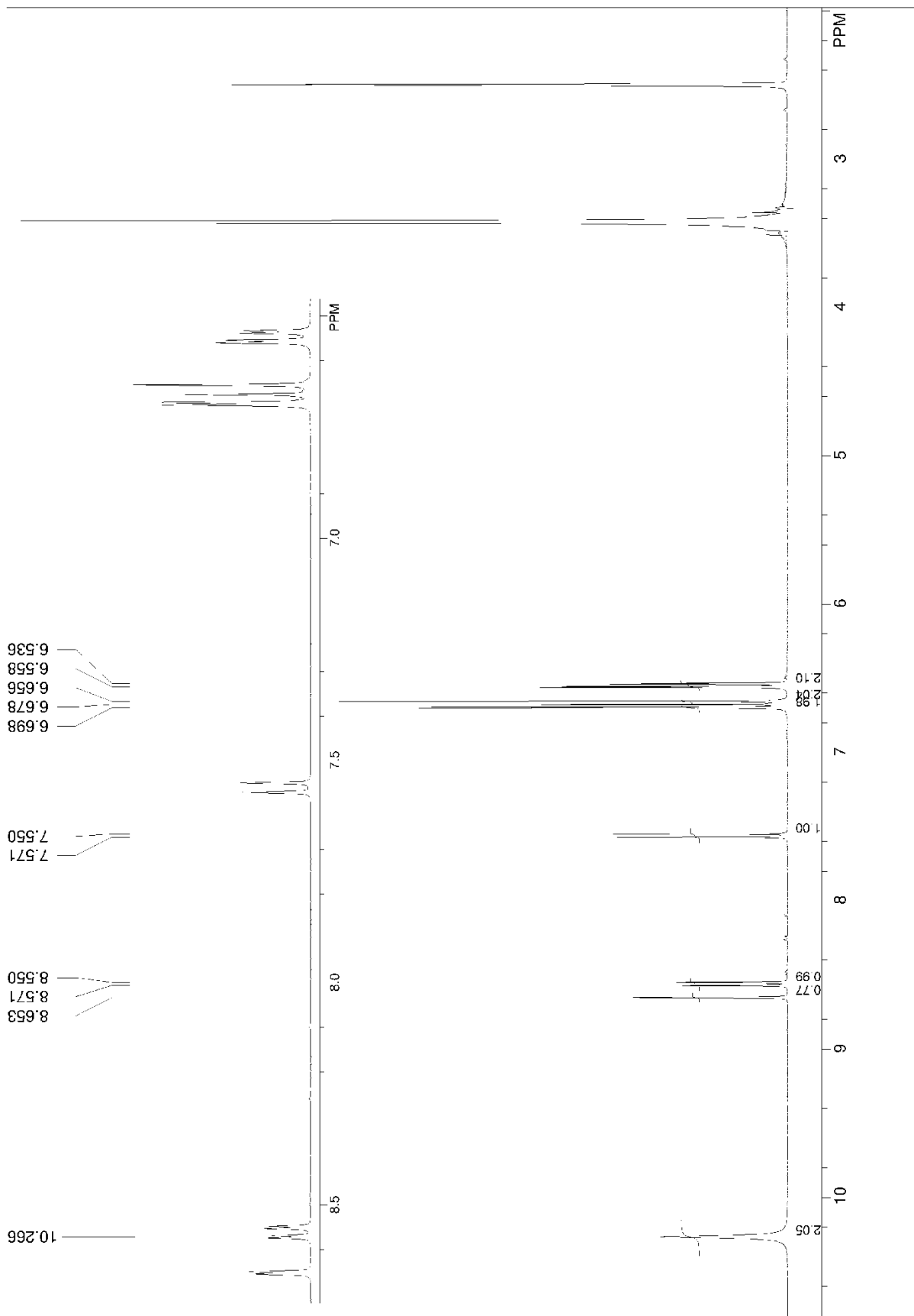


Figure A1: ^1H NMR spectrum of 4'-nitrofluorescein (400 MHz, $\text{DMSO-}d_6$).

Appendices

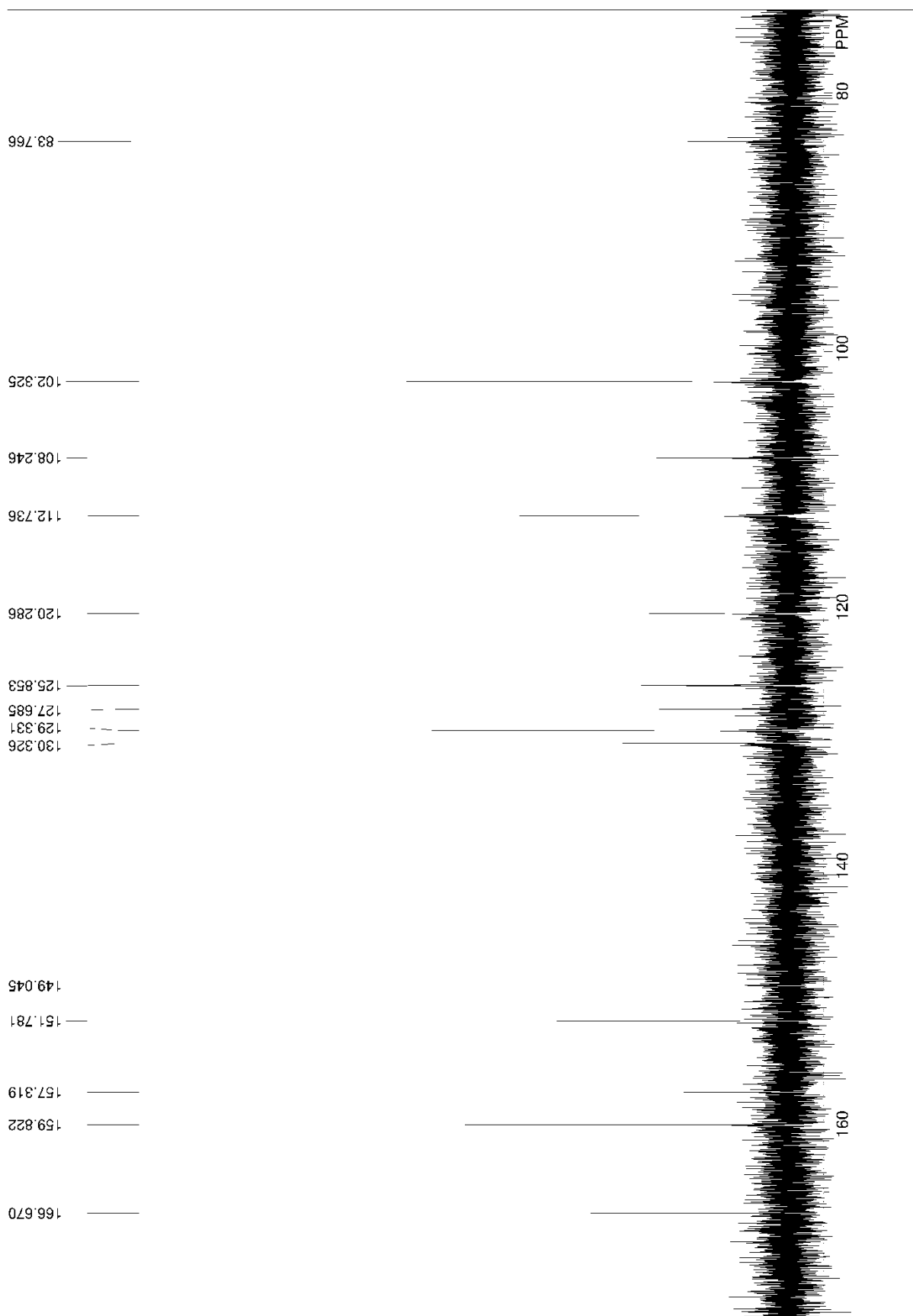


Figure A2: ^{13}C NMR spectrum of 4'-nitrofluorescein (101 MHz, $\text{DMSO-}d_6$).

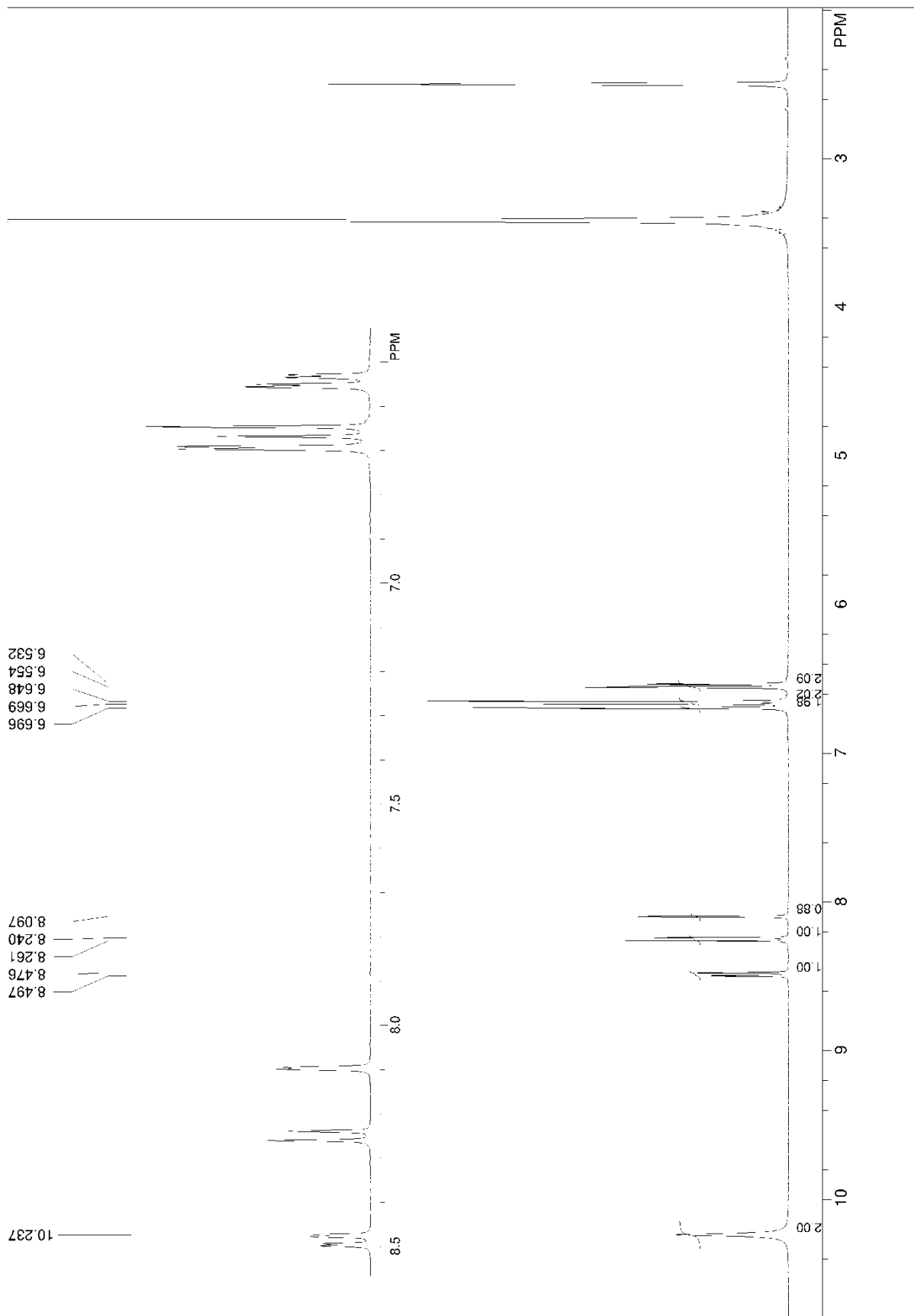


Figure A3: ^1H NMR spectrum of 5'-nitrofluorescein (400 MHz, $\text{DMSO-}d_6$).

Appendices

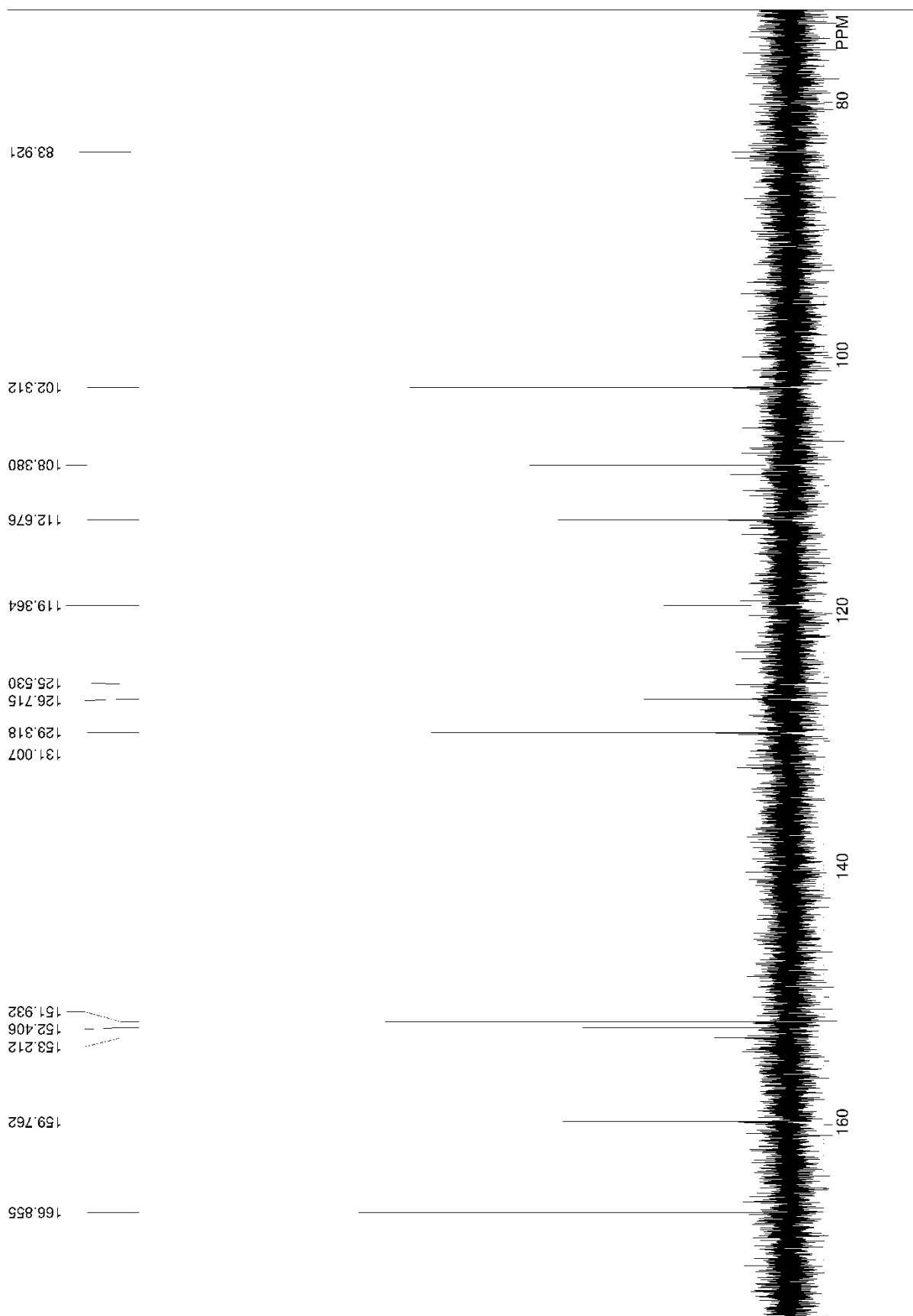


Figure A4: ¹³C NMR spectrum of 5'-nitrofluorescein (101 MHz, DMSO-*d*₆).

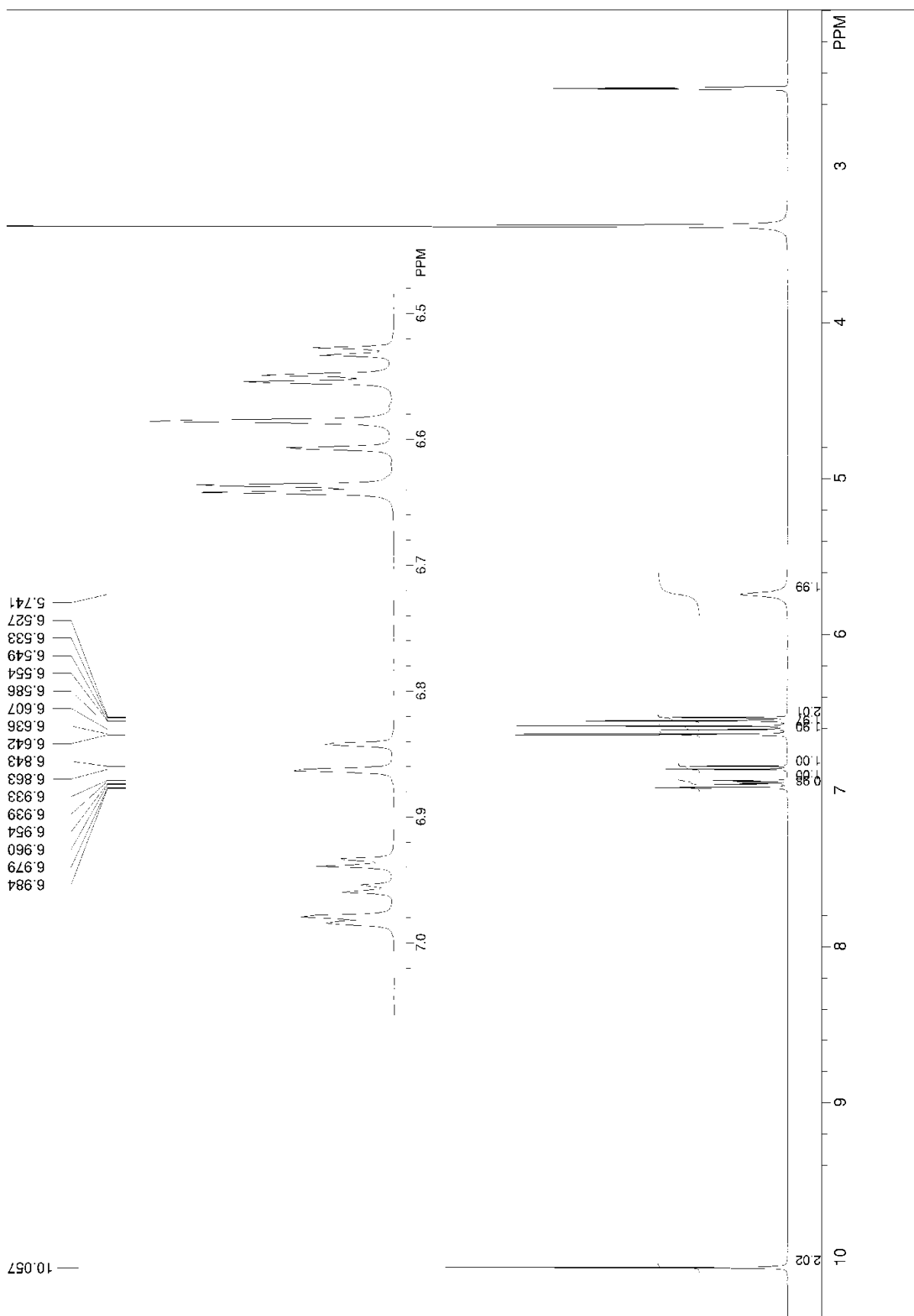


Figure A5: ^1H NMR spectrum of 4'-aminofluorescein (400 MHz, $\text{DMSO-}d_6$).

Appendices

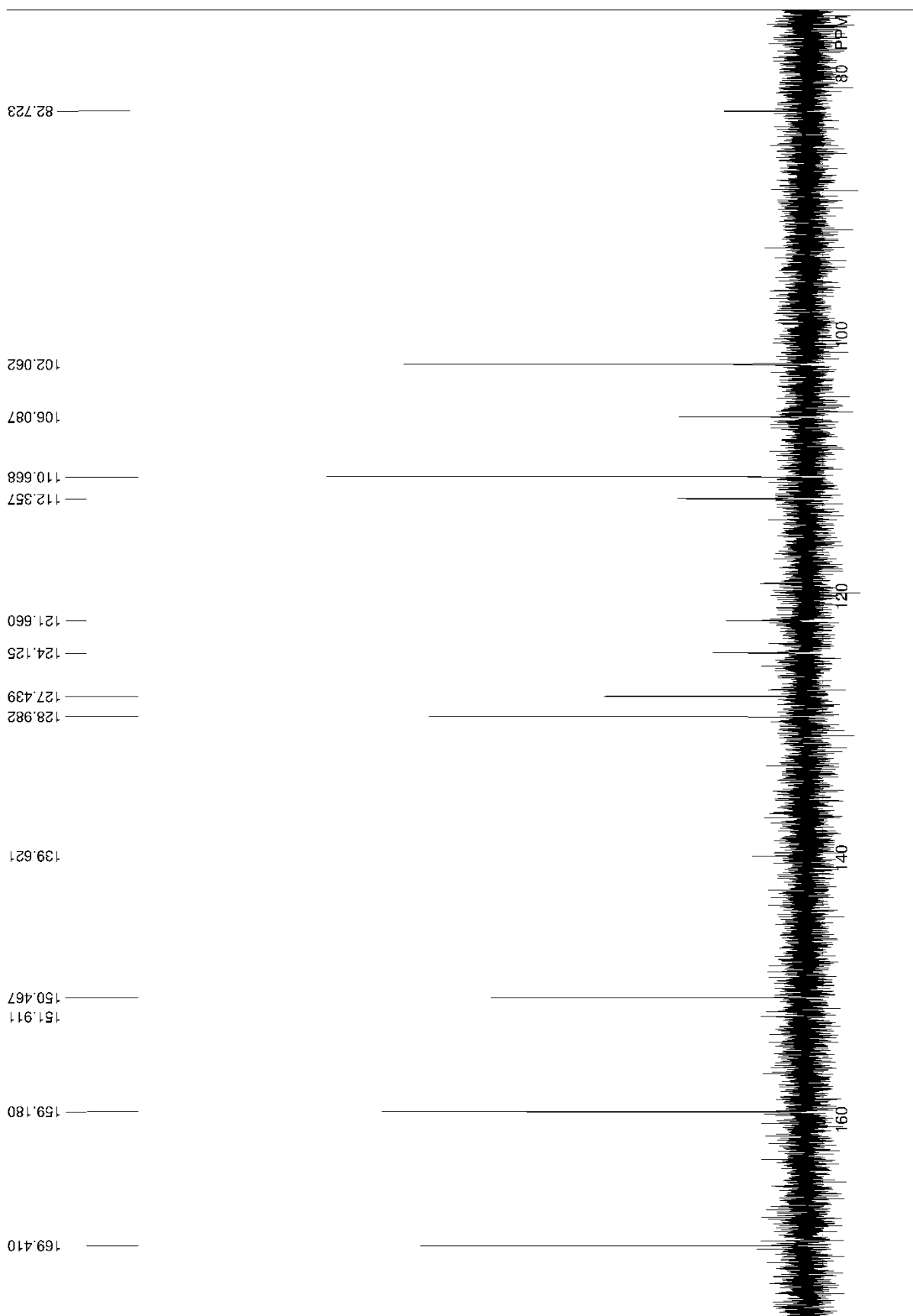


Figure A6: ^{13}C NMR spectrum of 4'-aminofluorescein (101 MHz, $\text{DMSO-}d_6$).

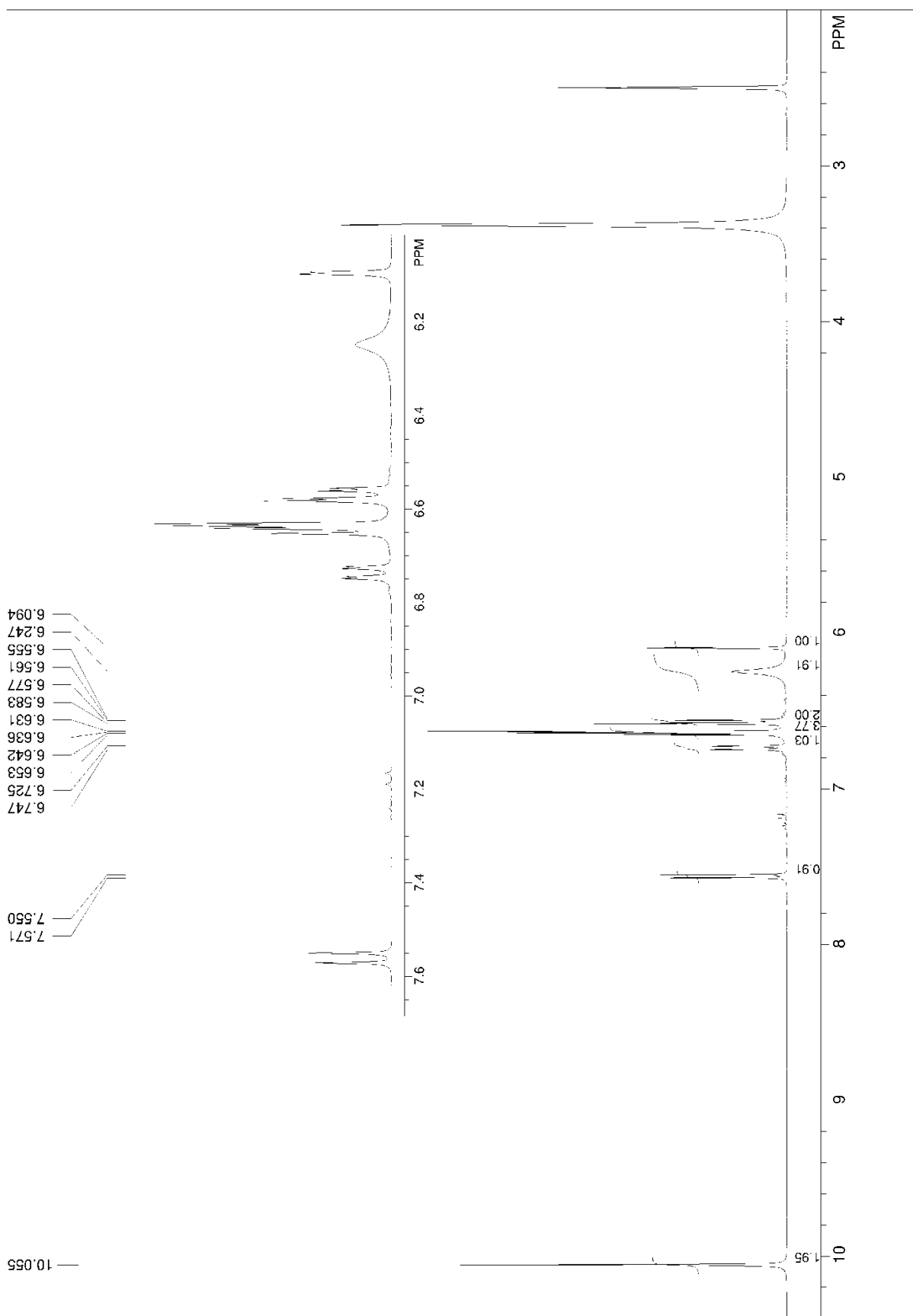


Figure A7: ^1H NMR spectrum of 5'-aminofluorescein (400 MHz, $\text{DMSO-}d_6$).

Appendices

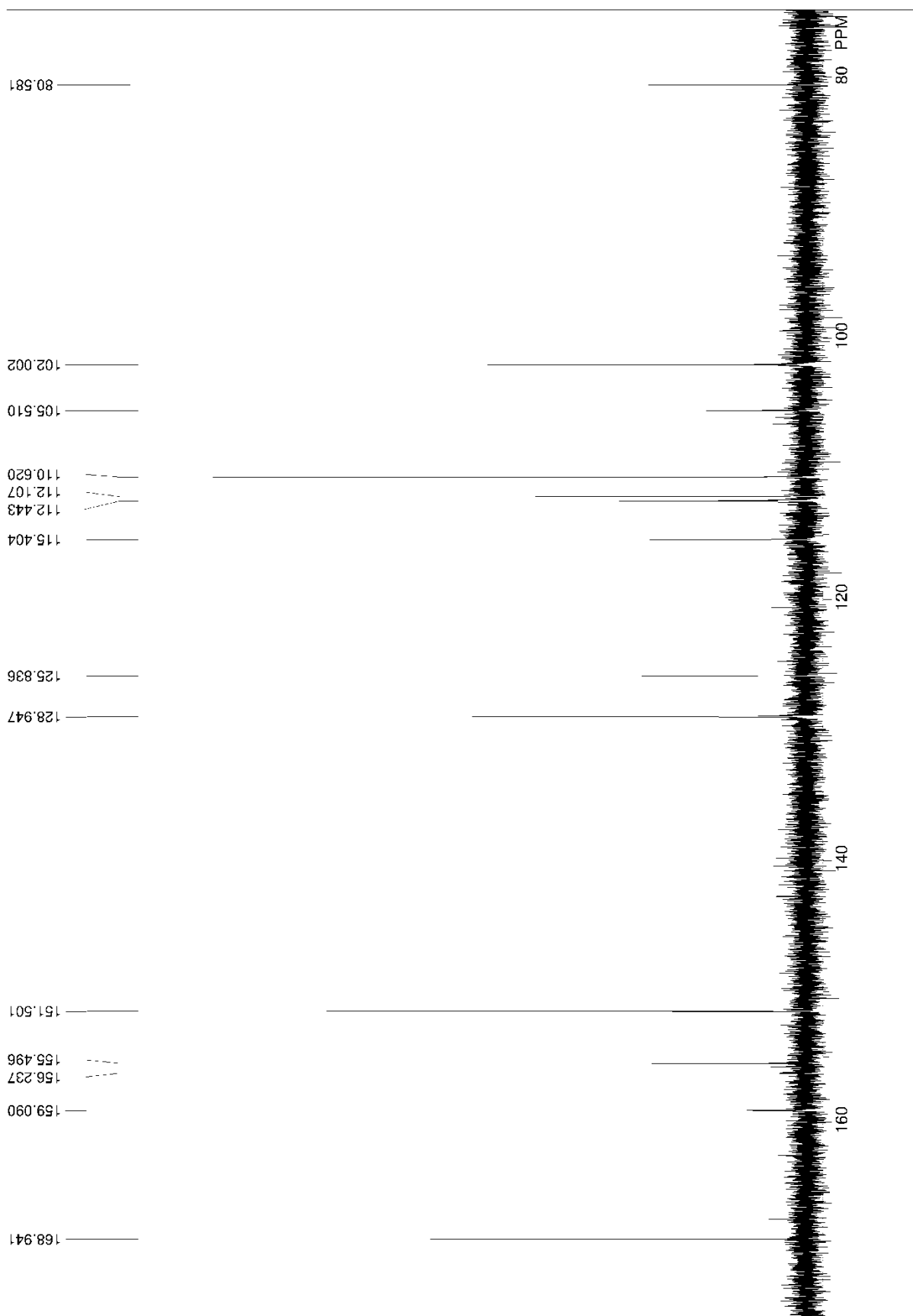


Figure A8: ^{13}C NMR spectrum of 5'-aminofluorescein (101 MHz, $\text{DMSO-}d_6$).

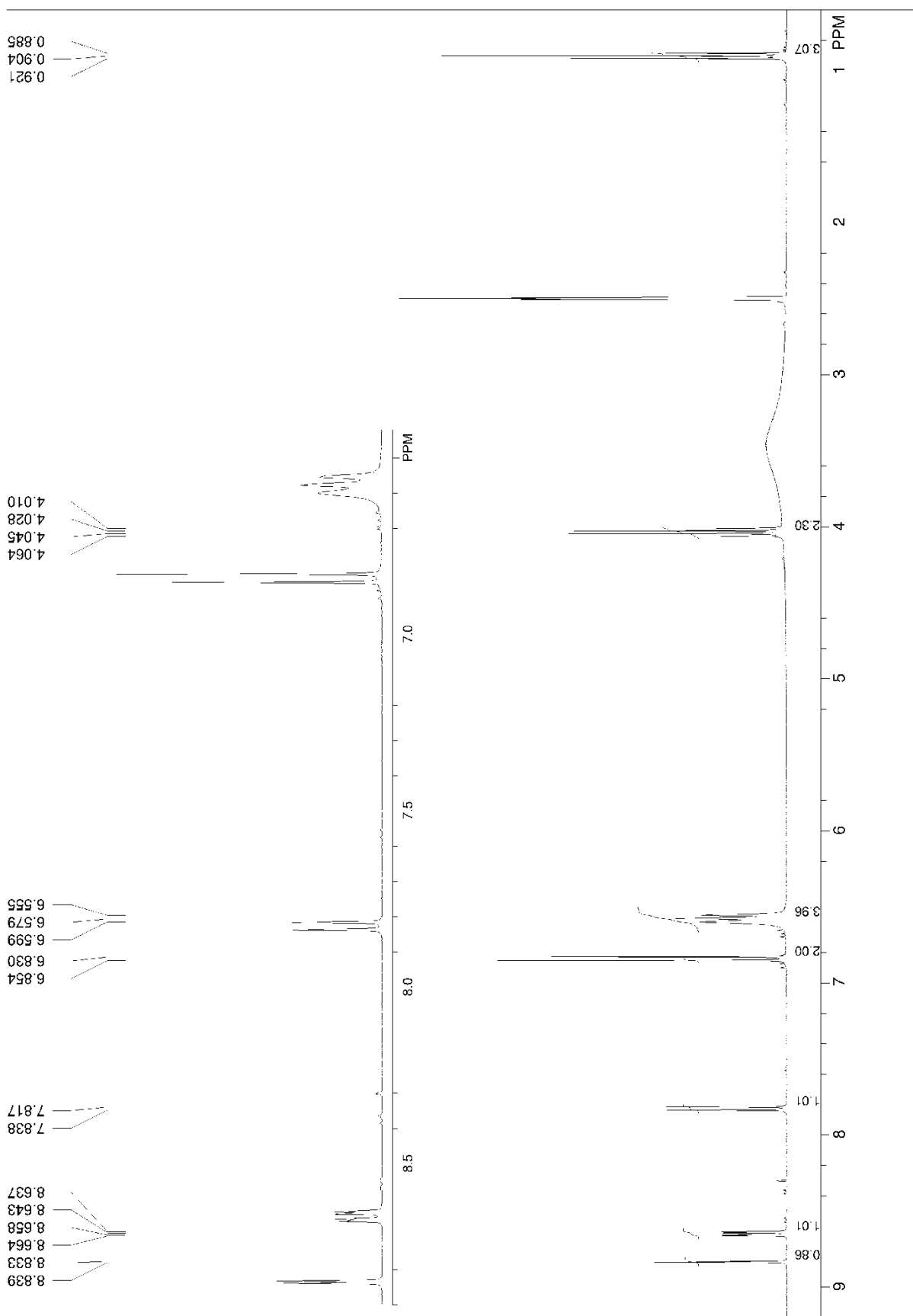


Figure A9: ^1H NMR spectrum of 4'-nitrofluorescein ethyl ester (400 MHz, $\text{DMSO-}d_6$).

Appendices

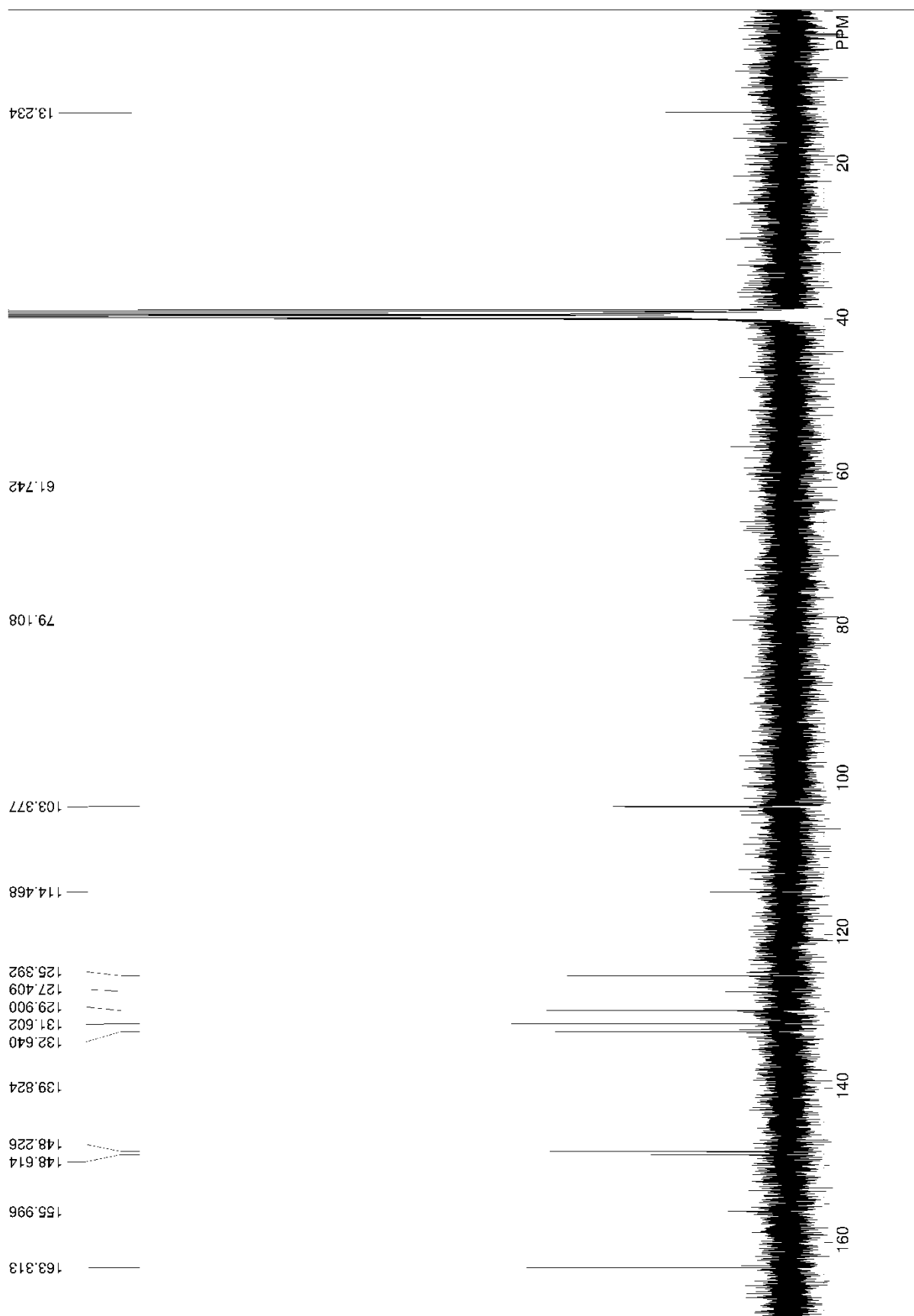


Figure A10: ^{13}C NMR spectrum of 4'-nitrofluorescein ethyl ester (101 MHz, $\text{DMSO-}d_6$).

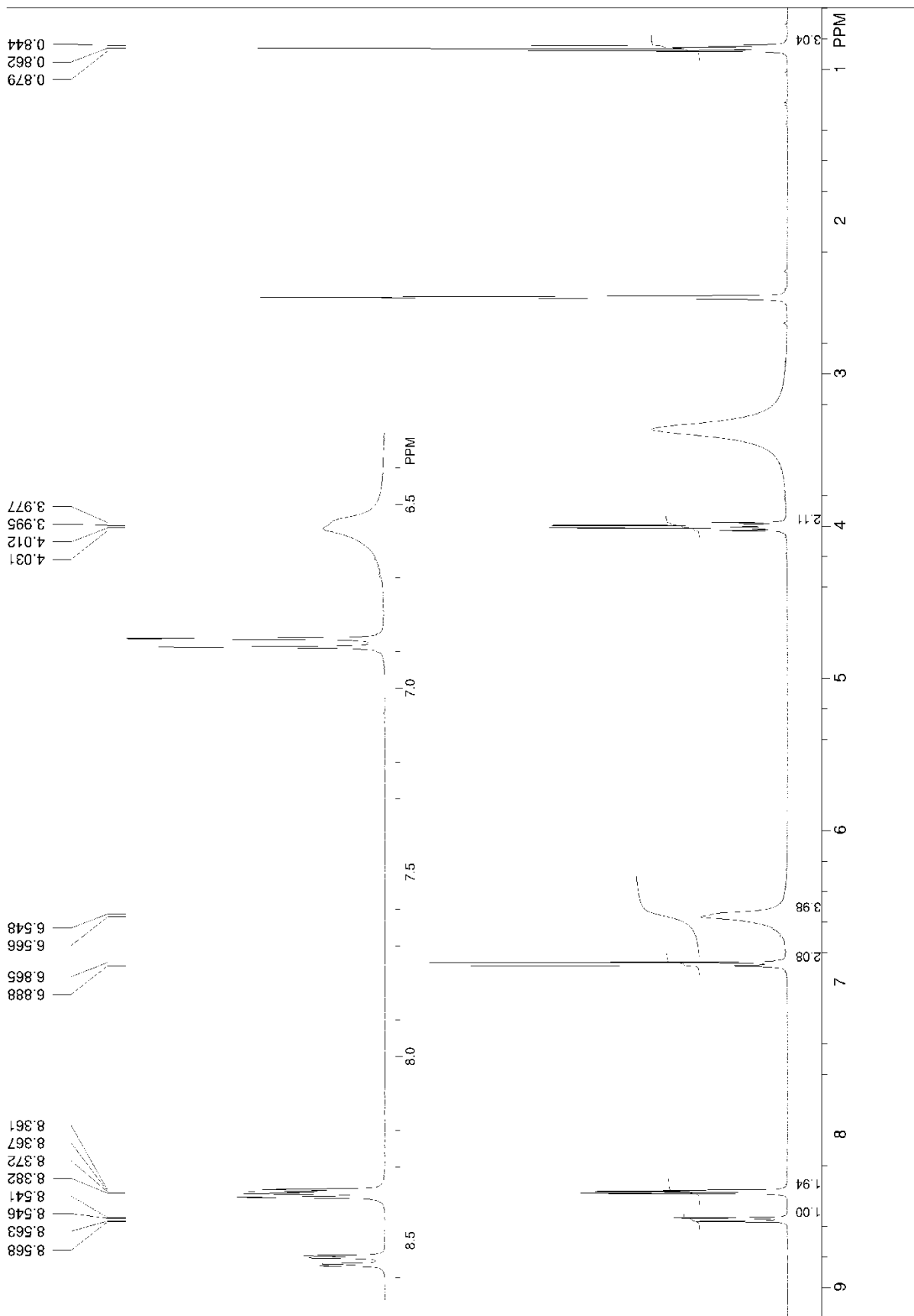


Figure A11: ^1H NMR spectrum of 5'-nitrofluorescein ethyl ester (400 MHz, $\text{DMSO-}d_6$).

Appendices

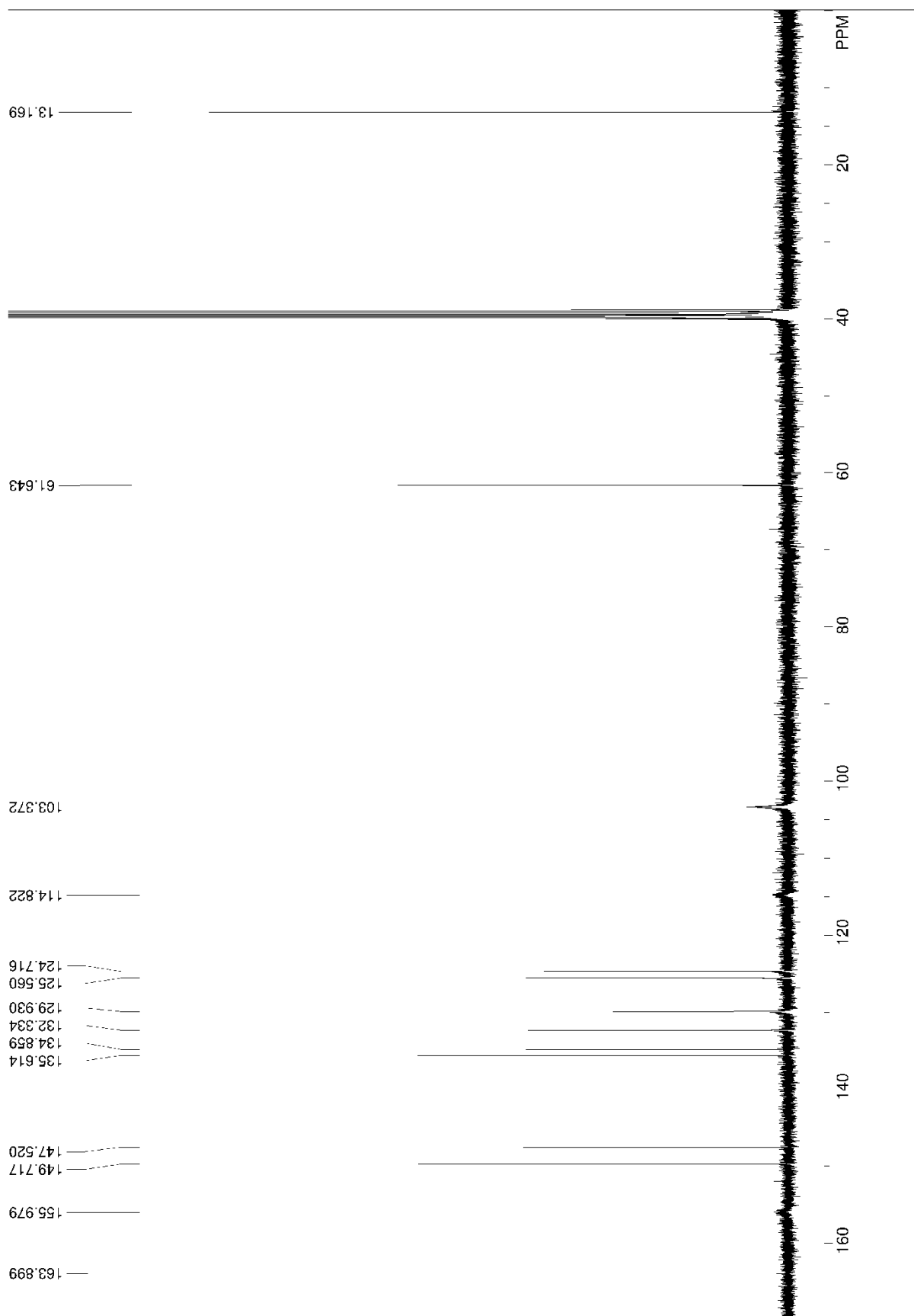


Figure A12: ^{13}C NMR spectrum of 5'-nitrofluorescein ethyl ester (101 MHz, $\text{DMSO-}d_6$).

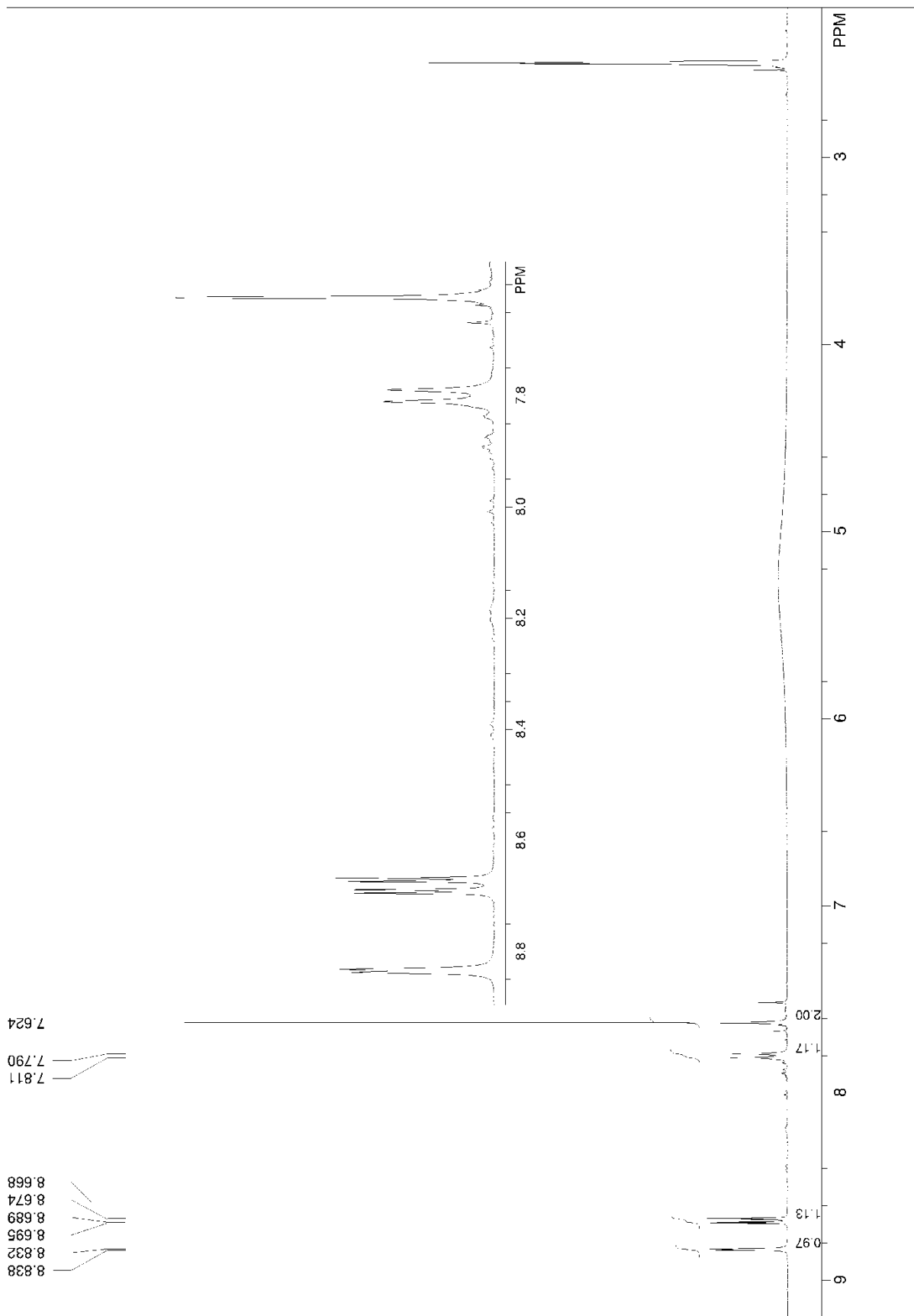


Figure A13: ^1H NMR spectrum of 2,4,5,7,4'-pentanitrofluorescein (400 MHz, $\text{DMSO-}d_6$).

Appendices

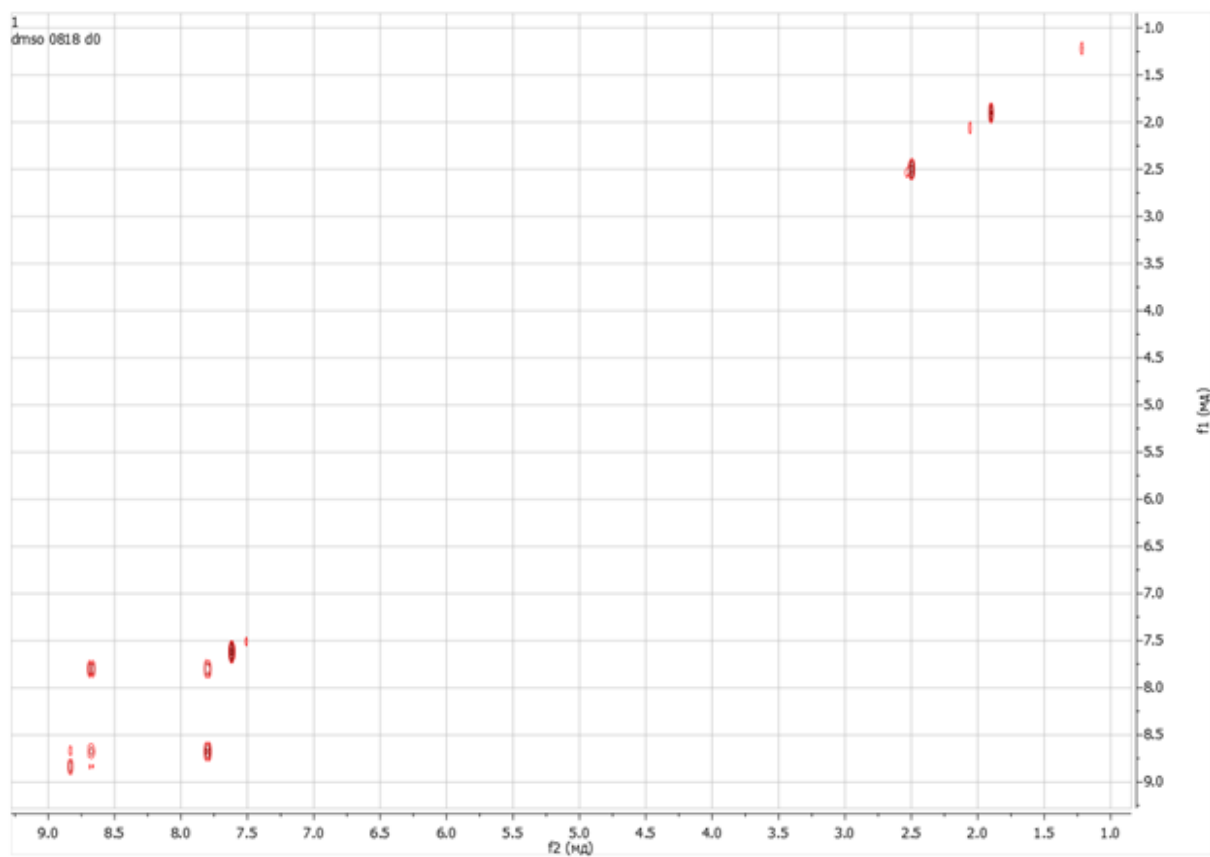


Figure A14: ^1H - ^1H COSY NMR spectrum of 2,4,5,7,4'-pentanitrofluorescein (400 MHz, DMSO- d_6).

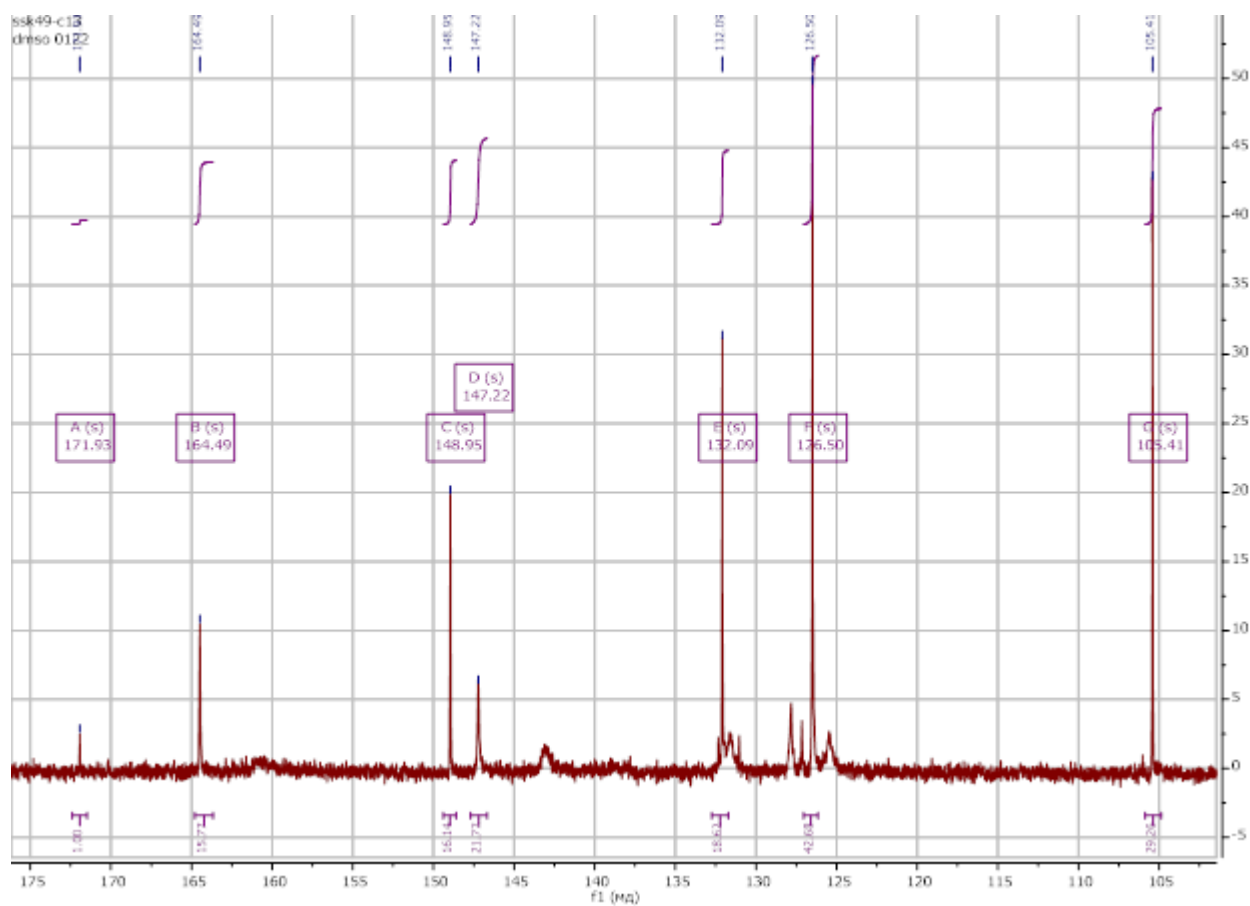


Figure A15: ^{13}C NMR spectrum of 2,4,5,7,4'-pentanitrofluorescein: (101 MHz, $\text{DMSO-}d_6$) δ 171.93, 164.49, 148.95, 147.22, 132.09, 126.50, 105.41, 20.99.

Appendices

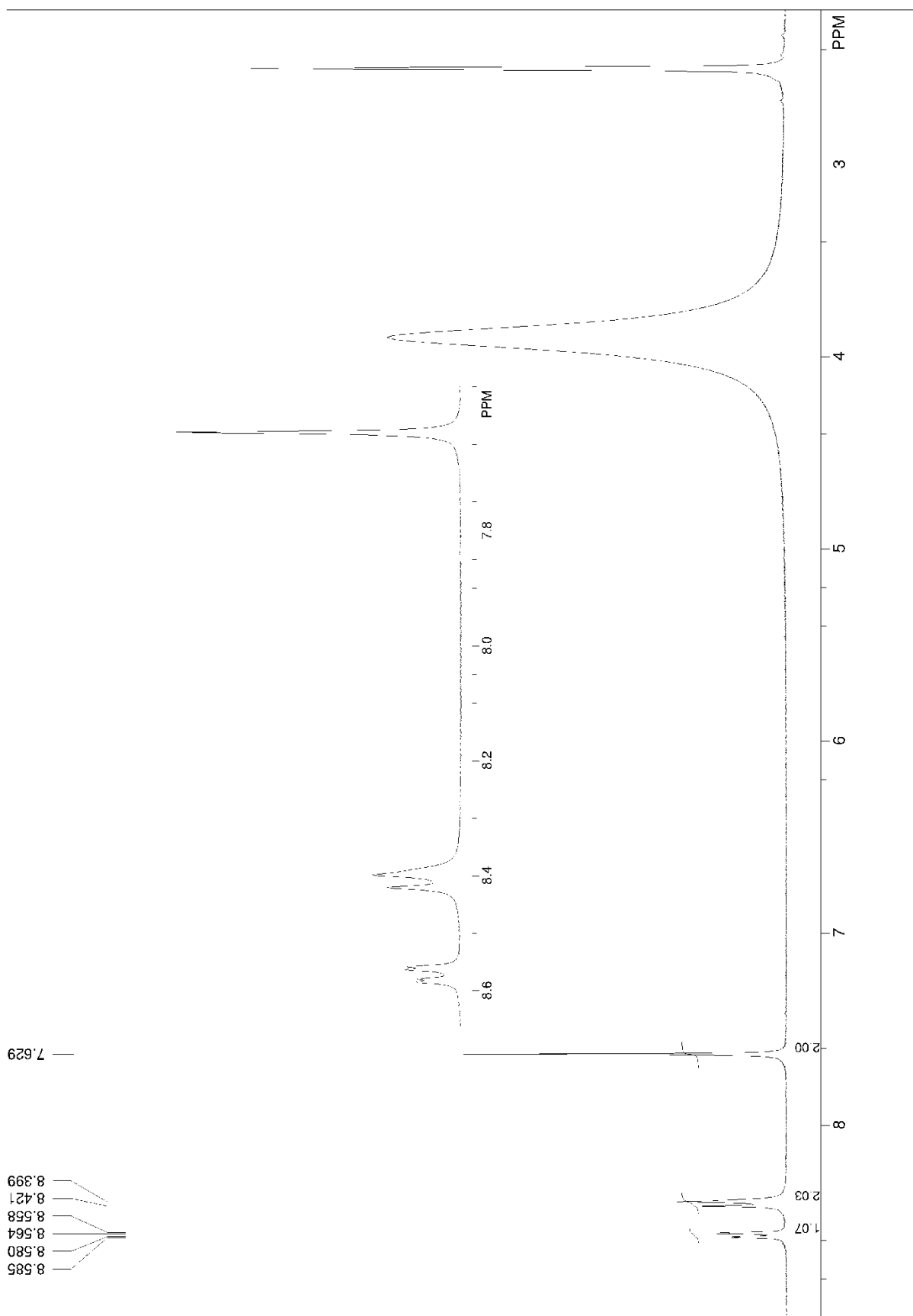


Figure A16: ^1H NMR spectrum of 2,4,5,7,5'-pentanitrofluorescein (400 MHz, $\text{DMSO-}d_6$).

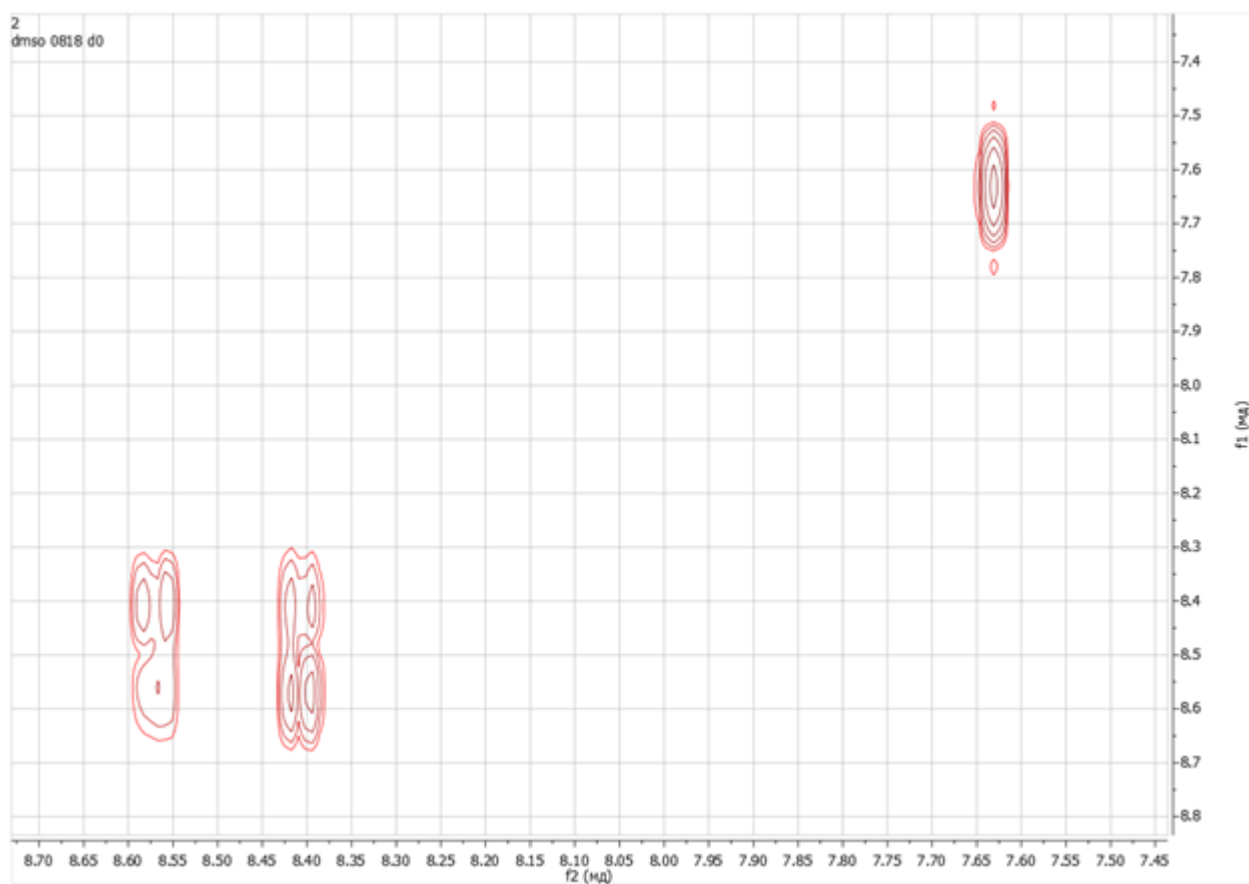
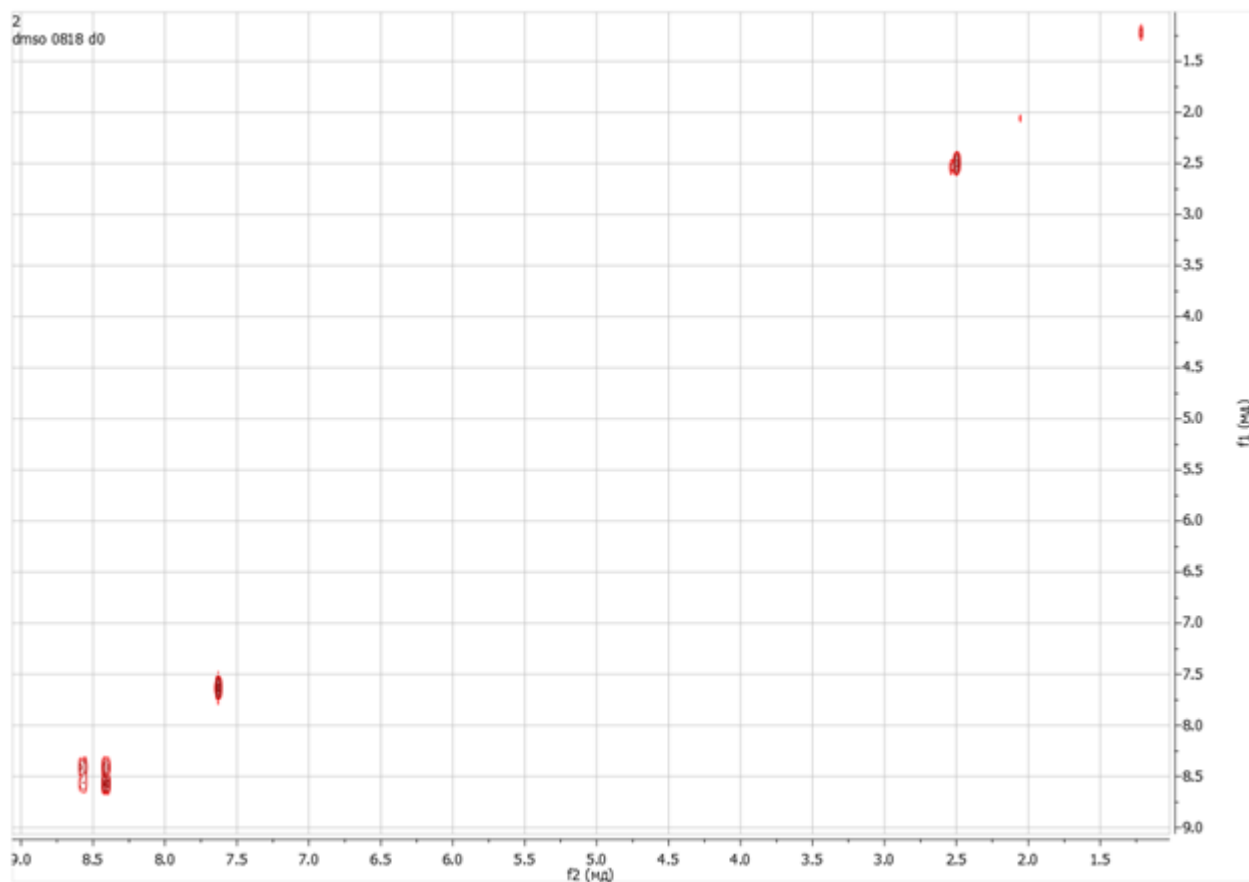


Figure A17: ^1H - ^1H COSY NMR spectrum of 2,4,5,7,5'-pentanitrofluorescein (400 MHz, $\text{DMSO-}d_6$).

Appendices

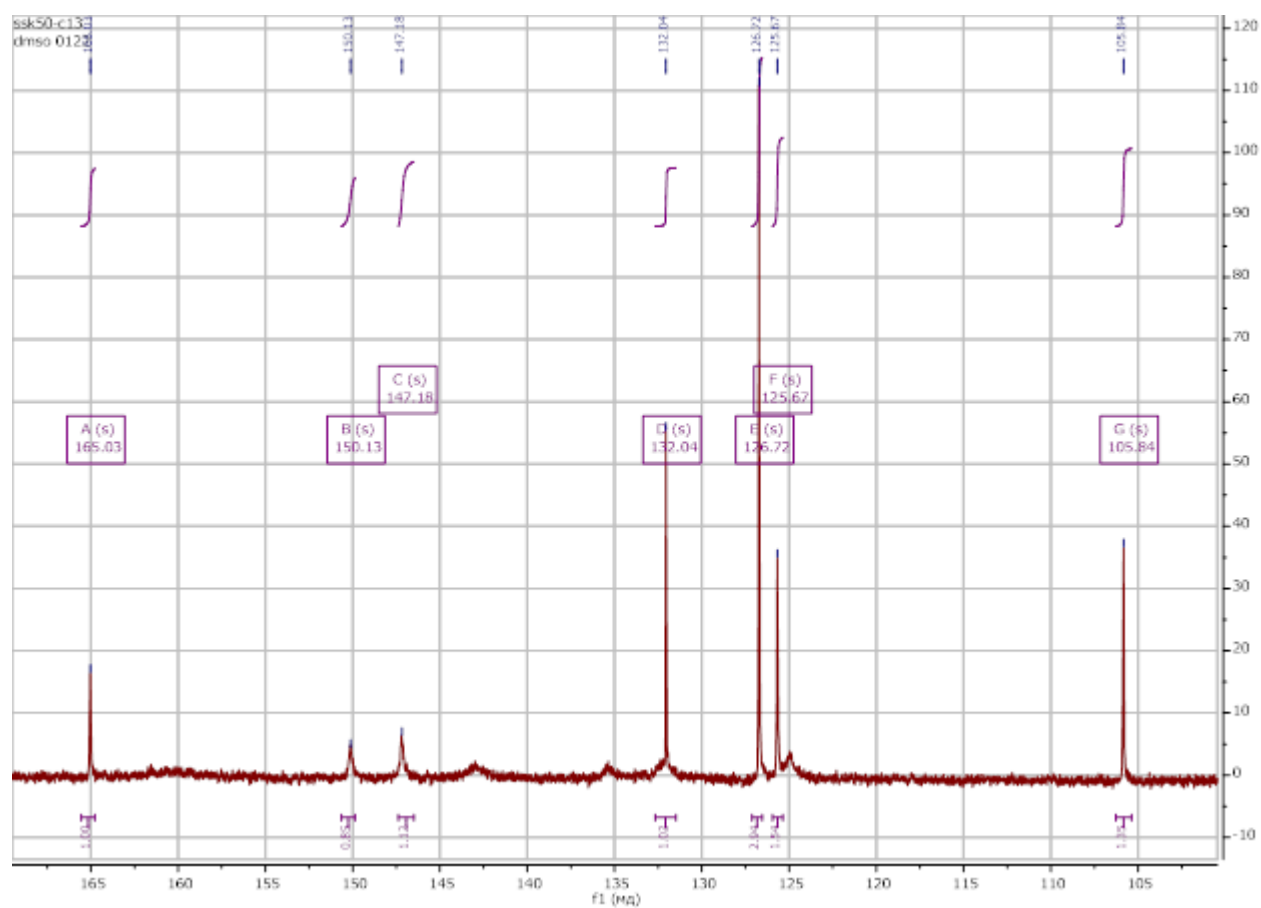


Figure A18: ^{13}C NMR spectrum of 2,4,5,7,5'-pentanitrofluorescein: (101 MHz, $\text{DMSO-}d_6$) δ 165.03, 150.13, 147.18, 132.04, 126.72, 125.67, 105.84.

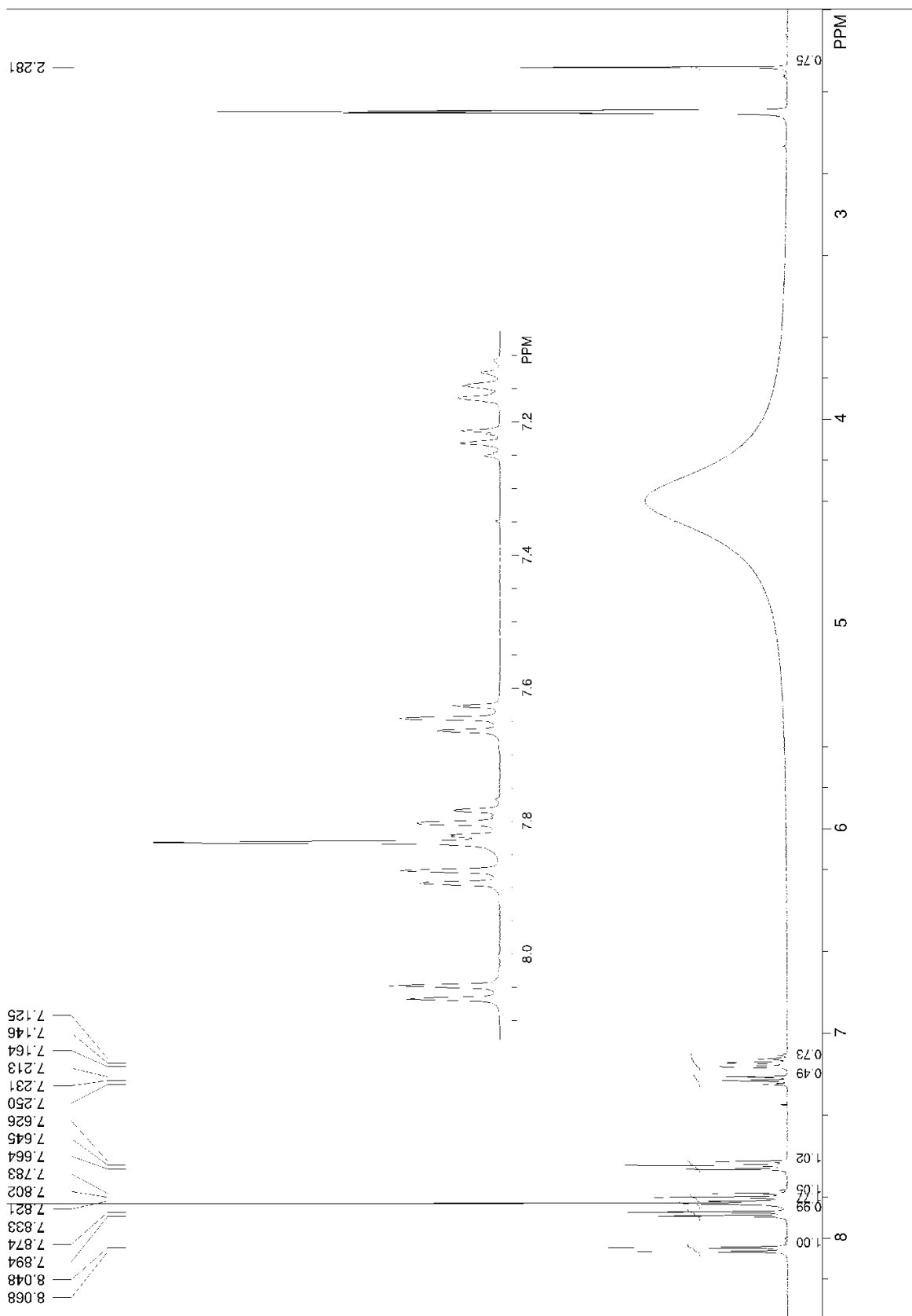
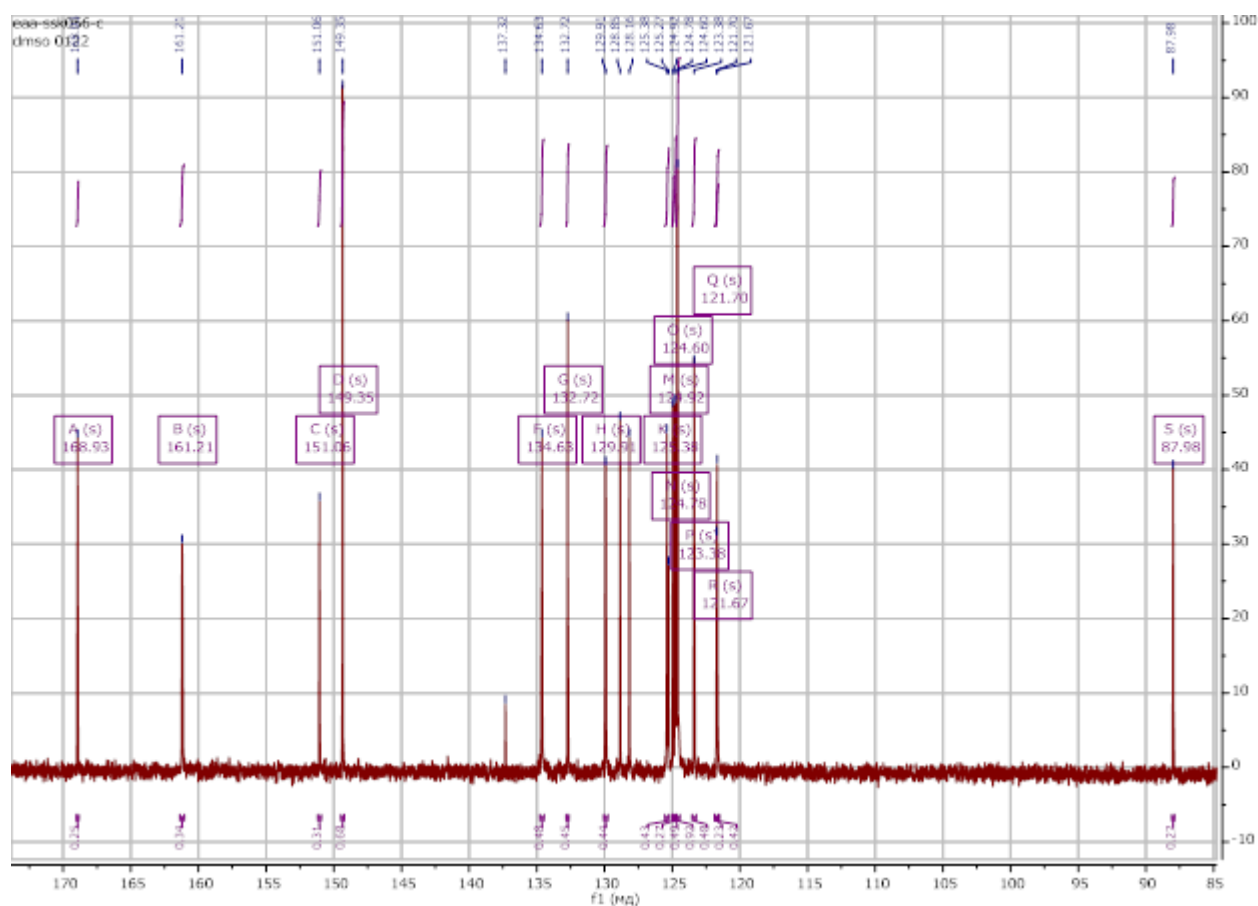


Figure A19: ^1H NMR spectrum of 2,4,5,7-tetranitrofluorescein with the cleaved pyran ring (3,3-bis(2',4'-dihydroxy-3,5-dinitrophenyl)-2-benzofuran-1(3H)-one) (400 MHz, $\text{DMSO-}d_6$).

Appendices



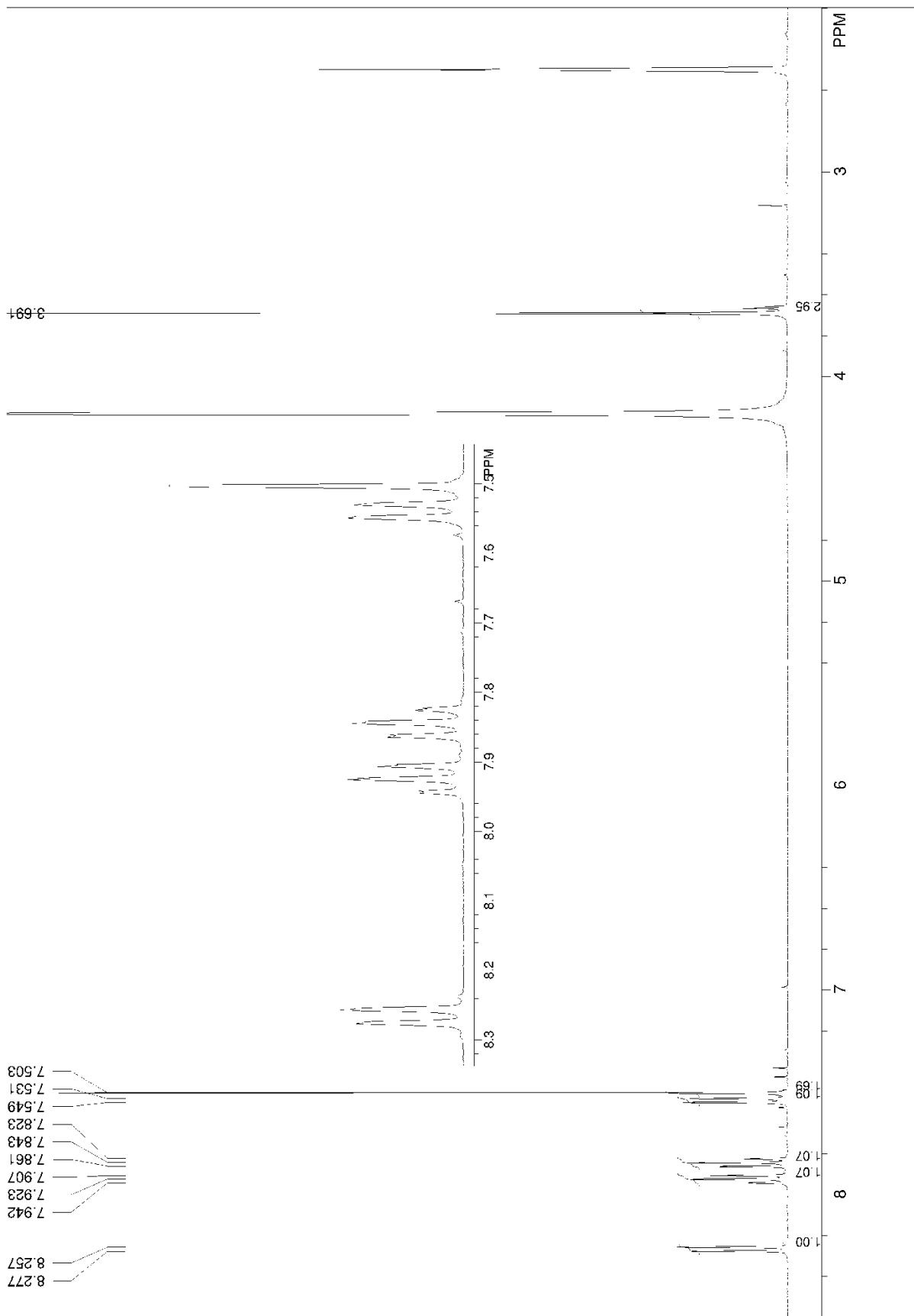


Figure A21: ^1H NMR spectrum of 2,4,5,7-tetranitrofluorescein methyl ester (400 MHz, $\text{DMSO-}d_6$).

Appendices

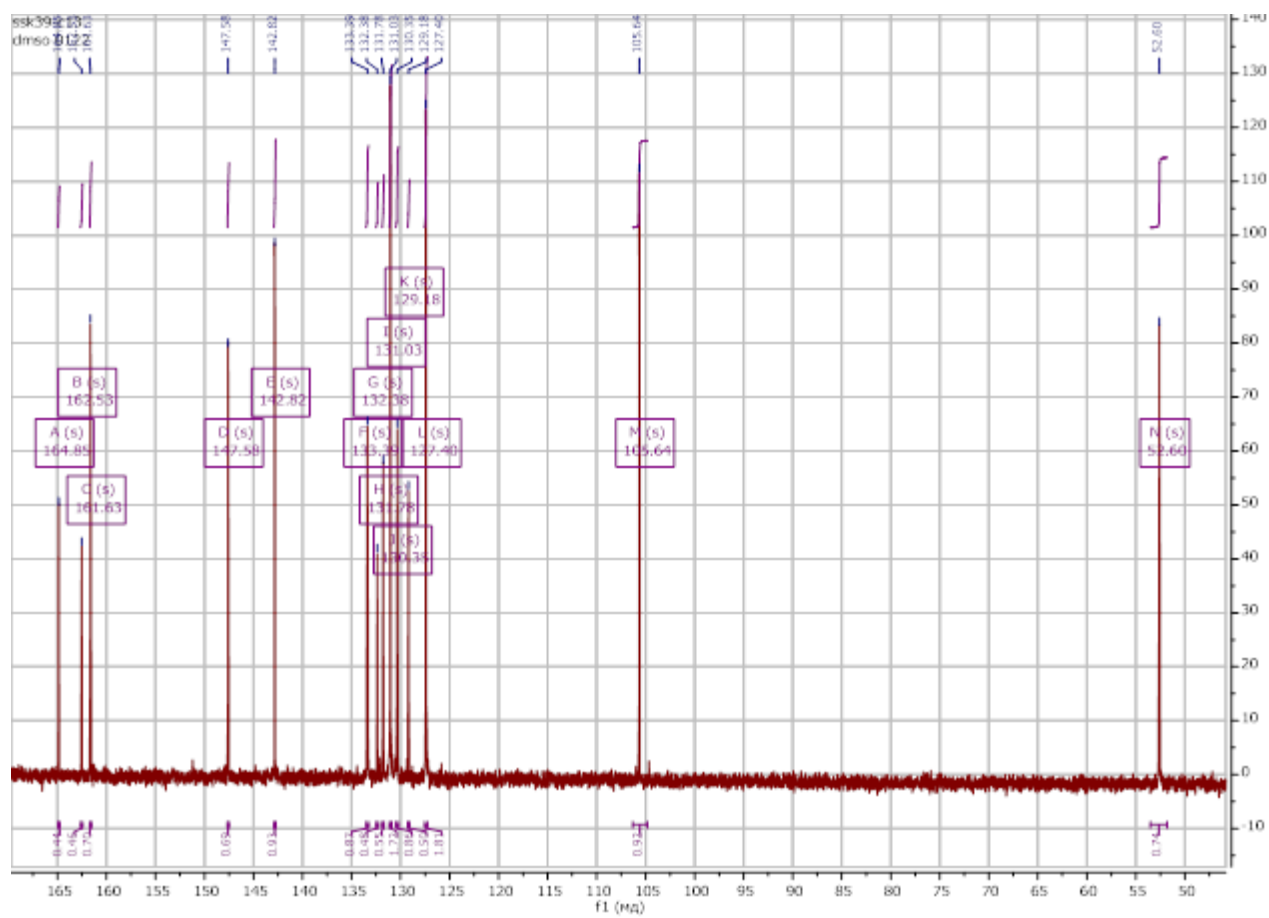


Figure A22: ^{13}C NMR spectrum of 2,4,5,7-tetranitrofluorescein methyl ester (methyl 2-(3,6-dihydroxy-2,4,5,7-tetranitro-9H-xanthen-9-yl)benzoate): (101 MHz, $\text{DMSO-}d_6$) δ 164.85, 162.53, 161.63, 147.58, 142.82, 133.39, 132.38, 131.78, 131.03, 130.35, 129.18, 127.40, 105.64, 52.60 ppm.

Appendix B: The $pa_{H^+}^*$ values and ionic strength of buffer solutions in acetonitrile with 4 mass % DMSO

The $pa_{H^+}^*$ values and ionic strength of buffer solutions in acetonitrile with 4 mass % DMSO, from ref. [1].

The parameters of ionic equilibrium in the buffer systems, necessary for calculations, are taken from ref. [2]. The $K_{HA_2}^f$ values for salicylic and benzoic acids are 2.5×10^2 and 2.2×10^3 M^{-1} , respectively. The dissociation constants of sodium hydrosalicylate and tetraethylammonium benzoate are 5.0×10^{-3} and 3.5×10^{-4} M, respectively. For picric acid, 2,4-dinitrophenol, and 2,6-dinitrophenol, $pK_{HA} = 3.30, 8.68,$ and 8.73 , respectively. The dissociation constants of sodium salts of 2,4- and 2,6-dinitrophenol 1.4×10^{-3} and 3.5×10^{-4} M.

Table B1: The $pa_{H^+}^*$ values and ionic strength of buffer solutions in acetonitrile with 4 mass % DMSO: salicylic acid + 0.00487 M sodium salicylate, 25 °C

Salicylic acid, M	$pa_{H^+}^*$	I, M
0.1733	6.27	0.0041
0.1722	6.28	0.0041
0.1570	6.35	0.0041
0.1037	6.69	0.0038
0.0948	6.76	0.0037
0.0948	6.76	0.0037
0.0689	7.01	0.0035
0.0584	7.14	0.0034
0.0555	7.18	0.0033
0.0420	7.40	0.0031
0.0118	8.31	0.0021
0.0050	8.86	0.0017
0.0022	9.32	0.0015

Appendices

1. Moskaeva, E.G., Mosharenkova, O.V., Shekhovtsov, S.V., Mchedlov-Petrosyan, N.O., Protolytic equilibrium of tetra- and pentanitrofluoresceins in a binary solvent acetonitrile – dimethyl sulfoxide (mass ratio 96 : 4), Ukrainian Chem J., V. 87., No. 5., P. 25–37, (2021).
<http://ucj.org.ua/10.33609/2708-129X.87.05.2021.25-37>.
2. Gensh K. V., Zevatskii Yu. E., Samoylov D.V., Shekhovtsov S.V., Lebed A. V., Goga S.T., Mchedlov-Petrosyan N.O., Ionic equilibrium in mixtures of polar protophobic and protophilic non-hydrogen bond donor solvents: Acids, salts, and indicators in acetonitrile with 4 mass % dimethylsulfoxide. J. Mol. Liquids, 322, 114560, (2020).

Table B2: The $pa_{H^+}^*$ values and ionic strength of 2,6-dinitrophenolate buffer solutions in acetonitrile with 4 mass % DMSO, 25 °C

2,6-Dinitrophenol	Sodium 2,6-dinitrophenolate	$pa_{H^+}^*$	<i>I</i> , M
0.3619	0.0510	6.76	0.0049
0.3547	0.0510	6.77	0.0049
0.3521	0.0510	6.78	0.0049
0.2997	0.0048	6.29	0.0012
0.2954	0.0048	6.23	0.0012
0.2881	0.0048	6.31	0.0012
0.1590	0.0048	6.57	0.0012
0.1362	0.0048	6.64	0.0012
0.1317	0.0048	6.65	0.0012
0.0090	0.0040	7.77	0.0011
0.0045	0.0040	8.07	0.0011

Table B3: The $pa_{H^+}^*$ values and ionic strength of 2,4-dinitrophenolate buffer solutions in acetonitrile with 4 mass % DMSO, 25 °C

2,4-Dinitrophenol	Sodium 2,4-dinitrophenolate	$pa_{H^+}^*$	<i>I</i> , M
0.1086	0.0040	6.30	0.0018
0.0698	0.0010	6.18	0.0006
0.0551	0.0008	6.25	0.0005
0.0549	0.0008	6.26	0.0005
0.0519	0.0005	6.14	0.0004
0.0455	0.0004	6.14	0.0003
0.0449	0.0004	6.15	0.0003
0.0270	0.0040	7.12	0.0014
0.0090	0.0040	7.68	0.0012
0.0045	0.0040	8.01	0.0012
0.0018	0.0040	8.42	0.0011

Appendix C: Steady-state absorption spectra of esters of fluorescein in DMSO

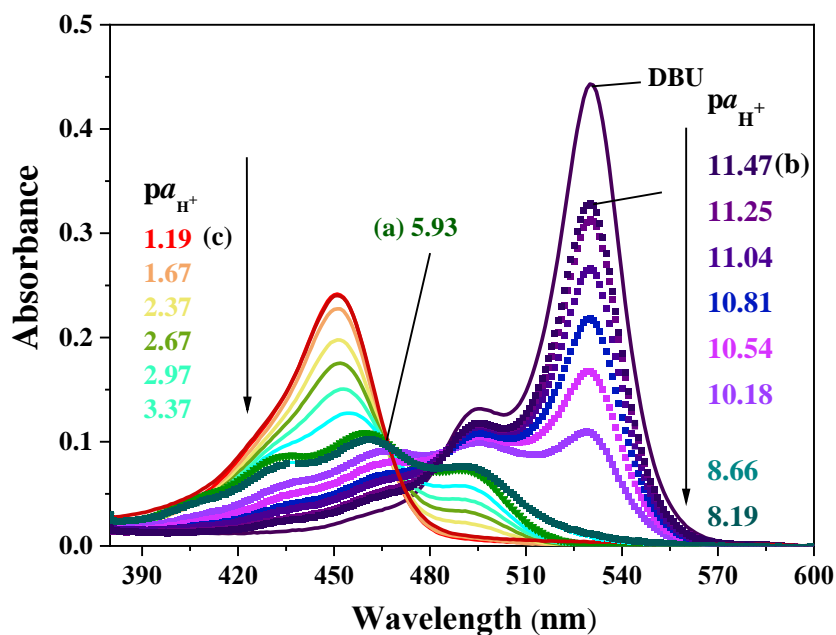


Figure C1: Steady-state absorption spectra of ethyl ester of fluorescein in DMSO at different pK_{aH^+} values in salicylate (a) and benzoate (b) buffer solutions and in *p*-toluenesulfonic acid solutions (c).

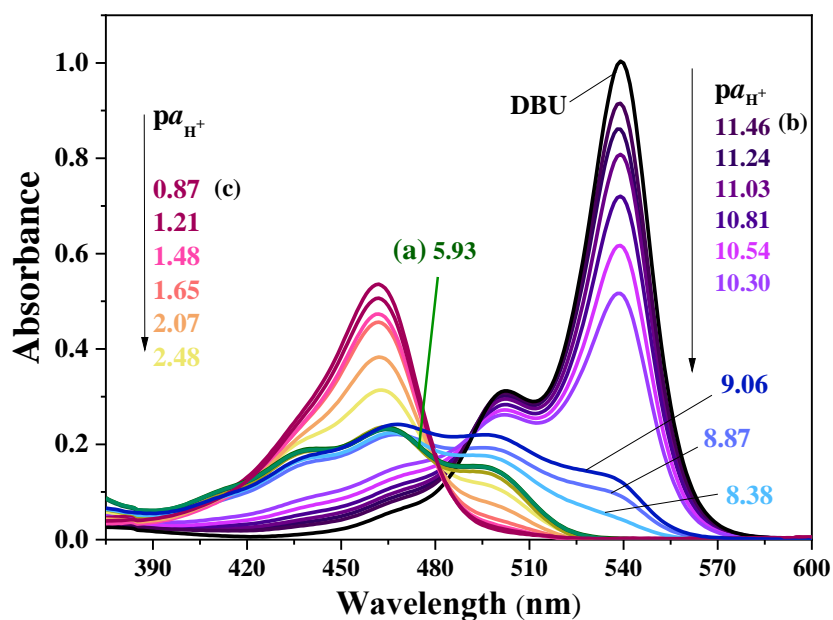


Figure C2: Steady-state absorption spectra of methyl ester of 5'-nitrofluorescein in DMSO at different pK_{aH^+} values in salicylate (a) and benzoate (b) buffer solutions and in *p*-toluenesulfonic acid solutions (c).

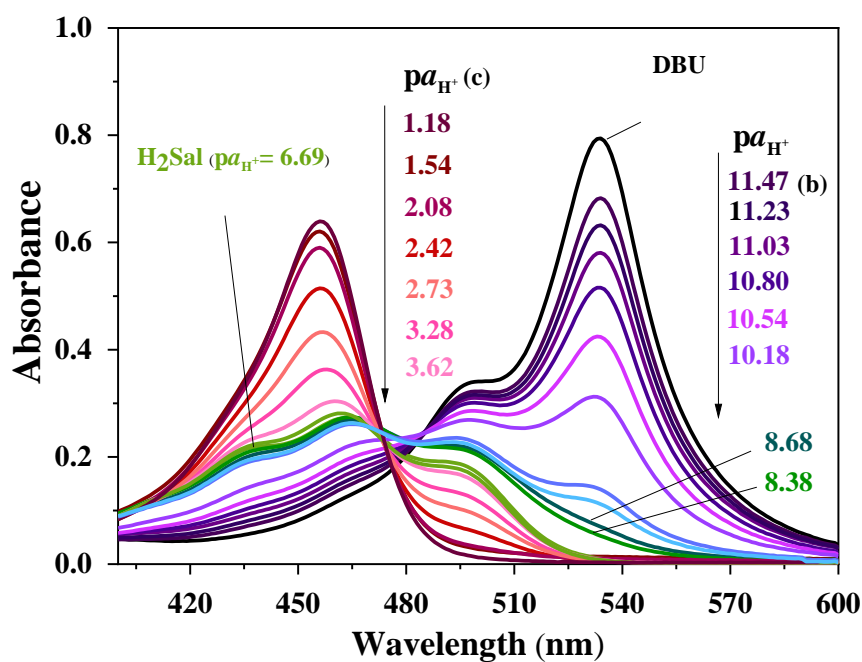


Figure C3: Steady-state absorption spectra of ethyl ester of 4'-nitrofluorescein in DMSO at different $pK_{a_{H^+}}$ values in salicylate (a) and benzoate (b) buffer solutions and in *p*-toluenesulfonic acid solutions (c).

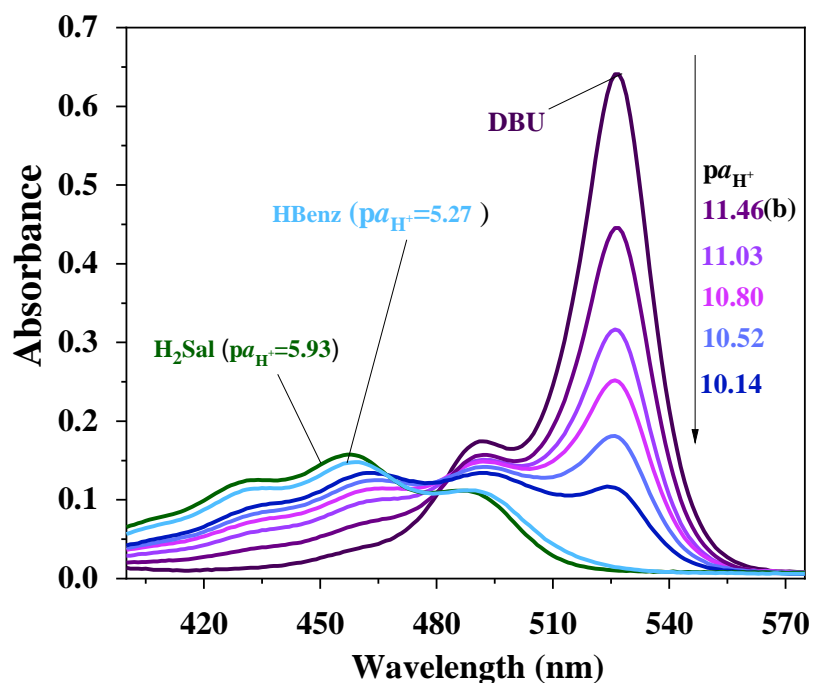


Figure C4: Steady-state absorption spectra of ethyl ester of 5'-aminofluorescein in DMSO at different $pK_{a_{H^+}}$ values in salicylate (a) and benzoate (b) buffer solutions and in *p*-toluenesulfonic acid solutions (c).

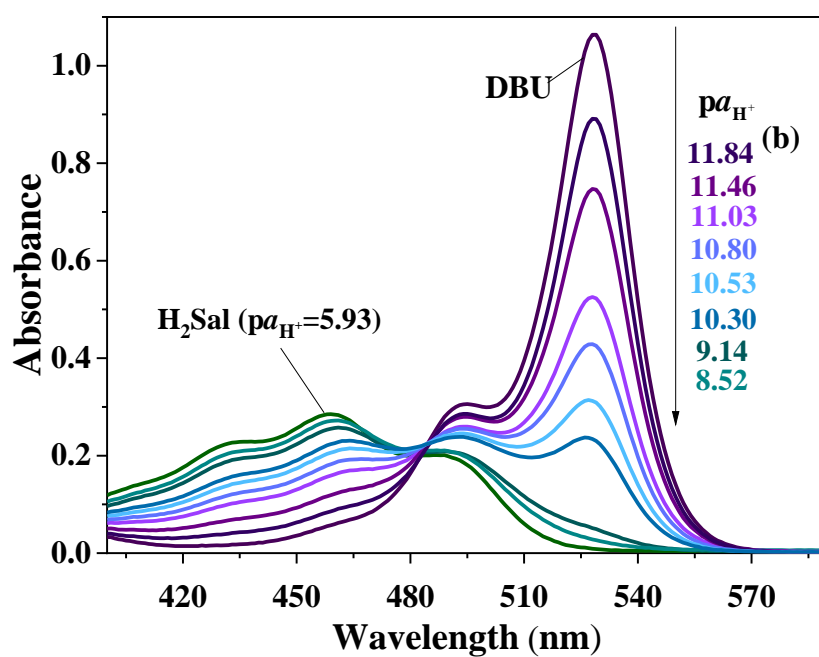


Figure C5: Steady-state absorption spectra of methyl ester of 5'-aminofluorescein in DMSO at different pK_a values in salicylate (a) and benzoate (b) buffer solutions and in *p*-toluenesulfonic acid solutions (c).

Appendix D: The parameters of the fluorescence decays of BDP1 and BDP2

Table D1: The fitting parameters of the fluorescence decays of BDP1 using multiexponential functions: fluorescence lifetime components (τ_i , ps) and their relative contributions (A_i , normalized to the sum of positive components).

X (BuOH)	A_1	τ_1	A_2	τ_2	A_3	τ_3	χ^2
0.00	5577	4.38±0.02	5848	2.83±0.03			0.993
0.10	3571	4.58±0.03	7739	2.95±0.02			0.993
0.19	4298	4.38±0.03	7120	2.73±0.02			0.990
0.29	3742	4.44±0.03	7816	2.75±0.02			0.990
0.39	4966	4.10±0.02	6459	2.56±0.02			1.094
0.48	2114	4.76±0.04	9122	2.879±0.015	1648	0.14±0.04	0.998
0.58	1943	4.70±0.04	8149	2.855±0.016	2958	0.22±0.03	0.999
0.66	3410	4.37±0.03	8019	2.60±0.02			1.02
0.77	2017	4.74±0.04	8783	2.767±0.016	1852	0.118±0.04	0.972
0.86	1869	4.69±0.04	8432	2.767±0.015	1822	0.13±0.04	0.990
0.95	1618	4.84±0.05	8424	2.788±0.015	1760	0.16±0.04	0.976

Appendices

Table D2: The parameters of the fluorescence decays of BDP1: k_{rad} (ps), k_{nonrad} (ps)

X (BuOH)	ε	η , mPa*s	k_{rad} (ps ⁻¹)	k_{nonrad} (ps ⁻¹)	$\Delta\nu_{Stokes}$, cm ⁻¹	Φ_{fluo} , %
0.00	35.93	0.3326	0.5446	278.2	531.09	0.1954
0.10	32.41	0.3599	0.5708	299.4	494.74	0.1903
0.19	29.39	0.4087	0.5228	297.8	527.12	0.1752
0.29	26.81	0.4754	0.4934	302.8	492.89	0.1627
0.39	24.64	0.5602	0.4957	308.9	491.04	0.1602
0.48	22.81	0.6674	0.4932	352.0	527.12	0.1399
0.58	21.30	0.8047	0.5853	394.4	455.11	0.1482
0.66	20.16	0.9638	0.4437	319.5	455.11	0.1387
0.77	19.03	1.2190	0.4395	370.7	523.19	0.1384
0.86	18.19	1.5296	0.5860	374.2	523.19	0.1564
0.95	17.49	1.9357	0.6253	372.7	453.41	0.1675

Table D3: The fitting parameters of the fluorescence decays of BDP2 using multiexponential functions: fluorescence lifetime components (τ_i , ps) and their relative contributions (A_i , normalized to the sum of positive components).

X (BuO H)	A_1	τ_1	A_2	τ_2	χ^2
0.00	18827	0.1584±0.0007			1.12
0.10	17865	0.1669±0.0006	945000	0.00100±0.00005	0.991
0.20	18288	0.1745±0.0007	449100	0.00105±0.00005	1.09
0.29	17310	0.1821±0.0006	1184800	0.001100±0.000016	0.977
0.39	16666	0.1903±0.0007	643500	0.00126±0.00003	1.018
0.49	16864	0.1979±0.0006	1241500	0.001003±0.000018	0.971
0.59	16343	0.2090±0.0007	684300	0.00130±0.00002	0.982
0.68	16209	0.2146±0.0007	1420300	0.001060±0.000015	0.975
0.78	15953	0.2287±0.0008	556200	0.00133±0.00003	0.994
0.88	235.1	0.350±0.03	16153.8	0.02405±0.0009	0.975
0.98	1429.1	0.357±0.007	14731.9	0.02559±0.0010	0.997

Appendices

Table D4: The parameters of the fluorescence decays of BDP2: k_{rad} (ps), k_{nonrad} (ps)

X (BuOH)	ε	η , mPa*s	k_{rad} , (ps ⁻¹)	k_{nonrad} ,(ps ⁻¹)	$\Delta\nu_{Stokes}$, cm ⁻¹	Φ_{fluo} , %
0.00	35.93	0.3326	30.24	5852	630.04	0.5141
0.10	32.31	0.3611	43.714	7830	630.04	0.5552
0.20	29.21	0.4126	28.26	4857	703.25	0.5785
0.29	26.81	0.4756	46.00	7697	703.25	0.5940
0.39	24.55	0.5646	40.99	6546	625.07	0.6222
0.49	22.66	0.6788	83.46	6843	625.07	1.2049
0.59	21.10	0.8279	82.76	5935	622.60	1.3753
0.68	19.94	1.004	154.2	6506	622.60	2.3153
0.78	18.88	1.263	128.7	5124	622.60	2.4504
0.88	18.02	1.612	120.5	3906	622.60	2.9915
0.98	17.30	2.078	101.9	3630	582.52	2.7299